Understanding Mitofusin 2: Insights from Disease-Associated Alleles

Nyssa Becker Samanas

A dissertation

submitted in partial fulfillment of the

requirements for the degree of

Doctor of Philosophy

University of Washington

2019

Reading Committee:

Suzanne Hoppins , Chair

David Hockenbery

James Hurley

Program Authorized to Offer Degree:

Molecular and Cellular Biology

University of Washington

Abstract

Understanding Mitofusin 2: Insights from Disease-Associated Alleles

Nyssa Becker Samanas

Chair of Supervisory Committee:

Suzanne Hoppins

Department of Biochemistry

Mitofusin 2 (Mfn2) is an outer mitochondrial membrane protein responsible for mitochondrial fusion. Mitochondrial fusion is essential for cellular health and survival. Mutations in Mfn2 cause the peripheral neuropathy Charcot-Marie-Tooth Type 2A, however, the etiology of the disease as well as the molecular mechanism of Mfn2-mediated mitochondrial fusion are not fully understood. Comparison to related proteins indicates a potential model of mitofusin activity, but details have yet to be filled in. Due to the lack of structural and biochemical information available about Mfn2, I used disease-associated alleles of Mfn2 to perform a structure-function analysis to learn about the molecular mechanism of Mfn2.

I first sought to identify domains of Mfn2 essential to its fusion activity. I found that the C-terminus of Mfn2 is essential to mitochondrial fusion, while the N-terminus and the middle stalk domain can be modified without gross morphological changes of mitochondria. I next examined the role of Mfn2 in response to oxidative stress and found that this response, at least in our system, is different dependent on the exact stressor and is dependent on Mfn2. I also report that oxidative environments cause a change in Mfn2 assembly in isolated mitochondria.

Finally, I report that the integrity of a major predicted hinge region of Mfn2 is essential for correct mitochondrial fusion using a series of microscopy based and biochemical assays. This is likely due to its contribution to the ability of Mfn2 to assemble within mitochondrial membranes to form oligomers capable of mitochondrial fusion.

Table of contents

LIST OF FIGURES

Acknowledgements

Graduate school has been a time of learning, struggling, and growing. I have become a better scientist, co-worker, and person, which would not have happened without so many people. Suzanne Hoppins, my advisor, has been a wonderful guide through my journey from clueless rotation student to capable scientist. All the members of the Hoppins lab gave me invaluable advice, support, and encouragement. I would especially like to thank Brittany Whitley, who was a wonderful baymate for so many years.

My family and friends back in Wisconsin have been such a great cheering section and were so understanding of how infrequently I could come back. Thank you to all of you who worked around my schedule and met up with little notice.

My family here in Seattle has been through so much the last six years. Elodie, you have been my buddy throughout grad school. You have kept me grounded and always been ready to make me smile and remember it's not the end of the world when science goes wrong for a day. Your questions and creativity are amazing to me, and I have tried to remember to keep those qualities in my work. Lyra, you came in and shook our lives, but I wouldn't trade you for all the papers in the world. Your intensity and determination are spectacular, and your very existence has allowed me to finish this journey.

Evan deserves his own paragraph, and this work is dedicated to him. We've gone from moving to Seattle with almost nothing to building a family and making a home in the last six years. Thank you for your endless love and support. Two pregnancies, two home purchases, and five moves in six years would have been a lot even if I weren't in grad school, but I had to make it harder on us. Thank you for always telling me that we were in this together; this has truly been a team effort.

Chapter 1: Introduction

1.1 Mitochondria and mitochondrial morphology

Mitochondria are best known as the powerhouse of the cell due to their role of producing the majority of the ATP in most cell types through the process of oxidative phosphorylation (Ernster and Schatz 1981). However, the true role of the mitochondria in the eukaryotic cell is significantly broader. Mitochondria are able to import calcium and serve as a calcium sequestration compartment vital to Ca_{2+} signaling in the cell (Slater and Cleland 1953; De Stefani, Rizzuto, and Pozzan 2016). Reactive oxygen species made in the mitochondria also function as signaling molecules, cementing the role of mitochondria as a signaling organelle (Chandel et al. 1998). Additionally, mitochondria are a central regulator of apoptosis by the regulated release of pro-apoptotic factors such as cytochrome C, Smac, and Omi (Wang and Youle 2011). Mitochondrial dysfunction is associated with a host of diseases including neurodegenerative diseases, cardiovascular disease, cancer, and diabetes (Sorrentino, Menzies, and Auwerx 2017; Wallace, Fan, and Procaccio 2010; Picard, Wallace, and Burelle 2016).

Mitochondrial and cellular function is highly influenced by the morphology of the organelles (Pernas and Scorrano 2015). Both the distribution and the connectivity of mitochondria within a cell are dynamic (Mishra and Chan 2014). Baseline mitochondrial morphology varies among tissues from long, tubular mitochondria in fibroblasts to smaller, ovoid mitochondria in skeletal muscle to highly clustered mitochondria between the inner and outer segment of cone photoreceptors (Shitara et al. 2010; Giarmarco et al. 2017). In addition to different baseline morphologies, the status of the mitochondrial network is also responsive to changes in physiological states of the cell. For example, mild stresses induce a highly connected network of mitochondria while severe or prolonged stress is associated with fragmentation of the mitochondrial network which is further correlated with apoptosis (Shutt and McBride 2013). During the cell cycle, the mitochondrial morphology changes from a connected network to a

fragmented collection of mitochondria and back (Horbay and Bilyy 2016). Much like mitochondrial dysfunction, disruption of mitochondrial dynamics is implicated in disease states such as peripheral and central neurodegenerative diseases (Vital and Vital 2012; Celardo et al. 2014; Pareyson et al. 2015), and diabetes (Wada and Nakatsuka 2016; Rovira-Llopis et al. 2017).

1.2 Proteins responsible for mammalian mitochondrial dynamics

1.2.1 Mitochondrial trafficking

The various mitochondrial morphologies are regulated by trafficking, fusion, and division of individual organelles. Correct localization of mitochondria is especially important in polarized cells such as neurons or migrating cells where energy demands and the physiological environment vary across the cell. Mitochondria are moved though the cytoplasm along microtubules by transport proteins of the kinesin, which moves mitochondria toward the plus end of microtubules, and dynein, which moves the mitochondria toward the minus end of microtubules, families (Pilling et al. 2006). Mitochondrial transport requires adaptor proteins which connect the mitochondrial membrane to the transport machinery. In mammals, mitochondrial rho GTPases (Miro1 and Miro2) are mitochondrial outer membrane proteins that interreact with the adaptor proteins TRAK1/TRAK2 which connect the mitochondria to the transport machinery (Fransson, Ruusala, and Aspenström 2006; Koutsopoulos et al. 2010).

1.2.2 Network connectivity

The opposing processes of mitochondrial fusion and division are both regulated by mechanochemical enzymes of the dynamin related protein (DRP) family of large GTPases. This family of membrane remodeling proteins is characterized by a large, globular GTPase domain connected to a membrane interaction domain by a stalk region composed of helical bundles (Figure 1) (Jimah and Hinshaw 2019).

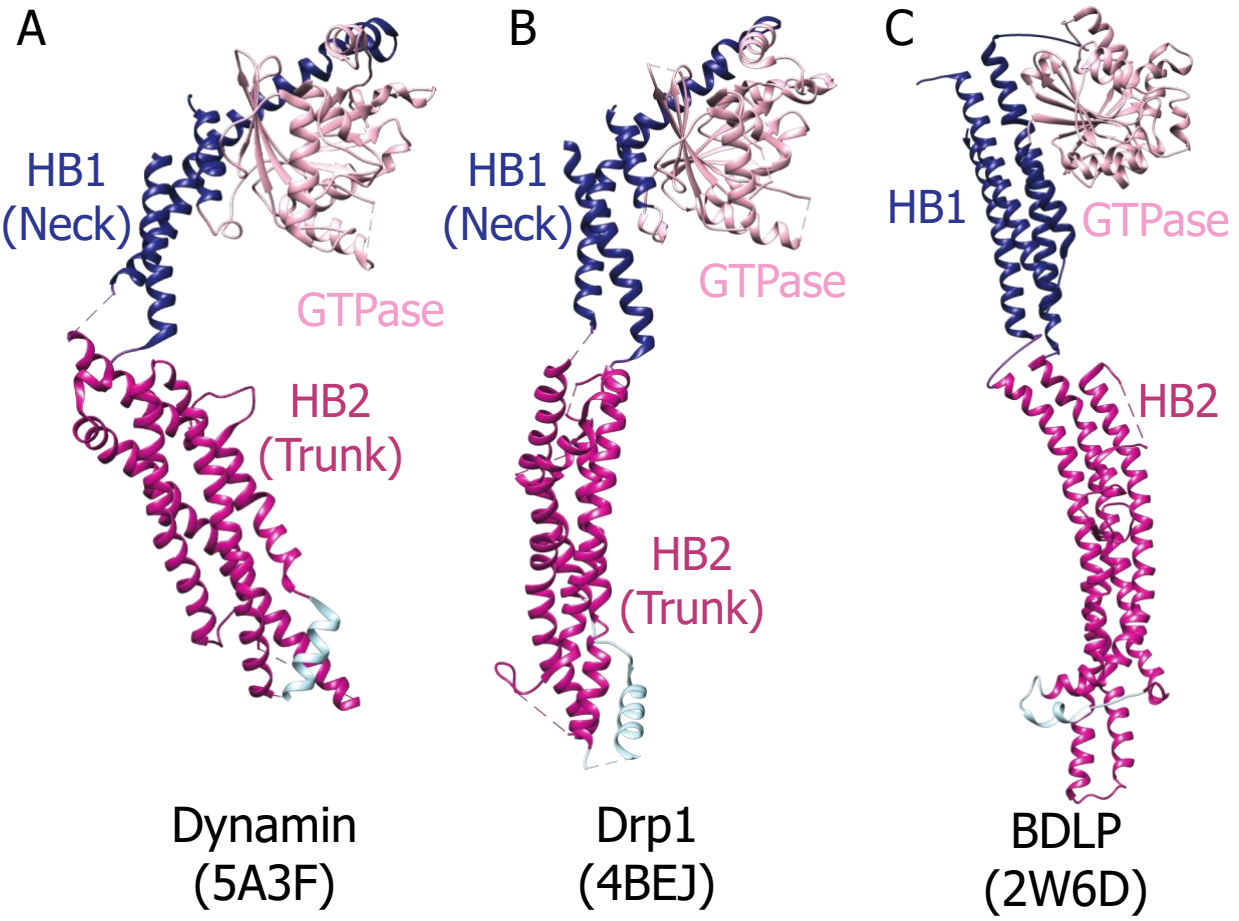

Figure 1.1. Domain architecture of selected dynamin related proteins (DRPs). Common DRP domains in A) Dynamin, B) Dynamin-related protein 1, and C) Bacterial dynamin like protein include a nucleotide binding and hydrolysis domain (GTPase, light pink); a membrane interacting domain (light blue); and an extended helical region between the two which is divided into two regions (HB1/Neck/Bundle Signaling Element, navy blue; and HB2/Trunk, dark pink).

1.2.3 Mitochondrial Division

In mammals, mitochondrial division is accomplished by dynamin related protein 1 (Drp1) (Smirnova et al. 2001). Drp1 functions in a manner very similar to the mechanism of the prototypical family member, dynamin. Drp1 is recruited to putative division sites in the mitochondrial membrane by adaptors proteins Fis1, Mff, MiD49, and MiD51 (Loson et al. 2013). Once at the membrane, Drp1 assembles into highly stereotyped helices around the mitochondria

that involve several interaction domains between monomers (Jimah and Hinshaw 2019). Assembly triggers GTP hydrolysis which is connected to a major conformational change that effectively narrows the inner diameter of the helix and leads to mitochondrial division (Mears et al. 2011).

1.2.4 Mitochondrial Fusion

Mitochondrial fusion is regulated in mammals by mitofusins (Mfn1 and Mfn2) on the outer mitochondrial membrane and optic atrophy 1 (Opa1) on the inner mitochondrial membrane (Santel and Fuller 2001; Eura 2003; Olichon et al. 2003). These proteins are all members of the same protein family as Drp1 yet must function through distinct molecular mechanisms as they catalyze membrane fusion rather than division. The general biochemical characteristics of DRPs including assembly, nucleotide hydrolysis, and large conformational changes have been demonstrated for mitofusins, but the precise way in which these properties lead to membrane fusion is only just beginning to be understood (Chen et al. 2003; Ishihara, Eura, and Mihara 2004; Detmer and Chan 2007; Yan et al. 2018).

Multiple lines of biochemical inquiry including co-immunoprecipitation, sucrose gradient sizing, and blue native-PAGE have indicated that Mfn1 and Mfn2 form both homooligomeric and heterooligomeric complexes (Chen et al. 2003; Eura 2003; Ishihara et al. 2004; Koshiba et al. 2004; Engelhart and Hoppins 2019). Several studies indicate that the most efficient fusion complex includes both Mfn1 and Mfn2, suggesting a functional difference between the two proteins (Eura 2003; Detmer and Chan 2007b; Hoppins et al. 2011).

The role of GTP hydrolysis in mitofusin function is not yet well understood, although the proteins have been known to function as GTPases almost since they were discovered (Ishihara, Eura, and Mihara 2004). Recent structural work has shed light on the structural basis of

mitofusin GTP hydrolysis and suggests that, like other DRPs, nucleotide binding is required for dimerization which precedes nucleotide hydrolysis. Minimal structures of the GTPase region and first helical bundle of Mfn1 allowed the discovery of a dimerization interface between the GTPase domains of Mfn1 molecules that allows interaction in a nucleotide-dependent manner (Cao et al. 2017; Yan et al. 2018).

Additionally, this minimal construct has shown that, for Mfn1, the nucleotide state of the GTPase domain can alter the position of the GTPase region relative to HB1, indicating that nucleotide-dependent conformational changes are likely important for mitofusin functioning as they are for other DRPs (Yan et al. 2018; Jimah and Hinshaw 2019). While these studies cannot address the possibility of a conformational change of the relative positions of the two helical bundles, analysis of the closely structurally related protein BLDP indicates that it is likely that mitofusins can exist in a "closed" state where HB1 and HB2 are in close proximity (see Figure 1.3 for approximate structure) and an "open" state where they are much further apart (see Figure 1.1 for approximate structure). Movement around this region of the protein would be consistent with the conformational states observed in other family members (Jimah and Hinshaw 2019).

This information results in a model of mitochondrial fusion consisting of several steps. First, the mitochondria that are to fuse must be tethered together through interactions of mitofusins on opposite membranes (Figure 1.2A). Then the mitofusins form some oligomeric assembly (Figure 1.2B) that stimulates nucleotide hydrolysis. Lastly, a conformational change of the mitofusins (Figure 1.2C) results in disruption and mixing of the two outer membranes (Figure 1.2D).

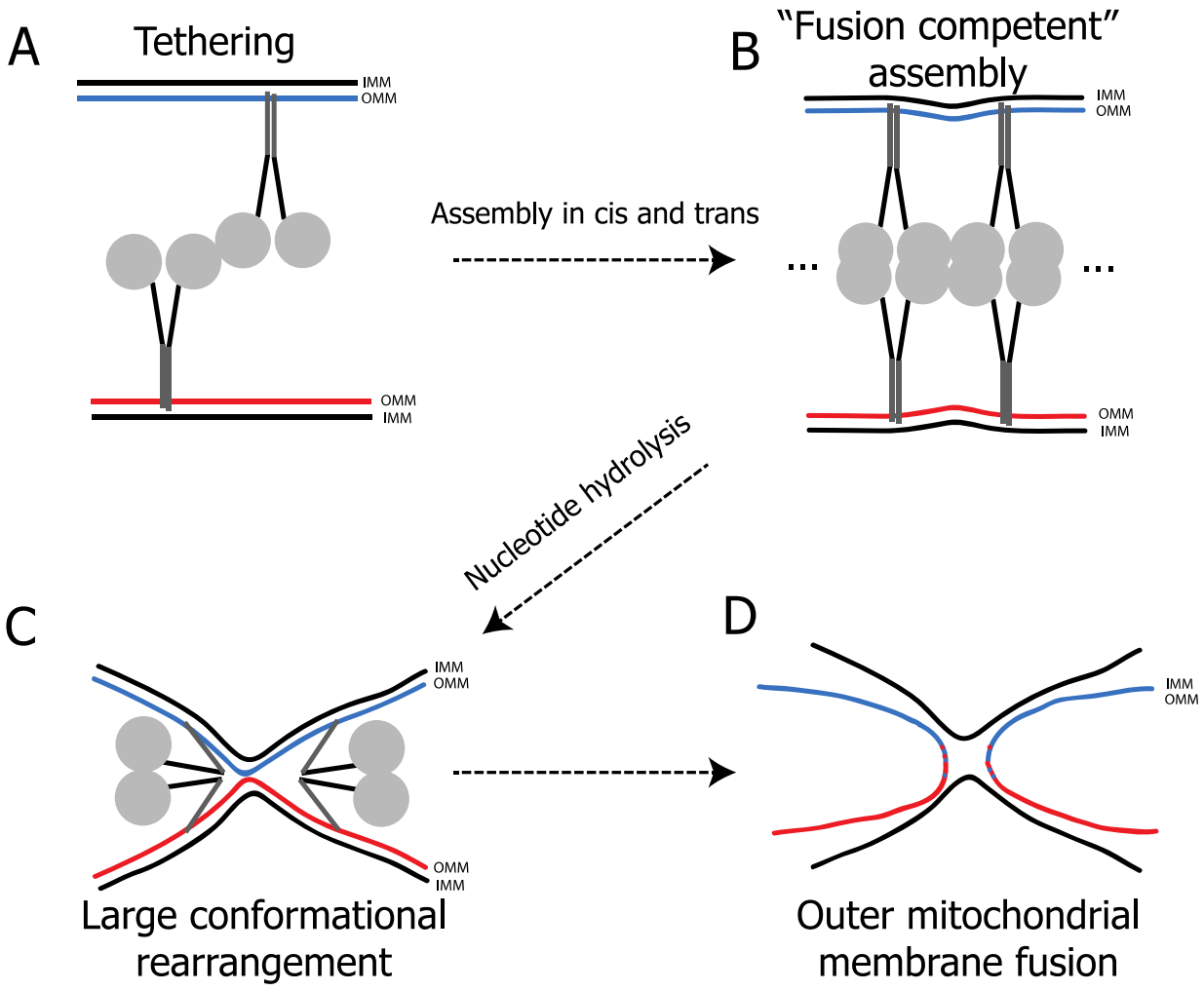

Figure 1.2. Model of outer mitochondrial membrane fusion.
A) Mitofusins on separate mitochondria are tethered by interactions between mitofusin molecules on opposite outer membranes. **B)** Assembly of mitofusin molecules on the same membrane (in cis) and on opposite membranes (in trans) leads to the formation of an assembly that can facilitate outer mitochondrial membrane fusion. **C)** Nucleotide hydrolysis leads to a large structural rearrangement of the mitofusin proteins that disrupts the mitochondrial membranes and brings them into close proximity. **D)** Outer mitochondrial membranes mix completing the process of outer membrane fusion.

1.2.5 Regulation

As the morphology of the mitochondrial network changes in a regulated manner, the proteins that mediate changes in morphology must also be regulated. Drp1 is regulated by post translational modifications of the protein itself as well as interactions with the adaptor proteins

that facilitate interaction between Drp1 and the mitochondrial membrane (Harder et al. 2004; Cribbs and Strack 2007; Han et al. 2008; Otera et al. 2010; Wang et al. 2011; Gawlowski et al. 2012; Guo et al. 2013; Loson et al. 2013; Prudent et al. 2015; Atkins et al. 2016; Bian et al. 2019; Ganesan et al. 2019). In a similar manner, both mitofusins have been reported to be post-translationally modified (Chen and Dorn 2013; Sugiura et al. 2013; Lee et al. 2014; Park et al. 2014; Pyakurel et al. 2015; McLelland et al. 2018; Ferreira et al. 2019) and Mfn2 has been shown to interact with the pro-apoptotic Bcl-2 protein Bax in a manner that modifies its fusion efficiency (Karbowski et al. 2002; Guo et al. 2007; Shen et al. 2007; Cleland et al. 2011; Hoppins et al. 2011). Thus, mitochondrial connectivity can be altered by inputs impinging on both the division and the fusion machinery to result in effective regulated morphological changes.

1.3 Unique aspects of Mfn2

1.3.1 Mfn2 and Charcot-Marie-Tooth Type 2A

While mitochondrial dysfunction in general is implicated in many diseases, there is a single neurodegenerative disease that is genetically linked to Mfn2, Charcot Marie Tooth syndrome type 2A (CMT2A) (Züchner et al. 2004). This disease is mainly caused by autosomal dominant missense mutations in the *MFN2* gene, although a few nonsense, recessive, or compound heterozygous cases have been reported (Stuppia et al. 2015). CMT2A is a progressive peripheral neuropathy of the distal motor neurons that leads to weakness, sensory loss, gait impairment and foot deformations (Gemignani and Marbini 2001). Mutations that cause CMT2A have been reported throughout the gene, complicating the assignment of the etiology of CMT phenotypes to one domain or function of Mfn2. However, when these mutations are mapped onto a predicted structure of Mfn2, it appears that certain areas of the protein contain more concentrated mutations (<5 bp between CMT2A alleles). These regions include sections of the GTPase domain, a section of HB1 (mutations in all three helices in the same short length of the

helix), and the region immediately abutting and including the loops that connect HB1 to HB2 (Figure 1.3).

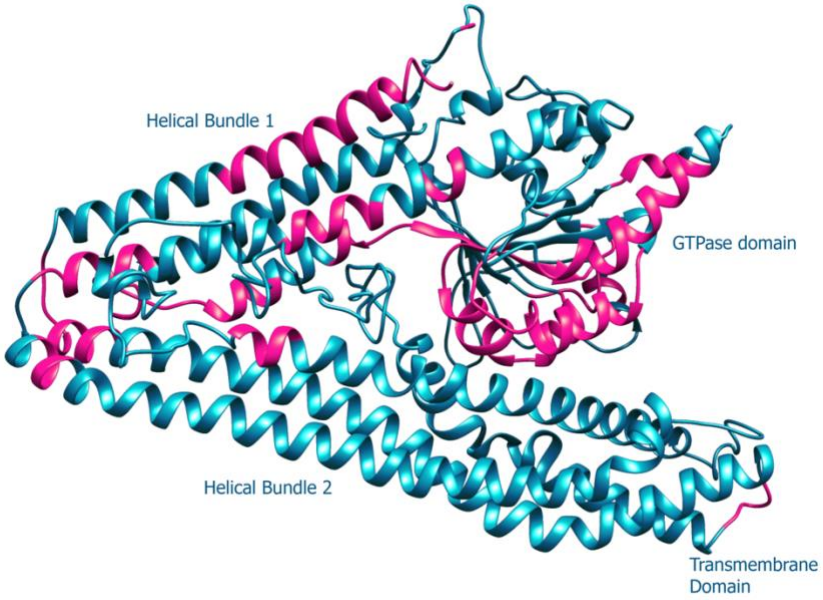

Figure 1.3. Model of Mfn2 structure with areas of concentrated CMT2A mutations highlighted.
Areas of concentrated CMT2A mutations ("hotspots") are defined as less than 5 base pairs between reported mutations and are shown in pink.

Patient biopsies suggest the mitochondrial origin of CMT2A may be due to a defect in transport of the mitochondria through the axons along with mitochondria dysfunction and morphological changes (Baloh et al. 2007; Vallat et al. 2008; Calvo et al. 2009; Cartoni and Martinou 2009). However, mechanistic understanding of the disease has been difficult to achieve as disease models of CMT2A caused by Mfn2 mutations have generally failed to fully recapitulate the defects seen in patients. A mouse model of a GTPase domain mutation (T105M) expressed in motor neurons resulted in CMT2A-like phenotypes of reduced number of axons and muscle mass (Detmer et al. 2008). However, this required homozygous expression of the transgene and was present from birth rather than presenting as a degenerative disease. Another mouse model

using a different disease-associated allele (R94Q) reported phenotypes that more closely resemble patients in both motor ability and mitochondrial location in axons (Cartoni et al. 2010). The limitation of this model is that it still relies on overexpression of the mutant allele in neurons. A knock-in model at the same location but with a different mutant allele (R94W) displayed mild neuropathy symptoms rather than the severe CMT phenotype of patients with this mutation (Strickland et al. 2014). Because both patient biopsies and murine models fail to define how Mfn2 mutations lead to disease, understanding the mechanics of how Mfn2 works is likely an important step in understanding and treating CMT2A.

1.3.2 Non-fusion roles of Mfn2

In addition to the observation that mutations in Mfn2 but not Mfn1 lead to CMT2A, there have been reports that Mfn2 is unique from Mfn1 in having multiple roles aside from mitochondrial fusion. Mfn2 has been reported to tether mitochondria to endoplasmic reticulum (de Brito and Scorrano 2008), but this report has been questioned by other studies that suggest an increase of ER-mitochondria contacts when Mfn2 is deleted (Filadi et al. 2015). Mfn2 is also an inhibitor of cell proliferation in normal and cancerous cells (K.-H. Chen et al. 2004; Chen et al. 2014; Xu et al. 2017). There are numerous other functions that have been reported for Mfn2 with varying levels of evidence. Because of its broad role in cellular function and its association with disease, increasing our understanding of the mechanisms by which this protein works could inform scientists in multiple fields.

1.4 References

Atkins K, Dasgupta A, Chen K, Mewburn J, Archer SL. 2016. The role of Drp1 adaptor proteins MiD49 and MiD51 in mitochondrial fission : implications for human disease. :1861–1874. doi:10.1042/CS20160030.

Baloh RH, Schmidt RE, Pestronk A, Milbrandt J. 2007. Altered axonal mitochondrial transport in the pathogenesis of Charcot-Marie-Tooth disease from mitofusin 2 mutations. *J Neurosci*. 27(2):422–430. doi:10.1523/JNEUROSCI.4798-06.2007.

Bian X, Xu J, Zhao H, Zheng Q, Xiao X, Ma X, Li Y, Du X, Liu X. 2019. Zinc-Induced SUMOylation of Dynamin-Related Protein 1 Protects the Heart against Ischemia-Reperfusion Injury. *Oxid Med Cell Longev*. 2019:1–11. doi:10.1155/2019/1232146.

Brandt T, Cavellini L, Kühlbrandt W, Cohen MM. 2016. A mitofusin-dependent docking ring complex triggers mitochondrial fusion in vitro. *Elife*. 5:1–23. doi:10.7554/eLife.14618.

de Brito OM, Scorrano L. 2008. Mitofusin 2 tethers endoplasmic reticulum to mitochondria. *Nature*. 456(7222):605–10. doi:10.1038/nature07534.

Cairns RA, Harris IS, Mak TW. 2011. Regulation of cancer cell metabolism. *Nat Rev Cancer*. 11(2):85–95. doi:10.1038/nrc2981.

Calvo J, Funalot B, Ouvrier R a, Lazaro L, Toutain A, De Mas P, Bouche P, Gilbert-Dussardier B, Arne-Bes M-C, Carrière J-P, et al. 2009. Genotype-phenotype correlations in Charcot-Marie-Tooth disease type 2 caused by mitofusin 2 mutations. *Arch Neurol*. 66(12):1511–1516. doi:10.1001/archneurol.2009.284.

Cao Y-L, Meng S, Chen Y, Feng J-X, Gu D-D, Yu B, Li Y-J, Yang J-Y, Liao S, Chan DC, et al. 2017. MFN1 structures reveal nucleotide-triggered dimerization critical for mitochondrial fusion. *Nature*.:1–5. doi:10.1038/nature21077.

Cartoni R, Arnaud E, Médard JJ, Poirot O, Courvoisier DS, Chrast R, Martinou JC. 2010. Expression of mitofusin 2R94Q in a transgenic mouse leads to Charcot-Marie-Tooth neuropathy type 2A. *Brain*. 133(5):1460–1469. doi:10.1093/brain/awq082.

Cartoni R, Martinou JC. 2009. Role of mitofusin 2 mutations in the physiopathology of Charcot-Marie-Tooth disease type 2A. *Exp Neurol*. 218(2):268–273. doi:10.1016/j.expneurol.2009.05.003.

Celardo I, Martins LM, Gandhi S. 2014. Unravelling mitochondrial pathways to Parkinson's disease. *Br J Pharmacol*. 171(8):1943–1957. doi:10.1111/bph.12433.

Chandel NS, Maltepe E, Goldwasser E, Mathieu CE, Simon MC, Schumacker PT. 1998. Mitochondrial reactive oxygen species trigger hypoxia-induced transcription. *Proc Natl Acad Sci U S A*. 95(September):11715–11720.

Chappie JS, Acharya S, Liu Y-W, Leonard M, Pucadyil TJ, Schmid SL. 2009. An Intramolecular Signaling Element that Modulates Dynamin Function In Vitro and In Vivo. *Mol Biol Cell*. 20:3561–3571. doi:10.1091/mbc.E09.

Chen H, Detmer SA, Ewald AJ, Griffin EE, Fraser SE, Chan DC. 2003. Mitofusins Mfn1 and Mfn2 coordinately regulate mitochondrial fusion and are essential for embryonic development. *J Cell Biol*. 160:189–200. doi:10.1083/jcb.200211046.

Chen K-H, Guo X, Ma D, Guo Y, Li Q, Yang D, Li P, Qiu X, Wen S, Xiao R-P, et al. 2004. Dysregulation of HSG triggers vascular proliferative disorders. *Nat Cell Biol*. 6(9):872–883. doi:10.1038/ncb1161.

Chen KH, Dasgupta A, Ding J, Indig FE, Ghosh P, L. Longo D. 2014. Role of mitofusin 2 (Mfn2) in controlling cellular proliferation. *FASEB J*. 28(1):382–394. doi:10.1096/fj.13-230037.

Chen KH, Guo X, Ma D, Guo Y, Li Q, Yang D, Li P, Qiu X, Wen S, Xiao RP, et al. 2004. Dysregulation of HSG triggers vascular proliferative disorders. *Nat Cell Biol*. 6(9):872–883. doi:10.1038/ncb1161.

Chen Y, Dorn GW. 2013. PINK1-Phosphorylated Mitofusin 2 is a Parkin Receptor for Culling Damaged Mitochondria. *Science (80-)*. 340(April):471–476.

Cleland MM, Norris KL, Karbowski M, Wang C, Suen D-F, Jiao S, George NM, Luo X, Li Z, Youle RJ. 2011. Bcl-2 family interaction with the mitochondrial morphogenesis machinery. *Cell*

Death Differ. 18(2):235–247. doi:10.1038/cdd.2010.89.

Cribbs JT, Strack S. 2007. Reversible phosphorylation of Drp1 by cyclic AMP-dependent protein kinase and calcineurin regulates mitochondrial fission and cell death. *EMBO Rep*. 8(10):939–944. doi:10.1038/sj.embor.7401062.

Delaunay A, Isnard AD, Toledano MB. 2000. H2O2 sensing through oxidation of the Yap1 transcription factor. *EMBO J*. 19(19):5157–5166. doi:10.1093/emboj/19.19.5157.

Detmer Scott A, Chan DC. 2007a. Complementation between mouse Mfn1 and Mfn2 protects mitochondrial fusion defects caused by CMT2A disease mutations. *J Cell Biol*. 176(4):405–14. doi:10.1083/jcb.200611080.

Detmer Scott A, Chan DC. 2007b. Functions and dysfunctions of mitochondrial dynamics. *Nat Rev Mol Cell Biol*. 8(november):870–879. doi:10.1038/nrm2275.

Detmer Scott A., Chan DC. 2007. Complementation between mouse Mfn1 and Mfn2 protects mitochondrial fusion defects caused by CMT2A disease mutations. *J Cell Biol*. 176(4):405–414. doi:10.1083/jcb.200611080.

Detmer SA, Velde C Vande, Cleveland DW, Chan DC. 2008. Hindlimb gait defects due to motor axon loss and reduced distal muscles in a transgenic mouse model of Charcot - Marie - Tooth type 2A. *Hum Mol Genet*. 17(3):367–375. doi:10.1093/hmg/ddm314.

Du C, Fang M, Li Y, Li L, Wang X. 2000. Smac, a Mitochondrial Protein that Promotes Cytochrome c-Dependent Caspase Activation by Eliminating IAP Inhibition Hid, and Grim in terms of IAP neutralization and is the. *Cell*. 102:33–42.

Ekman D, Björklund ÅK, Frey-Skött J, Elofsson A. 2005. Multi-domain proteins in the three kingdoms of life: Orphan domains and other unassigned regions. *J Mol Biol*. 348(1):231–243. doi:10.1016/j.jmb.2005.02.007.

Engelhart EA, Hoppins S. 2019. A catalytic domain variant of Mitofusin requiring a wildtype paralog for function uncouples mitochondrial outer-membrane tethering and fusion. *J Biol Chem*. 1(8):jbc.RA118.006347. doi:10.1074/jbc.RA118.006347.

Ernster L, Schatz G. 1981. Mitochondria : A Historical Review. 91(December).

Eura Y. 2003. Two Mitofusin Proteins, Mammalian Homologues of FZO, with Distinct Functions Are Both Required for Mitochondrial Fusion. *J Biochem*. 134(3):333–344. doi:10.1093/jb/mvg150.

Federico A, Cardaioli E, Da Pozzo P, Formichi P, Gallus GN, Radi E. 2012. Mitochondria, oxidative stress and neurodegeneration. *J Neurol Sci*. 322(1–2):254–262. doi:10.1016/j.jns.2012.05.030.

Feely SME, Laura M, Siskind CE, Sottile S, Davis M, Gibbons VS, Reilly MM, Shy ME. 2011. MFN2 mutations cause severe phenotypes in most patients with CMT2A. *Neurology*. 76(20):1690–6. doi:10.1212/WNL.0b013e31821a441e.

Ferreira JCB, Campos JC, Qvit N, Qi X, Bozi LHM, Bechara LRG, Lima VM, Queliconi BB, Disatnik MH, Dourado PMM, et al. 2019. A selective inhibitor of mitofusin 1-βIIPKC association improves heart failure outcome in rats. *Nat Commun*. 10(1). doi:10.1038/s41467-018-08276-6.

Filadi R, Greotti E, Turacchio G, Luini A, Pozzan T, Pizzo P. 2015. Mitofusin 2 ablation increases endoplasmic reticulum–mitochondria coupling. *Proc Natl Acad Sci*. doi:10.1073/pnas.1504880112.

Franco A, Kitsis RN, Fleischer JA, Gavathiotis E, Kornfeld OS, Gong G, Biris N, Benz A, Qvit N, Donnelly SK, et al. 2016. Correcting mitochondrial fusion by manipulating mitofusin conformations. *Nature*.:1–20. doi:10.1038/nature20156.

Fransson Å, Ruusala A, Aspenström P. 2006. The atypical Rho GTPases Miro-1 and Miro-2 have essential roles in mitochondrial trafficking. *Biochem Biophys Res Commun*. 344(2):500–510. doi:10.1016/j.bbrc.2006.03.163.

Ganesan V, Willis SD, Chang KT, Beluch S, Cooper KF, Strich R. 2019. Cyclin C directly stimulates Drp1 GTP affinity to mediate stress-induced mitochondrial hyperfission. *Mol Biol Cell*. 30(3):302–311. doi:10.1091/mbc.E18-07-0463.

Gawlowski T, Suarez J, Scott B, Torres-Gonzalez M, Wang H, Schwappacher R, Han X, Yates JR,

Hoshijima M, Dillmann W. 2012. Modulation of dynamin-related protein 1 (DRP1) function by increased O-linked-β-N-acetylglucosamine modification (O-GlcNAc) in cardiac myocytes. *J Biol Chem*. 287(35):30024–30034. doi:10.1074/jbc.M112.390682.

Gemignani F, Marbini A. 2001. Charcot-Marie-Tooth disease (CMT): Distinctive phenotypic and genotypic features in CMT type 2. *J Neurol Sci*. 184(1):1–9. doi:10.1016/S0022-510X(00)00497-4.

Giarmarco MM, Cleghorn WM, Sloat SR, Hurley JB, Brockerhoff SE. 2017. Mitochondria Maintain Distinct Ca 2+ Pools in Cone Photoreceptors . *J Neurosci*. 37(8):2061–2072. doi:10.1523/jneurosci.2689-16.2017.

Gilbert HF. 1995. Thiol-Disulfide Exchange Equilibria and Bond Stability. *Methods Enzymol*. 251:8–28.

Giustarini D, Colombo G, Garavaglia ML, Astori E, Portinaro NM, Reggiani F, Badalamenti S, Aloisi AM, Santucci A, Rossi R, et al. 2017. Assessment of glutathione/glutathione disulphide ratio and S-glutathionylated proteins in human blood, solid tissues, and cultured cells. *Free Radic Biol Med*. 112(August):360–375. doi:10.1016/j.freeradbiomed.2017.08.008.

Giustarini D, Dalle-Donne I, Tsikas D, Rossi R. 2009. Oxidative stress and human diseases: Origin, link, measurement, mechanisms, and biomarkers. *Crit Rev Clin Lab Sci*. 46(5–6):241–281. doi:10.3109/10408360903142326.

Gomes LC, Benedetto G Di, Scorrano L. 2011. During autophagy mitochondria elongate, are spared from degradation and sustain cell viability. *Nat Cell Biol*. 13(5):589–598. doi:10.1038/ncb2220.

Grek CL, Zhang J, Manevich Y, Townsend DM, Tew KD. 2013. Causes and consequences of cysteine s-glutathionylation. *J Biol Chem*. 288(37):26497–26504. doi:10.1074/jbc.R113.461368.

Griffin EE, Chan DC. 2006. Domain interactions within Fzo1 oligomers are essential for mitochondrial fusion. *J Biol Chem*. 281(24):16599–606. doi:10.1074/jbc.M601847200.

Guo C, Hildick KL, Luo J, Dearden L, Wilkinson KA, Henley JM. 2013. SENP3-mediated

deSUMOylation of dynamin-related protein 1 promotes cell death following ischaemia. *EMBO J*. 32(11):1514–1528. doi:10.1038/emboj.2013.65.

Guo X, Chen KH, Guo Y, Liao H, Tang J, Xiao RP. 2007. Mitofusin 2 triggers vascular smooth muscle cell apoptosis via mitochondrial death pathway. *Circ Res*. 101(11):1113–1122. doi:10.1161/CIRCRESAHA.107.157644.

Han X, Lu Y, Li S, Kaitsuka T, Sato Y, Tomizawa K, Nairn AC, Takei K, Matsui H, Matsushita M. 2008. JCB : ARTICLE. 182(3):573–585. doi:10.1083/jcb.200802164.

Harder Z, Zunino R, McBride H. 2004. Sumo1 conjugates mitochondrial substrates and participates in mitochondrial fission. *Curr Biol*. 14(4):340–345. doi:10.1016/S0960-9822(04)00084-3.

Hoppins S, Edlich F, Cleland MM, Banerjee S, McCaffery JM, Youle RJ, Nunnari J. 2011. The Soluble Form of Bax Regulates Mitochondrial Fusion via MFN2 Homotypic Complexes. *Mol Cell*. 41(2):150–160. doi:10.1016/j.molcel.2010.11.030.

Horbay R, Bilyy R. 2016. Mitochondrial dynamics during cell cycling. *Apoptosis*. 21(12):1327–1335. doi:10.1007/s10495-016-1295-5.

Iqbal S, Hood DA. 2014. Oxidative stress-induced mitochondrial fragmentation and movement in skeletal muscle myoblasts. *Am J Physiol - Cell Physiol*. 306(12):1176–1183. doi:10.1152/ajpcell.00017.2014.

Ishihara N, Eura Y, Mihara K. 2004. Mitofusin 1 and 2 play distinct roles in mitochondrial fusion reactions via GTPase activity. *J Cell Sci*. 117(26):6535–6546. doi:10.1242/jcs.01565.

James SJ, Rose S, Melnyk S, Jernigan S, Blossom S, Pavliv O, Gaylor DW. 2009. Cellular and mitochondrial glutathione redox imbalance in lymphoblastoid cells derived from children with autism. *FASEB J*. 23(8):2374–2383. doi:10.1096/fj.08-128926.

Jendrach M, Mai S, Pohl S, Vöth M, Bereiter-Hahn J. 2008. Short- and long-term alterations of mitochondrial morphology, dynamics and mtDNA after transient oxidative stress. *Mitochondrion*. 8(4):293–304. doi:10.1016/j.mito.2008.06.001.

Jimah JR, Hinshaw JE. 2019. Structural Insights into the Mechanism of Dynamin Superfamily Proteins. *Trends Cell Biol*. 29(3):257–273. doi:10.1016/j.tcb.2018.11.003.

Karbowski M, Lee Y, Gaume B, Jeong S, Frank S, Nechushtan A, Santel A, Fuller M, Smith CL, Youle RJ. 2002. Spatial and temporal association of Bax with during apoptosis. 159(6):931–938. doi:10.1083/jcb.200209124.

Karbowski M, Norris KL, Cleland MM, Jeong S-Y, Youle RJ. 2006. Role of Bax and Bak in mitochondrial morphogenesis. *Nature*. 443(October):658–662. doi:10.1038/nature05111.

Kim YM, Youn SW, Sudhahar V, Das A, Chandhri R, Cuervo Grajal H, Kweon J, Leanhart S, He L, Toth PT, et al. 2018. Redox Regulation of Mitochondrial Fission Protein Drp1 by Protein Disulfide Isomerase Limits Endothelial Senescence. *Cell Rep*. 23(12):3565–3578. doi:10.1016/j.celrep.2018.05.054.

Koshiba T, Detmer S a, Kaiser JT, Chen H, McCaffery JM, Chan DC. 2004. Structural basis of mitochondrial tethering by mitofusin complexes. *Science*. 305(5685):858–862. doi:10.1126/science.1099793.

Kosower NS, Kosower EM, Wertheim B, Correa WS. 1969. Diamide, a new reagent for the intracellular oxidation of glutathione to the disulfide. *Biochem Biophys Res Commun*. 37(4):593–596. doi:10.1016/0006-291X(69)90850-X.

Koutsopoulos OS, Laine D, Osellame L, Chudakov DM, Parton RG, Frazier AE, Ryan MT. 2010. Human Miltons associate with mitochondria and induce microtubule-dependent remodeling of mitochondrial networks. *Biochim Biophys Acta - Mol Cell Res*. 1803(5):564–574. doi:10.1016/j.bbamcr.2010.03.006.

Labbé K, Murley A, Nunnari J. 2014. Determinants and Functions of Mitochondrial Behavior. *Annu Rev Cell Dev Biol*. 30(1):357–391. doi:10.1146/annurev-cellbio-101011-155756.

Lebeau J, Saunders JM, Moraes VWR, Madhavan A, Madrazo N, Anthony MC, Wiseman RL. 2018. The PERK Arm of the Unfolded Protein Response Regulates Mitochondrial Morphology during Acute Endoplasmic Reticulum Stress. *Cell Rep*. 22(11):2827–2836.

doi:10.1016/j.celrep.2018.02.055.

Lee D, Redfern O, Orengo C. 2007. Predicting protein function from sequence and structure. *Nat Rev Mol Cell Biol*. 8(12):995–1005. doi:10.1038/nrm2281.

Lee J-Y, Kapur M, Li M, Choi M-C, Choi S, Kim H-J, Kim I, Lee E, Taylor JP, Yao T-P. 2014. MFN1 deacetylation activates adaptive mitochondrial fusion and protects metabolically challenged mitochondria. *J Cell Sci*. 127(22):4954–4963. doi:10.1242/jcs.157321.

Liu J, Noel JK, Low HH. 2018. Structural basis for membrane tethering by a bacterial dynamin-like pair. *Nat Commun*. 9(1):1–12. doi:10.1038/s41467-018-05523-8.

Liu X, Kim CN, Yang J, Jemmerson R, Wang X. 1996. Induction of Apoptotic Program in Cell-Free Extracts: Requirement for dATP and Cytochrome C. *Cell*. 86(July):147–157.

Loson OC, Song Z, Chen H, Chan DC. 2013. Fis1, Mff, MiD49, and MiD51 mediate Drp1 recruitment in mitochondrial fission. *Mol Biol Cell*. 24(5):659–667. doi:10.1091/mbc.e12-10-0721.

Low HH, Löwe J. 2006. A bacterial dynamin-like protein. *Nature*. 444(7120):766–769. doi:10.1038/nature05312.

Low HH, Sachse C, Amos LA, Löwe J. 2009. Structure of a Bacterial Dynamin-like Protein Lipid Tube Provides a Mechanism For Assembly and Membrane Curving. *Cell*. 139(7):1342–1352. doi:10.1016/j.cell.2009.11.003.

Mattie S, Riemer J, Wideman JG, McBride HM. 2018. A new mitofusin topology places the redox-regulated C terminus in the mitochondrial intermembrane space. *J Cell Biol*. 217(2):507–515. doi:10.1083/jcb.201611194.

McLelland GL, Goiran T, Yi W, Dorval G, Chen CX, Lauinger ND, Krahn AI, Valimehr S, Rakovic A, Rouiller I, et al. 2018. Mfn2 ubiquitination by PINK1/parkin gates the p97-dependent release of ER from mitochondria to drive mitophagy. *Elife*. 7:1–35. doi:10.7554/eLife.32866.

Mears JA, Lackner LL, Fang S, Ingerman E, Nunnari J, Hinshaw JE. 2011. Conformational changes in Dnm1 support a contractile mechanism for mitochondrial fission. *Nat Struct Mol*

Biol. 18(1):20–27. doi:10.1038/nsmb.1949.

Mishra P, Chan DC. 2014. Mitochondrial dynamics and inheritance during cell division, development and disease. *Nat Rev Mol Cell Biol*. 15(10):634–646. doi:10.1038/nrm3877.

Mitra K, Wunder C, Roysam B, Lin G, Lippincott-Schwartz J. 2009. A hyperfused mitochondrial state achieved at G1-S regulates cyclin E buildup and entry into S phase. *Proc Natl Acad Sci*. 106(29):11960–11965. doi:10.1073/pnas.0904875106.

Olichon A, Baricault L, Gas N, Guillou E, Valette A, Belenguer P, Lenaers G. 2003. Loss of OPA1 perturbates the mitochondrial inner membrane structure and integrity, leading to cytochrome c release and apoptosis. *J Biol Chem*. 278(10):7743–7746. doi:10.1074/jbc.C200677200.

Ong S-B, Kalkhoran SB, Cabrera-Fuentes H a., Hausenloy DJ. 2015. Mitochondrial fusion and fission proteins as novel therapeutic targets for treating cardiovascular disease. *Eur J Pharmacol*.:1–11. doi:10.1016/j.ejphar.2015.04.056.

Østergaard H, Tachibana C, Winther JR. 2004. Monitoring disulfide bond formation in the eukaryotic cytosol. *J Cell Biol*. 166(3):337–345. doi:10.1083/jcb.200402120.

Otera H, Wang C, Cleland MM, Setoguchi K, Yokota S, Youle RJ, Mihara K. 2010. Mff is an essential factor for mitochondrial recruitment of Drp1 during mitochondrial fission in mammalian cells. *J Cell Biol*. 191(6):1141–1158. doi:10.1083/jcb.201007152.

Pareyson D, Saveri P, Sagnelli A, Piscosquito G. 2015. Mitochondrial dynamics and inherited peripheral nerve diseases. *Neurosci Lett*. 596:66–77. doi:10.1016/j.neulet.2015.04.001.

Park YY, Nguyen OTK, Kang H, Cho H. 2014. MARCH5-mediated quality control on acetylated Mfn1 facilitates mitochondrial homeostasis and cell survival. *Cell Death Dis*. 5(4):e1172-12. doi:10.1038/cddis.2014.142.

Pernas L, Scorrano L. 2015. Mito-Morphosis: Mitochondrial Fusion, Fission, and Cristae Remodeling as Key Mediators of Cellular Function. *Annu Rev Physiol*. 78(1):505–531. doi:10.1146/annurev-physiol-021115-105011.

Picard M, Wallace DC, Burelle Y. 2016. The rise of mitochondria in medicine. *Mitochondrion*.

30:105–116. doi:10.1016/j.mito.2016.07.003.

Pilling AD, Horiuchi D, Lively CM, Saxton WM. 2006. Kinesin-1 and Dynein are the primary motors for fast transport of mitochondria in Drosophila motor axons. *Mol Biol Cell*. 17(April):2057–2068. doi:10.1091/mbc.E05.

Pócsi I, Miskei M, Karányi Z, Emri T, Ayoubi P, Pusztahelyi T, Balla G, Prade RA. 2005. Comparison of gene expression signatures of diamide, H2O2 and menadione exposed Aspergillus nidulans cultures - Linking genome-wide transcriptional changes to cellular physiology. *BMC Genomics*. 6:1–18. doi:10.1186/1471-2164-6-182.

Prudent J, Zunino R, Sugiura A, Mattie S, Shore GC, McBride HM. 2015. MAPL SUMOylation of Drp1 Stabilizes an ER/Mitochondrial Platform Required for Cell Death. *Mol Cell*. 59(6):941–955. doi:10.1016/j.molcel.2015.08.001.

Pyakurel A, Savoia C, Scorrano L, Pyakurel A, Savoia C, Hess D, Scorrano L. 2015. Extracellular Regulated Kinase Phosphorylates Mitofusin 1 to Control Mitochondrial Morphology and Article Extracellular Regulated Kinase Phosphorylates Mitofusin 1 to Control Mitochondrial Morphology and Apoptosis. *Mol Cell*.:1–11. doi:10.1016/j.molcel.2015.02.021.

Qi Y, Yan L, Yu C, Guo X, Zhou X, Hu X, Huang X, Rao Z, Lou Z, Hu J. 2016. Structures of human mitofusin 1 provide insight into mitochondrial tethering.

Rambold AS, Kostelecky B, Elia N, Lippincott-Schwartz J. 2011. Tubular network formation protects mitochondria from autophagosomal degradation during nutrient starvation. *Proc Natl Acad Sci*. 108(25):10190–10195. doi:10.1073/pnas.1107402108.

Redpath CJ, Bou Khalil M, Drozdzal G, Radisic M, McBride HM. 2013. Mitochondrial Hyperfusion during Oxidative Stress Is Coupled to a Dysregulation in Calcium Handling within a C2C12 Cell Model. *PLoS One*. 8(7). doi:10.1371/journal.pone.0069165.

Rocha AG, Franco A, Krezel AM, Rumsey JM, Alberti JM, Knight WC, Biris N, Zacharioudakis E, Janetka JW, Baloh RH, et al. 2018a. MFN2 agonists reverse mitochondrial defects in preclinical models of Charcot-Marie-Tooth disease type 2A. *Science (80-)*. 360(6386):336–341.

doi:10.1126/science.aao1785.

Rocha AG, Franco A, Krezel AM, Rumsey JM, Alberti JM, Knight WC, Biris N, Zacharioudakis E, Janetka JW, Baloh RH, et al. 2018b. MFN2 agonists reverse mitochondrial defects in preclinical models of Charcot-Marie-Tooth disease type 2A. *Science (80-)*. 360(6386):336–341. doi:10.1126/science.aao1785.

Rovira-Llopis S, Bañuls C, Diaz-Morales N, Hernandez-Mijares A, Rocha M, Victor VM. 2017. Mitochondrial dynamics in type 2 diabetes: Pathophysiological implications. *Redox Biol*. 11(January):637–645. doi:10.1016/j.redox.2017.01.013.

Santel a, Fuller MT. 2001. Control of mitochondrial morphology by a human mitofusin. *J Cell Sci*. 114:867–874.

Scorrano L. 2013. Keeping mitochondria in shape: A matter of life and death. *Eur J Clin Invest*. 43(8):886–893. doi:10.1111/eci.12135.

Sena LA, Chandel NS. 2012. Physiological roles of mitochondrial reactive oxygen species. *Mol Cell*. 48(2):158–167. doi:10.1016/j.molcel.2012.09.025.

Shen T, Zheng M, Cao C, Chen C, Tang J, Zhang W, Cheng H, Chen KH, Xiao RP. 2007. Mitofusin-2 is a major determinant of oxidative stress-mediated heart muscle cell apoptosis. *J Biol Chem*. 282(32):23354–23361. doi:10.1074/jbc.M702657200.

SHITARA H, SHIMANUKI M, HAYASHI J-I, YONEKAWA H. 2010. Global Imaging of Mitochondrial Morphology in Tissues Using Transgenic Mice Expressing Mitochondrially Targeted Enhanced Green Fluorescent Protein. *Exp Anim*. 59(1):99–103. doi:10.1538/expanim.59.99.

Shutt T, Geoffrion M, Milne R, McBride HM. 2012. The intracellular redox state is a core determinant of mitochondrial fusion. *EMBO Rep*. 13(10):909–915. doi:10.1038/embor.2012.128.

Shutt TE, McBride HM. 2013. Staying cool in difficult times: Mitochondrial dynamics, quality control and the stress response. *Biochim Biophys Acta - Mol Cell Res*. 1833(2):417–424.

doi:10.1016/j.bbamcr.2012.05.024.

Slater EC, Cleland KW. 1953. The effect of calcium on the respiratory and phosphorylative activities of heart-muscle sarcosomes. *Biochem J*. 55(4):566–580. doi:10.1042/bj0550566.

Slivka A, Spina MB, Cohen G. 1987. Reduced and oxidized glutathione in human and monkey brain. *Neurosci Lett*. 74(1):112–118. doi:10.1016/0304-3940(87)90061-9.

Smirnova E, Griparic L, Shurland D-L, van der Bliek AM. 2001. Dynamin-related Protein Drp1 Is Required for Mitochondrial Division in Mammalian Cells. *Mol Biol Cell*. 12(8):2245–2256. doi:10.1091/mbc.12.8.2245.

Sorrentino V, Menzies KJ, Auwerx J. 2017. Repairing Mitochondrial Dysfunction in Disease. *Annu Rev Pharmacol Toxicol*. 58(1):353–389. doi:10.1146/annurev-pharmtox-010716-104908.

De Stefani D, Rizzuto R, Pozzan T. 2016. Enjoy the Trip: Calcium in Mitochondria Back and Forth. *Annu Rev Biochem*. 85(1):161–192. doi:10.1146/annurev-biochem-060614-034216.

Strickland A V, Rebelo AP, Zhang F, Price J, Bolon B, Silva JP, Wen R, Züchner S. 2014. Characterization of the Mitofusin 2 R94W Mutation in a Knock-in Mouse Model. *J Peripher Nerv Syst*. 164:152–164. doi:10.1111/jns5.12066.

Stuppia G, Rizzo F, Riboldi G, Del Bo R, Nizzardo M, Simone C, Comi GP, Bresolin N, Corti S. 2015. MFN2-related neuropathies: Clinical features, molecular pathogenesis and therapeutic perspectives. *J Neurol Sci*. doi:10.1016/j.jns.2015.05.033.

Suen D, Norris KL, Youle RJ. 2008. Mitochondrial dynamics and apoptosis. (301):1577–1590. doi:10.1101/gad.1658508.GENES.

Sugiura A, Nagashima S, Tokuyama T, Amo T, Matsuki Y, Ishido S, Kudo Y, McBride HM, Fukuda T, Matsushita N, et al. 2013. MITOL regulates endoplasmic reticulum-mitochondria contacts via Mitofusin2. *Mol Cell*. 51(1):20–34. doi:10.1016/j.molcel.2013.04.023.

Susin SA, Zamzami N, Castedo M, Hirsch T, Marchetti P, Macho A, Daugas E, Geuskens M, Kroemer G. 1996. Bcl-2 Inhibits the Mitochondrial Release of an Apoptotic Protease. *J Exp Med*. 184(October):1331–1341.

Suzuki M, Youle RJ, Tjandra N. 2000. Structure of Bax. *Cell*. 103(4):645–654. doi:10.1016/s0092-8674(00)00167-7.

Suzuki Y, Imai Y, Nakayama H, Takahashi K, Takio K, Takahashi R. 2001. A serine protease, HtrA2, is released from the mitochondria and interacts with XIAP, inducing cell death. *Mol Cell*. 8(3):613–621. doi:10.1016/S1097-2765(01)00341-0.

Thaher O, Wolf C, Dey PN, Pouya A, Wüllner V, Tenzer S, Methner A. 2017. The thiol switch C684 in Mitofusin-2 mediates redox-induced alterations of mitochondrial shape and respiration. *Neurochem Int*.:5–11. doi:10.1016/j.neuint.2017.05.009.

Thorpe GW, Fong CS, Alic N, Higgins VJ, Dawes IW. 2004. Cells have distinct mechanisms to maintain protection against different reactive oxygen species: Oxidative-stress-response genes. *Proc Natl Acad Sci*. 101(17):6564–6569. doi:10.1073/pnas.0305888101.

Tondera D, Grandemange S, Jourdain A, Karbowski M, Mattenberger Y, Herzig S, Da Cruz S, Clerc P, Raschke I, Merkwirth C, et al. 2009. SLP-2 is required for stress-induced mitochondrial hyperfusion. *EMBO J*. 28(November 2008):1589–1600. doi:10.1038/emboj.2009.89.

Twig G, Elorza A, Molina AJA, Mohamed H, Wikstrom JD, Walzer G, Stiles L, Haigh SE, Katz S, Las G, et al. 2008. Fission and selective fusion govern mitochondrial segregation and elimination by autophagy. *EMBO J*. 27(2):433–446. doi:10.1038/sj.emboj.7601963.

Vallat J-M, Ouvrier R a, Pollard JD, Magdelaine C, Zhu D, Nicholson G a, Grew S, Ryan MM, Funalot B. 2008. Histopathological findings in hereditary motor and sensory neuropathy of axonal type with onset in early childhood associated with mitofusin 2 mutations. *J Neuropathol Exp Neurol*. 67(11):1097–1102. doi:10.1097/NEN.0b013e31818b6cbc.

Verhagen AM, Ekert PG, Pakusch M, Silke J, Connonlly LM, Reid GE, Moritz RL, Simpson RJ, Vaux DL. 2000. Identification of DIABLO, a Mammalian Protein that Promotes Apoptosis by Binding to and Antagonizing IAP Proteins. *Cell*. 102(1):43–53. doi:10.1016/S0896-6273(00)80282-2.

Verhoeven K, Claeys KG, Züchner S, Schröder JM, Weis J, Ceuterick C, Jordanova A, Nelis E, De

Vriendt E, Van Hul M, et al. 2006. MFN2 mutation distribution and genotype/phenotype correlation in Charcot-Marie-Tooth type 2. *Brain*. 129(8):2093–2102. doi:10.1093/brain/awl126.

Vital A, Vital C. 2012. Mitochondria and peripheral neuropathies. *J Neuropathol Exp Neurol*. 71(12):1036–46. doi:10.1097/NEN.0b013e3182764d47.

Wada J, Nakatsuka A. 2016. Mitochondrial Dynamics and Mitochondrial Dysfunction in Diabetes. *Acta Med Okayama*. 70(3):151–8. doi:10.18926/AMO/54413.

Wallace DC, Fan W, Procaccio V. 2010. Mitochondrial Energetics and Therapeutics. *Annu Rev Pathol Mech Dis*. 5(1):297–348. doi:10.1146/annurev.pathol.4.110807.092314.

Wang C, Youle RJ. 2011. The role of mitochondria in apoptosis. *BMB Rep*. 41(1):11–22. doi:10.5483/bmbrep.2008.41.1.011.

Wang H, Song P, Du L, Tian W, Yue W, Liu M, Li D, Wang B, Zhu Y, Cao C, et al. 2011. Parkin ubiquitinates Drp1 for proteasome-dependent degradation: Implication of dysregulated mitochondrial dynamics in Parkinson disease. *J Biol Chem*. 286(13):11649–11658. doi:10.1074/jbc.M110.144238.

Wang K, Yan R, Cooper KF, Strich R. 2015. Cyclin C mediates stress-induced mitochondrial fission and apoptosis. *Mol Biol Cell*. 26(6):1030–1043. doi:10.1091/mbc.E14-08-1315.

Wang W, Zhang F, Li L, Tang F, Siedlak SL, Fujioka H, Liu Y, Su B, Pi Y, Wang X. 2015. MFN2 couples glutamate excitotoxicity and mitochondrial dysfunction in motor neurons. *J Biol Chem*. 290(1):168–182. doi:10.1074/jbc.M114.617167.

Wemmie JA, Steggerda SM, Moye-Rowley WS. 1997. The Saccharomyces cerevisiae AP-1 protein discriminates between oxidative stress elicited by the oxidants H 2O 2 and diamide. *J Biol Chem*. 272(12):7908–7914. doi:10.1074/jbc.272.12.7908.

Willems P, Wanschers BFJ, Esseling J, Szklarczyk R, Kudla U, Duarte I, Forkink M, Nooteboom M, Swarts H, Gloerich J, et al. 2013. BOLA1 is an aerobic protein that prevents mitochondrial morphology changes induced by glutathione depletion. *Antioxidants Redox Signal*. 18(2):129–

138. doi:10.1089/ars.2011.4253.

Wu S, Zhou F, Zhang Z, Xing D. 2011. Mitochondrial oxidative stress causes mitochondrial fragmentation via differential modulation of mitochondrial fission-fusion proteins. *FEBS J*. 278(6):941–954. doi:10.1111/j.1742-4658.2011.08010.x.

Xiying F, Rajaa H, George A. B. 2013. H2O2-induced mitochondrial fragmentation in C2C12 myocytes. *Free Radic Biol Med*. 18(9):1199–1216. doi:10.1016/j.micinf.2011.07.011.Innate.

Xu K, Chen G, Li X, Wu X, Chang Z, Xu J, Zhu Y, Yin P, Liang X, Dong L. 2017. MFN2 suppresses cancer progression through inhibition of mTORC2/Akt signaling. *Sci Rep*. 7(February):1–13. doi:10.1038/srep41718.

Yan L, Qi Y, Huang X, Yu C, Lan L, Guo X, Rao Z, Hu J, Lou Z. 2018. Structural basis for GTP hydrolysis and conformational change of MFN1 in mediating membrane fusion. *Nat Struct Mol Biol*. 25(3):233–243. doi:10.1038/s41594-018-0034-8.

Yang J, Zhang Y. 2015. I-TASSER server: New development for protein structure and function predictions. *Nucleic Acids Res*. 43(W1):W174–W181. doi:10.1093/nar/gkv342.

Yesylevskyy SO, Kharkyanen VN, Demchenko AP. 2006. Dynamic protein domains: Identification, interdependence, and stability. *Biophys J*. 91(2):670–685. doi:10.1529/biophysj.105.078584.

Yoon Y-S, Yoon D-S, Lim IK, Yoon S-H, Chung H-Y, Rojo M, Malka F, Jou M-J, Martinou J-C, Yoon G. 2006. Formation of Elongated Giant Mitochondria in DFO-Induced Cellular Senescence: Involvement of Enhanced Fusion Process Through Modulation of Fis1. *J Cell Physiol*. 209(1):468–480. doi:10.1002/JCP.

Zahedi A, Phandthong R, Chaili A, Leung S, Omaiye E, Talbot P. 2019. Mitochondrial Stress Response in Neural Stem Cells Exposed to Electronic Cigarettes. *iScience*. 16:250–269. doi:10.1016/j.isci.2019.05.034.

Zhang G-E, Jin H-L, Lin X-K, Chen C, Liu X-S, Zhang Q, Yu J-R. 2013. Anti-tumor effects of mfn2 in gastric cancer. *Int J Mol Sci*. 14:13005–21. doi:10.3390/ijms140713005.

Zhang Y. 2009. I-TASSER: Fully automated protein structure prediction in CASP8. *Proteins Struct Funct Bioinforma*. 77(SUPPL. 9):100–113. doi:10.1002/prot.22588.

Zheng M, Xiao RP. 2010. Role of mitofusin 2 in cardiovascular oxidative injury. *J Mol Med*. 88(10):987–991. doi:10.1007/s00109-010-0675-5.

Zhou Y, Lutz CM, Baloh RH, Zhou Y, Carmona S, Muhammad AKMG, Bell S, Landeros J, Vazquez M, Ho R, et al. 2019. Restoring mitofusin balance prevents axonal degeneration in a Charcot-Marie-Tooth type 2A model Graphical abstract Find the latest version : Restoring mitofusin balance prevents axonal degeneration in a Charcot-Marie-Tooth type 2A model.

Zorov DB, Filburn CR, Klotz LO, Zweier JL, Sollott SJ. 2000. Reactive oxygen species (ROS)-induced ROS release: A new phenomenon accompanying induction of the mitochondrial permeability transition in cardiac myocytes. *J Exp Med*. 192(7):1001–1014. doi:10.1084/jem.192.7.1001.

Züchner S, Mersiyanova I V, Muglia M, Bissar-Tadmouri N, Rochelle J, Dadali EL, Zappia M, Nelis E, Patitucci A, Senderek J, et al. 2004. Mutations in the mitochondrial GTPase mitofusin 2 cause Charcot-Marie-Tooth neuropathy type 2A. *Nat Genet*. 36(5):449–451. doi:10.1038/ng1341.

Chapter 2: Survey of Mfn2 CMT2A-associated variants in three different domains

2.1 Introduction

The majority of eukaryotic proteins are composed of multiple structural protein domains (Ekman et al. 2005). Protein domains are modular, three-dimensional segments that are quasi-independent functional building blocks of proteins (Yesylevskyy, Kharkyanen, and Demchenko 2006). The arrangement and interaction of domains can, to some extent, determine the protein's capabilities as well as assist in the defining of protein families. Structural/functional domains can sometimes be predicted from amino acid sequence and homology, allowing for prediction of structure and/or activity of uncharacterized proteins (Lee, Redfern, and Orengo 2007). For the membrane remodeling family of dynamin-related proteins, defining domains include a nucleotide binding and hydrolysis domain (GTPase domain), a structural helical stalk, and a domain that interacts with membranes, either directly or through adaptor proteins (Figure 1.1) (Jimah and Hinshaw 2019). Family members can have other domains as well. For example, some have a bundle signaling element that regulates the GTPase domain's activity (Chappie et al. 2009).

Mfn2 possesses all three of the defining domains of a membrane remodeling DRP, and also has many additional reported functions aside from mitochondrial membrane remodeling (K.H. Chen et al. 2004; Züchner et al. 2004; Guo et al. 2007; de Brito and Scorrano 2008; Cleland et al. 2011; Xu et al. 2017). I hypothesized that some domains of Mfn2 would contribute to its fusion activity while others would be involved in other Mfn2 functions. Therefore, I decided to characterize mutations predicted to fall in different domains of Mfn2. Within fusion, there are three obvious properties of Mfn2 that could be affected by mutations: mitochondrial tethering, assembly into a fusion competent state, or conformational changes.

Two interaction partners that have been reported for Mfn2 are Mfn1 and the pro-apoptotic protein Bax. Assigning a domain to facilitating the interaction of Mfn2 with either of these proteins would enhance our understanding of the structure/function relationship of Mfn2. Interaction between Mfn2 and Mfn1 or Bax has been shown to increase mitochondrial fusion efficiency of Mfn2 (Hoppins et al. 2011) which is due to a physical interaction between the Mfn2 and either Mfn1 or Bax (other refs showing Mfn1/2 interaction) (H. Chen et al. 2003; Eura 2003; Ishihara, Eura, and Mihara 2004; Koshiba et al. 2004; Cleland et al. 2011). I hypothesized that at least one of the domains I decided to study might impact the ability of Mfn2 to interact with Mfn1 and/or Bax.

2.2 Methods and Materials

2.2.1 Cell line generation

Mouse Mfn2 cDNA fused to a FLAG epitope tag was inserted into pBABE-hygro (Addgene #1765) multiple cloning site by restriction enzyme digest. Mutations were introduced to the Mfn2 retroviral vector by PCR-based site directed mutagenesis followed by Gibson assembly or restriction enzyme digest followed by ligation. Plasmids were transfected into retroviral packaging PlatE cells (Cell Biolabs) by FuGENE™ HD transfection reagent (Promega). Viral supernatant was applied to Mfn2-null mouse embryonic fibroblasts (MEFs) at 48 and 72 hours post transfection in the presence of 8 mg/ml polybrene. Approximately 24 hours after the final infection, cells that incorporated the plasmid were selected by addition of 200 μg/mL hygromycin to the media for 2-3 days.

Cells expressing the plasmid were plated at low density and clusters of cells each derived from a single cell were collected onto sterile filter paper dots soaked in trypsin and expanded. After expansion, cells were lysed in RIPA buffer (25 mM Tris-HCl pH 7.6; 150 mM NaCl; 1% NP-40;

1% sodium deoxycholate; 0.1% SDS) and the lysate was separated by SDS-PAGE and transferred to nitrocellulose membrane. The membrane was then probed with anti-Mfn2 antibody to determine the expression level of Mfn2. Tubulin was used as a loading control to compare MFn2 expression levels to that of wild type cells. Cells expressing Mfn2-FLAG at .8-3x of wild type were selected for further characterization.

2.2.2 Western blot

Samples were run on an SDS-PAGE gel and transferred onto nitrocellulose at 100 V for 50 minutes in 1X transfer buffer (25 mM Tris, 192 mM glycine, 20% methanol). Membranes were blocked in 4% milk for at least 45 minutes and were probed with anti-Mfn1, anti-Mfn2 (Sigma), anti-EIF2a (Cell Signaling Technology), anti-phospho-EIF2a (Cell Signaling Technology), anti-Caspase 3 (Cell Signaling Technology), or anti-αTubulin (Invitrogen) antibody for 4 hours at room temperature or overnight at 4°C. Membranes were incubated with DyLight secondary antibody (Invitrogen) at room temperature for 1 hour. Membranes were imaged on LI-COR Imaging System (LI-COR Biosciences).

2.2.3 Microscopy

All cells were plated in No. 1.5 glass-bottomed dishes (MatTek). Mouse embryonic fibroblasts were incubated with 0.1 μg/mL Mitotracker Red CMX Ros (Invitrogen) for 15 minutes at 37°C with 5% CO_2, washed and incubated with complete media for at least 45 minutes prior to imaging. MEFs were imaged at 37°C. A Z-series with a step size of 0.3 μm was collected with a Nikon Ti-E widefield microscope with a 63X NA 1.4 oil objective (Nikon), a solid-state light source (Spectra X, Lumencor), and an sCMOS camera (Zyla 5.5 Megapixel). Each cell line was imaged by a blinded researcher on at least three separate occasions (n > 100 cells per experiment).

2.2.4 Morphology image analysis

Images were deconvolved using 8-15 iterations of 3D Landweber deconvolution by Nikon Elements software. Deconvolved images of mitochondrial morphology were then scored as follows: reticular indicates that fewer than 30% of the mitochondria in the cell were fragments (fragments defined as mitochondria less than 2.5 μm in length); fragmented indicates that most of the mitochondria in the cell were less than 2 μm in length. Maximum intensity projections were created using Photoshop (Adobe).

2.2.5 Tethering construct assay

Hela cells were plated in No. 1.5 glass-bottomed dishes (MatTek). The day before imaging, the cells were transfected with 1μg Mfn2 ΔGTPase DNA (pBABE-hygro vector) and 1μg mitoCFP (pBABE-puro vector) DNA for visualization using Lipofectamine 3000® (Thermo Fisher). 24-48 hours after transfection, cells were imaged as described in the "*Microscopy*" section.

2.2.6 Co-immunoprecipitation

For each sample, approximately 10_7 cells were collected, pelleted, and rinsed with phosphate buffered saline (PBS). Pellets were then resuspended in 1 mL of lysis buffer (50 mM Tris pH 7.5; 150 mM NaCl; 1mM $MgCl_2$; 1% IGEPAL-CA-630; 5% glycerol, 1X HALT protease inhibitor cocktail (Fisher Scientific)) and incubated for 5 minutes on ice. The lysate was cleared by centrifugation at 4000 x g for 15 min at 4°C and the supernatant was transferred to a new tube. Lysate was bound to anti-FLAG conjugated magnetic beads (Miltenyi Biotec, Inc.) on ice for 30 minutes. Lysates were bound to equilibrated columns (Miltenyi Biotec, Inc.) and washed 3x with wash buffer 1 (50 mM Tris pH 7.5; 150 mM NaCl; 1mM $MgCl_2$; 0.05% IGEPAL-CA-630; 5% glycerol) and 2x with wash buffer 2 (50 mM Tris pH 7.5; 150 mM NaCl; 1mM $MgCl_2$; 5%

glycerol). Immunoprecipitate was eluted from the columns with Laemmli buffer (0.06 M Tris-HCl pH 6.8; 2.5% SDS; 5% beta mercaptoethanol; 5% sucrose; 0.004% bromophenol blue). Samples of the total (1.5%), soluble (1.5%), flow through (1.5%), first wash (1.5%), and elution (50%) were separated by SDS-PAGE and transferred to nitrocellulose membrane for immunoblotting.

2.2.7 Sucrose gradients

For each genotype, 15 cm plates of MEFs were grown to ~90% confluency. Cells were harvested by trypsin dissociation, pelleted, and washed in mitochondrial isolation buffer (MIB) (0.2 M sucrose, 10 mM Tris-MOPS [pH 7.4], 1 mM EGTA). The cell pellet was resuspended in one cell pellet volume of cold MIB, and cells were homogenized by 12 to 15 strokes on ice with a Kontes Potter-Elvehjem tissue grinder set at 400 RPM. The homogenate was centrifuged (500 × *g*, 5 min, 4°C) to remove nuclei and unbroken cells, and homogenization of the pellet fraction was repeated followed by centrifugation at 500 × *g*, 5 min, 4°C. The supernatant fractions were combined and centrifuged again at 500 × *g*, 5 min, 4°C to remove remaining debris. The supernatant was transferred to a clean microfuge tube and centrifuged (7400 × *g*, 10 min, 4°C) to pellet a crude mitochondrial fraction. The pellet was suspended in one pellet volume MIB and the concentration of mitochondrial proteins was determined by Bradford assay. Isolated mitochondria were frozen at -80°C.

To set up gradients, 2.5 ml 20% or 25% sucrose and 2.5 mL 5% sucrose in gradient buffer (20 mM HEPES-KOH pH 7.4; 50 mM NaCl; 2.5 mM $MgCl_2$; 0.1 mM EDTA; 0.02% digitonin) were layered in an ultracentrifuge tube and sealed with parafilm. A gradient was created by setting the tubes horizontally for two hours at room temperature and then vertically for 1 hour at 4°C. Crude mitochondria (100μg) were lysed with 1.5% digitonin in gradient buffer and layered on top of the gradients. A marker cocktail (GE Healthcare) was layered on an additional gradient

for sizing. Gradients were centrifuged in an ultracentrifuge at 100,000 x g for 16 hours at 4°C. 525 μL fractions were collected and concentrated by 12.5% TCA precipitation. Samples were reconstituted in 1x Laemmli buffer and separated by SDS-PAGE and immunoblotted for Mfn2.

2.2.8 Evaluation of endoplasmic reticulum stress response

Mouse embryonic fibroblasts in 10 cm tissue culture dishes were treated with 1μM thapsigargin for the indicated time. After ER stress treatment, cells were rinsed in PBS and lysed in 200 μL lysis buffer (20 mM Tris-HCl pH 7.6, 150 mM NaCl, 1 mM EDTA, 1 mM EGTA, 1% TritonX-100, 1X Halt Protease Inhibitor Cocktail, ETDA-Free [Thermo Scientific]) for 5 minutes. Cell lysates were collected by cell scraping and sonicated for 2-3 seconds. Lysates were cleared by centrifugation at 15.000 x g for 5 minutes at 4°C. The supernatant was moved to a clean tube and flash frozen in liquid nitrogen and stored at -80°C.

2.2.9 Plasmids & primers

The following plasmids were purchased from Addgene: pBABE-hygro (#1765) and pBABE-puro (#1764). The following primers were used for restriction enzyme digest followed by in gel ligation (RE) or site directed mutagenesis (SDM):

$Mfn2_{Q45R}$ F: (5' – ATCAATGGAATCTTTGAGCGGCTGGGGGCCTACATCC – 3') (RE)

$Mfn2_{Q45R}$ R: (5' – TCTCTTGGATGTAGGCCCCCAGCCGCTCAAAGATTCCATTGATC – 3') (RE)

$Mfn2_{V69F}$ F: (5' – AACACAGAACTGGACCCGTTTACCACGGAAGAGCAGG – 3') (RE)

$Mfn2_{V69F}$ R: (5' – TGCTCTTCCGTGGTAAACGGGTCCAGTTCTGTGTTC – 3') (RE)

$Mfn2_{L76P}$ F: (5' – TTACCACGGAAGAGCAGGTCCCGGACGTCAAAGGGTACCTGTCC – 3') (SDM)

$Mfn2_{L76P}$ R: (5' – GGACAGGTACCCTTTGACGTCCGGGACCTGCTCTTCCGTGGTAA – 3') (SDM)

$Mfn2_{R94Q}$ F: (5' – ATCAGCGAAGTGCTGGCCCAGCGGCACATGAAGGTGG – 3') (SDM)

$Mfn2_{R94Q}$ R: (5' – CCACCTTCATGTGCCGCTGGGCCAGCACTTCGCTGAT – 3') (SDM)

Mfn2$_{K98E}$ F: (5’ – TGGCCAGGCGGCACATGGAGGTGGCTTTTTTTGGCCGG – 3’) (SDM)

Mfn2$_{K98E}$ R: (5’ – TCGTCCGGCCAAAAAAAGCCACCTCCATGTGCCGCCTGGCCAG – 3’) (SDM)

Mfn2$_{H361Y}$ F: (5’ – CCAAATTTGAGCAGTACACAGTCCGGGCC – 3’) (SDM)

Mfn2$_{H361Y}$ R: (5’ – GGCCCGGACTGTGTACTGCTCAAATTTGG – 3’) (SDM)

Mfn2$_{C390R}$ F: (5’ – GAGCAGCGGGTTTATCGCCTAGAAATGCGG – 3’) (SDM)

Mfn2$_{C390R}$ R: (5’ – CCGCATTTCTAGGCGATAAACCCGCTGCTC – 3’) (SDM)

Mfn2$_{P456L}$ F: (5’ – GGACTTCCACCCATCCCTAGTTGTCCTCAAGG – 3’) (SDM)

Mfn2$_{P456L}$ R: (5’ – CCTTGAGGACAACTAGGGATGGGTGGAAGTCC – 3’) (SDM)

Mfn2$_{L710P}$ F: (5’ – GACATCACCCGAGATAATCCGGAGCAGGAAATTGCTGC – 3’) (RE)

Mfn2$_{L710P}$ R: (5’ – GCAGCAATTTCCTGCTCCGGATTATCTCGGGTGATGTC – 3’) (RE)

Mfn2$_{A738V}$ F: (5’ – AGGAATAAAGTTGGCTGGTTGG – 3’) (SDM)

Mfn2$_{A738V}$ R: (5’ – CCAACCAGCCAACTTTATTCCTGAGC – 3’) (SDM)

Mfn2$_{W740S}$ F: (5’ – CAGGAATAAAGCTGGCAGCTTGGACAGCGAACTC – 3’) (RE)

Mfn2$_{W740S}$ R: (5’ – GAGTTCGCTGTCCAAGCTGCCAGCTTTATTCCTG – 3’) (RE)

Mfn2$_{\Delta GTPase}$ F: (5’ – CGCCGGCCGGATCCATGCAGTCTGCAGTAAAGACC – 3’) (SDM)

Mfn2$_{\Delta GTPase}$ R: (5’ – GGTCTTTACTGCAGACTGCATGGATCCGGCCGGCG – 3’) (SDM)

Amp1: (5’ – AGAATTATGCAGTGCTGCC – 3’) (SDM)

Amp2: (5’ – GGCAGCACTGCATAATTCT – 3’) (SDM)

2.3 Results

2.3.1 Mutations to be examined

I chose to examine CMT2A-associated mutations of Mfn2 that lay outside the GTPase domain. While CMT2A mutations are most concentrated in the GTPase domain, we reasoned that these would likely affect the mitochondrial fusion role of Mfn2 as all dynamin related proteins rely on GTP hydrolysis to remodel membranes. We decided to exclude GTPase domain mutants from our survey to allow us to focus on finding domains that had other important roles in Mfn2 function. We first turned to linear domain homology maps and models of domain architecture as well as lists of MFN2 mutations reported to cause CMT2A to group Mfn2 mutations into putative domain. We chose to focus on three domains that we termed the N-terminal domain (amino acids 1-98, proximal to the GTPase domain), the stalk domain (amino acids 352-615, between the GTPase domain and the transmembrane domain), and the C-terminal domain (amino acids 693-747, distal to the transmembrane region) (Figure 2.1). We selected 5 mutations from the N-terminal domain (Q45R, V69F, L76P, R94Q, and K98E), 3 from the stalk domain (H361Y, C390R, and P456L), and 3 from the C-terminal domain (L710P, A738V, and W740S) for characterization (Figure 2.1).

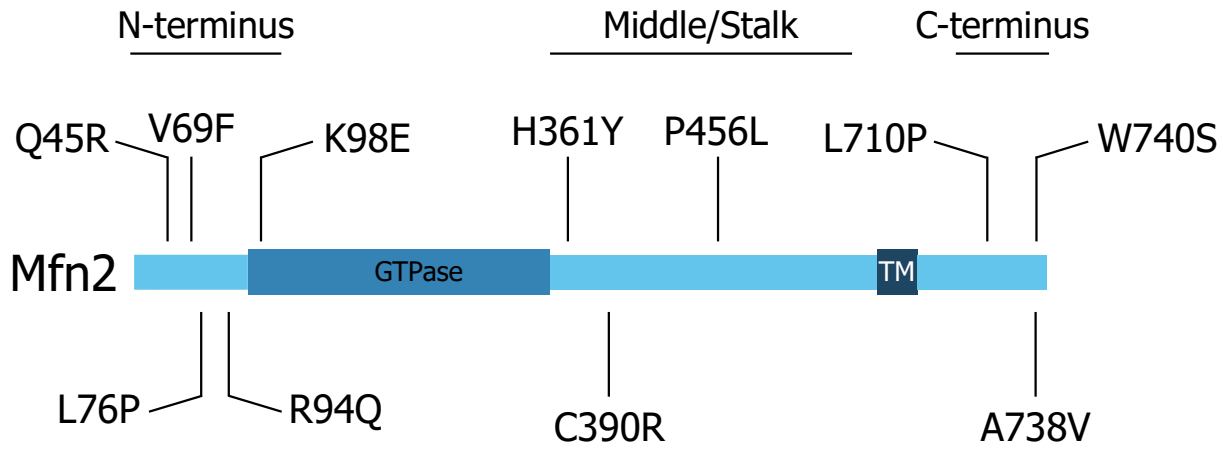

Figure 2.1. Disease-associated mutations in this study.
Domain schematic showing the linear placement of the CMT2A amino acids in this chapter. GTPase = GTPase domain. TM = transmembrane domain (double pass). Narrower light blue regions are mainly helical. Mutations classified as N-terminal, middle or stalk, and C-terminal are labeled at their approximate location.

2.3.2 Disease-associated mutations have a spectrum of effects on mitochondrial morphology

I began by examining the ability of each of these variants to rescue mitochondrial morphology in Mfn2-null mouse embryonic fibroblasts. Each variant was introduced into the cells by a viral transduction system and screened for stable expression at approximately wild type levels. The mitochondrial networks in cells expanded from single cells were visualized and the mitochondrial morphology was scored as fragmented (< 50% of mitochondria greater than 2.5um in length) or fused (> 50% of mitochondria longer than 2.5um). Mfn2-null cells with an empty vector displayed a mostly fragmented mitochondrial network, while those expressing Mfn2^{WT}-FLAG had a reticular mitochondrial network indistinguishable from wild type cells (Figure 2.2). Most of the mutant forms of Mfn2 I examined rescued the reticular morphology in Mfn2-null cells to varying degrees (Figure 2.2). However, the cells expressing Mfn2 with amino acid substitutions in the C-terminal domain (L710P, A738V, W740S) remained mostly fragmented (~80%), indicating that this region is essential for the fusion activity of Mfn2 (Figure 2.2). The N-terminal mutants (Q45R, V69F, L76P, R94Q, and K98E) did not reveal a clear pattern of mitochondrial morphology ranging from 40-70% of cells displaying a reticular mitochondrial network, preventing me from determining with certainty whether this region was important for fusion. It is possible that this means there are subdomains within this region. However, the variation in the level of rescue went up as the average rescue decreased, meaning

that maybe these variants (Q45R and L76P) are more susceptible to changes in the cellular environment (Figure 2.2). Expression of each of the three variants in the stalk domain (H361Y, C390R, and P456L) resulted in mostly reticular networks all to about the same degree (Figure 2.2). This indicates that the middle coiled-coil region may be more vital for other Mfn2 functions than for fusion or that a biochemical fusion defect caused by amino substitutions in this region are masked by the cellular environment.

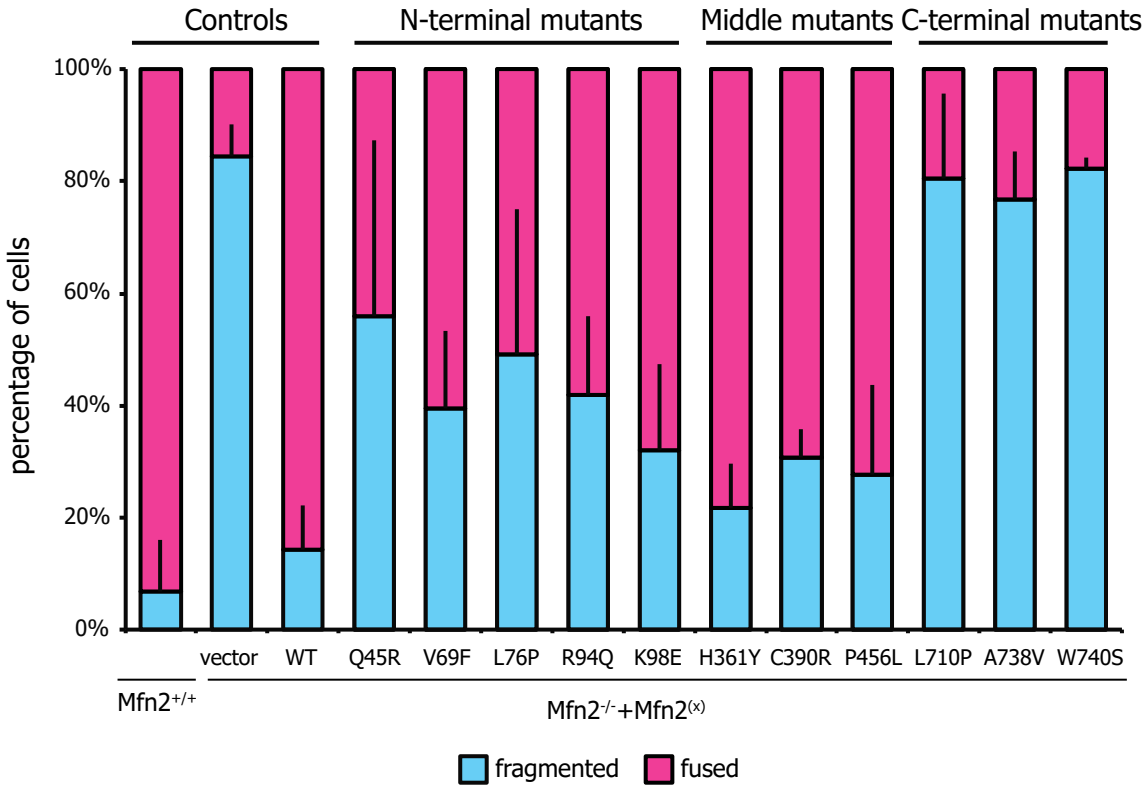

Figure 2.2. Mitochondrial morphology in mouse embryonic fibroblasts stably expressing CMT2A mutant forms of Mfn2.
Cells were scored as having a fused or fragmented mitochondrial network and quantified as the average proportion in each category ± standard deviation. N ≥ 3 experiments of at least 100 cells per experiment.

2.3.3 C-terminal domain mutations and mitochondrial tethering

Because the C-terminal mutants were not able to rescue reticular mitochondrial networks in MEFs, I decided to determine how they might be disrupting fusion. Structural analysis and expression of the Mfn1 C-terminal alpha helix has implicated this region in the tethering of mitochondria to one another (Koshiba et al. 2004). When a fragment of Mfn1 containing this helix (heptad repeat (HR) 2) was expressed and purified, it could form a stable dimer with both itself and the HR2 from Mfn2 when examined by co-immunoprecipitation. When this fragment was crystallized, it was found to form antiparallel coiled coils. When this group then expressed an Mfn1 construct lacking the GTPase domain, the mitochondria became aggregated in this study. Electron microscopy of these aggregates suggested that they were composed of closely apposed, or tethered, mitochondria. Proline substitutions predicted to disrupt this helix ($Mfn1_{L691P}$ and $Mfn1_{L705P}$) were shown to abolish this tethering activity (Koshiba et al. 2004) leading to the conclusion that the C-terminal helix of Mfn1 tethers mitochondria. I decided to determine whether any of the Mfn2 C-terminal mutants I had examined impaired fusion by similarly disrupting mitochondrial tethering. $Mfn2_{L710P}$ is analogous to $Mfn1_{L691P}$, so I expected it to have a similar effect in the Mfn2 ΔGTPase construct.

Unlike the increase in mitochondrial aggregates caused by Mfn1 reported by Koshiba and colleagues, I saw a small increase in hyperfused mitochondria (scored as almost all of the mitochondria belonging to the same connected network) with the expression of the analogous Mfn2 construct lacking the GTPase domain in Hela cells (Figure 2.3). Because this result was so different from previously reported data, I decided to express the Mfn1 ΔGTPase protein in these cells. This experiment also revealed an increase in reticular or hyperfused rather than aggregated mitochondria (Figure 2.3). Looking back at images from the supplemental information from the report by Koshiba, et al. (2004), I discovered that one of the example cells transfected with this construct contained mitochondria that I would have scored as hyperfused

rather than aggregated. Therefore, the disagreement of our two studies may be at least partially due to a difference in definition of aggregated versus hyperfused mitochondria. Mfn1$_{\Delta GTPase}$ expression resulted in more fusion than Mfn2$_{\Delta GTPase}$ expression, indicating that if hyperfusion does represent the tethering ability of this protein fragment, Mfn1$_{\Delta GTPase}$ is a stronger tether than Mfn2$_{\Delta GTPase}$.

Expressing the ΔGTPase construct including the W740S mutation did not change the morphological pattern from the wild type version. This indicates that this mutation does not disrupt how the Mfn2 ΔGTPase protein affects mitochondrial fusion in these cells (Figure 2.3). When the ΔGTPase protein included the L710P or A738V substitution, there was a much larger increase in hyperfused mitochondria and very few fragmented mitochondria (Figure 2.3) indicating that these two mutants alter the quality of

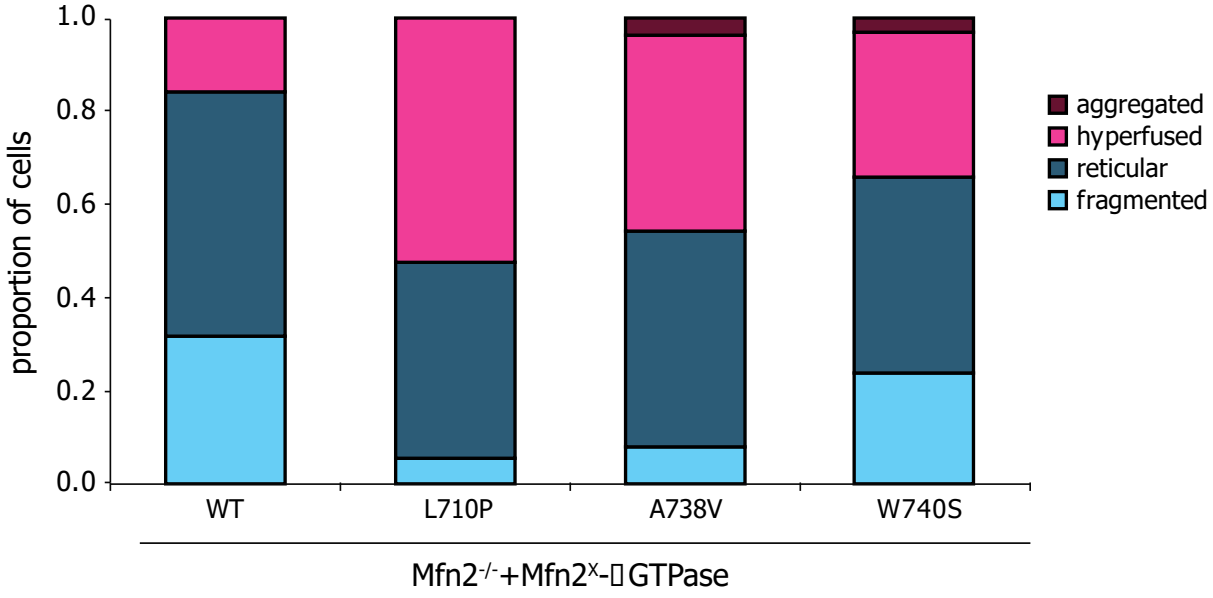

Figure 2.3. Mitochondrial morphology of Hela cells overexpressing "tethering" constructs.
Cells were scored as having a fused, fragmented, hyperfused, or aggregated mitochondrial network and quantified as the average proportion in each category. N ≥ 1 experiment of at least 100 cells per experiment.

this protein in a way that enhances its ability to increase mitochondrial fusion in these cells. Koshiba and colleagues interpreted their data to mean that the C-terminal helix of Mfn1 functions as a tether between mitochondria. My data does not exclude this region from functioning as a tether, but it does indicate that the manner in which it tethers would not prevent the progression of mitochondrial fusion. A tether that does not block subsequent fusion would be expected to increase mitochondrial fusion because according to the current model, tethering is the first step required for mitochondrial fusion. However, more recent structural data suggests that the very C-terminal portion of this helix is actually part of a four-helix bundle connected to the GTPase domain (HB1) that is essential for the stability of the GTPase domain of Mfn1. The deletion of the GTPase domain in these experiments may allow this helix to assume a conformation that is not relevant to one found in the context of the full-length protein. A way to test whether the Mfn1 or 2 C-terminal domain forms a tether in the context of the full length protein, I could introduce the mutations reported to alter the activity of the ΔGTPase variant into full length mitofusin and perform the tethering co-immunoprecipitation assay using purified mitochondria developed in our lab (Engelhart and Hoppins 2019). If the results I have reported truly reflect the ability of $Mfn2_{L710P}$, $Mfn2_{A738V}$, or $Mfn2_{W740S}$ variants to tether, that would mean that it is not the tethering step of mitochondrial fusion that is deficient in these variants. Future work on these mutations could examine the subsequent steps of mitochondrial fusion, assembly and conformational changes, to determine how these variants prevent mitochondrial fusion in cells (Figure 2.2)

2.3.4 N-terminal and stalk domain mutants show variable interactions with Mfn1

Because minimal mutants did not seem to act as a singular domain, I decided to test the ability of some of these mutations to interact with known interactors and to form oligomeric assemblies to determine whether the differences in their fusion activity could be explained by different affinities for binding partners. Mfn2 has been shown to physically interact not only with itself,

but with the other proteins associated with mitochondrial membrane fusion: Mfn1 (Chen et al. 2003; Ishihara et al. 2004). Additionally, Mfn2 specifically has been shown to be regulated by the pro-apoptotic protein Bax which may be via a physical interaction between the two(Cleland et al. 2011; Hoppins et al. 2011). Therefore, the next property of these mutants I assessed was their ability to interact with Bax a by co-immunoprecipitation. I was never able to detect an interaction between Mfn2 and Bax using our co-immunoprecipitation protocol, so I was not able to compare the mutant versions of Mfn2 to the wild type. Co-immunoprecipitation assays in our lab have improved in methodology since these results were obtained, so I would repeat these experiments with the new protocols. It is also possible that Bax only strongly interacts with Mfn2 under certain conditions such as stress. Treating cells in manners shown to increase mitochondrial fusion may stabilize the interaction between Bax and Mfn2 and allow detection of this interaction.

It has been previously reported that fusion occurs most efficiently when both Mfn1 and Mfn2 are involved (Hoppins et al. 2011). Therefore, I decided to test whether the fusion activity of Mfn2 variants correlated with their ability to interact with Mfn1. I was able to detect interactions between Mfn2 and Mfn1 (Figure 2.4). The amount of Mfn1 signal in the elution after Mfn2 co-immunoprecipitation compared to that in the total lysate fraction was about 25% (Figure 2.4). The N-terminal and stalk domain mutants I examined using this assay displayed varying degrees of interaction with Mfn1. Two N-terminal variants (V69F and L76P) interacted with Mfn1 similarly to wild type Mfn2. The other two variants designated as N-terminal (Q45R and R94Q) co-precipitated less Mfn1 than wild type (Figure 2.4). This means that the finding that $Mfn2_{Q45R}$ and $Mfn2_{R94Q}$ may be due at least in part to a decreased affinity for Mfn1. This is supported by the correlation between the extent of morphological rescue of these two variants with the strength of the interaction with Mfn1: $Mfn2_{R94Q}$ interacted with Mfn1 slightly more than $Mfn2_{Q45R}$ and also rescued mitochondrial morphology slightly more when expressed in cells.

Conversely, the stalk domain mutant, Mfn2$_{C390R}$, showed an increased interaction with Mfn1 compared to wild type. This is also consistent with the morphological analysis in which expression of Mfn2$_{C390R}$ resulted in a reticular network in the majority (~70%) of cells.

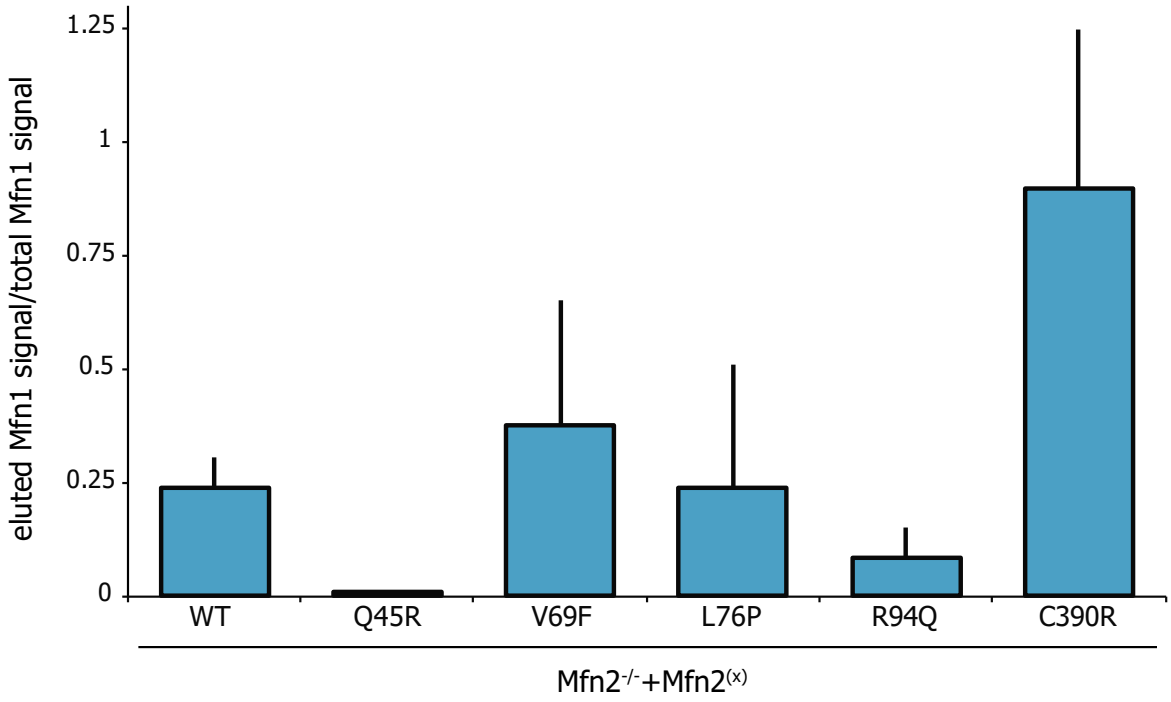

Figure 2.4. Interaction of Mfn1 with Mfn2 mutations.
Immunoprecipitation of epitope tagged Mfn2 of the noted genotypes was probed for Mfn1. Data are expressed as the ratio of eluted Mfn1 signal to input Mfn1 signal. Bar indicate mean ± standard deviation from n ≥ 3 experiments.

The variation in co-immunoprecipitation data for the N-terminal variants is consistent with the morphological data. Together, these findings indicate that this designation may be too broad and that the section of Mfn2 proximal to the GTPase domain may not behave as one domain. Further dividing this region by amino acid position does not yield better congruency as the greatest differences appear to be between mutations closest to one another in amino acid sequence. Alternative grouping may be suggested by the Mfn1 interaction findings. In this assay, Mfn2$_{V69F}$ and Mfn2$_{L76P}$ did not alter interaction between Mfn1 and Mfn2, but Mfn2$_{Q45R}$ and

Mfn2$_{R94Q}$ did. This may indicate that interaction between the two mitofusins is in fact dependent on the N-terminal region of Mfn2, but that it is facilitated mainly by charged amino acids because both Q45R and R94Q involve a change in the charge of the amino acid

2.3.5 Assembly of Mfn2$_{C390R}$

Because the middle domain mutant C390R showed increased interaction with Mfn1, I decided to test whether this mutant existed in different assembly states from wild type Mfn2. The interaction between Mfn2 and Mfn1 detected in the co-immunoprecipitation assay could represent a dimer of Mfn1 and Mfn2 or a larger assembly that includes both of these proteins. As assembly is expected to be a vital step in mitochondrial fusion, it is possible that the mild difference in mitochondrial morphology between cells expressing Mfn2$_{WT}$ and Mfn2$_{C390R}$ could be due to a difference in the assembly states favored by each protein. To test this possibility, I utilized sucrose gradients to determine the size of Mfn2-containing assemblies from isolated mitochondria. Wild type Mfn2 appeared mainly in the fractions corresponding to the marker sizes 140-242 (Figure 2.5). This is most congruent with an assembly the size of a dimer. Mfn2$_{C390R}$ displayed a pattern of Mfn2-containing assemblies similar to Mfn2$_{WT}$ (Figure 2.5), with most of the protein in the fractions representing a dimer. There were two visible differences between the assembly size profile of Mfn2$_{C390R}$ and Mfn2$_{WT}$. There was slightly more Mfn2$_{C390R}$ found in the fractions corresponding to assembly sizes larger than 440 kDa and less in the fraction containing the 66 kDa marker, which roughly corresponds to the size of the Mfn2 monomer. Therefore, there appears to be a slight bias of Mfn2$_{C390R}$ toward larger assemblies, but as a whole it shows mostly wild-type assembly patterns.

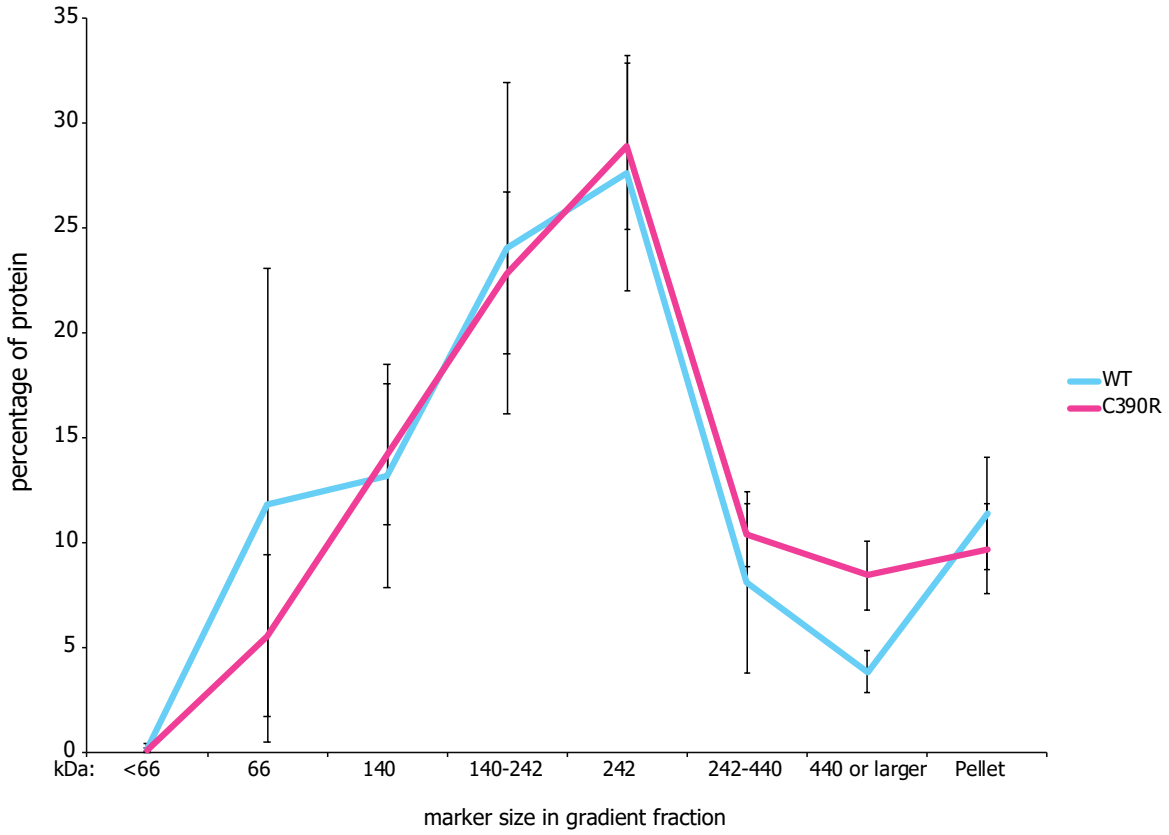

Figure 2.5. Mfn2 protein assembly state in isolated mitochondria.
Isolated mitochondria were solubilized, and the lysate was layered on top of a 5-20% sucrose gradient. Fractions were taken and analyzed by western blot for Mfn2. Assembly size was determined by identification of marker proteins layered on a control sucrose gradient.

The findings presented here could explain the slight morphological difference and the increase in interaction with Mfn1 as follows: Most of the Mfn2 exists as a homodimer (Mfn2-Mfn2), but some percentage of the protein is also contained in larger assemblies that also include Mfn1 (440 kDa or larger). As more of the Mfn2$_{C390R}$ was present in these large species, this could explain the increased interaction with Mfn1 seen by co-immunoprecipitation. I speculate that because Mfn2$_{C390R}$ showed a mild fusion defect in cells, it is plausible that this assembly is different from the assembly needed to facilitate fusion. Thus, this variant of Mfn2 would need to

move out of this presumably inactive assembly and into an active one, rather than going directly from dimer to active assembly. Because the larger assembly size seen by sucrose gradient likely represents both my hypothetical inactive and active assemblies, I would need to gain more resolution in this size region to attempt to determine if I could distinguish two larger assemblies that would represent each of these populations. I could first attempt to do this by blue native PAGE under the same conditions as these sucrose gradients to see if I could replicate the finding that more Mfn2$_{C390R}$ exists in higher molecular weight assemblies. I could then test whether I observe different bands at higher molecular weights that could represent active and inactive assemblies. To attempt to begin to determine whether these species represent active or inactive assemblies, I could isolate mitochondria from synchronized cells undergoing mitosis, when mitochondria are largely fragmented and from cells at G1-S phase, when mitochondria are highly connected(Mitra et al. 2009). If there is a difference in the assemblies formed in these two conditions, I could begin to draw conclusions of the assembly state of the mitofusins that are active versus inactive. I could then go back at determine whether Mfn2$_{C390R}$ exists in more inactive assemblies than Mfn2$_{WT}$.

2.4 Conclusions and Future Directions

This study aimed to assign functionality to three broad domains of Mfn2. By examining mitochondrial morphology in Mfn2-null cells expressing disease-associate variants of Mfn2, I was able to determine that the C-terminal domain of Mfn2 (distal to the transmembrane domains) is essential for the mitochondrial fusion activity of Mfn2. This is consistent with a previous report that suggests that the equivalent domain of Mfn1 is essential for pre-fusion tethering of mitofusins (Koshiba et al. 2004). However, my findings with Mfn2 did not lead to the significant increase in mitochondrial aggregation seen in this study. This may indicate that the C-terminus of Mfn2 does not act as a tether or that tethers mediated by Mfn2 do not block

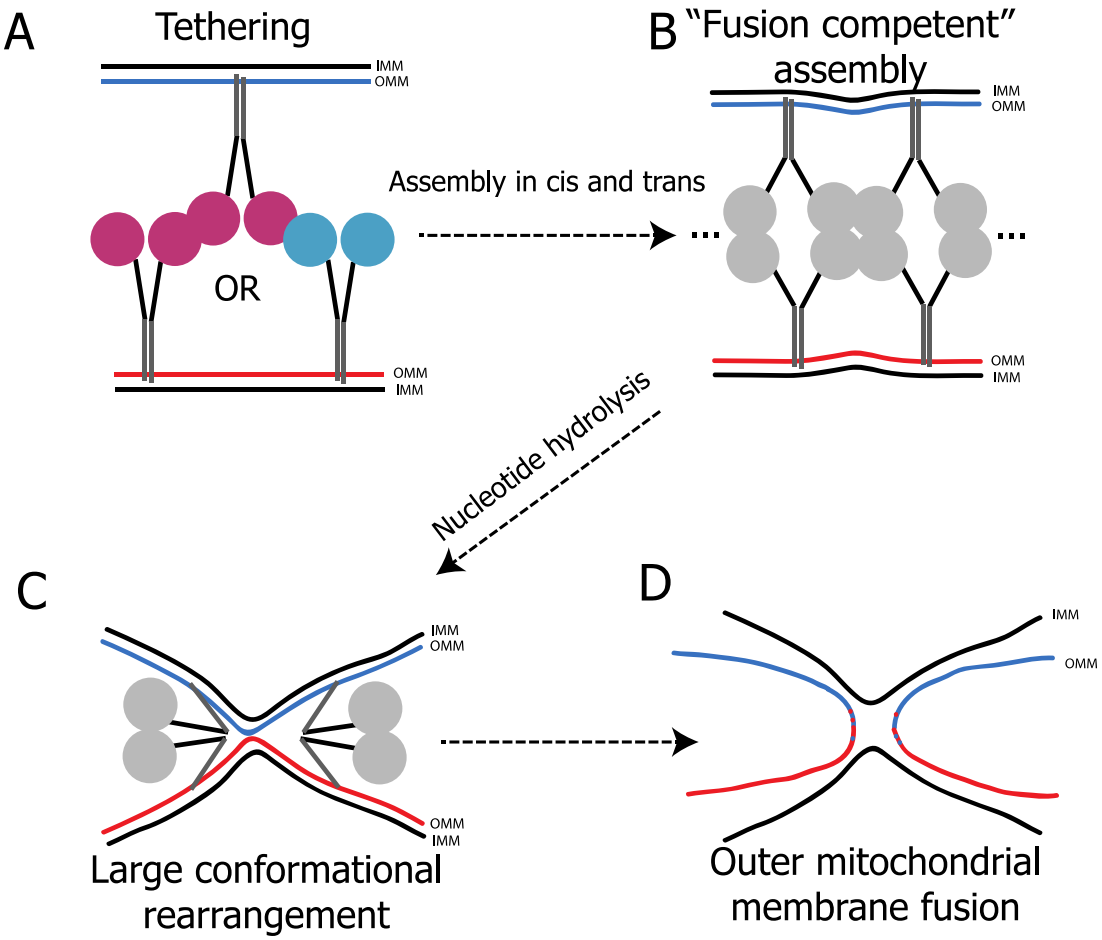

Figure 2.6. Model of mitochondrial fusion.
A) Tethering is facilitated by interactions between Mfn1-Mfn1(pink) or Mfn1 (pink) - Mfn2 (blue) on separate mitochondria. B) After mitochondria are tethered changes (i.e. nucleotide binding and/or conformational changes) lead to further assembly of mitofusin molecules into a machine capable of fusion. C) Nucleotide hydrolysis leads to a large conformational change that disrupts and brings the mitochondrial membranes close together. D) Outer mitochondrial membranes fuse.

the procession of the rest of the fusion reaction. The hypothesis that Mfn2 is not an effective tether on its own is supported by later work I have done that shows that Mfn2 homotypic interactions cannot be observed in trans by co-immunoprecipitation (Chapter 4). If tethering is not a main responsibility of Mfn2, our model of mitochondrial fusion would need to be updated to indicate that the tethers that hold mitochondria together are mediated by either Mfn1

proteins on each membrane or Mfn1 protein on one membrane and Mfn2 protein on the other (Figure 2.6).

This work should be confirmed more rigorously by increasing the sample size and number of experiments and could be followed up by future studies utilizing a co-immunoprecipitation assay that can detect interactions between mitofusins in trans. I could also use this assay to determine whether $Mfn2_{L710P}$ or $Mfn2_{A738V}$ increase tethering activity of Mfn2, which would explain the increase in hyperfusion mediated by these variants in the ΔGTPase form of the protein relative to Mfn2 wild type ΔGTPase.

Expressing Mfn2 with amino acid substitutions in the N-terminal and stalk domains each resulted in partial rescue of the reticular mitochondrial networks in Mfn2-null cells. Mutations in the stalk domain did not seem to greatly impair mitochondrial fusion in cells, opening the possibility that this region is either vital to other activities of Mfn2 or plays a regulatory role in mitochondrial fusion that is not apparent in baseline mitochondrial morphology analysis. Further studies of this region could focus on other reported activities of Mfn2 or mitochondrial fusion activity under stress conditions.

Analyzing the effects of amino acid substitutions in the N-terminal domain was more difficult. They had higher variability both on an individual mutation basis (standard deviation) and between the mutations within the proposed domain. It is thus impossible based on this study to determine whether the region proximal to the GTPase domain is vital for mitochondrial fusion or even acts as a single region in cells. Fortunately, new structural information has been obtained from crystallographic studies of Mfn1 and structural homology modeling with the related protein bacterial dynamin like protein (BLDP) since these experiments were performed. Structural predictions suggest that the mitofusin proteins are closest in structure to BDLP of all the DRPs, and recently obtained Mfn1 structures reinforce the appropriateness of using BDLP as

a model of full length mitofusin structure. This information suggests much different domain groupings than we assigned based on the linear sequence (Figure 2.7). We now know that the helical stalk between the GTPase domain and the transmembrane domain is made of 2 helical bundles (HB1 and HB2) and that the region distal to the transmembrane domain folds back up into these helical bundles. Examining the variants originally classified as N-terminal in the context of this information might allow us to make more sense of this data.

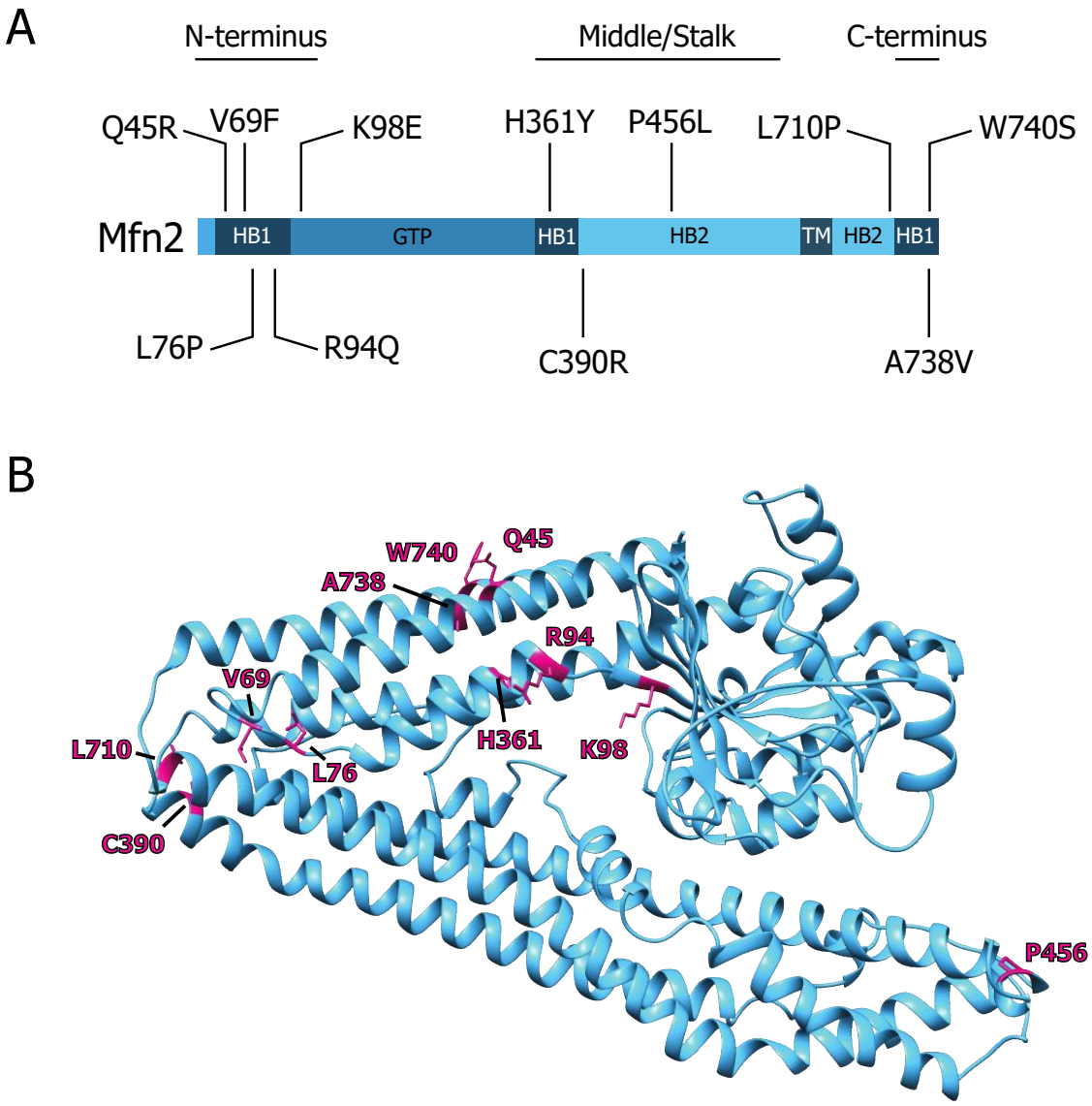

Figure 2.7. Disease-associated mutations in this study.
A) Domain schematic showing the linear placement of the CMT2A-associated amino acids in this chapter. GTP = GTPase domain. HB1 = helical bundle 1. HB2 = helical bundle 2. TM = transmembrane domain (double pass). Mutations classified as N-terminal, middle or stalk, and C-terminal are labeled. **B)** CMT2A mutations mapped to a model of Mfn2 based on the closely related protein BDLP (PDB 2J69). Mutants are labeled and colored pink.

Using the predicted boundaries of these helical bundles and mapping the mutations onto a structural prediction based on BDLP yields much smaller groupings. Amino acids R94 and K98 are pointing in a similar direction near the HB1/GTPase boundary, Q45, A738, and W740 are near each other within two neighboring helices of HB1, V69 and L76 are predicted to be in a loop connecting two helices of HB1, and C390, and L710 are near the boundary between HB1 and HB2 (Figure 2.7). In this model, H361 and P456 do not group well with any of the other mutations and are in HB1 (H361) or close to the transmembrane region (P456). However, this new grouping still does not fully explain the morphological data (Figure 2.8). Therefore, even with more domain information about Mfn2, I am still not able to confidently say that any particular group of the mutations I examined here affect Mfn2 in the same way, especially when it comes to fusion ability.

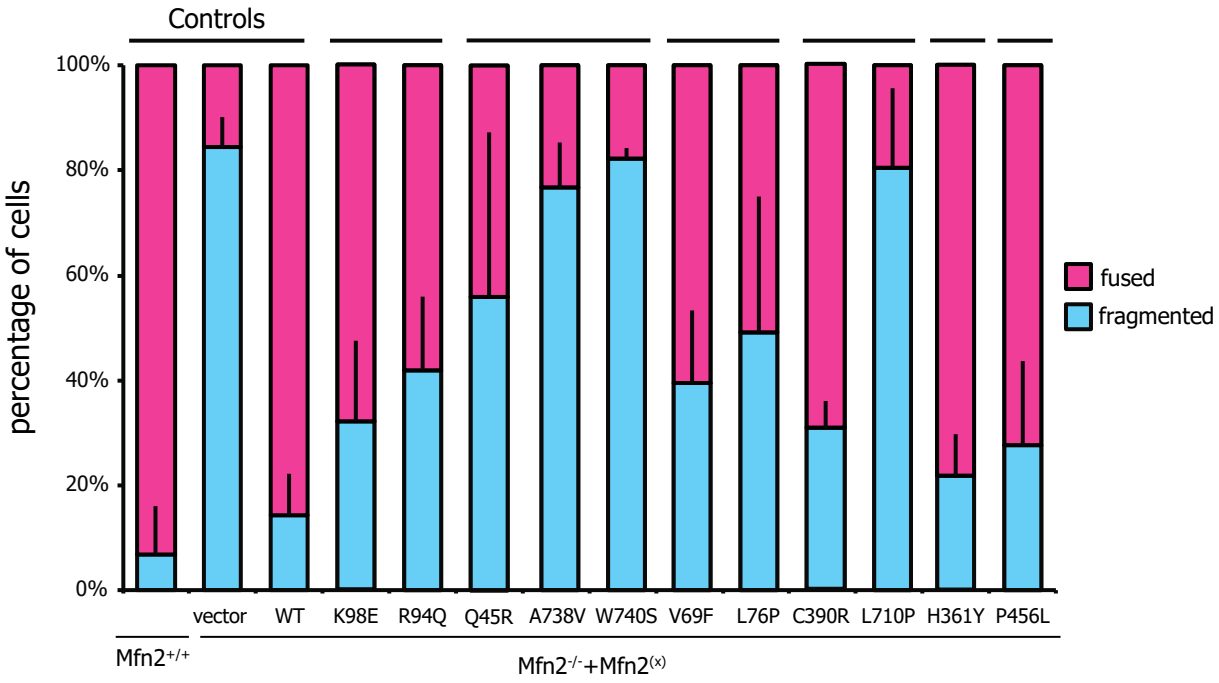

Figure 2.8. Mitochondrial morphology in mouse embryonic fibroblasts stably expressing CMT2A mutant forms of Mfn2, updated groupings.
Cells were scored as having a fused or fragmented mitochondrial network and quantified as the average proportion in each category ± standard deviation. N ≥ 3 experiments of at least 100 cells per experiment.

Especially relevant to model-based grouping of the N-terminal mutations is that the N-terminus of Mnf2 is likely not correctly modeled. Mfn2 has 21 amino acids at its N-terminus that are not conserved in Mfn1. Homology based modeling of Mfn2 either leaves out these amino acids or (as in the model in Figure 2.7), skips some amino acids later in the sequence. V69 and L76 are modeled to be separated by one amino acid in this model, but they are actually seven amino acids apart. Better sequence alignment occurs starting at the GTPase domain, so the structure is likely more reliable at and after the GTPase domain. Therefore, alternative approaches are still necessary. A better approach to this study might be to base the choice of CMT2A-associated variants I study on the areas of Mfn2 that appear to be CMT2A "hotspots" (Figure 1.3). Perhaps different hotspots represent important structural regions of Mfn2 that differentially affect Mfn2 activity.

Another approach to studying the N-terminal region of Mfn2 would be to focus on the very first helix of Mfn2. This angle stems from the recent description of a pair of bacterial dynamin like proteins that form heterooligomers by the binding of the first helix (H1) of one partner to a region in the GTPase domain of the other (Liu, Noel, and Low 2018). The only mutation in the predicted H1 of Mfn2 examined here was $Mfn2_{Q45R}$, which stood out from the other mutations in that it had both the lowest level of morphological rescue of the N-terminal variants (Figure 2.2) as well as very low detectable interaction with Mfn1 by co-immunoprecipitation (Figure 2.3). Further studies could determine whether other mutations in this domain also inhibit binding of Mfn2 to Mfn1. I could also determine whether the inability of $Mfn2_{Q45R}$ to interact with Mfn1 is different between cis and trans interactions. If there is a difference, this information would help us to make hypotheses on the differences in the Mfn1/Mfn2 assembly interfaces in cis and trans.

This research allowed me to both make theoretical updates to our working model of mitochondrial outer membrane fusion and to have background information for later projects.

While I was not able to assign specific activities to domains, the information I gathered allowed me to identify some areas where our knowledge of Mfn2 structure and function was lacking and to narrow down the questions I asked.

2.5 Acknowledgements for Chapter 2:

Special thanks to Dan Vail, who made the DNA for Mfn2$_{H361Y, C390R, and P456L}$ and to Suzanne Hoppins who made the DNA for Mfn2$_{L710P and W740S}$ and to Emily Engelhart, who made the DNA for Mfnw$_{A738V}$.

2.6 References

Atkins K, Dasgupta A, Chen K, Mewburn J, Archer SL. 2016. The role of Drp1 adaptor proteins MiD49 and MiD51 in mitochondrial fission : implications for human disease. :1861–1874. doi:10.1042/CS20160030.

Baloh RH, Schmidt RE, Pestronk A, Milbrandt J. 2007. Altered axonal mitochondrial transport in the pathogenesis of Charcot-Marie-Tooth disease from mitofusin 2 mutations. *J Neurosci*. 27(2):422–430. doi:10.1523/JNEUROSCI.4798-06.2007.

Bian X, Xu J, Zhao H, Zheng Q, Xiao X, Ma X, Li Y, Du X, Liu X. 2019. Zinc-Induced SUMOylation of Dynamin-Related Protein 1 Protects the Heart against Ischemia-Reperfusion Injury. *Oxid Med Cell Longev*. 2019:1–11. doi:10.1155/2019/1232146.

Brandt T, Cavellini L, Kühlbrandt W, Cohen MM. 2016. A mitofusin-dependent docking ring complex triggers mitochondrial fusion in vitro. *Elife*. 5:1–23. doi:10.7554/eLife.14618.

de Brito OM, Scorrano L. 2008. Mitofusin 2 tethers endoplasmic reticulum to mitochondria. *Nature*. 456(7222):605–10. doi:10.1038/nature07534.

Cairns RA, Harris IS, Mak TW. 2011. Regulation of cancer cell metabolism. *Nat Rev Cancer*. 11(2):85–95. doi:10.1038/nrc2981.

Calvo J, Funalot B, Ouvrier R a, Lazaro L, Toutain A, De Mas P, Bouche P, Gilbert-Dussardier B, Arne-Bes M-C, Carrière J-P, et al. 2009. Genotype-phenotype correlations in Charcot-Marie-Tooth disease type 2 caused by mitofusin 2 mutations. *Arch Neurol*. 66(12):1511–1516. doi:10.1001/archneurol.2009.284.

Cao Y-L, Meng S, Chen Y, Feng J-X, Gu D-D, Yu B, Li Y-J, Yang J-Y, Liao S, Chan DC, et al. 2017. MFN1 structures reveal nucleotide-triggered dimerization critical for mitochondrial fusion. *Nature*.:1–5. doi:10.1038/nature21077.

Cartoni R, Arnaud E, Médard JJ, Poirot O, Courvoisier DS, Chrast R, Martinou JC. 2010. Expression of mitofusin 2R94Q in a transgenic mouse leads to Charcot-Marie-Tooth neuropathy type 2A. *Brain*. 133(5):1460–1469. doi:10.1093/brain/awq082.

Cartoni R, Martinou JC. 2009. Role of mitofusin 2 mutations in the physiopathology of Charcot-Marie-Tooth disease type 2A. *Exp Neurol*. 218(2):268–273. doi:10.1016/j.expneurol.2009.05.003.

Celardo I, Martins LM, Gandhi S. 2014. Unravelling mitochondrial pathways to Parkinson's disease. *Br J Pharmacol*. 171(8):1943–1957. doi:10.1111/bph.12433.

Chandel NS, Maltepe E, Goldwasser E, Mathieu CE, Simon MC, Schumacker PT. 1998. Mitochondrial reactive oxygen species trigger hypoxia-induced transcription. *Proc Natl Acad Sci U S A*. 95(September):11715–11720.

Chappie JS, Acharya S, Liu Y-W, Leonard M, Pucadyil TJ, Schmid SL. 2009. An Intramolecular Signaling Element that Modulates Dynamin Function In Vitro and In Vivo. *Mol Biol Cell*. 20:3561–3571. doi:10.1091/mbc.E09.

Chen H, Detmer SA, Ewald AJ, Griffin EE, Fraser SE, Chan DC. 2003. Mitofusins Mfn1 and Mfn2 coordinately regulate mitochondrial fusion and are essential for embryonic development. *J Cell Biol*. 160:189–200. doi:10.1083/jcb.200211046.

Chen K-H, Guo X, Ma D, Guo Y, Li Q, Yang D, Li P, Qiu X, Wen S, Xiao R-P, et al. 2004. Dysregulation of HSG triggers vascular proliferative disorders. *Nat Cell Biol*. 6(9):872–883.

doi:10.1038/ncb1161.

Chen KH, Dasgupta A, Ding J, Indig FE, Ghosh P, L. Longo D. 2014. Role of mitofusin 2 (Mfn2) in controlling cellular proliferation. *FASEB J*. 28(1):382–394. doi:10.1096/fj.13-230037.

Chen KH, Guo X, Ma D, Guo Y, Li Q, Yang D, Li P, Qiu X, Wen S, Xiao RP, et al. 2004. Dysregulation of HSG triggers vascular proliferative disorders. *Nat Cell Biol*. 6(9):872–883. doi:10.1038/ncb1161.

Chen Y, Dorn GW. 2013. PINK1-Phosphorylated Mitofusin 2 is a Parkin Receptor for Culling Damaged Mitochondria. *Science (80-)*. 340(April):471–476.

Cleland MM, Norris KL, Karbowski M, Wang C, Suen D-F, Jiao S, George NM, Luo X, Li Z, Youle RJ. 2011. Bcl-2 family interaction with the mitochondrial morphogenesis machinery. *Cell Death Differ*. 18(2):235–247. doi:10.1038/cdd.2010.89.

Cribbs JT, Strack S. 2007. Reversible phosphorylation of Drp1 by cyclic AMP-dependent protein kinase and calcineurin regulates mitochondrial fission and cell death. *EMBO Rep*. 8(10):939–944. doi:10.1038/sj.embor.7401062.

Delaunay A, Isnard AD, Toledano MB. 2000. H2O2 sensing through oxidation of the Yap1 transcription factor. *EMBO J*. 19(19):5157–5166. doi:10.1093/emboj/19.19.5157.

Detmer Scott A, Chan DC. 2007a. Complementation between mouse Mfn1 and Mfn2 protects mitochondrial fusion defects caused by CMT2A disease mutations. *J Cell Biol*. 176(4):405–14. doi:10.1083/jcb.200611080.

Detmer Scott A, Chan DC. 2007b. Functions and dysfunctions of mitochondrial dynamics. *Nat Rev Mol Cell Biol*. 8(november):870–879. doi:10.1038/nrm2275.

Detmer Scott A., Chan DC. 2007. Complementation between mouse Mfn1 and Mfn2 protects mitochondrial fusion defects caused by CMT2A disease mutations. *J Cell Biol*. 176(4):405–414. doi:10.1083/jcb.200611080.

Detmer SA, Velde C Vande, Cleveland DW, Chan DC. 2008. Hindlimb gait defects due to motor axon loss and reduced distal muscles in a transgenic mouse model of Charcot - Marie - Tooth

type 2A. *Hum Mol Genet*. 17(3):367–375. doi:10.1093/hmg/ddm314.

Du C, Fang M, Li Y, Li L, Wang X. 2000. Smac, a Mitochondrial Protein that Promotes Cytochrome c-Dependent Caspase Activation by Eliminating IAP Inhibition Hid, and Grim in terms of IAP neutralization and is the. *Cell*. 102:33–42.

Ekman D, Björklund ÅK, Frey-Skött J, Elofsson A. 2005. Multi-domain proteins in the three kingdoms of life: Orphan domains and other unassigned regions. *J Mol Biol*. 348(1):231–243. doi:10.1016/j.jmb.2005.02.007.

Engelhart EA, Hoppins S. 2019. A catalytic domain variant of Mitofusin requiring a wildtype paralog for function uncouples mitochondrial outer-membrane tethering and fusion. *J Biol Chem*. 1(8):jbc.RA118.006347. doi:10.1074/jbc.RA118.006347.

Ernster L, Schatz G. 1981. Mitochondria : A Historical Review. 91(December).

Eura Y. 2003. Two Mitofusin Proteins, Mammalian Homologues of FZO, with Distinct Functions Are Both Required for Mitochondrial Fusion. *J Biochem*. 134(3):333–344. doi:10.1093/jb/mvg150.

Federico A, Cardaioli E, Da Pozzo P, Formichi P, Gallus GN, Radi E. 2012. Mitochondria, oxidative stress and neurodegeneration. *J Neurol Sci*. 322(1–2):254–262. doi:10.1016/j.jns.2012.05.030.

Feely SME, Laura M, Siskind CE, Sottile S, Davis M, Gibbons VS, Reilly MM, Shy ME. 2011. MFN2 mutations cause severe phenotypes in most patients with CMT2A. *Neurology*. 76(20):1690–6. doi:10.1212/WNL.0b013e31821a441e.

Ferreira JCB, Campos JC, Qvit N, Qi X, Bozi LHM, Bechara LRG, Lima VM, Queliconi BB, Disatnik MH, Dourado PMM, et al. 2019. A selective inhibitor of mitofusin 1-βIIPKC association improves heart failure outcome in rats. *Nat Commun*. 10(1). doi:10.1038/s41467-018-08276-6.

Filadi R, Greotti E, Turacchio G, Luini A, Pozzan T, Pizzo P. 2015. Mitofusin 2 ablation increases endoplasmic reticulum–mitochondria coupling. *Proc Natl Acad Sci*. doi:10.1073/pnas.1504880112.

Franco A, Kitsis RN, Fleischer JA, Gavathiotis E, Kornfeld OS, Gong G, Biris N, Benz A, Qvit N, Donnelly SK, et al. 2016. Correcting mitochondrial fusion by manipulating mitofusin conformations. *Nature*.:1–20. doi:10.1038/nature20156.

Fransson Å, Ruusala A, Aspenström P. 2006. The atypical Rho GTPases Miro-1 and Miro-2 have essential roles in mitochondrial trafficking. *Biochem Biophys Res Commun*. 344(2):500–510. doi:10.1016/j.bbrc.2006.03.163.

Ganesan V, Willis SD, Chang KT, Beluch S, Cooper KF, Strich R. 2019. Cyclin C directly stimulates Drp1 GTP affinity to mediate stress-induced mitochondrial hyperfission. *Mol Biol Cell*. 30(3):302–311. doi:10.1091/mbc.E18-07-0463.

Gawlowski T, Suarez J, Scott B, Torres-Gonzalez M, Wang H, Schwappacher R, Han X, Yates JR, Hoshijima M, Dillmann W. 2012. Modulation of dynamin-related protein 1 (DRP1) function by increased O-linked-β-N-acetylglucosamine modification (O-GlcNAc) in cardiac myocytes. *J Biol Chem*. 287(35):30024–30034. doi:10.1074/jbc.M112.390682.

Gemignani F, Marbini A. 2001. Charcot-Marie-Tooth disease (CMT): Distinctive phenotypic and genotypic features in CMT type 2. *J Neurol Sci*. 184(1):1–9. doi:10.1016/S0022-510X(00)00497-4.

Giarmarco MM, Cleghorn WM, Sloat SR, Hurley JB, Brockerhoff SE. 2017. Mitochondria Maintain Distinct Ca 2+ Pools in Cone Photoreceptors . *J Neurosci*. 37(8):2061–2072. doi:10.1523/jneurosci.2689-16.2017.

Gilbert HF. 1995. Thiol-Disulfide Exchange Equilibria and Bond Stability. *Methods Enzymol*. 251:8–28.

Giustarini D, Colombo G, Garavaglia ML, Astori E, Portinaro NM, Reggiani F, Badalamenti S, Aloisi AM, Santucci A, Rossi R, et al. 2017. Assessment of glutathione/glutathione disulphide ratio and S-glutathionylated proteins in human blood, solid tissues, and cultured cells. *Free Radic Biol Med*. 112(August):360–375. doi:10.1016/j.freeradbiomed.2017.08.008.

Giustarini D, Dalle-Donne I, Tsikas D, Rossi R. 2009. Oxidative stress and human diseases:

Origin, link, measurement, mechanisms, and biomarkers. *Crit Rev Clin Lab Sci*. 46(5–6):241–281. doi:10.3109/10408360903142326.

Gomes LC, Benedetto G Di, Scorrano L. 2011. During autophagy mitochondria elongate, are spared from degradation and sustain cell viability. *Nat Cell Biol*. 13(5):589–598. doi:10.1038/ncb2220.

Grek CL, Zhang J, Manevich Y, Townsend DM, Tew KD. 2013. Causes and consequences of cysteine s-glutathionylation. *J Biol Chem*. 288(37):26497–26504. doi:10.1074/jbc.R113.461368.

Griffin EE, Chan DC. 2006. Domain interactions within Fzo1 oligomers are essential for mitochondrial fusion. *J Biol Chem*. 281(24):16599–606. doi:10.1074/jbc.M601847200.

Guo C, Hildick KL, Luo J, Dearden L, Wilkinson KA, Henley JM. 2013. SENP3-mediated deSUMOylation of dynamin-related protein 1 promotes cell death following ischaemia. *EMBO J*. 32(11):1514–1528. doi:10.1038/emboj.2013.65.

Guo X, Chen KH, Guo Y, Liao H, Tang J, Xiao RP. 2007. Mitofusin 2 triggers vascular smooth muscle cell apoptosis via mitochondrial death pathway. *Circ Res*. 101(11):1113–1122. doi:10.1161/CIRCRESAHA.107.157644.

Han X, Lu Y, Li S, Kaitsuka T, Sato Y, Tomizawa K, Nairn AC, Takei K, Matsui H, Matsushita M. 2008. JCB : ARTICLE. 182(3):573–585. doi:10.1083/jcb.200802164.

Harder Z, Zunino R, McBride H. 2004. Sumo1 conjugates mitochondrial substrates and participates in mitochondrial fission. *Curr Biol*. 14(4):340–345. doi:10.1016/S0960-9822(04)00084-3.

Hoppins S, Edlich F, Cleland MM, Banerjee S, McCaffery JM, Youle RJ, Nunnari J. 2011. The Soluble Form of Bax Regulates Mitochondrial Fusion via MFN2 Homotypic Complexes. *Mol Cell*. 41(2):150–160. doi:10.1016/j.molcel.2010.11.030.

Horbay R, Bilyy R. 2016. Mitochondrial dynamics during cell cycling. *Apoptosis*. 21(12):1327–1335. doi:10.1007/s10495-016-1295-5.

Iqbal S, Hood DA. 2014. Oxidative stress-induced mitochondrial fragmentation and movement

in skeletal muscle myoblasts. *Am J Physiol - Cell Physiol*. 306(12):1176–1183. doi:10.1152/ajpcell.00017.2014.

Ishihara N, Eura Y, Mihara K. 2004. Mitofusin 1 and 2 play distinct roles in mitochondrial fusion reactions via GTPase activity. *J Cell Sci*. 117(26):6535–6546. doi:10.1242/jcs.01565.

James SJ, Rose S, Melnyk S, Jernigan S, Blossom S, Pavliv O, Gaylor DW. 2009. Cellular and mitochondrial glutathione redox imbalance in lymphoblastoid cells derived from children with autism. *FASEB J*. 23(8):2374–2383. doi:10.1096/fj.08-128926.

Jendrach M, Mai S, Pohl S, Vöth M, Bereiter-Hahn J. 2008. Short- and long-term alterations of mitochondrial morphology, dynamics and mtDNA after transient oxidative stress. *Mitochondrion*. 8(4):293–304. doi:10.1016/j.mito.2008.06.001.

Jimah JR, Hinshaw JE. 2019. Structural Insights into the Mechanism of Dynamin Superfamily Proteins. *Trends Cell Biol*. 29(3):257–273. doi:10.1016/j.tcb.2018.11.003.

Karbowski M, Lee Y, Gaume B, Jeong S, Frank S, Nechushtan A, Santel A, Fuller M, Smith CL, Youle RJ. 2002. Spatial and temporal association of Bax with during apoptosis. 159(6):931–938. doi:10.1083/jcb.200209124.

Karbowski M, Norris KL, Cleland MM, Jeong S-Y, Youle RJ. 2006. Role of Bax and Bak in mitochondrial morphogenesis. *Nature*. 443(October):658–662. doi:10.1038/nature05111.

Kim YM, Youn SW, Sudhahar V, Das A, Chandhri R, Cuervo Grajal H, Kweon J, Leanhart S, He L, Toth PT, et al. 2018. Redox Regulation of Mitochondrial Fission Protein Drp1 by Protein Disulfide Isomerase Limits Endothelial Senescence. *Cell Rep*. 23(12):3565–3578. doi:10.1016/j.celrep.2018.05.054.

Koshiba T, Detmer S a, Kaiser JT, Chen H, McCaffery JM, Chan DC. 2004. Structural basis of mitochondrial tethering by mitofusin complexes. *Science*. 305(5685):858–862. doi:10.1126/science.1099793.

Kosower NS, Kosower EM, Wertheim B, Correa WS. 1969. Diamide, a new reagent for the intracellular oxidation of glutathione to the disulfide. *Biochem Biophys Res Commun*.

37(4):593–596. doi:10.1016/0006-291X(69)90850-X.

Koutsopoulos OS, Laine D, Osellame L, Chudakov DM, Parton RG, Frazier AE, Ryan MT. 2010. Human Miltons associate with mitochondria and induce microtubule-dependent remodeling of mitochondrial networks. *Biochim Biophys Acta - Mol Cell Res*. 1803(5):564–574. doi:10.1016/j.bbamcr.2010.03.006.

Labbé K, Murley A, Nunnari J. 2014. Determinants and Functions of Mitochondrial Behavior. *Annu Rev Cell Dev Biol*. 30(1):357–391. doi:10.1146/annurev-cellbio-101011-155756.

Lebeau J, Saunders JM, Moraes VWR, Madhavan A, Madrazo N, Anthony MC, Wiseman RL. 2018. The PERK Arm of the Unfolded Protein Response Regulates Mitochondrial Morphology during Acute Endoplasmic Reticulum Stress. *Cell Rep*. 22(11):2827–2836. doi:10.1016/j.celrep.2018.02.055.

Lee D, Redfern O, Orengo C. 2007. Predicting protein function from sequence and structure. *Nat Rev Mol Cell Biol*. 8(12):995–1005. doi:10.1038/nrm2281.

Lee J-Y, Kapur M, Li M, Choi M-C, Choi S, Kim H-J, Kim I, Lee E, Taylor JP, Yao T-P. 2014. MFN1 deacetylation activates adaptive mitochondrial fusion and protects metabolically challenged mitochondria. *J Cell Sci*. 127(22):4954–4963. doi:10.1242/jcs.157321.

Liu J, Noel JK, Low HH. 2018. Structural basis for membrane tethering by a bacterial dynamin-like pair. *Nat Commun*. 9(1):1–12. doi:10.1038/s41467-018-05523-8.

Liu X, Kim CN, Yang J, Jemmerson R, Wang X. 1996. Induction of Apoptotic Program in Cell-Free Extracts: Requirement for dATP and Cytochrome C. *Cell*. 86(July):147–157.

Loson OC, Song Z, Chen H, Chan DC. 2013. Fis1, Mff, MiD49, and MiD51 mediate Drp1 recruitment in mitochondrial fission. *Mol Biol Cell*. 24(5):659–667. doi:10.1091/mbc.e12-10-0721.

Low HH, Löwe J. 2006. A bacterial dynamin-like protein. *Nature*. 444(7120):766–769. doi:10.1038/nature05312.

Low HH, Sachse C, Amos LA, Löwe J. 2009. Structure of a Bacterial Dynamin-like Protein Lipid

Tube Provides a Mechanism For Assembly and Membrane Curving. *Cell*. 139(7):1342–1352. doi:10.1016/j.cell.2009.11.003.

Mattie S, Riemer J, Wideman JG, McBride HM. 2018. A new mitofusin topology places the redox-regulated C terminus in the mitochondrial intermembrane space. *J Cell Biol*. 217(2):507–515. doi:10.1083/jcb.201611194.

McLelland GL, Goiran T, Yi W, Dorval G, Chen CX, Lauinger ND, Krahn AI, Valimehr S, Rakovic A, Rouiller I, et al. 2018. Mfn2 ubiquitination by PINK1/parkin gates the p97-dependent release of ER from mitochondria to drive mitophagy. *Elife*. 7:1–35. doi:10.7554/eLife.32866.

Mears JA, Lackner LL, Fang S, Ingerman E, Nunnari J, Hinshaw JE. 2011. Conformational changes in Dnm1 support a contractile mechanism for mitochondrial fission. *Nat Struct Mol Biol*. 18(1):20–27. doi:10.1038/nsmb.1949.

Mishra P, Chan DC. 2014. Mitochondrial dynamics and inheritance during cell division, development and disease. *Nat Rev Mol Cell Biol*. 15(10):634–646. doi:10.1038/nrm3877.

Mitra K, Wunder C, Roysam B, Lin G, Lippincott-Schwartz J. 2009. A hyperfused mitochondrial state achieved at G1-S regulates cyclin E buildup and entry into S phase. *Proc Natl Acad Sci*. 106(29):11960–11965. doi:10.1073/pnas.0904875106.

Olichon A, Baricault L, Gas N, Guillou E, Valette A, Belenguer P, Lenaers G. 2003. Loss of OPA1 perturbates the mitochondrial inner membrane structure and integrity, leading to cytochrome c release and apoptosis. *J Biol Chem*. 278(10):7743–7746. doi:10.1074/jbc.C200677200.

Ong S-B, Kalkhoran SB, Cabrera-Fuentes H a., Hausenloy DJ. 2015. Mitochondrial fusion and fission proteins as novel therapeutic targets for treating cardiovascular disease. *Eur J Pharmacol*.:1–11. doi:10.1016/j.ejphar.2015.04.056.

Østergaard H, Tachibana C, Winther JR. 2004. Monitoring disulfide bond formation in the eukaryotic cytosol. *J Cell Biol*. 166(3):337–345. doi:10.1083/jcb.200402120.

Otera H, Wang C, Cleland MM, Setoguchi K, Yokota S, Youle RJ, Mihara K. 2010. Mff is an essential factor for mitochondrial recruitment of Drp1 during mitochondrial fission in

mammalian cells. *J Cell Biol*. 191(6):1141–1158. doi:10.1083/jcb.201007152.

Pareyson D, Saveri P, Sagnelli A, Piscosquito G. 2015. Mitochondrial dynamics and inherited peripheral nerve diseases. *Neurosci Lett*. 596:66–77. doi:10.1016/j.neulet.2015.04.001.

Park YY, Nguyen OTK, Kang H, Cho H. 2014. MARCH5-mediated quality control on acetylated Mfn1 facilitates mitochondrial homeostasis and cell survival. *Cell Death Dis*. 5(4):e1172-12. doi:10.1038/cddis.2014.142.

Pernas L, Scorrano L. 2015. Mito-Morphosis: Mitochondrial Fusion, Fission, and Cristae Remodeling as Key Mediators of Cellular Function. *Annu Rev Physiol*. 78(1):505–531. doi:10.1146/annurev-physiol-021115-105011.

Picard M, Wallace DC, Burelle Y. 2016. The rise of mitochondria in medicine. *Mitochondrion*. 30:105–116. doi:10.1016/j.mito.2016.07.003.

Pilling AD, Horiuchi D, Lively CM, Saxton WM. 2006. Kinesin-1 and Dynein are the primary motors for fast transport of mitochondria in Drosophila motor axons. *Mol Biol Cell*. 17(April):2057–2068. doi:10.1091/mbc.E05.

Pócsi I, Miskei M, Karányi Z, Emri T, Ayoubi P, Pusztahelyi T, Balla G, Prade RA. 2005. Comparison of gene expression signatures of diamide, H2O2 and menadione exposed Aspergillus nidulans cultures - Linking genome-wide transcriptional changes to cellular physiology. *BMC Genomics*. 6:1–18. doi:10.1186/1471-2164-6-182.

Prudent J, Zunino R, Sugiura A, Mattie S, Shore GC, McBride HM. 2015. MAPL SUMOylation of Drp1 Stabilizes an ER/Mitochondrial Platform Required for Cell Death. *Mol Cell*. 59(6):941–955. doi:10.1016/j.molcel.2015.08.001.

Pyakurel A, Savoia C, Scorrano L, Pyakurel A, Savoia C, Hess D, Scorrano L. 2015. Extracellular Regulated Kinase Phosphorylates Mitofusin 1 to Control Mitochondrial Morphology and Article Extracellular Regulated Kinase Phosphorylates Mitofusin 1 to Control Mitochondrial Morphology and Apoptosis. *Mol Cell*.:1–11. doi:10.1016/j.molcel.2015.02.021.

Qi Y, Yan L, Yu C, Guo X, Zhou X, Hu X, Huang X, Rao Z, Lou Z, Hu J. 2016. Structures of

human mitofusin 1 provide insight into mitochondrial tethering.

Rambold AS, Kostelecky B, Elia N, Lippincott-Schwartz J. 2011. Tubular network formation protects mitochondria from autophagosomal degradation during nutrient starvation. *Proc Natl Acad Sci*. 108(25):10190–10195. doi:10.1073/pnas.1107402108.

Redpath CJ, Bou Khalil M, Drozdzal G, Radisic M, McBride HM. 2013. Mitochondrial Hyperfusion during Oxidative Stress Is Coupled to a Dysregulation in Calcium Handling within a C2C12 Cell Model. *PLoS One*. 8(7). doi:10.1371/journal.pone.0069165.

Rocha AG, Franco A, Krezel AM, Rumsey JM, Alberti JM, Knight WC, Biris N, Zacharioudakis E, Janetka JW, Baloh RH, et al. 2018a. MFN2 agonists reverse mitochondrial defects in preclinical models of Charcot-Marie-Tooth disease type 2A. *Science (80-)*. 360(6386):336–341. doi:10.1126/science.aao1785.

Rocha AG, Franco A, Krezel AM, Rumsey JM, Alberti JM, Knight WC, Biris N, Zacharioudakis E, Janetka JW, Baloh RH, et al. 2018b. MFN2 agonists reverse mitochondrial defects in preclinical models of Charcot-Marie-Tooth disease type 2A. *Science (80-)*. 360(6386):336–341. doi:10.1126/science.aao1785.

Rovira-Llopis S, Bañuls C, Diaz-Morales N, Hernandez-Mijares A, Rocha M, Victor VM. 2017. Mitochondrial dynamics in type 2 diabetes: Pathophysiological implications. *Redox Biol*. 11(January):637–645. doi:10.1016/j.redox.2017.01.013.

Santel a, Fuller MT. 2001. Control of mitochondrial morphology by a human mitofusin. *J Cell Sci*. 114:867–874.

Scorrano L. 2013. Keeping mitochondria in shape: A matter of life and death. *Eur J Clin Invest*. 43(8):886–893. doi:10.1111/eci.12135.

Sena LA, Chandel NS. 2012. Physiological roles of mitochondrial reactive oxygen species. *Mol Cell*. 48(2):158–167. doi:10.1016/j.molcel.2012.09.025.

Shen T, Zheng M, Cao C, Chen C, Tang J, Zhang W, Cheng H, Chen KH, Xiao RP. 2007. Mitofusin-2 is a major determinant of oxidative stress-mediated heart muscle cell apoptosis. *J*

Biol Chem. 282(32):23354–23361. doi:10.1074/jbc.M702657200.

SHITARA H, SHIMANUKI M, HAYASHI J-I, YONEKAWA H. 2010. Global Imaging of Mitochondrial Morphology in Tissues Using Transgenic Mice Expressing Mitochondrially Targeted Enhanced Green Fluorescent Protein. *Exp Anim*. 59(1):99–103. doi:10.1538/expanim.59.99.

Shutt T, Geoffrion M, Milne R, McBride HM. 2012. The intracellular redox state is a core determinant of mitochondrial fusion. *EMBO Rep*. 13(10):909–915. doi:10.1038/embor.2012.128.

Shutt TE, McBride HM. 2013. Staying cool in difficult times: Mitochondrial dynamics, quality control and the stress response. *Biochim Biophys Acta - Mol Cell Res*. 1833(2):417–424. doi:10.1016/j.bbamcr.2012.05.024.

Slater EC, Cleland KW. 1953. The effect of calcium on the respiratory and phosphorylative activities of heart-muscle sarcosomes. *Biochem J*. 55(4):566–580. doi:10.1042/bj0550566.

Slivka A, Spina MB, Cohen G. 1987. Reduced and oxidized glutathione in human and monkey brain. *Neurosci Lett*. 74(1):112–118. doi:10.1016/0304-3940(87)90061-9.

Smirnova E, Griparic L, Shurland D-L, van der Bliek AM. 2001. Dynamin-related Protein Drp1 Is Required for Mitochondrial Division in Mammalian Cells. *Mol Biol Cell*. 12(8):2245–2256. doi:10.1091/mbc.12.8.2245.

Sorrentino V, Menzies KJ, Auwerx J. 2017. Repairing Mitochondrial Dysfunction in Disease. *Annu Rev Pharmacol Toxicol*. 58(1):353–389. doi:10.1146/annurev-pharmtox-010716-104908.

De Stefani D, Rizzuto R, Pozzan T. 2016. Enjoy the Trip: Calcium in Mitochondria Back and Forth. *Annu Rev Biochem*. 85(1):161–192. doi:10.1146/annurev-biochem-060614-034216.

Strickland A V, Rebelo AP, Zhang F, Price J, Bolon B, Silva JP, Wen R, Züchner S. 2014. Characterization of the Mitofusin 2 R94W Mutation in a Knock-in Mouse Model. *J Peripher Nerv Syst*. 164:152–164. doi:10.1111/jns5.12066.

Stuppia G, Rizzo F, Riboldi G, Del Bo R, Nizzardo M, Simone C, Comi GP, Bresolin N, Corti S.

2015. MFN2-related neuropathies: Clinical features, molecular pathogenesis and therapeutic perspectives. *J Neurol Sci*. doi:10.1016/j.jns.2015.05.033.

Suen D, Norris KL, Youle RJ. 2008. Mitochondrial dynamics and apoptosis. (301):1577–1590. doi:10.1101/gad.1658508.GENES.

Sugiura A, Nagashima S, Tokuyama T, Amo T, Matsuki Y, Ishido S, Kudo Y, McBride HM, Fukuda T, Matsushita N, et al. 2013. MITOL regulates endoplasmic reticulum-mitochondria contacts via Mitofusin2. *Mol Cell*. 51(1):20–34. doi:10.1016/j.molcel.2013.04.023.

Susin SA, Zamzami N, Castedo M, Hirsch T, Marchetti P, Macho A, Daugas E, Geuskens M, Kroemer G. 1996. Bcl-2 Inhibits the Mitochondrial Release of an Apoptotic Protease. *J Exp Med*. 184(October):1331–1341.

Suzuki M, Youle RJ, Tjandra N. 2000. Structure of Bax. *Cell*. 103(4):645–654. doi:10.1016/s0092-8674(00)00167-7.

Suzuki Y, Imai Y, Nakayama H, Takahashi K, Takio K, Takahashi R. 2001. A serine protease, HtrA2, is released from the mitochondria and interacts with XIAP, inducing cell death. *Mol Cell*. 8(3):613–621. doi:10.1016/S1097-2765(01)00341-0.

Thaher O, Wolf C, Dey PN, Pouya A, Wüllner V, Tenzer S, Methner A. 2017. The thiol switch C684 in Mitofusin-2 mediates redox-induced alterations of mitochondrial shape and respiration. *Neurochem Int*.:5–11. doi:10.1016/j.neuint.2017.05.009.

Thorpe GW, Fong CS, Alic N, Higgins VJ, Dawes IW. 2004. Cells have distinct mechanisms to maintain protection against different reactive oxygen species: Oxidative-stress-response genes. *Proc Natl Acad Sci*. 101(17):6564–6569. doi:10.1073/pnas.0305888101.

Tondera D, Grandemange S, Jourdain A, Karbowski M, Mattenberger Y, Herzig S, Da Cruz S, Clerc P, Raschke I, Merkwirth C, et al. 2009. SLP-2 is required for stress-induced mitochondrial hyperfusion. *EMBO J*. 28(November 2008):1589–1600. doi:10.1038/emboj.2009.89.

Twig G, Elorza A, Molina AJA, Mohamed H, Wikstrom JD, Walzer G, Stiles L, Haigh SE, Katz S, Las G, et al. 2008. Fission and selective fusion govern mitochondrial segregation and

elimination by autophagy. *EMBO J*. 27(2):433–446. doi:10.1038/sj.emboj.7601963.

Vallat J-M, Ouvrier R a, Pollard JD, Magdelaine C, Zhu D, Nicholson G a, Grew S, Ryan MM, Funalot B. 2008. Histopathological findings in hereditary motor and sensory neuropathy of axonal type with onset in early childhood associated with mitofusin 2 mutations. *J Neuropathol Exp Neurol*. 67(11):1097–1102. doi:10.1097/NEN.0b013e31818b6cbc.

Verhagen AM, Ekert PG, Pakusch M, Silke J, Connonlly LM, Reid GE, Moritz RL, Simpson RJ, Vaux DL. 2000. Identification of DIABLO, a Mammalian Protein that Promotes Apoptosis by Binding to and Antagonizing IAP Proteins. *Cell*. 102(1):43–53. doi:10.1016/S0896-6273(00)80282-2.

Verhoeven K, Claeys KG, Züchner S, Schröder JM, Weis J, Ceuterick C, Jordanova A, Nelis E, De Vriendt E, Van Hul M, et al. 2006. MFN2 mutation distribution and genotype/phenotype correlation in Charcot-Marie-Tooth type 2. *Brain*. 129(8):2093–2102. doi:10.1093/brain/awl126.

Vital A, Vital C. 2012. Mitochondria and peripheral neuropathies. *J Neuropathol Exp Neurol*. 71(12):1036–46. doi:10.1097/NEN.0b013e3182764d47.

Wada J, Nakatsuka A. 2016. Mitochondrial Dynamics and Mitochondrial Dysfunction in Diabetes. *Acta Med Okayama*. 70(3):151–8. doi:10.18926/AMO/54413.

Wallace DC, Fan W, Procaccio V. 2010. Mitochondrial Energetics and Therapeutics. *Annu Rev Pathol Mech Dis*. 5(1):297–348. doi:10.1146/annurev.pathol.4.110807.092314.

Wang C, Youle RJ. 2011. The role of mitochondria in apoptosis. *BMB Rep*. 41(1):11–22. doi:10.5483/bmbrep.2008.41.1.011.

Wang H, Song P, Du L, Tian W, Yue W, Liu M, Li D, Wang B, Zhu Y, Cao C, et al. 2011. Parkin ubiquitinates Drp1 for proteasome-dependent degradation: Implication of dysregulated mitochondrial dynamics in Parkinson disease. *J Biol Chem*. 286(13):11649–11658. doi:10.1074/jbc.M110.144238.

Wang K, Yan R, Cooper KF, Strich R. 2015. Cyclin C mediates stress-induced mitochondrial

fission and apoptosis. *Mol Biol Cell*. 26(6):1030–1043. doi:10.1091/mbc.E14-08-1315.

Wang W, Zhang F, Li L, Tang F, Siedlak SL, Fujioka H, Liu Y, Su B, Pi Y, Wang X. 2015. MFN2 couples glutamate excitotoxicity and mitochondrial dysfunction in motor neurons. *J Biol Chem*. 290(1):168–182. doi:10.1074/jbc.M114.617167.

Wemmie JA, Steggerda SM, Moye-Rowley WS. 1997. The Saccharomyces cerevisiae AP-1 protein discriminates between oxidative stress elicited by the oxidants H 2O 2 and diamide. *J Biol Chem*. 272(12):7908–7914. doi:10.1074/jbc.272.12.7908.

Willems P, Wanschers BFJ, Esseling J, Szklarczyk R, Kudla U, Duarte I, Forkink M, Nooteboom M, Swarts H, Gloerich J, et al. 2013. BOLA1 is an aerobic protein that prevents mitochondrial morphology changes induced by glutathione depletion. *Antioxidants Redox Signal*. 18(2):129–138. doi:10.1089/ars.2011.4253.

Wu S, Zhou F, Zhang Z, Xing D. 2011. Mitochondrial oxidative stress causes mitochondrial fragmentation via differential modulation of mitochondrial fission-fusion proteins. *FEBS J*. 278(6):941–954. doi:10.1111/j.1742-4658.2011.08010.x.

Xiying F, Rajaa H, George A. B. 2013. H2O2-induced mitochondrial fragmentation in C2C12 myocytes. *Free Radic Biol Med*. 18(9):1199–1216. doi:10.1016/j.micinf.2011.07.011.Innate.

Xu K, Chen G, Li X, Wu X, Chang Z, Xu J, Zhu Y, Yin P, Liang X, Dong L. 2017. MFN2 suppresses cancer progression through inhibition of mTORC2/Akt signaling. *Sci Rep*. 7(February):1–13. doi:10.1038/srep41718.

Yan L, Qi Y, Huang X, Yu C, Lan L, Guo X, Rao Z, Hu J, Lou Z. 2018. Structural basis for GTP hydrolysis and conformational change of MFN1 in mediating membrane fusion. *Nat Struct Mol Biol*. 25(3):233–243. doi:10.1038/s41594-018-0034-8.

Yang J, Zhang Y. 2015. I-TASSER server: New development for protein structure and function predictions. *Nucleic Acids Res*. 43(W1):W174–W181. doi:10.1093/nar/gkv342.

Yesylevskyy SO, Kharkyanen VN, Demchenko AP. 2006. Dynamic protein domains: Identification, interdependence, and stability. *Biophys J*. 91(2):670–685.

doi:10.1529/biophysj.105.078584.

Yoon Y-S, Yoon D-S, Lim IK, Yoon S-H, Chung H-Y, Rojo M, Malka F, Jou M-J, Martinou J-C, Yoon G. 2006. Formation of Elongated Giant Mitochondria in DFO-Induced Cellular Senescence: Involvement of Enhanced Fusion Process Through Modulation of Fis1. *J Cell Physiol*. 209(1):468–480. doi:10.1002/JCP.

Zahedi A, Phandthong R, Chaili A, Leung S, Omaiye E, Talbot P. 2019. Mitochondrial Stress Response in Neural Stem Cells Exposed to Electronic Cigarettes. *iScience*. 16:250–269. doi:10.1016/j.isci.2019.05.034.

Zhang G-E, Jin H-L, Lin X-K, Chen C, Liu X-S, Zhang Q, Yu J-R. 2013. Anti-tumor effects of mfn2 in gastric cancer. *Int J Mol Sci*. 14:13005–21. doi:10.3390/ijms140713005.

Zhang Y. 2009. I-TASSER: Fully automated protein structure prediction in CASP8. *Proteins Struct Funct Bioinforma*. 77(SUPPL. 9):100–113. doi:10.1002/prot.22588.

Zheng M, Xiao RP. 2010. Role of mitofusin 2 in cardiovascular oxidative injury. *J Mol Med*. 88(10):987–991. doi:10.1007/s00109-010-0675-5.

Zhou Y, Lutz CM, Baloh RH, Zhou Y, Carmona S, Muhammad AKMG, Bell S, Landeros J, Vazquez M, Ho R, et al. 2019. Restoring mitofusin balance prevents axonal degeneration in a Charcot-Marie-Tooth type 2A model Graphical abstract Find the latest version : Restoring mitofusin balance prevents axonal degeneration in a Charcot-Marie-Tooth type 2A model.

Zorov DB, Filburn CR, Klotz LO, Zweier JL, Sollott SJ. 2000. Reactive oxygen species (ROS)-induced ROS release: A new phenomenon accompanying induction of the mitochondrial permeability transition in cardiac myocytes. *J Exp Med*. 192(7):1001–1014. doi:10.1084/jem.192.7.1001.

Züchner S, Mersiyanova I V, Muglia M, Bissar-Tadmouri N, Rochelle J, Dadali EL, Zappia M, Nelis E, Patitucci A, Senderek J, et al. 2004. Mutations in the mitochondrial GTPase mitofusin 2 cause Charcot-Marie-Tooth neuropathy type 2A. *Nat Genet*. 36(5):449–451. doi:10.1038/ng1341.

Chapter 3: Mfn2 and oxidative stress

3.1 Introduction

Mitochondria are a hub of cellular stress response (Labbé, Murley, and Nunnari 2014). The most well-known of the mitochondrial stress-related roles is arguably the sequestration and regulated release of pro-apoptotic factors such as cytochrome C, Smac/DIABLO, AIF, and HtrA2 to commit the cell to apoptosis in response to stress (Liu et al. 1996; Susin et al. 1996; Du et al. 2000; Verhagen et al. 2000; Suzuki et al. 2001). During stressful conditions that are severe, prolonged, or result in mitochondrial membrane depolarization, mitochondrial generally become fragmented (Shutt and McBride 2013). This fragmentation helps facilitate efficient cytochrome c release and apoptosis as well as effective clearance of damaged mitochondria by mitophagy (Suen, Norris, and Youle 2008; Twig et al. 2008). During mild stresses, however, mitochondria tend to become highly connected which is correlated with increased ATP production and decreased mitophagy (Tondera et al. 2009; Gomes, Benedetto, and Scorrano 2011; Rambold et al. 2011). Highly connected mitochondria have been reported after a variety of stressful conditions including starvation, UV irradiation, and multiple drug treatments (Tondera et al. 2009; Lebeau et al. 2018; Zahedi et al. 2019). Thus, mitochondrial dynamics are vital to efficient responses to stress at all intensities, allowing the mitochondria to increase respiration and ATP production to deal with mild stresses and facilitate pro-apoptotic factors during severe or prolonged stress.

As one of the main sources of reactive oxidative species (ROS) in cells, mitochondria have a unique requirement to deal with oxidative stress and changes in the local redox state. Mitochondria generate superoxide from the electron transport chain at complex I and III. Superoxide is dismutated by superoxide dismutase (SOD) into hydrogen peroxide (H_2O_2) in either the mitochondrial matrix (SOD2) or cytosol (SOD1). One of the main ways H_2O_2 is reduced to H_2O is by the oxidation of glutathione (GSH) to its oxidized form (GSSG) by

glutathione peroxidase. Thus, the ratio of GSH:GSSG in the cell can be seen as a proxy for the redox state of the cell. During normal conditions in most cell types, the intracellular (cytosolic) GSH:GSSG ratio is on the order of magnitude of 100:1 (Slivka et al. 1987; Østergaard et al. 2004). However, during times of oxidative stress, this ratio can decrease dramatically (Gilbert 1995; Giustarini et al. 2009; James et al. 2009; Giustarini et al. 2017). This system maintains the cellular redox environment but can be overwhelmed during times of oxidative stress created by extracellular or mitochondrial ROS. When this happens, the excess H_2O_2 goes on to cause oxidative damage to DNA, lipids, and proteins throughout the cell. Changes in mitochondrial morphology have been associated with oxidative stress conditions, but the morphological response does not appear uniform. Both fragmented and hyperfused mitochondrial morphology have been reported upon induction of oxidative stress by different methods in various cell types (Yoon et al. 2006; Jendrach et al. 2008; Wu et al. 2011; Shutt et al. 2012; Redpath et al. 2013; Willems et al. 2013; Iqbal and Hood 2014; K. Wang et al. 2015; Thaher et al. 2017). One study that reported increased mitochondrial connectivity after oxidative stress and suggest that this is dependent on the regulated formation of disulfide bonds involving cysteines of Mfn2 (Shutt et al. 2012). One of the mutations that I had screened in the domain scanning study resulted in altering a cysteine in Mfn2 to an arginine. The replacement of cysteine at this position by phenylalanine has also been associated with CMT2A (Feely et al. 2011). Thus, the cysteine at amino acid position 390 is likely important for Mfn2 function as mutating this sulfur-containing amino acid to either a basic or bulky aromatic amino acid both cause disease. Therefore, I decided to build upon existing studies to discover how oxidative stress might affect Mfn2 and mitochondrial morphology and whether the response is dependent on the cysteine at amino acid position 390.

3.2 Methods

3.2.1 Cell line generation

Mouse Mfn2 cDNA fused to a FLAG epitope tag was inserted into pBABE-hygro (Addgene #1765) multiple cloning site by restriction enzyme digest. Mutations were introduced to the Mfn2 retroviral vector by PCR-based site directed mutagenesis followed by Gibson assembly or restriction enzyme digest followed by ligation. Plasmids were transfected into retroviral packaging PlatE cells (Cell Biolabs) by FuGENE™ HD transfection reagent (Promega). Viral supernatant was applied to Mfn2-null mouse embryonic fibroblasts (MEFs) at 48 and 72 hours post transfection in the presence of 8 mg/ml polybrene. Approximately 24 hours after the final infection, cells that incorporated the plasmid were selected by addition of 200 μg/mL hygromycin to the media for 2-3 days.

Cells expressing the plasmid were plated at low density and clusters of cells each derived from a single cell were collected onto sterile filter paper dots soaked in trypsin and expanded. After expansion, cells were lysed in RIPA buffer (25 mM Tris-HCl pH 7.6; 150 mM NaCl; 1% NP-40; 1% sodium deoxycholate; 0.1% SDS) and the lysate was separated by SDS-PAGE and transferred to nitrocellulose membrane. The membrane was then probed with anti-Mfn2 antibody to determine the expression level of Mfn2. Tubulin was used as a loading control to compare MFn2 expression levels to that of wild type cells. Cells expressing Mfn2-FLAG at .8-3x of wild type were selected for further characterization.

3.2.2 Western blot

Samples were run on an SDS-PAGE gel and transferred onto nitrocellulose at 100 V for 50 minutes in 1X transfer buffer (25 mM Tris, 192 mM glycine, 20% methanol). Membranes were blocked in 4% milk for at least 45 minutes and were probed with anti-Mfn1, anti-Mfn2 (Sigma),

anti-EIF2a (Cell Signaling Technology), anti-phospho-EIF2a (Cell Signaling Technology), anti-Caspase 3 (Cell Signaling Technology), or anti-αTubulin (Invitrogen) antibody for 4 hours at room temperature or overnight at 4°C. Membranes were incubated with DyLight secondary antibody (Invitrogen) at room temperature for 1 hour. Membranes were imaged on LI-COR Imaging System (LI-COR Biosciences).

3.2.3 Microscopy

All cells were plated in No. 1.5 glass-bottomed dishes (MatTek). Mouse embryonic fibroblasts were incubated with 0.1 μg/mL Mitotracker Red CMX Ros (Invitrogen) for 15 minutes at 37°C with 5% CO_2, washed and incubated with complete media with no drug, diamide, or H_2O_2 prior to imaging. MEFs were imaged at 37°C with 5% CO_2. A Z-series with a step size of 0.3 μm was collected with a Nikon Ti-E widefield microscope with a 63X NA 1.4 oil objective (Nikon), a solid-state light source (Spectra X, Lumencor), and an sCMOS camera (Zyla 5.5 Megapixel). Each cell line was imaged by a blinded researcher on at least three separate occasions (n > 100 cells per experiment).

3.2.4 Image analysis

Images were deconvolved using 8-15 iterations of 3D Landweber deconvolution. Deconvolved images were then analyzed using Nikon Elements software. Maximum intensity projections were created using Photoshop (Adobe). Mitochondrial morphology was scored as follows: reticular indicates that fewer than 30% of the mitochondria in the cell were fragments (fragments defined as mitochondria less than 2 μm in length); fragmented indicates that most of the mitochondria in the cell were less than 2 μm in length; aggregated indicates fragmented mitochondria that were not distributed throughout the cytosol.

3.2.5 In vitro mitochondrial fusion

An equivalent mass (12.5 μg) of mtTagRFP and mtCFP mitochondria were mixed, washed in 500uL MIB and concentrated by centrifugation (7400 × *g*, 10 min, 4°C). Following a 10 min incubation on ice, the supernatant was removed and the mitochondrial pellet was resuspended in 10 μl fusion buffer (20mM PIPES-KOH [pH 6.8], 150mM KOAc, 5mM $Mg(OAc)_2$, 0.4M sorbitol, 0.12 mg/ml creatine phosphokinase, 40mM creatine phosphate, 1.5mM ATP, 1.5mM GTP) or 10 μl cytosol-enriched buffer (2.5 μL of the cytosol-enriched fraction obtained from WT MEFs and 7.5 μL fusion buffer) with or without 1 mM oxidized or reduced glutathione (GSSG or GSH). Fusion reactions were incubated at 37°C for 60 minutes.

3.2.6 Analysis of in vitro mitochondrial fusion

Mitochondria were imaged on depression microscope slides by pipetting 4 μL fusion reaction onto a 3% low-melt agarose bed, made in modified fusion buffer (20 mM PIPES-KOH [pH 6.8], 150 mM KOAc, 5 mM $Mg(OAc)_2$, 0.4 M sorbitol). A Z-series of 6 0.2 μm steps was collected with a Nikon Ti-E widefield microscope with a 100X NA 1.4 oil objective (Nikon), a solid state light source (Spectra X, Lumencor), and a sCMOS camera (Zyla 5.5 Megapixel). For each condition tested, mitochondrial fusion was assessed by counting ≥ 300 total mitochondria per condition from ≥ 4 images per condition (50 – 200 mitochondria per image collected), and fusion was scored by colocalization of the red and cyan fluorophores in three dimensions.

3.2.7 Biochemical studies of GSSG and Mfn2

Isolated mitochondria (30 μg) were incubated with or without 1.5 mM GTP and with or without 0.5 mM GSSG in fusion buffer at 37°C for 1 hr. Mitochondria were lysed in laemmli buffer (0.06 M Tris-HCl pH 6.8; 2.5% SDS; 5% beta mercaptoethanol; 5% sucrose; 0.004% bromophenol

blue), loaded on a 3-8% NuPAGE Tris-Acetate gel (Fisher Scientific), and processed by western blot.

3.3 Results

3.3.1 Mitochondrial fusion in vitro depends on the redox state of the environment and is altered by amino acid substitutions

It has been previously reported that an oxidizing environment induced by oxidized glutathione (GSSG) increases the fusion activity of mitochondria with wild type Mfn2, while a reducing environment decreases fusion efficiency (Shutt et al. 2012). I was able to repeat this finding, although to a much smaller degree than that shown in the previous study (Figure 3.1A). I observed a ~10% increase in mitochondrial fusion compared to the 100% increase seen in the comparable experiment by Shutt and colleagues (2012). This may be explained by technical differences in the assays used to analyze fusion between our groups. The 2012 study used a split luciferase plate-reader assay while I used a two-fluorophore fluorescence microscopy assay. Additionally, the mitochondria in the 2012 study were incubated at a concentration of 4 μg/μL while the mitochondria in my assay are incubated at 2.5 μg/μL. Shutt reported that the increase in fusion due to GSSG was dependent on mitochondrial concentration. At a mitochondrial concentration of 1 μg/μL, they saw no stimulation by GSSG and at 10 μg/μL the stimulation was reduced to approximately 30% above the basal reaction (Shutt et al. 2012). Thus, an increase of 10% fusion efficiency is not out of line with previously reported data.

To determine whether the cysteine at position 390 mediates the increase in mitochondrial fusion in vitro, I performed the same experiment with mitochondria isolated from Mfn2-null mouse embryonic fibroblasts
stably expressing one of the two disease-associated reported mutations of C390 in Mfn2: C390R and C390F. The mitochondria with $Mfn2_{C390R\ or\ F}$ exhibited lower rates of fusion when incubated in an oxidizing environment compared to both wild type mitochondria and the same

mitochondria at basal conditions (Figure 3.1A). Thus, not only does the cysteine at position 390 facilitate the increase in fusion, alteration of this cysteine reverses the phenotype.

To more closely mimic the cellular environment, I repeated this assay in buffer including cytosol-enriched fraction. As previously reported, the addition of cytosol increased fusion rates in all populations of mitochondria I examined (Hoppins et al. 2011; Shutt et al. 2012; Engelhart and Hoppins 2019). To determine whether the redox environment in the context of cytosol altered fusion activity in these mitochondria, I performed the cytosol-enriched fusion reaction with either 1uM GSSG or 1uM GSH. Wild type mitochondria demonstrated increased fusion in cytosol-stimulated oxidative conditions (GSSG), but lower fusion activity when incubated in a cytosol-stimulated reducing environment (GSH) (Figure 3.1B). This is consistent with the results from the assay without cytosol. Also consistent with previous results Mfn2$_{C390R/F}$ displayed a reversed pattern of fusion efficiency compared to wild type controls in the presence of cytosol-enriched fraction (Figure 3.1B). Mitochondria with both variants displayed lower fusion when incubated with cytosol and oxidized glutathione (GSSG), and Mfn2$_{C390R}$ resulted in mitochondria that fused more efficiently with reduced glutathione (GSH) (C390F was not tested). This indicates that the response of Mfn2 to the redox environment is altered by mutation of this cysteine and that this alteration persists, but its magnitude is reduced (~40% reduction in fusion without cytosol versus ~25%

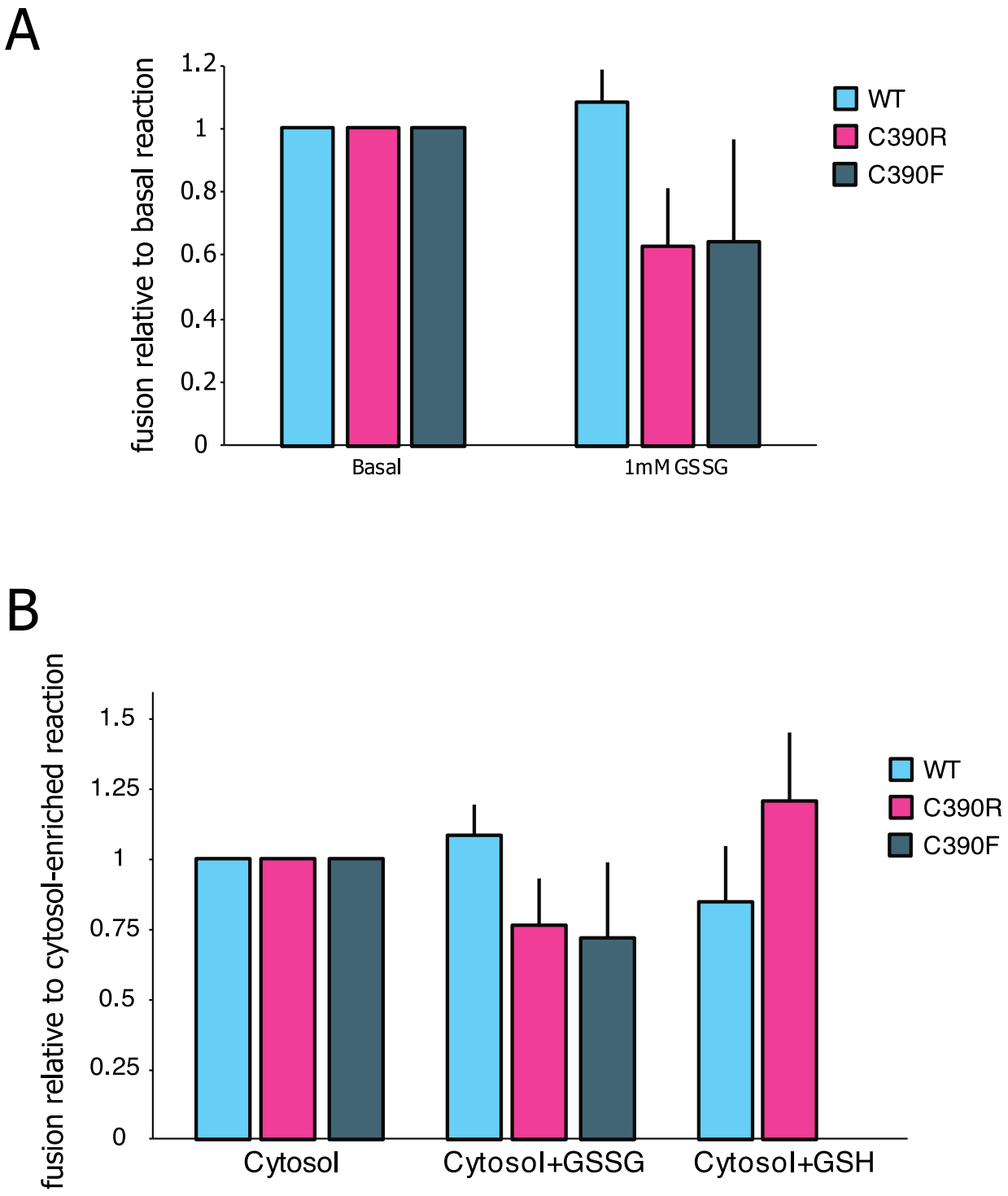

Figure 3.1. Effect of redox environment on mitochondrial fusion in vitro.
A) Mitochondria were isolated from wild type cells or clonal populations of Mfn2-null cells transduced with the indicated Mfn2 variant. The mitochondria were subjected to the in vitro fusion conditions at 37°C for 60 minutes with or without 1mM GSSG. The data are represented as relative to basal fusion reactions performed in parallel. Error bars indicate mean + standard deviation from at least three independent experiments.

Figure 3.1, cont. B) The same mitochondria from A were subjected to in vitro fusion conditions including cytosol enriched fraction with or without 1mM GSSG or GSH. The data are represented as relative to cytosol enriched fusion reactions performed in parallel. Error bars indicate mean + standard deviation from at least three independent experiments.

reduction in fusion with cytosol) in the presence of cytosol. This could be due to a direct effect of a specific cytosolic factor on Mfn2 or to the fact that the cytosol is a largely reducing environment, thus shifting the redox potential in the in vitro fusion reaction toward less oxidating in these experiments. The latter explanation is refuted by the equal increase in mitochondrial fusion facilitated by wild type Mfn2 seen in the GSSG-containing buffer with or without cytosol (both were ~9%). Therefore, I favor the explanation that specific cellular factor(s) are responsible for mitgating the inhibitory effect of GSSG on $Mfn2_{C390R\ or\ F}$-mediated mitochondrial fusion.

3.3.2 Biochemical assessment of Mfn2 in an oxidizing environment

There is evidence that, when exposed to an oxidizing environment, Mfn2 forms oligomeric species detectable by analysis on a non-reducing gel (Shutt et al. 2012). These species are likely due to the formation of intermolecular disulfide bonds, as the higher molecular weight species are significantly larger than the monomeric form of Mfn2 (Shutt, et al. 2012). Because the in vitro fusion assay suggested that $Mfn2_{C390R\ or\ F}$ behave differently in oxidizing environments than $Mfn2_{WT}$, I decided to examine whether the loss of this cysteine affects the ability of Mfn2 to form oligomeric species when oxidized. I tested this question by examining the assembly state of Mfn2 protein from isolated mitochondria by non-reducing gel. In this experiment, wild type Mfn2 did indeed form larger (~170 kDa), likely oligomeric species when incubated with the oxidizing agent GSSG (Figure 3.2A). There were no significant differences in the presence of higher molecular weight species between wild type Mfn2 and $Mfn2_{C390R}$ after GSSG treatment (Figure 3.2B). If these species are assumed to represent interactions mediated by disulfide

bonds, this finding would indicate this cysteine is not directly involved in disulfide bonds involving Mfn2 in oxidative stress conditions. it may be involved in conformational states or changes that responds to oxidative stress. Somewhat surprisingly, in the untreated condition, an appreciable amount of $Mfn2_{C390R}$ migrated as a group of oligomeric species of approximately the same size, but not the same pattern as those induced by GSSG treatment (Figure 3.2). This pattern was not seen in wild type Mfn2. This could be interpreted to mean that C390 is important for maintaining appropriate conformational states of Mfn2, and when it is altered, Mfn2 favors a conformation that facilitates interactions (perhaps mediated by disulfide bonds) that are different than those made upon oxidative stress induction. These interactions could be different in terms of the identities of the proteins involved and/or the conformations of these proteins.

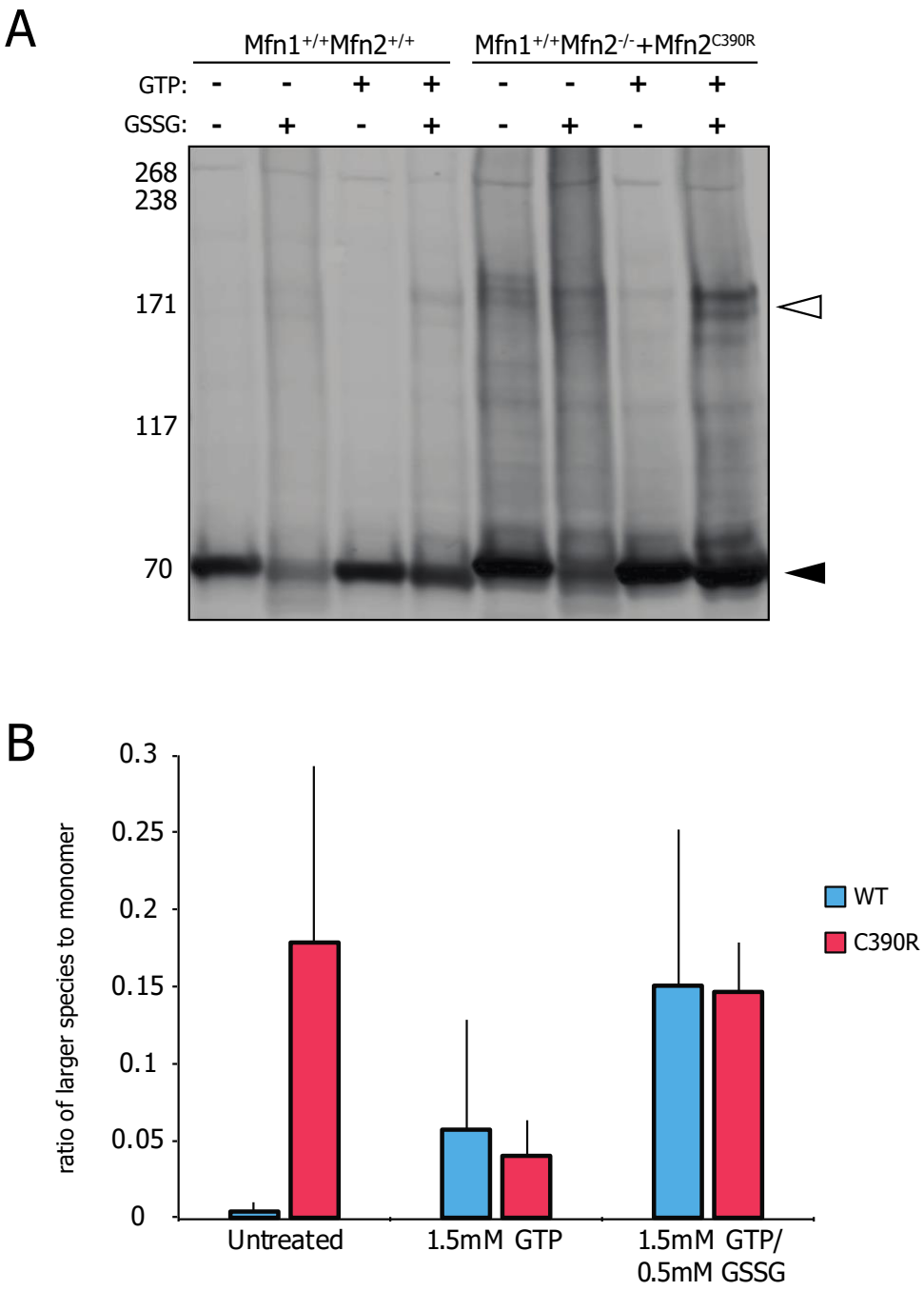

Figure 3.2. Mfn2 forms oligomeric assemblies when exposed to oxidizing conditions.
A) Mitochondria were isolated from wild type cells or clonal populations of Mfn2-null cells transduced with Mfn2$_{C390R}$. Mitochondria were incubated with either nucleotide or nucleotide and oxidized glutathione at 37°C for 1 hr. Analysis under non-reducing conditions revealed both monomeric (filled arrowhead) and oligomeric (outlined arrowhead) species of Mfn2 **B**) Quantification of the data described in A. The amount of signal in the larger species was divided by that in the monomeric species. Error bars equal mean + standard deviation from at least three independent experiments.

3.3.3 Oxidative stress and mitofusin-dependent mitochondrial morphology

I next decided to see if the in vitro results I observed were recapitulated by morphological differences in cells. I treated mouse embryonic fibroblasts expressing wild type Mfn2, no Mfn2, or Mfn2$_{C390R \text{ or } F}$ stably transduced into an Mfn2-null background with two different oxidative stressors. Hydrogen peroxide (H_2O_2) is a general oxidizing agent that damages proteins, lipids, and DNA at high concentrations, but acts as a signaling molecule involved in maintaining homeostasis and adapting to stress at lower concentrations (Sena and Chandel 2012). Excess H_2O_2 would lead to a decrease in the GSH:GSSG ratio through its reaction with glutathione peroxidases. Diamide is a more specific thiol oxidizer that targets GSH quickly and preferentially (Kosower et al. 1969) and thus directly shifts the GSH:GSSG ratio down.

When treated with H_2O_2, mitochondria in all cells became mainly fragmented (Figure 3.3), representing a shift in the balance of fusion and division toward the latter. Indeed, treatment with hydrogen peroxide has been shown to activate Drp1 (Iqbal and Hood 2014; K. Wang et al. 2015; Kim et al. 2018). Conversely, diamide treatment resulted in a hyperconnected network in wild type cells (Figure 3.3). This finding was not particularly surprising because of the variation of mitochondrial morphology previously reported in response to these two stressors. Most studies that used H_2O_2 reported fragmented mitochondria (Jendrach et al. 2008; Xiying et al. 2013; Iqbal and Hood 2014; Thaher et al. 2017), while studies that used diamide to induce oxidative stress more commonly reported increased mitochondrial connectivity (Shutt et al. 2012; Redpath et al. 2013). Differential responses to unique inducers of oxidative stresses have been reported before, (Wemmie et al. 1997; Delaunay et al. 2000; Thorpe et al. 2004; Pócsi et al. 2005), but my study represents the first examination of mitochondrial morphology after both H_2O_2 and diamide treatments and is the first to count mitochondrial morphology among the group of outcomes uniquely regulated by different inducers of oxidative stress.

Cells lacking Mfn2 displayed very little fusion after diamide treatment (Figure 3.3), indicating that Mfn2 is required for mitochondrial fusion induced by oxidative stress due to diamide. Both $Mfn2_{C390R}$ and $Mfn2_{C390F}$ displayed a similar proportion of cells with hyperfused mitochondria

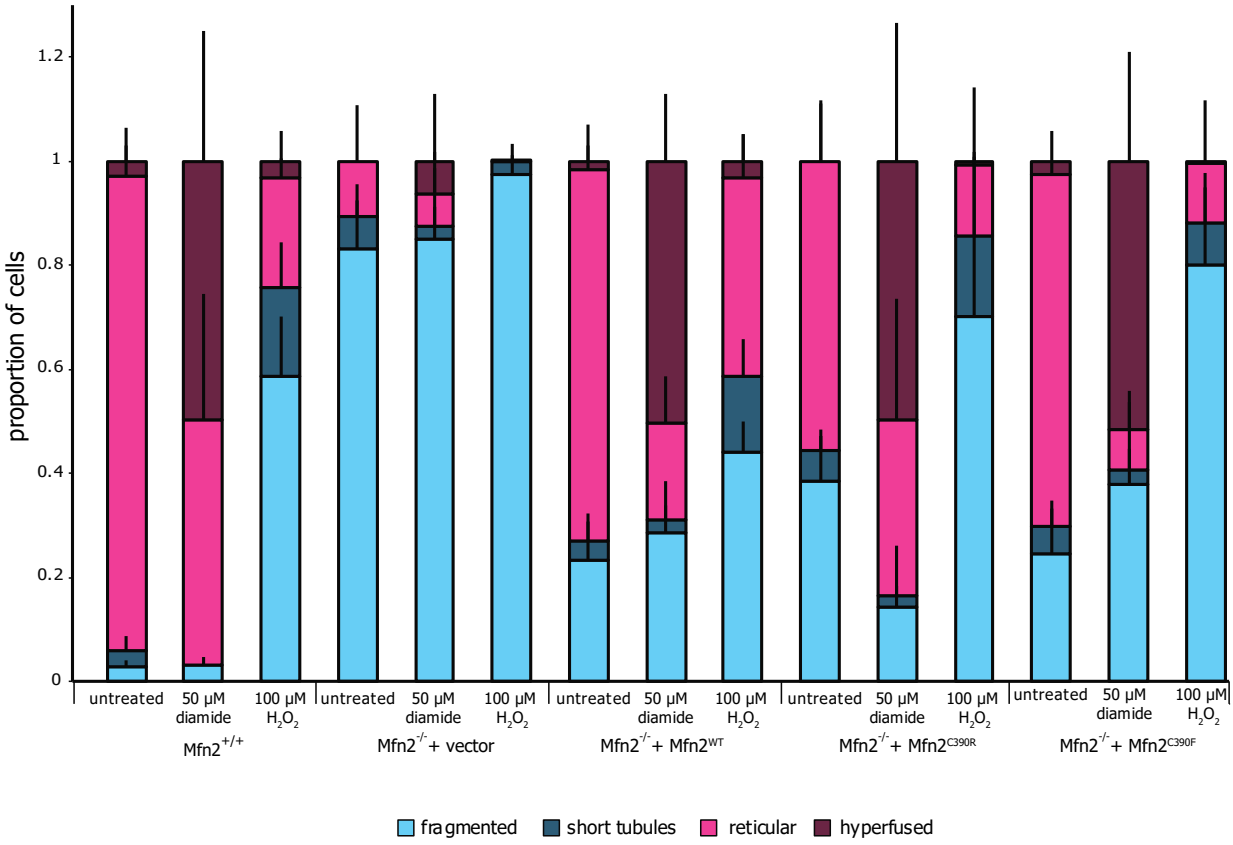

Figure 3.3. Mitochondrial morphology in cells exposed to oxidative stress. Quantification of mitochondrial networks in wild type ($Mfn2_{+/+}$) or Mfn2-null ($Mfn2_{-/-}$) mouse embryonic fibroblasts expressing the indicated Mfn2 variant. Cells were either untreated, treated with 50 µM diamide for one hour or 100 µM H_2O_2 for two hours. Mitochondria were stained with Mitotracker Red CMXRos before drug treatment and visualized by fluorescence microscopy. Error bars indicate mean + standard deviation from three blinded experiments (n ≧ 100 cells per population per experiment).

with diamide treatment as wild type (Figure 3.3). These results suggest that the cellular environment obfuscates the inhibition of fusion seen under oxidative conditions in vitro which was unexpected as addition of cytosol enriched fraction to the in vitro fusion assay did not alter the inhibition of fusion of Mfn2$_{C390R\ or\ F}$ mitochondria by GSSG (compare to Figure 3.1). This could indicate that the hyperfusion response in cells is dependent on factors or conditions that are present in whole cells but not in the fusion assay which allow both wild type Mfn2 and Mfn2$_{C390R\ or\ F}$ to facilitate increased fusion. The finding that the loss of cysteine at this position does not block mitochondrial hyperfusion after diamide treatment indicates that this response does not depend on disulfide bonds involving this site. However, the cell-free fusion results indicate that without the contribution of some cytosolic factor, these variants of Mfn2 are inhibited by oxidative conditions. The addition of cytosol to this assay somewhat mitigated this inhibition (Figure 3.1). Thus, the finding that Mfn2$_{C390R\ or\ F}$ does not prevent diamide-responsive hyperfusion is not completely unexpected. Diamide treatment increased the proportion of both fragmented and hyperfused mitochondrial networks in cells expressing Mfn2$_{C390R\ or\ F}$. In wild type cells, diamide increased hyperfused networks only. This may indicate that both the fusion and division machinery are activated upon diamide-induced stress, but wild type Mfn2 activation is stronger than Drp1 activation, while Mfn2$_{C390R\ or\ F}$ activation is not as overpowering. This activation could be due to post translational modifications. Drp1 has already been shown to be post-translational modified during oxidative stress. Perhaps Mfn2 is also modified upon oxidative stress, and the difference in conformational states proposed above impacts the ability of Mfn2 to be modified.

An alternative explanation for the differences in findings among my assays is that the final redox potential in each assay is likely different. Future work could focus on ensuring that comparisons are made between assays at the same redox potential.

3.3.4 Diamide-induced hyperfusion is dependent on Mfn2 rather than Mfn1

Because Mfn2-null cells did not display an increase in mitochondrial connectivity with diamide treatment, I decided to test whether the hyperfusion in this stress condition could be assigned specifically to Mfn2 versus Mfn1. This would be a novel finding as stress induced hyperfusion was originally described to be facilitated by Mfn1 rather than Mfn2 (Tondera et al. 2009). The results of a pilot study suggest that oxidative stress-induced hyperfusion is indeed mediated

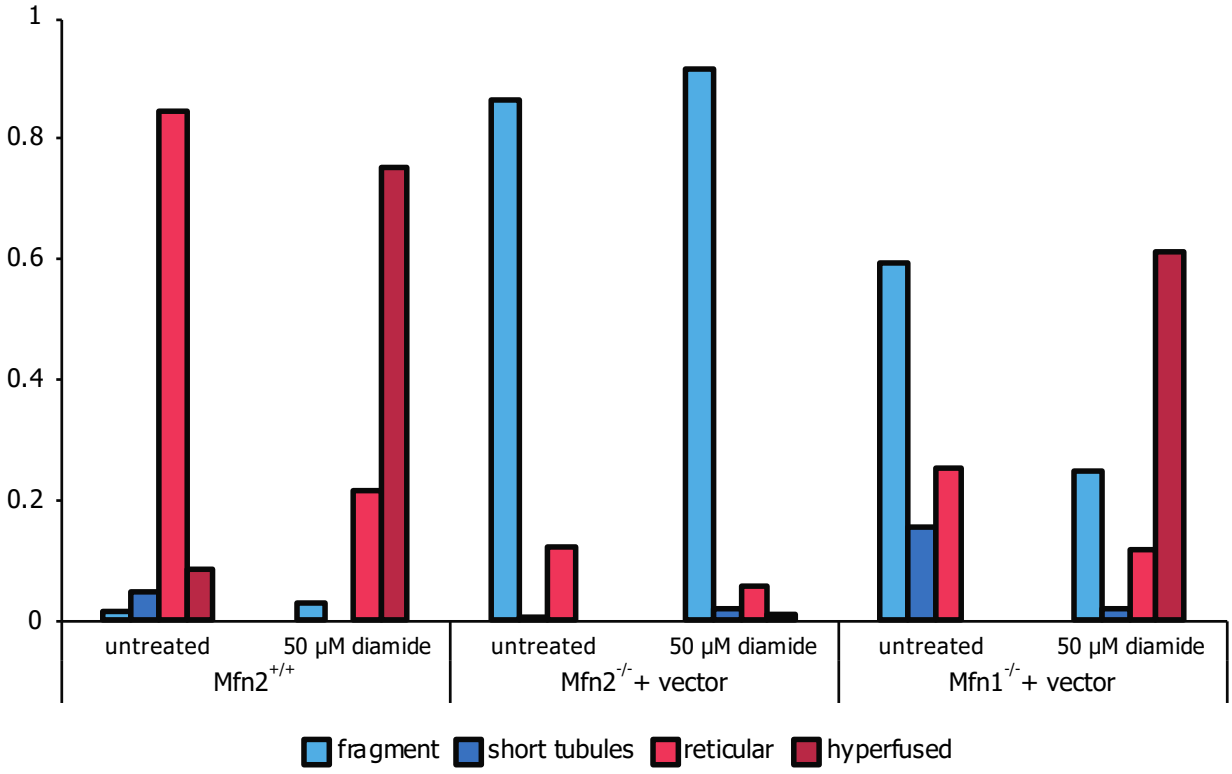

Figure 4. Mitofusin 2-mediated response of mitochondrial morphology to oxidative stress.
Quantification of mitochondrial networks in wild type (Mfn2$_{+/+}$), Mfn2-null (Mfn2$_{-/-}$), or Mfn1-null (Mfn1$_{-/-}$) mouse embryonic fibroblasts. Cells were either untreated or treated with 50 μM diamide for one hour. Mitochondria were stained with Mitotracker Red CMXRos before drug treatment and visualized by fluorescence microscopy.

specifically by Mfn2. When treated with diamide, Mfn2-null cells displayed very little hyperfusion, while Mfn1-null cells frequently contained hyperfused mitochondria (Figure 3.4).

3.4 Conclusions/Discussion

This analysis in this chapter is consistent with the hypothesis that Mfn2 plays a role in the mitochondrial response to oxidative stress. Additionally, $Mfn2^{C390R \text{ or } F}$ seem to react differently to certain oxidative stressors than $Mfn2^{WT}$ in vitro. In vitro fusion analysis indicated that this difference is more clearly seen in the absence of the cellular milieu. This could be due to differences in the redox potential seen by the mitochondria in the two assays, or to a cellular factor that enhances the effect of oxidative stress on Mfn2, perhaps a post-translational modification. The latter explanation is supported by the finding that the increase in fusion rate of wild type mitochondria seen in vitro is much smaller than the significant hyperfusion seen in the cellular analysis. I could test this hypothesis by isolating Mfn2 (and/or Drp1) from cells under control conditions or oxidative stress and using mass spectrometry to find post translational modifications. An attractive first PTM to target would be glutathionylation, which has been reported to be increased during periods of oxidative stress (Grek et al. 2013).

Biochemical analysis revealed that there were differences in the oligomeric species formed by either $Mfn2^{WT}$ or $Mfn2^{C390R}$ in untreated mitochondria but not upon oxidizing treatment of isolated mitochondria. The work reported here as well as previously (Shutt, et al. 2012) suggest that these stress-induced oligomers are essential for Mfn2-mediated hyperfusion. The ability of $Mfn2^{C390R}$ to form the same oligomeric species as $Mfn2^{WT}$ in this assay agrees with the result that $Mfn2^{C390R}$ can support mitochondrial hyperfusion in cells. The assembly difference seen in untreated conditions may help explain the difference in fusion rates seen by these isolated mitochondria if cytosolic factors help $Mfn2^{C390R}$ to transition from the untreated assembly

pattern to the oxidative stress-induced assembly pattern. Future work could focus on determining the composition of these oligomeric species. The identification of the proteins involved in these oligomers would provide knowledge of how Mfn2 is regulated during oxidative stress.

The changes in the response of Mfn2 to oxidative stress seen in vitro cannot be linked to disulfide bonds involving C390 because there was no difference in Mfn2 assembly in isolated mitochondria or in mitochondrial morphology between wild type and C390 variants under oxidative stress. If this difference is not due to alterations in the disulfide binding profile of Mfn2, it could be due to the aforementioned potential post translation modifications or changes in the protein's conformation. C390 is located near a predicted hinge region of Mfn2, so altering this residue may change the functioning of this hinge. An alteration in conformational state or changes could lead to a difference in the assembly patterns of the protein, explaining the biochemical results. Hinge region mutations were also implicated in the first study to test the mechanism of oxidative stress-induced mitochondrial hyperfusion (Shutt, et al. 2012), so this hypothesis has a precedent in the literature. I could test this hypothesis by characterizing the response of other reported variants in or near this hinge (see Chapter 4 for examples) to oxidative stress and determining whether they behave similarly to $Mfn2^{C390R \text{ or } F}$. See Chapter 4 for a more in-depth discussion of this proposed hinge in Mfn2.

My results also contribute to a current debate in the field regarding the structure and function of the C-terminus of Mfn2. This region has been hypothesized to function as a tether (see Chapter 2 for more discussion), as a vital structural element of HB1, or as a responder to oxidative stress that resides in the intermembrane space. Proponents of this final hypothesis suggest that C-terminal tags interfere with the ability of the protein to be imported in the correct conformation and leads to the positioning outside the mitochondria. They also argue that this alternative

placement does not interfere with Mfn2 fusion activity but that residence of the Mfn2 C-terminus is required for redox regulation of Mfn2 (Mattie et al. 2018). All of my analyses involving the $Mfn2_{C390R \text{ or } F}$ variants involved a C-terminal FLAG tag, and both these proteins did demonstrate increased fusion after oxidative stress in cells. This indicates that either the tag does not alter the location of the Mfn2 C-terminus or that localization to the mitochondrial intermembrane space is not required for redox regulation of Mfn2.

Finally, this study contributed the valuable insight that hyperfusion due to oxidative stress seems to occur via Mfn2 rather than Mfn1. This would be the first stressor examined that shows this pattern. Mfn1 has one more cysteine than Mfn2, and only half of the cysteines are conserved between Mfn1 and Mfn2. Therefore, it is possible that oxidative conditions have different effects on the disulfide bonding profile of these two proteins that render Mfn1 unable to facilitate fusion.

3.5 References

Atkins K, Dasgupta A, Chen K, Mewburn J, Archer SL. 2016. The role of Drp1 adaptor proteins MiD49 and MiD51 in mitochondrial fission : implications for human disease. :1861–1874. doi:10.1042/CS20160030.

Baloh RH, Schmidt RE, Pestronk A, Milbrandt J. 2007. Altered axonal mitochondrial transport in the pathogenesis of Charcot-Marie-Tooth disease from mitofusin 2 mutations. *J Neurosci*. 27(2):422–430. doi:10.1523/JNEUROSCI.4798-06.2007.

Bian X, Xu J, Zhao H, Zheng Q, Xiao X, Ma X, Li Y, Du X, Liu X. 2019. Zinc-Induced SUMOylation of Dynamin-Related Protein 1 Protects the Heart against Ischemia-Reperfusion Injury. *Oxid Med Cell Longev*. 2019:1–11. doi:10.1155/2019/1232146.

Brandt T, Cavellini L, Kühlbrandt W, Cohen MM. 2016. A mitofusin-dependent docking ring complex triggers mitochondrial fusion in vitro. *Elife*. 5:1–23. doi:10.7554/eLife.14618.

de Brito OM, Scorrano L. 2008. Mitofusin 2 tethers endoplasmic reticulum to mitochondria. *Nature*. 456(7222):605–10. doi:10.1038/nature07534.

Cairns RA, Harris IS, Mak TW. 2011. Regulation of cancer cell metabolism. *Nat Rev Cancer*. 11(2):85–95. doi:10.1038/nrc2981.

Calvo J, Funalot B, Ouvrier R a, Lazaro L, Toutain A, De Mas P, Bouche P, Gilbert-Dussardier B, Arne-Bes M-C, Carrière J-P, et al. 2009. Genotype-phenotype correlations in Charcot-Marie-Tooth disease type 2 caused by mitofusin 2 mutations. *Arch Neurol*. 66(12):1511–1516. doi:10.1001/archneurol.2009.284.

Cao Y-L, Meng S, Chen Y, Feng J-X, Gu D-D, Yu B, Li Y-J, Yang J-Y, Liao S, Chan DC, et al. 2017. MFN1 structures reveal nucleotide-triggered dimerization critical for mitochondrial fusion. *Nature*.:1–5. doi:10.1038/nature21077.

Cartoni R, Arnaud E, Médard JJ, Poirot O, Courvoisier DS, Chrast R, Martinou JC. 2010. Expression of mitofusin 2R94Q in a transgenic mouse leads to Charcot-Marie-Tooth neuropathy type 2A. *Brain*. 133(5):1460–1469. doi:10.1093/brain/awq082.

Cartoni R, Martinou JC. 2009. Role of mitofusin 2 mutations in the physiopathology of Charcot-Marie-Tooth disease type 2A. *Exp Neurol*. 218(2):268–273. doi:10.1016/j.expneurol.2009.05.003.

Celardo I, Martins LM, Gandhi S. 2014. Unravelling mitochondrial pathways to Parkinson's disease. *Br J Pharmacol*. 171(8):1943–1957. doi:10.1111/bph.12433.

Chandel NS, Maltepe E, Goldwasser E, Mathieu CE, Simon MC, Schumacker PT. 1998. Mitochondrial reactive oxygen species trigger hypoxia-induced transcription. *Proc Natl Acad Sci U S A*. 95(September):11715–11720.

Chappie JS, Acharya S, Liu Y-W, Leonard M, Pucadyil TJ, Schmid SL. 2009. An Intramolecular Signaling Element that Modulates Dynamin Function In Vitro and In Vivo. *Mol Biol Cell*. 20:3561–3571. doi:10.1091/mbc.E09.

Chen H, Detmer SA, Ewald AJ, Griffin EE, Fraser SE, Chan DC. 2003. Mitofusins Mfn1 and Mfn2 coordinately regulate mitochondrial fusion and are essential for embryonic development. *J Cell Biol*. 160:189–200. doi:10.1083/jcb.200211046.

Chen K-H, Guo X, Ma D, Guo Y, Li Q, Yang D, Li P, Qiu X, Wen S, Xiao R-P, et al. 2004. Dysregulation of HSG triggers vascular proliferative disorders. *Nat Cell Biol*. 6(9):872–883. doi:10.1038/ncb1161.

Chen KH, Dasgupta A, Ding J, Indig FE, Ghosh P, L. Longo D. 2014. Role of mitofusin 2 (Mfn2) in controlling cellular proliferation. *FASEB J*. 28(1):382–394. doi:10.1096/fj.13-230037.

Chen KH, Guo X, Ma D, Guo Y, Li Q, Yang D, Li P, Qiu X, Wen S, Xiao RP, et al. 2004. Dysregulation of HSG triggers vascular proliferative disorders. *Nat Cell Biol*. 6(9):872–883. doi:10.1038/ncb1161.

Chen Y, Dorn GW. 2013. PINK1-Phosphorylated Mitofusin 2 is a Parkin Receptor for Culling Damaged Mitochondria. *Science (80-)*. 340(April):471–476.

Cleland MM, Norris KL, Karbowski M, Wang C, Suen D-F, Jiao S, George NM, Luo X, Li Z, Youle RJ. 2011. Bcl-2 family interaction with the mitochondrial morphogenesis machinery. *Cell*

Death Differ. 18(2):235–247. doi:10.1038/cdd.2010.89.

Cribbs JT, Strack S. 2007. Reversible phosphorylation of Drp1 by cyclic AMP-dependent protein kinase and calcineurin regulates mitochondrial fission and cell death. *EMBO Rep*. 8(10):939–944. doi:10.1038/sj.embor.7401062.

Delaunay A, Isnard AD, Toledano MB. 2000. H2O2 sensing through oxidation of the Yap1 transcription factor. *EMBO J*. 19(19):5157–5166. doi:10.1093/emboj/19.19.5157.

Detmer Scott A, Chan DC. 2007a. Complementation between mouse Mfn1 and Mfn2 protects mitochondrial fusion defects caused by CMT2A disease mutations. *J Cell Biol*. 176(4):405–14. doi:10.1083/jcb.200611080.

Detmer Scott A, Chan DC. 2007b. Functions and dysfunctions of mitochondrial dynamics. *Nat Rev Mol Cell Biol*. 8(november):870–879. doi:10.1038/nrm2275.

Detmer Scott A., Chan DC. 2007. Complementation between mouse Mfn1 and Mfn2 protects mitochondrial fusion defects caused by CMT2A disease mutations. *J Cell Biol*. 176(4):405–414. doi:10.1083/jcb.200611080.

Detmer SA, Velde C Vande, Cleveland DW, Chan DC. 2008. Hindlimb gait defects due to motor axon loss and reduced distal muscles in a transgenic mouse model of Charcot - Marie - Tooth type 2A. *Hum Mol Genet*. 17(3):367–375. doi:10.1093/hmg/ddm314.

Du C, Fang M, Li Y, Li L, Wang X. 2000. Smac, a Mitochondrial Protein that Promotes Cytochrome c-Dependent Caspase Activation by Eliminating IAP Inhibition Hid, and Grim in terms of IAP neutralization and is the. *Cell*. 102:33–42.

Ekman D, Björklund ÅK, Frey-Skött J, Elofsson A. 2005. Multi-domain proteins in the three kingdoms of life: Orphan domains and other unassigned regions. *J Mol Biol*. 348(1):231–243. doi:10.1016/j.jmb.2005.02.007.

Engelhart EA, Hoppins S. 2019. A catalytic domain variant of Mitofusin requiring a wildtype paralog for function uncouples mitochondrial outer-membrane tethering and fusion. *J Biol Chem*. 1(8):jbc.RA118.006347. doi:10.1074/jbc.RA118.006347.

Ernster L, Schatz G. 1981. Mitochondria : A Historical Review. 91(December).

Eura Y. 2003. Two Mitofusin Proteins, Mammalian Homologues of FZO, with Distinct Functions Are Both Required for Mitochondrial Fusion. *J Biochem*. 134(3):333–344. doi:10.1093/jb/mvg150.

Federico A, Cardaioli E, Da Pozzo P, Formichi P, Gallus GN, Radi E. 2012. Mitochondria, oxidative stress and neurodegeneration. *J Neurol Sci*. 322(1–2):254–262. doi:10.1016/j.jns.2012.05.030.

Feely SME, Laura M, Siskind CE, Sottile S, Davis M, Gibbons VS, Reilly MM, Shy ME. 2011. MFN2 mutations cause severe phenotypes in most patients with CMT2A. *Neurology*. 76(20):1690–6. doi:10.1212/WNL.0b013e31821a441e.

Ferreira JCB, Campos JC, Qvit N, Qi X, Bozi LHM, Bechara LRG, Lima VM, Queliconi BB, Disatnik MH, Dourado PMM, et al. 2019. A selective inhibitor of mitofusin 1-βIIPKC association improves heart failure outcome in rats. *Nat Commun*. 10(1). doi:10.1038/s41467-018-08276-6.

Filadi R, Greotti E, Turacchio G, Luini A, Pozzan T, Pizzo P. 2015. Mitofusin 2 ablation increases endoplasmic reticulum–mitochondria coupling. *Proc Natl Acad Sci*. doi:10.1073/pnas.1504880112.

Franco A, Kitsis RN, Fleischer JA, Gavathiotis E, Kornfeld OS, Gong G, Biris N, Benz A, Qvit N, Donnelly SK, et al. 2016. Correcting mitochondrial fusion by manipulating mitofusin conformations. *Nature*.:1–20. doi:10.1038/nature20156.

Fransson Å, Ruusala A, Aspenström P. 2006. The atypical Rho GTPases Miro-1 and Miro-2 have essential roles in mitochondrial trafficking. *Biochem Biophys Res Commun*. 344(2):500–510. doi:10.1016/j.bbrc.2006.03.163.

Ganesan V, Willis SD, Chang KT, Beluch S, Cooper KF, Strich R. 2019. Cyclin C directly stimulates Drp1 GTP affinity to mediate stress-induced mitochondrial hyperfission. *Mol Biol Cell*. 30(3):302–311. doi:10.1091/mbc.E18-07-0463.

Gawlowski T, Suarez J, Scott B, Torres-Gonzalez M, Wang H, Schwappacher R, Han X, Yates JR,

Hoshijima M, Dillmann W. 2012. Modulation of dynamin-related protein 1 (DRP1) function by increased O-linked-β-N-acetylglucosamine modification (O-GlcNAc) in cardiac myocytes. *J Biol Chem*. 287(35):30024–30034. doi:10.1074/jbc.M112.390682.

Gemignani F, Marbini A. 2001. Charcot-Marie-Tooth disease (CMT): Distinctive phenotypic and genotypic features in CMT type 2. *J Neurol Sci*. 184(1):1–9. doi:10.1016/S0022-510X(00)00497-4.

Giarmarco MM, Cleghorn WM, Sloat SR, Hurley JB, Brockerhoff SE. 2017. Mitochondria Maintain Distinct Ca 2+ Pools in Cone Photoreceptors . *J Neurosci*. 37(8):2061–2072. doi:10.1523/jneurosci.2689-16.2017.

Gilbert HF. 1995. Thiol-Disulfide Exchange Equilibria and Bond Stability. *Methods Enzymol*. 251:8–28.

Giustarini D, Colombo G, Garavaglia ML, Astori E, Portinaro NM, Reggiani F, Badalamenti S, Aloisi AM, Santucci A, Rossi R, et al. 2017. Assessment of glutathione/glutathione disulphide ratio and S-glutathionylated proteins in human blood, solid tissues, and cultured cells. *Free Radic Biol Med*. 112(August):360–375. doi:10.1016/j.freeradbiomed.2017.08.008.

Giustarini D, Dalle-Donne I, Tsikas D, Rossi R. 2009. Oxidative stress and human diseases: Origin, link, measurement, mechanisms, and biomarkers. *Crit Rev Clin Lab Sci*. 46(5–6):241–281. doi:10.3109/10408360903142326.

Gomes LC, Benedetto G Di, Scorrano L. 2011. During autophagy mitochondria elongate, are spared from degradation and sustain cell viability. *Nat Cell Biol*. 13(5):589–598. doi:10.1038/ncb2220.

Grek CL, Zhang J, Manevich Y, Townsend DM, Tew KD. 2013. Causes and consequences of cysteine s-glutathionylation. *J Biol Chem*. 288(37):26497–26504. doi:10.1074/jbc.R113.461368.

Griffin EE, Chan DC. 2006. Domain interactions within Fzo1 oligomers are essential for mitochondrial fusion. *J Biol Chem*. 281(24):16599–606. doi:10.1074/jbc.M601847200.

Guo C, Hildick KL, Luo J, Dearden L, Wilkinson KA, Henley JM. 2013. SENP3-mediated

deSUMOylation of dynamin-related protein 1 promotes cell death following ischaemia. *EMBO J*. 32(11):1514–1528. doi:10.1038/emboj.2013.65.

Guo X, Chen KH, Guo Y, Liao H, Tang J, Xiao RP. 2007. Mitofusin 2 triggers vascular smooth muscle cell apoptosis via mitochondrial death pathway. *Circ Res*. 101(11):1113–1122. doi:10.1161/CIRCRESAHA.107.157644.

Han X, Lu Y, Li S, Kaitsuka T, Sato Y, Tomizawa K, Nairn AC, Takei K, Matsui H, Matsushita M. 2008. JCB : ARTICLE. 182(3):573–585. doi:10.1083/jcb.200802164.

Harder Z, Zunino R, McBride H. 2004. Sumo1 conjugates mitochondrial substrates and participates in mitochondrial fission. *Curr Biol*. 14(4):340–345. doi:10.1016/S0960-9822(04)00084-3.

Hoppins S, Edlich F, Cleland MM, Banerjee S, McCaffery JM, Youle RJ, Nunnari J. 2011. The Soluble Form of Bax Regulates Mitochondrial Fusion via MFN2 Homotypic Complexes. *Mol Cell*. 41(2):150–160. doi:10.1016/j.molcel.2010.11.030.

Horbay R, Bilyy R. 2016. Mitochondrial dynamics during cell cycling. *Apoptosis*. 21(12):1327–1335. doi:10.1007/s10495-016-1295-5.

Iqbal S, Hood DA. 2014. Oxidative stress-induced mitochondrial fragmentation and movement in skeletal muscle myoblasts. *Am J Physiol - Cell Physiol*. 306(12):1176–1183. doi:10.1152/ajpcell.00017.2014.

Ishihara N, Eura Y, Mihara K. 2004. Mitofusin 1 and 2 play distinct roles in mitochondrial fusion reactions via GTPase activity. *J Cell Sci*. 117(26):6535–6546. doi:10.1242/jcs.01565.

James SJ, Rose S, Melnyk S, Jernigan S, Blossom S, Pavliv O, Gaylor DW. 2009. Cellular and mitochondrial glutathione redox imbalance in lymphoblastoid cells derived from children with autism. *FASEB J*. 23(8):2374–2383. doi:10.1096/fj.08-128926.

Jendrach M, Mai S, Pohl S, Vöth M, Bereiter-Hahn J. 2008. Short- and long-term alterations of mitochondrial morphology, dynamics and mtDNA after transient oxidative stress. *Mitochondrion*. 8(4):293–304. doi:10.1016/j.mito.2008.06.001.

Jimah JR, Hinshaw JE. 2019. Structural Insights into the Mechanism of Dynamin Superfamily Proteins. *Trends Cell Biol*. 29(3):257–273. doi:10.1016/j.tcb.2018.11.003.

Karbowski M, Lee Y, Gaume B, Jeong S, Frank S, Nechushtan A, Santel A, Fuller M, Smith CL, Youle RJ. 2002. Spatial and temporal association of Bax with during apoptosis. 159(6):931–938. doi:10.1083/jcb.200209124.

Karbowski M, Norris KL, Cleland MM, Jeong S-Y, Youle RJ. 2006. Role of Bax and Bak in mitochondrial morphogenesis. *Nature*. 443(October):658–662. doi:10.1038/nature05111.

Kim YM, Youn SW, Sudhahar V, Das A, Chandhri R, Cuervo Grajal H, Kweon J, Leanhart S, He L, Toth PT, et al. 2018. Redox Regulation of Mitochondrial Fission Protein Drp1 by Protein Disulfide Isomerase Limits Endothelial Senescence. *Cell Rep*. 23(12):3565–3578. doi:10.1016/j.celrep.2018.05.054.

Koshiba T, Detmer S a, Kaiser JT, Chen H, McCaffery JM, Chan DC. 2004. Structural basis of mitochondrial tethering by mitofusin complexes. *Science*. 305(5685):858–862. doi:10.1126/science.1099793.

Kosower NS, Kosower EM, Wertheim B, Correa WS. 1969. Diamide, a new reagent for the intracellular oxidation of glutathione to the disulfide. *Biochem Biophys Res Commun*. 37(4):593–596. doi:10.1016/0006-291X(69)90850-X.

Koutsopoulos OS, Laine D, Osellame L, Chudakov DM, Parton RG, Frazier AE, Ryan MT. 2010. Human Miltons associate with mitochondria and induce microtubule-dependent remodeling of mitochondrial networks. *Biochim Biophys Acta - Mol Cell Res*. 1803(5):564–574. doi:10.1016/j.bbamcr.2010.03.006.

Labbé K, Murley A, Nunnari J. 2014. Determinants and Functions of Mitochondrial Behavior. *Annu Rev Cell Dev Biol*. 30(1):357–391. doi:10.1146/annurev-cellbio-101011-155756.

Lebeau J, Saunders JM, Moraes VWR, Madhavan A, Madrazo N, Anthony MC, Wiseman RL. 2018. The PERK Arm of the Unfolded Protein Response Regulates Mitochondrial Morphology during Acute Endoplasmic Reticulum Stress. *Cell Rep*. 22(11):2827–2836.

doi:10.1016/j.celrep.2018.02.055.

Lee D, Redfern O, Orengo C. 2007. Predicting protein function from sequence and structure. *Nat Rev Mol Cell Biol*. 8(12):995–1005. doi:10.1038/nrm2281.

Lee J-Y, Kapur M, Li M, Choi M-C, Choi S, Kim H-J, Kim I, Lee E, Taylor JP, Yao T-P. 2014. MFN1 deacetylation activates adaptive mitochondrial fusion and protects metabolically challenged mitochondria. *J Cell Sci*. 127(22):4954–4963. doi:10.1242/jcs.157321.

Liu J, Noel JK, Low HH. 2018. Structural basis for membrane tethering by a bacterial dynamin-like pair. *Nat Commun*. 9(1):1–12. doi:10.1038/s41467-018-05523-8.

Liu X, Kim CN, Yang J, Jemmerson R, Wang X. 1996. Induction of Apoptotic Program in Cell-Free Extracts: Requirement for dATP and Cytochrome C. *Cell*. 86(July):147–157.

Loson OC, Song Z, Chen H, Chan DC. 2013. Fis1, Mff, MiD49, and MiD51 mediate Drp1 recruitment in mitochondrial fission. *Mol Biol Cell*. 24(5):659–667. doi:10.1091/mbc.e12-10-0721.

Low HH, Löwe J. 2006. A bacterial dynamin-like protein. *Nature*. 444(7120):766–769. doi:10.1038/nature05312.

Low HH, Sachse C, Amos LA, Löwe J. 2009. Structure of a Bacterial Dynamin-like Protein Lipid Tube Provides a Mechanism For Assembly and Membrane Curving. *Cell*. 139(7):1342–1352. doi:10.1016/j.cell.2009.11.003.

Mattie S, Riemer J, Wideman JG, McBride HM. 2018. A new mitofusin topology places the redox-regulated C terminus in the mitochondrial intermembrane space. *J Cell Biol*. 217(2):507–515. doi:10.1083/jcb.201611194.

McLelland GL, Goiran T, Yi W, Dorval G, Chen CX, Lauinger ND, Krahn AI, Valimehr S, Rakovic A, Rouiller I, et al. 2018. Mfn2 ubiquitination by PINK1/parkin gates the p97-dependent release of ER from mitochondria to drive mitophagy. *Elife*. 7:1–35. doi:10.7554/eLife.32866.

Mears JA, Lackner LL, Fang S, Ingerman E, Nunnari J, Hinshaw JE. 2011. Conformational changes in Dnm1 support a contractile mechanism for mitochondrial fission. *Nat Struct Mol*

Biol. 18(1):20–27. doi:10.1038/nsmb.1949.

Mishra P, Chan DC. 2014. Mitochondrial dynamics and inheritance during cell division, development and disease. *Nat Rev Mol Cell Biol*. 15(10):634–646. doi:10.1038/nrm3877.

Mitra K, Wunder C, Roysam B, Lin G, Lippincott-Schwartz J. 2009. A hyperfused mitochondrial state achieved at G1-S regulates cyclin E buildup and entry into S phase. *Proc Natl Acad Sci*. 106(29):11960–11965. doi:10.1073/pnas.0904875106.

Olichon A, Baricault L, Gas N, Guillou E, Valette A, Belenguer P, Lenaers G. 2003. Loss of OPA1 perturbates the mitochondrial inner membrane structure and integrity, leading to cytochrome c release and apoptosis. *J Biol Chem*. 278(10):7743–7746. doi:10.1074/jbc.C200677200.

Ong S-B, Kalkhoran SB, Cabrera-Fuentes H a., Hausenloy DJ. 2015. Mitochondrial fusion and fission proteins as novel therapeutic targets for treating cardiovascular disease. *Eur J Pharmacol*.:1–11. doi:10.1016/j.ejphar.2015.04.056.

Østergaard H, Tachibana C, Winther JR. 2004. Monitoring disulfide bond formation in the eukaryotic cytosol. *J Cell Biol*. 166(3):337–345. doi:10.1083/jcb.200402120.

Otera H, Wang C, Cleland MM, Setoguchi K, Yokota S, Youle RJ, Mihara K. 2010. Mff is an essential factor for mitochondrial recruitment of Drp1 during mitochondrial fission in mammalian cells. *J Cell Biol*. 191(6):1141–1158. doi:10.1083/jcb.201007152.

Pareyson D, Saveri P, Sagnelli A, Piscosquito G. 2015. Mitochondrial dynamics and inherited peripheral nerve diseases. *Neurosci Lett*. 596:66–77. doi:10.1016/j.neulet.2015.04.001.

Park YY, Nguyen OTK, Kang H, Cho H. 2014. MARCH5-mediated quality control on acetylated Mfn1 facilitates mitochondrial homeostasis and cell survival. *Cell Death Dis*. 5(4):e1172-12. doi:10.1038/cddis.2014.142.

Pernas L, Scorrano L. 2015. Mito-Morphosis: Mitochondrial Fusion, Fission, and Cristae Remodeling as Key Mediators of Cellular Function. *Annu Rev Physiol*. 78(1):505–531. doi:10.1146/annurev-physiol-021115-105011.

Picard M, Wallace DC, Burelle Y. 2016. The rise of mitochondria in medicine. *Mitochondrion*.

30:105–116. doi:10.1016/j.mito.2016.07.003.

Pilling AD, Horiuchi D, Lively CM, Saxton WM. 2006. Kinesin-1 and Dynein are the primary motors for fast transport of mitochondria in Drosophila motor axons. *Mol Biol Cell*. 17(April):2057–2068. doi:10.1091/mbc.E05.

Pócsi I, Miskei M, Karányi Z, Emri T, Ayoubi P, Pusztahelyi T, Balla G, Prade RA. 2005. Comparison of gene expression signatures of diamide, H2O2 and menadione exposed Aspergillus nidulans cultures - Linking genome-wide transcriptional changes to cellular physiology. *BMC Genomics*. 6:1–18. doi:10.1186/1471-2164-6-182.

Prudent J, Zunino R, Sugiura A, Mattie S, Shore GC, McBride HM. 2015. MAPL SUMOylation of Drp1 Stabilizes an ER/Mitochondrial Platform Required for Cell Death. *Mol Cell*. 59(6):941–955. doi:10.1016/j.molcel.2015.08.001.

Pyakurel A, Savoia C, Scorrano L, Pyakurel A, Savoia C, Hess D, Scorrano L. 2015. Extracellular Regulated Kinase Phosphorylates Mitofusin 1 to Control Mitochondrial Morphology and Article Extracellular Regulated Kinase Phosphorylates Mitofusin 1 to Control Mitochondrial Morphology and Apoptosis. *Mol Cell*.:1–11. doi:10.1016/j.molcel.2015.02.021.

Qi Y, Yan L, Yu C, Guo X, Zhou X, Hu X, Huang X, Rao Z, Lou Z, Hu J. 2016. Structures of human mitofusin 1 provide insight into mitochondrial tethering.

Rambold AS, Kostelecky B, Elia N, Lippincott-Schwartz J. 2011. Tubular network formation protects mitochondria from autophagosomal degradation during nutrient starvation. *Proc Natl Acad Sci*. 108(25):10190–10195. doi:10.1073/pnas.1107402108.

Redpath CJ, Bou Khalil M, Drozdzal G, Radisic M, McBride HM. 2013. Mitochondrial Hyperfusion during Oxidative Stress Is Coupled to a Dysregulation in Calcium Handling within a C2C12 Cell Model. *PLoS One*. 8(7). doi:10.1371/journal.pone.0069165.

Rocha AG, Franco A, Krezel AM, Rumsey JM, Alberti JM, Knight WC, Biris N, Zacharioudakis E, Janetka JW, Baloh RH, et al. 2018a. MFN2 agonists reverse mitochondrial defects in preclinical models of Charcot-Marie-Tooth disease type 2A. *Science (80-)*. 360(6386):336–341.

doi:10.1126/science.aao1785.

Rocha AG, Franco A, Krezel AM, Rumsey JM, Alberti JM, Knight WC, Biris N, Zacharioudakis E, Janetka JW, Baloh RH, et al. 2018b. MFN2 agonists reverse mitochondrial defects in preclinical models of Charcot-Marie-Tooth disease type 2A. *Science (80-)*. 360(6386):336–341. doi:10.1126/science.aao1785.

Rovira-Llopis S, Bañuls C, Diaz-Morales N, Hernandez-Mijares A, Rocha M, Victor VM. 2017. Mitochondrial dynamics in type 2 diabetes: Pathophysiological implications. *Redox Biol*. 11(January):637–645. doi:10.1016/j.redox.2017.01.013.

Santel a, Fuller MT. 2001. Control of mitochondrial morphology by a human mitofusin. *J Cell Sci*. 114:867–874.

Scorrano L. 2013. Keeping mitochondria in shape: A matter of life and death. *Eur J Clin Invest*. 43(8):886–893. doi:10.1111/eci.12135.

Sena LA, Chandel NS. 2012. Physiological roles of mitochondrial reactive oxygen species. *Mol Cell*. 48(2):158–167. doi:10.1016/j.molcel.2012.09.025.

Shen T, Zheng M, Cao C, Chen C, Tang J, Zhang W, Cheng H, Chen KH, Xiao RP. 2007. Mitofusin-2 is a major determinant of oxidative stress-mediated heart muscle cell apoptosis. *J Biol Chem*. 282(32):23354–23361. doi:10.1074/jbc.M702657200.

SHITARA H, SHIMANUKI M, HAYASHI J-I, YONEKAWA H. 2010. Global Imaging of Mitochondrial Morphology in Tissues Using Transgenic Mice Expressing Mitochondrially Targeted Enhanced Green Fluorescent Protein. *Exp Anim*. 59(1):99–103. doi:10.1538/expanim.59.99.

Shutt T, Geoffrion M, Milne R, McBride HM. 2012. The intracellular redox state is a core determinant of mitochondrial fusion. *EMBO Rep*. 13(10):909–915. doi:10.1038/embor.2012.128.

Shutt TE, McBride HM. 2013. Staying cool in difficult times: Mitochondrial dynamics, quality control and the stress response. *Biochim Biophys Acta - Mol Cell Res*. 1833(2):417–424.

doi:10.1016/j.bbamcr.2012.05.024.

Slater EC, Cleland KW. 1953. The effect of calcium on the respiratory and phosphorylative activities of heart-muscle sarcosomes. *Biochem J*. 55(4):566–580. doi:10.1042/bj0550566.

Slivka A, Spina MB, Cohen G. 1987. Reduced and oxidized glutathione in human and monkey brain. *Neurosci Lett*. 74(1):112–118. doi:10.1016/0304-3940(87)90061-9.

Smirnova E, Griparic L, Shurland D-L, van der Bliek AM. 2001. Dynamin-related Protein Drp1 Is Required for Mitochondrial Division in Mammalian Cells. *Mol Biol Cell*. 12(8):2245–2256. doi:10.1091/mbc.12.8.2245.

Sorrentino V, Menzies KJ, Auwerx J. 2017. Repairing Mitochondrial Dysfunction in Disease. *Annu Rev Pharmacol Toxicol*. 58(1):353–389. doi:10.1146/annurev-pharmtox-010716-104908.

De Stefani D, Rizzuto R, Pozzan T. 2016. Enjoy the Trip: Calcium in Mitochondria Back and Forth. *Annu Rev Biochem*. 85(1):161–192. doi:10.1146/annurev-biochem-060614-034216.

Strickland A V, Rebelo AP, Zhang F, Price J, Bolon B, Silva JP, Wen R, Züchner S. 2014. Characterization of the Mitofusin 2 R94W Mutation in a Knock-in Mouse Model. *J Peripher Nerv Syst*. 164:152–164. doi:10.1111/jns5.12066.

Stuppia G, Rizzo F, Riboldi G, Del Bo R, Nizzardo M, Simone C, Comi GP, Bresolin N, Corti S. 2015. MFN2-related neuropathies: Clinical features, molecular pathogenesis and therapeutic perspectives. *J Neurol Sci*. doi:10.1016/j.jns.2015.05.033.

Suen D, Norris KL, Youle RJ. 2008. Mitochondrial dynamics and apoptosis. (301):1577–1590. doi:10.1101/gad.1658508.GENES.

Sugiura A, Nagashima S, Tokuyama T, Amo T, Matsuki Y, Ishido S, Kudo Y, McBride HM, Fukuda T, Matsushita N, et al. 2013. MITOL regulates endoplasmic reticulum-mitochondria contacts via Mitofusin2. *Mol Cell*. 51(1):20–34. doi:10.1016/j.molcel.2013.04.023.

Susin SA, Zamzami N, Castedo M, Hirsch T, Marchetti P, Macho A, Daugas E, Geuskens M, Kroemer G. 1996. Bcl-2 Inhibits the Mitochondrial Release of an Apoptotic Protease. *J Exp Med*. 184(October):1331–1341.

Suzuki M, Youle RJ, Tjandra N. 2000. Structure of Bax. *Cell*. 103(4):645–654. doi:10.1016/s0092-8674(00)00167-7.

Suzuki Y, Imai Y, Nakayama H, Takahashi K, Takio K, Takahashi R. 2001. A serine protease, HtrA2, is released from the mitochondria and interacts with XIAP, inducing cell death. *Mol Cell*. 8(3):613–621. doi:10.1016/S1097-2765(01)00341-0.

Thaher O, Wolf C, Dey PN, Pouya A, Wüllner V, Tenzer S, Methner A. 2017. The thiol switch C684 in Mitofusin-2 mediates redox-induced alterations of mitochondrial shape and respiration. *Neurochem Int*.:5–11. doi:10.1016/j.neuint.2017.05.009.

Thorpe GW, Fong CS, Alic N, Higgins VJ, Dawes IW. 2004. Cells have distinct mechanisms to maintain protection against different reactive oxygen species: Oxidative-stress-response genes. *Proc Natl Acad Sci*. 101(17):6564–6569. doi:10.1073/pnas.0305888101.

Tondera D, Grandemange S, Jourdain A, Karbowski M, Mattenberger Y, Herzig S, Da Cruz S, Clerc P, Raschke I, Merkwirth C, et al. 2009. SLP-2 is required for stress-induced mitochondrial hyperfusion. *EMBO J*. 28(November 2008):1589–1600. doi:10.1038/emboj.2009.89.

Twig G, Elorza A, Molina AJA, Mohamed H, Wikstrom JD, Walzer G, Stiles L, Haigh SE, Katz S, Las G, et al. 2008. Fission and selective fusion govern mitochondrial segregation and elimination by autophagy. *EMBO J*. 27(2):433–446. doi:10.1038/sj.emboj.7601963.

Vallat J-M, Ouvrier R a, Pollard JD, Magdelaine C, Zhu D, Nicholson G a, Grew S, Ryan MM, Funalot B. 2008. Histopathological findings in hereditary motor and sensory neuropathy of axonal type with onset in early childhood associated with mitofusin 2 mutations. *J Neuropathol Exp Neurol*. 67(11):1097–1102. doi:10.1097/NEN.0b013e31818b6cbc.

Verhagen AM, Ekert PG, Pakusch M, Silke J, Connonlly LM, Reid GE, Moritz RL, Simpson RJ, Vaux DL. 2000. Identification of DIABLO, a Mammalian Protein that Promotes Apoptosis by Binding to and Antagonizing IAP Proteins. *Cell*. 102(1):43–53. doi:10.1016/S0896-6273(00)80282-2.

Verhoeven K, Claeys KG, Züchner S, Schröder JM, Weis J, Ceuterick C, Jordanova A, Nelis E, De

Vriendt E, Van Hul M, et al. 2006. MFN2 mutation distribution and genotype/phenotype correlation in Charcot-Marie-Tooth type 2. *Brain*. 129(8):2093–2102. doi:10.1093/brain/awl126.

Vital A, Vital C. 2012. Mitochondria and peripheral neuropathies. *J Neuropathol Exp Neurol*. 71(12):1036–46. doi:10.1097/NEN.0b013e3182764d47.

Wada J, Nakatsuka A. 2016. Mitochondrial Dynamics and Mitochondrial Dysfunction in Diabetes. *Acta Med Okayama*. 70(3):151–8. doi:10.18926/AMO/54413.

Wallace DC, Fan W, Procaccio V. 2010. Mitochondrial Energetics and Therapeutics. *Annu Rev Pathol Mech Dis*. 5(1):297–348. doi:10.1146/annurev.pathol.4.110807.092314.

Wang C, Youle RJ. 2011. The role of mitochondria in apoptosis. *BMB Rep*. 41(1):11–22. doi:10.5483/bmbrep.2008.41.1.011.

Wang H, Song P, Du L, Tian W, Yue W, Liu M, Li D, Wang B, Zhu Y, Cao C, et al. 2011. Parkin ubiquitinates Drp1 for proteasome-dependent degradation: Implication of dysregulated mitochondrial dynamics in Parkinson disease. *J Biol Chem*. 286(13):11649–11658. doi:10.1074/jbc.M110.144238.

Wang K, Yan R, Cooper KF, Strich R. 2015. Cyclin C mediates stress-induced mitochondrial fission and apoptosis. *Mol Biol Cell*. 26(6):1030–1043. doi:10.1091/mbc.E14-08-1315.

Wang W, Zhang F, Li L, Tang F, Siedlak SL, Fujioka H, Liu Y, Su B, Pi Y, Wang X. 2015. MFN2 couples glutamate excitotoxicity and mitochondrial dysfunction in motor neurons. *J Biol Chem*. 290(1):168–182. doi:10.1074/jbc.M114.617167.

Wemmie JA, Steggerda SM, Moye-Rowley WS. 1997. The Saccharomyces cerevisiae AP-1 protein discriminates between oxidative stress elicited by the oxidants H 2O 2 and diamide. *J Biol Chem*. 272(12):7908–7914. doi:10.1074/jbc.272.12.7908.

Willems P, Wanschers BFJ, Esseling J, Szklarczyk R, Kudla U, Duarte I, Forkink M, Nooteboom M, Swarts H, Gloerich J, et al. 2013. BOLA1 is an aerobic protein that prevents mitochondrial morphology changes induced by glutathione depletion. *Antioxidants Redox Signal*. 18(2):129–

138. doi:10.1089/ars.2011.4253.

Wu S, Zhou F, Zhang Z, Xing D. 2011. Mitochondrial oxidative stress causes mitochondrial fragmentation via differential modulation of mitochondrial fission-fusion proteins. *FEBS J*. 278(6):941–954. doi:10.1111/j.1742-4658.2011.08010.x.

Xiying F, Rajaa H, George A. B. 2013. H2O2-induced mitochondrial fragmentation in C2C12 myocytes. *Free Radic Biol Med*. 18(9):1199–1216. doi:10.1016/j.micinf.2011.07.011.Innate.

Xu K, Chen G, Li X, Wu X, Chang Z, Xu J, Zhu Y, Yin P, Liang X, Dong L. 2017. MFN2 suppresses cancer progression through inhibition of mTORC2/Akt signaling. *Sci Rep*. 7(February):1–13. doi:10.1038/srep41718.

Yan L, Qi Y, Huang X, Yu C, Lan L, Guo X, Rao Z, Hu J, Lou Z. 2018. Structural basis for GTP hydrolysis and conformational change of MFN1 in mediating membrane fusion. *Nat Struct Mol Biol*. 25(3):233–243. doi:10.1038/s41594-018-0034-8.

Yang J, Zhang Y. 2015. I-TASSER server: New development for protein structure and function predictions. *Nucleic Acids Res*. 43(W1):W174–W181. doi:10.1093/nar/gkv342.

Yesylevskyy SO, Kharkyanen VN, Demchenko AP. 2006. Dynamic protein domains: Identification, interdependence, and stability. *Biophys J*. 91(2):670–685. doi:10.1529/biophysj.105.078584.

Yoon Y-S, Yoon D-S, Lim IK, Yoon S-H, Chung H-Y, Rojo M, Malka F, Jou M-J, Martinou J-C, Yoon G. 2006. Formation of Elongated Giant Mitochondria in DFO-Induced Cellular Senescence: Involvement of Enhanced Fusion Process Through Modulation of Fis1. *J Cell Physiol*. 209(1):468–480. doi:10.1002/JCP.

Zahedi A, Phandthong R, Chaili A, Leung S, Omaiye E, Talbot P. 2019. Mitochondrial Stress Response in Neural Stem Cells Exposed to Electronic Cigarettes. *iScience*. 16:250–269. doi:10.1016/j.isci.2019.05.034.

Zhang G-E, Jin H-L, Lin X-K, Chen C, Liu X-S, Zhang Q, Yu J-R. 2013. Anti-tumor effects of mfn2 in gastric cancer. *Int J Mol Sci*. 14:13005–21. doi:10.3390/ijms140713005.

Zhang Y. 2009. I-TASSER: Fully automated protein structure prediction in CASP8. *Proteins Struct Funct Bioinforma*. 77(SUPPL. 9):100–113. doi:10.1002/prot.22588.

Zheng M, Xiao RP. 2010. Role of mitofusin 2 in cardiovascular oxidative injury. *J Mol Med*. 88(10):987–991. doi:10.1007/s00109-010-0675-5.

Zhou Y, Lutz CM, Baloh RH, Zhou Y, Carmona S, Muhammad AKMG, Bell S, Landeros J, Vazquez M, Ho R, et al. 2019. Restoring mitofusin balance prevents axonal degeneration in a Charcot-Marie-Tooth type 2A model Graphical abstract Find the latest version : Restoring mitofusin balance prevents axonal degeneration in a Charcot-Marie-Tooth type 2A model.

Zorov DB, Filburn CR, Klotz LO, Zweier JL, Sollott SJ. 2000. Reactive oxygen species (ROS)-induced ROS release: A new phenomenon accompanying induction of the mitochondrial permeability transition in cardiac myocytes. *J Exp Med*. 192(7):1001–1014. doi:10.1084/jem.192.7.1001.

Züchner S, Mersiyanova I V, Muglia M, Bissar-Tadmouri N, Rochelle J, Dadali EL, Zappia M, Nelis E, Patitucci A, Senderek J, et al. 2004. Mutations in the mitochondrial GTPase mitofusin 2 cause Charcot-Marie-Tooth neuropathy type 2A. *Nat Genet*. 36(5):449–451. doi:10.1038/ng1341.

Chapter 4: Mfn2 requires Hinge 1 integrity for efficient nucleotide-dependent assembly and membrane fusion

This chapter is minimally altered from a manuscript of the same title under review for publication. Authors of this manuscript are Nyssa B. Samanas, Emily A. Engelhart, and Suzanne C. Hoppins

4.1 Abstract

Two mitofusin isoforms mediate mitochondrial outer membrane fusion in vertebrates. Mitofusins are members of the dynamin-related protein family, large GTPases that harness the energy from nucleotide hydrolysis to remodel membranes. Mitofusins possess four structural domains including the globular GTPase domain, two extended helical bundles, and a transmembrane region, that are connected by flexible linkers to facilitate conformational changes. The role of Hinge 1, the linker connecting the two helical bundles, in mitofusin-mediated membrane fusion is not well understood. To address this, we have characterized four variants with amino acid substitutions within this region of Mfn2. While a functional defect was not apparent in cells, a cell-free mitochondrial fusion assay revealed a fusion deficiency, which was rescued by the addition of cytosolic fraction. Consistent with this, all four variants had decreased nucleotide-dependent assembly, which was improved by the addition of recombinant purified Bax. In contrast, assembly of mitofusins across two membranes was unaffected as the formation of the trans complex was similar to wild type for all variants. Together, our data are consistent with a model where this region contributes to conformational changes that are important for higher order assembly. We further demonstrate that variants with substitutions in both helical bundles are more severely impaired than any single mutant, suggesting that both helical bundles contribute to this function.

4.2 Introduction

Mitochondrial dynamics have become increasingly recognized as an important indicator of and contributor to both cellular health and death. Mitochondrial shape and their cellular distribution change during the cell cycle, in response to stress, and as part of apoptosis (Tondera et al. 2009; Scorrano 2013; Labbé et al. 2014; Horbay and Bilyy 2016). Mitochondria are trafficked on microtubules and the overall shape and connectivity of the mitochondrial network is maintained or modified through mitochondrial fusion and division, which are mediated by membrane-remodeling large GTPase proteins of the dynamin related protein (DRP) family (Labbé et al. 2014). At steady state, it is estimated that mitochondrial fusion and division events are balanced. When mitochondrial division events exceed fusion events, the network fragments into many small individual mitochondria, and this fragmentation is associated with mitophagy and apoptosis. In contrast, when mitochondrial fusion occurs more frequently than division, the result is a more connected network comprised of longer mitochondria, which is associated with increased ATP production; i.e., during a cellular stress response. The importance of these processes and their regulation is highlighted by the association of dysregulated mitochondrial dynamics with various diseases such as Parkinson's disease, diabetes, and peripheral neuropathies (Züchner et al. 2004; Vital and Vital 2012; Celardo et al. 2014; Wada and Nakatsuka 2016; Rovira-Llopis et al. 2017).

Mitochondrial DRP-mediated fusion is poorly understood and is mechanistically distinct from both SNARE- and viral-mediated fusion. Fusion DRPs that reside in the outer and inner mitochondrial membranes are mitofusin 1, mitofusin 2 (Mfn1 and Mfn2) and Opa1, respectively. Mfn1 and Mfn2 are functionally related but non-redundant paralogs in mammalian cells (Santel and Fuller 2001; Chen et al. 2003; Eura 2003; Ishihara et al. 2004). Interestingly, mutations in Mfn2, but not Mfn1, are the main cause of the peripheral neuropathy Charcot Marie Tooth

Syndrome Type 2A (CMT2A) (Züchner et al. 2004). In CMT2A patients, distal nerve degeneration leads to weakness, sensory loss, gait impairment and foot deformations (Gemignani and Marbini 2001).

Fusion defects associated with some disease-associated variants of Mfn2 can be functionally complemented by Mfn1 (Detmer & Chan 2007b). Consistent with this, a recent report found that expression of exogenous Mfn1 in neurons of a CMT2A mouse model rescued axonal degradation (Zhou et al. 2019). The importance of the interaction between the mitofusin paralogs is further highlighted by the observation that the optimal fusion complex is composed of both Mfn1 and Mfn2 (Hoppins et al. 2011). As with other DRPs, both mitofusins exhibit nucleotide-dependent self-assembly, and the ability to form higher order oligomers has been correlated with fusion activity (Engelhart and Hoppins 2019). Further supporting a role for assembly in DRP-mediated fusion, intermolecular complementation has been observed between non-functional variants of the yeast mitofusin homolog Fzo1 that possess amino acid substitutions in distinct functional domains (Griffin and Chan 2006). Consistently, Fzo1 has been shown to form a large docking ring that generates an extensive area of contact at the interface of two mitochondria (Brandt et al. 2016).

Mitofusins contain four major structural domains including the GTPase domain, two sequential extended helical bundles (HB1 and HB2) connected by flexible loops, and a transmembrane domain (Figure 1). The domain organization is similar to the bacterial DRP (BDLP), which has been structurally characterized (Low and Löwe 2006; Low et al. 2009). In BLDP, the relative positions of these domains changes in different nucleotide states via changes in hinge regions that connect the domains, resulting in either an extended or a closed state (Figure 1A and B). It is hypothesized that mitofusin proteins undergo similar structural rearrangements around hinge regions (Jimah and Hinshaw 2019). Indeed, atomic structures of a minimal GTPase domain

construct of Mfn1 demonstrate that relative to the GTPase domain, HB1 can exist in two distinct, nucleotide-dependent conformations due to changes in Hinge 2 (Qi et al. 2016; Cao et al. 2017; Yan et al. 2018). Furthermore, mini-peptides or small molecules thought to alter the stability of the extended or closed state of mitofusin change the overall structure of the mitochondrial network in cells (Franco et al. 2016; Rocha et al. 2018a). The function of the region connecting HB1 and HB2 is relatively unexplored. To identify functionally informative variants of mitofusin and characterize the contribution of this region, we exploited the fact that amino acid substitutions in Mfn2 are associated with human disease. Several of these disease-associated substitutions occur near Hinge 1, consistent with our prediction that this domain is functionally important. To gain insight into the role of Hinge 1 in mitofusin-mediated membrane fusion, we interrogated the mitochondrial fusion activity and biochemical properties of disease-associated hinge variants. Our data indicate that this region is required for optimal mitochondrial fusion activity and efficient nucleotide-dependent assembly of Mfn2.

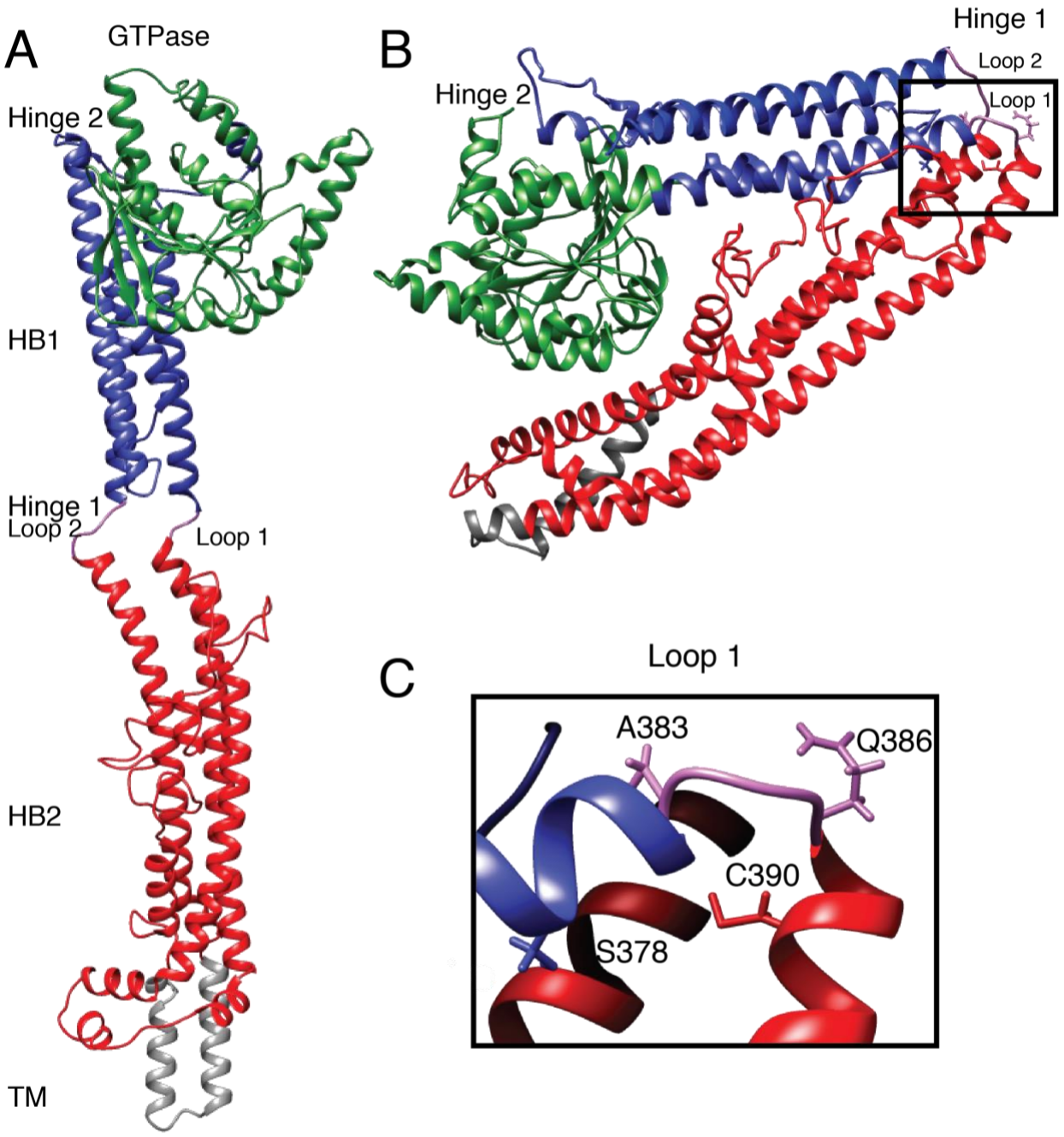

Figure 4.1. Structural model of the positions of Hinge 1 amino acid substitutions associated with CMT2A.
(A) Structural model of the predicted extended structure of Mfn2 based on the crystal structure of the structurally related protein BDLP with GMPPNP (PDB 2W6D). The GTPase domain is green, HB1 is blue, HB2 is red, the transmembrane (TM) domain is grey, and Loops 1/ 2 are purple. Structural prediction performed by I-TASSER server (Zhang 2009; Yang and Zhang 2015). **(B)** Structural model of the predicted closed structure of Mfn2 based on the crystal structure of the structurally related protein BDLP with GDP (PDB 2J69). Domains are colored as described in (A). Structural prediction performed by I-TASSER server (Zhang 2009; Yang and Zhang 2015). **(C)** Enlarged view of Loop 1 from Hinge 1 showing the positions of the CMT2A-related amino acids.

4.3 Results

4.3.1 Mfn2 hinge variants restore reticular mitochondrial morphology in Mfn2-null cells

We set out to characterize four mutant variants of Mfn2 with amino acid substitutions within or adjacent to Loop 1 of Hinge 1: S378P, A383V, Q386P, and C390F (Figure 1C and Table S1). We began by analyzing mitochondrial morphology in stable cell lines expressing mutant versions of Mfn2. To create these lines, we introduced either wild type or mutant *MFN2* with a C-terminal 3xFLAG tag into Mfn2-null mouse embryonic fibroblasts (MEFs) using retroviral transduction (Chen et al. 2003). Clonal populations expressing Mfn2 at near-endogenous levels were selected for characterization (Figure S1).

In wild type MEFs, mitochondria were in reticular networks where most of the mitochondria were longer than 2.5 μm (Figure 2, $Mfn1^{+/+}Mfn2^{+/+}$). Mfn2-null cells transduced with an empty vector, conversely, contained mainly fragmented individual mitochondria less than 2.5 μm in length (Figure 2, vector), which is consistent with published observations of Mfn2-null cells (Chen et al. 2003). Expression of wild type Mfn2 in Mfn2-null cells restored fusion activity and a reticular mitochondrial network in about 80% of cells (Figure 2, $Mfn2^{WT}$). Somewhat surprisingly, all Mfn2 mutant variants examined here ($Mfn2^{S378P}$, $Mfn2^{A383V}$, $Mfn2^{Q386P}$, and $Mfn2^{C390F}$) also restored a reticular mitochondrial network in Mfn2-null cells to a similar extent as $Mfn2^{WT}$. These results indicate that all four of these Mfn2 variants are stable and well-folded and support robust fusion activity in Mfn2-null fibroblasts. This is consistent with previously reported data that showed subsets of CMT2A associated mutations restored fusion activity (Detmer & Chan 2007; Engelhart & Hoppins 2019).

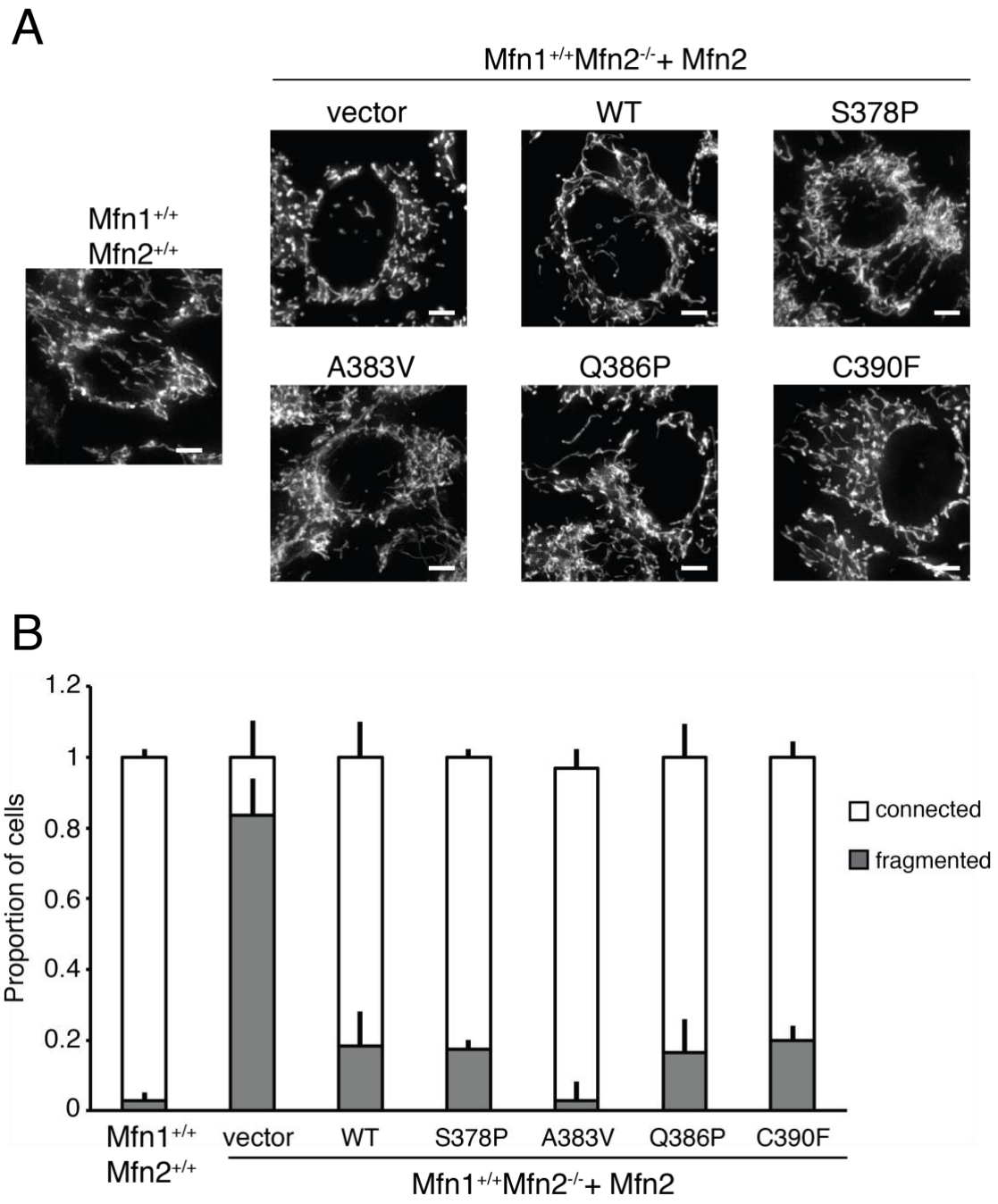

Figure 4.2. Mfn2 hinge variants support mitochondrial fusion in Mfn2-null cells. **(A)** Representative images of mitochondrial networks in wild type ($Mfn1^{+/+}Mfn2^{+/+}$) or Mfn2-null ($Mfn1^{+/+}Mfn2^{-/-}$) mouse embryonic fibroblasts expressing the indicated Mfn2 variant. Mitochondria were stained with Mitotracker Red CMXRos and visualized by fluorescence microscopy. Images represent a maximum intensity projection. Scale bars = 5 μm. **(B)** Quantification of mitochondrial morphology in cells represented in **(A)** Error bars indicate mean + standard deviation from three blinded experiments (n ≧ 100 cells per population per experiment).

4.3.2 Mfn2 hinge variants have an in vitro mitochondrial fusion defect

We reasoned that these substitutions may result in biochemical changes to the protein that were masked in the context of the cell, where many factors modulate the structure of the mitochondrial network. Therefore, we proceeded to characterize these mutant forms of Mfn2 in the context of isolated mitochondria. To quantify the mitochondrial fusion activity of the Mfn2 mutant variants in the absence of cytosolic factors, we utilized a cell-free mitochondrial fusion assay. Mitochondria isolated from cells expressing RFP or CFP targeted to the mitochondrial matrix were mixed, incubated in fusion buffer and then imaged by fluorescence microscopy. Fusion events were scored as the overlap of the two fluorophores in three dimensions. All assays were performed in parallel with mitochondria isolated from wild type cells, and data is expressed as a proportion of wild type controls. Mitochondria isolated from Mfn2-null cells transduced with empty vector fused at a much lower frequency than wild type controls (Figure 3A). Fusion of mitochondria isolated from the clonal population of Mfn2-null cells expressing $Mfn2^{WT}$ was similar to wild type controls (Figure 3A), consistent with the restoration of the mitochondrial morphology in cells. To quantify the fusion activity of the Mfn2 hinge mutants in vitro, mitochondria were isolated from each of the clonal populations described above. In each case, the mitochondrial fusion activity was significantly lower than wild type controls (Figure 3A).

The in vitro mitochondrial fusion data revealed that amino acid substitutions in this hinge region diminish the fusion activity of Mfn2. Given that we could not detect a mitochondrial fusion defect in cells, we predicted that a cytosolic factor could be enhancing fusion activity of the mutant variants. To test this in vitro, we performed the mitochondrial fusion assay in the presence of cytosol from wild type MEFs. As has been previously reported, the addition of the cytosol-enriched fraction to wild type mitochondria moderately stimulated fusion activity

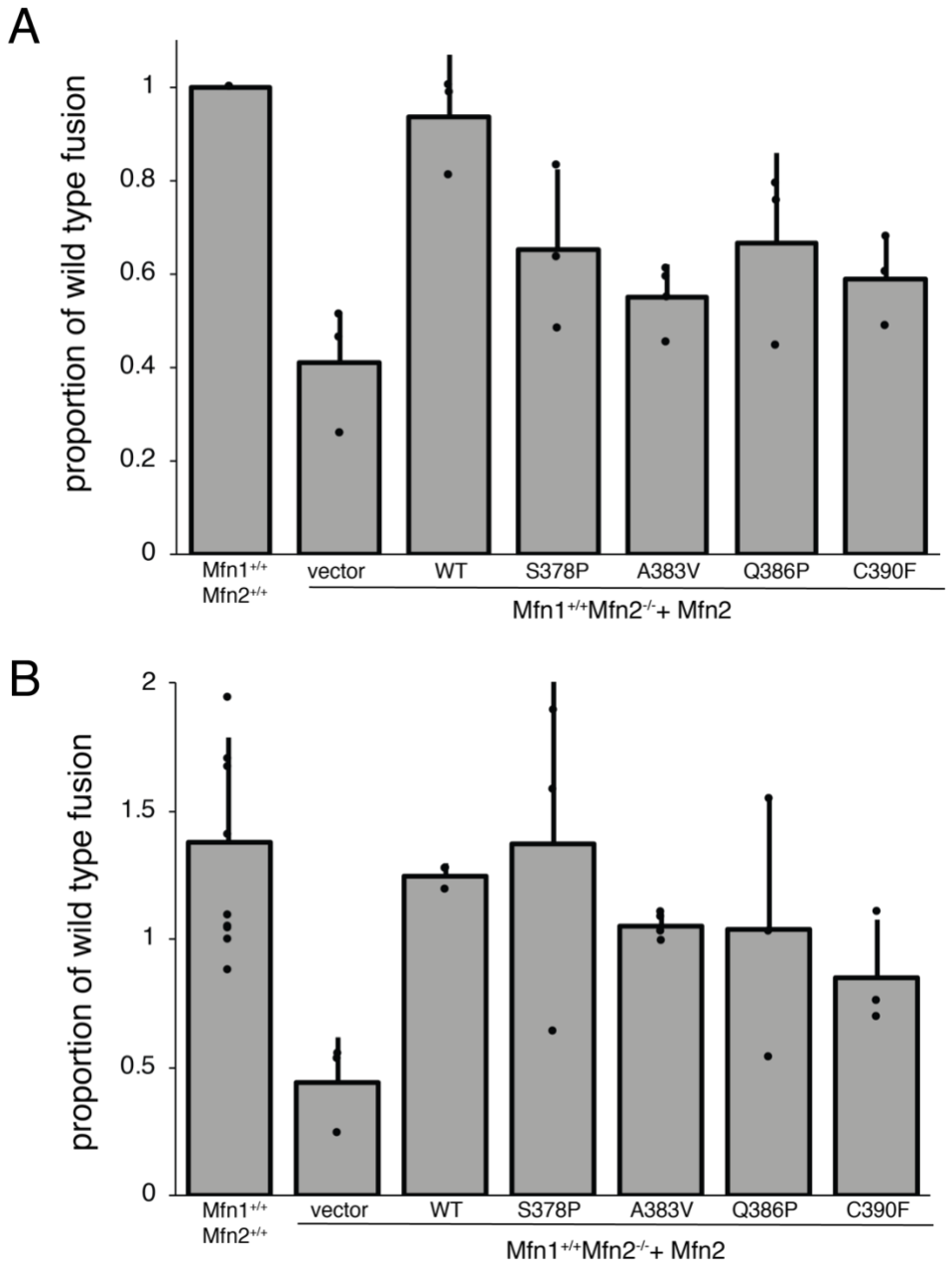

Figure 4.3. Mitochondrial in vitro fusion assay reveals a defect for all Mfn2 hinge variants.
(A) Mitochondria were isolated from wild type cells or clonal populations of Mfn2-null cells either transduced with empty vector or expressing the indicated Mfn2 variant were subject to in vitro fusion conditions at 37°C for 60 minutes. The data are represented as relative to wild type controls performed in parallel. Error bars indicate mean + standard deviation from at least three independent experiments and the statistical significance were determined by paired t-test analysis (*P<0.05). **(B)** Mitochondrial in vitro fusion assay performed as in (A) except with the addition of cytosol-enriched fraction to the reaction buffer. Data are represented as relative to wild type controls performed in parallel without cytosol added. Error bars indicate mean + standard deviation from at least three independent experiments

(Hoppins et al. 2011). In contrast, the cytosol-enriched fraction did not alter the fusion activity of mitochondria isolated from Mfn2-null cells, indicating that Mfn2, but not Mfn1, is regulated by the cytosolic factor (Figure 3B). The addition of cytosol also increased the fusion activity of mitochondria that possess the Mfn2 hinge variants similarly to wild type controls (Figure 3B). These data indicate that the fusion defect associated with the hinge mutant variants can be compensated for by cytosolic factors in cells.

4.3.3 Mfn2 hinge mutant variants interact with Mfn1 in cis and in trans

Mfn1 and Mfn2 physically interact in the same membrane, in cis, and across two membranes, in trans, as measured by co-immunoprecipitation (Chen et al. 2003; Scott A Detmer and Chan 2007a; Engelhart and Hoppins 2019). To determine if the Mfn2 hinge mutant variants interact with Mfn1 in cis or in trans, we tested whether Mfn1 would co-immunoprecipitate with Mfn2-FLAG. To distinguish between cis and trans, we mixed mitochondria that possess endogenous Mfn1 and Mfn2-FLAG with mitochondria that possess Mfn1-EGFP and endogenous Mfn2 (Figure 4A). In this way, three unique interactions with Mfn2-FLAG (Figure 4, filled arrowhead) could be assessed: (1) endogenous Mfn1 in cis (Figure 4, black arrow), (2) Mfn1-EGFP in trans (Figure 4, open arrowhead), and (3) endogenous Mfn2 in trans (Figure 4, white arrow). These reactions were performed in the presence of the GTP transition state mimic GDP-BeF_3, which has been shown to stabilize an interaction between mitofusin molecules and promote a tethering interaction, or BeF_3 alone as a negative control (Qi et al. 2016; Yan et al. 2018; Engelhart and Hoppins 2019). As expected, wild type Mfn2-FLAG immunoprecipitated both endogenous Mfn1 and Mfn1-EGFP (Figure 4). The amount of endogenous Mfn1 interacting in cis (Figure 4, black arrow) is not significantly different in the presence or absence of the transition state mimic. In contrast, the trans interaction is more robust in the presence of GDP-BeF_3 compared to BeF_3 alone (Figure 4, open arrowhead). Together, these data indicate that only the trans interaction is highly dependent on the nucleotide binding state of the mitofusin proteins. Each of the four Mfn2 hinge variants also immunoprecipitated Mfn1 in cis and in trans (Figure 4), indicating that there is no defect in the physical interaction with Mfn1 in either context. Interestingly, even in the presence of GDP-BeF_3, we could not detect an interaction in trans between Mfn2-FLAG and

endogenous Mfn2 (Figure 4, white arrow), which suggests that Mfn2 does not form a robust homotypic trans complex. This could indicate that Mfn2 homodimers are not usually responsible for mitochondrial tethering prior to outer mitochondrial membrane fusion (Figure 7A).

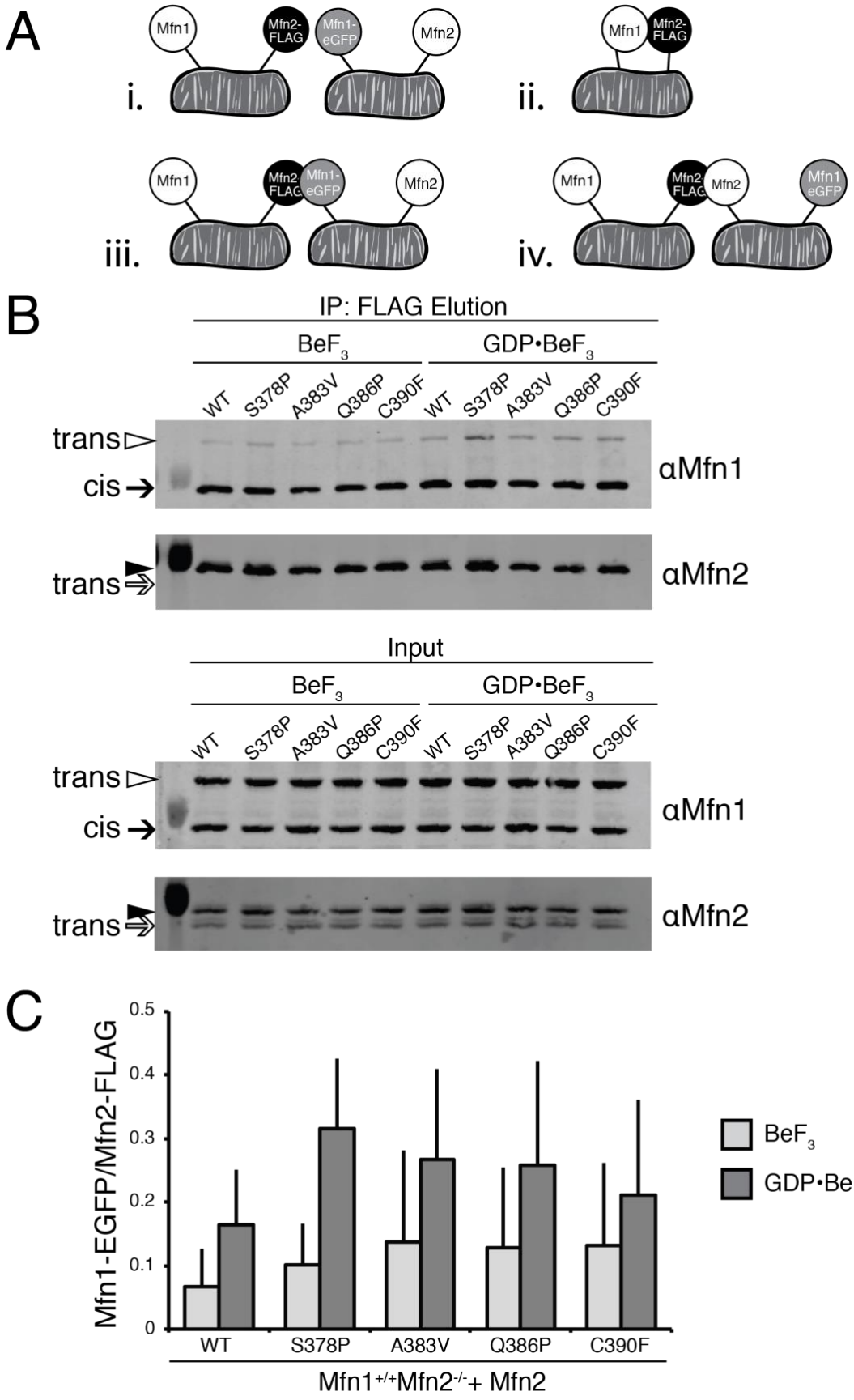
A
Mfn1
Mfn2-FLAG
Mfn1-eGFP
Mfn2
i.
ii.
iii.
iv.
B
IP: FLAG Elution
BeF3
GDP•BeF3
WT
S378P
A383V
Q386P
C390F
trans
cis
αMfn1
αMfn2
Input
C
Mfn1-EGFP/Mfn2-FLAG
0.5
0.4
0.3
0.2
0.1
0
Mfn1+/+Mfn2-/-+ Mfn2

Figure 4.4. Mfn2 hinge variants interact with Mfn1 in cis and trans.
(A) Schematic of the differential epitope labeling utilized in the co-immunoprecipitation assay. **(B)** Mitochondria were isolated from a clonal population of Mfn1-null cells expressing Mfn1^{WT}-EGFP at endogenous levels (Mfn1^{WT}Mfn2$^{+/+}$), and clonal populations of Mfn2-null cells expressing the indicated Mfn2-FLAG variants. Mitochondria that possess Mfn1-EGFP and Mfn2 were combined with mitochondria that possess Mfn1 and Mfn2-FLAG and these mixtures were incubated with BeF_3 in the absence or presence of GDP. Following lysis, immunoprecipitation was performed with α-FLAG magnetic beads. Proteins eluted from the beads were subjected to SDS-PAGE and immunoblotting with α-Mfn1 and α-Mfn2, as indicated. Arrows indicate endogenous Mfn1 (black) and Mfn2 (white); arrowheads indicate Mfn1-EGFP (white) and Mfn2-FLAG (black), respectively. Input represents 3% of the input and elution represents 37.5% of the immunoprecipitated protein. **(C)** Quantification of the percentage of Mfn1-EGFP in the elution compared to Mfn2-FLAG is shown as the mean + standard deviation of three independent experiments.

4.3.4 Nucleotide-dependent self-assembly is diminished in Mfn2 hinge mutant variants

Defects in mitofusin assembly correlate with reduced rates of mitochondrial fusion in vitro (Engelhart and Hoppins 2019). To determine the capacity of the Mfn2 hinge variants to assemble, we utilized blue native gel electrophoresis (BN-PAGE). Mitochondria were left untreated or were incubated with either GTP or the non-hydrolyzable analog GMPPNP. Mitochondria were then lysed and separated by BN-PAGE and subject to Western blot analysis. When mitochondria were untreated, $Mfn2^{WT}$ migrated mostly in assemblies that approximately correspond in size to a dimer (Figure 5A and C, arrow), with some protein migrating as larger assemblies (Figure 5A and C, arrowheads). When these mitochondria were instead incubated with nucleotide, the ratio of dimer to larger assemblies decreased, consistent with nucleotide-dependent assembly of Mfn2 into higher-order oligomers. Specifically, following incubation with GTP, more $Mfn2^{WT}$ migrated in two larger assemblies, with a notable increase in the ~450 kDa oligomer (Figure 5A, open arrowhead). Incubation of mitochondria with GMPPNP also promoted higher-order assembly with enhanced stability of a ~320 kDa oligomer and some protein migrating as the ~450 kDa oligomer (Figure 5A, closed and open arrowheads, respectively). Together, these data indicate that Mfn2 exists primarily as a dimer in the mitochondrial outer membrane and assembles into at least two larger oligomeric species in a nucleotide-dependent manner.

In untreated mitochondria, all of the Mfn2 hinge variants migrated similarly to wild type, with most of the protein in the dimer (Figure 5A). In the presence of GTP, the mutants also assembled similar to wild type, with the exception of $Mfn2^{S378P}$, which had less protein migrating as the 450 kDa oligomer compared to wild type. Each of the hinge mutants displayed altered assembly relative to wild type Mfn2 in the presence of GMPPNP (Figure 5B). Compared to $Mfn2^{WT}$, $Mfn2^{S378P}$, $Mfn2^{A383V}$, $Mfn2^{Q386P}$, and $Mfn2^{C390F}$ all showed a significantly decreased

amount of protein migrating as the 320 kDa oligomer (Figure 5B). These data indicate that amino acid substitutions in this hinge region prevent the stable assembly of Mfn2 into this oligomeric species in the presence of the non-hydrolyzable GTP analog.

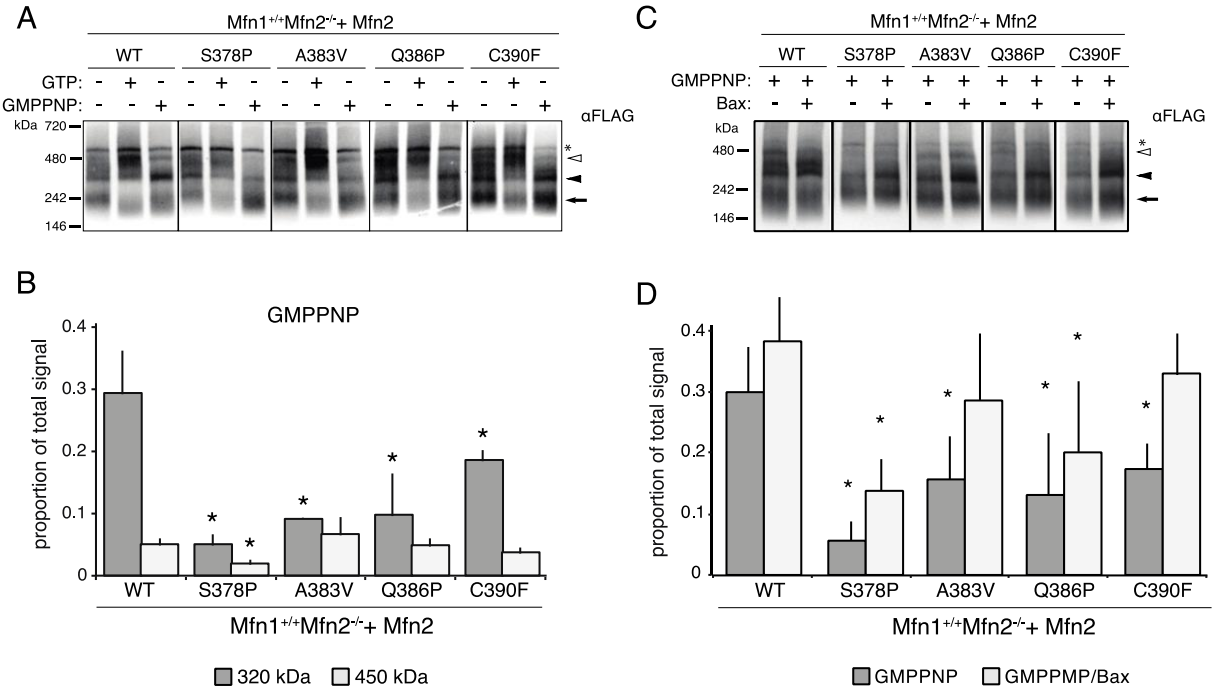

Figure 4.5. Mfn2 hinge variants have altered nucleotide-dependent assembly. **(A)** Mitochondria were isolated from clonal populations of Mfn2-null cells expressing the indicated Mfn2 variant. Mitochondria were either untreated or incubated with 2mM GTP or 2mM GMPPNP as indicated before lysis and separation by BN-PAGE followed by immunoblotting with anti-FLAG antibody. Arrow represents predicted dimer, closed arrowhead indicates ~320 kDa species, and open arrowhead indicates ~450 kDa species. Asterisk (*) indicates nonspecific signal. **(B)** Quantification of proportion of the total protein observed in the 320kDa or 450kDa band after treatment with GMPPNP (filled arrowhead). Error bars indicate mean + standard deviation from at least three independent experiments and the statistical significance were determined by paired t-test analysis between the indicated data and wild type (*P<0.05). **(C)** Mitochondria were prepared as in (A) and incubated with 2mM GMPPNP with or without 1μM recombinant purified Bax. Arrow represents predicted dimer, closed arrowhead indicates ~320 kDa species, and open arrowhead indicates ~450 kDa species. Asterisk (*) indicates nonspecific signal. **(D)** Quantification of proportion of the total protein observed in the 320kDa band. Error bars indicate mean + standard deviation from at least three independent experiments and the statistical significance were determined by paired t-test analysis between the indicated data and wild type (*P<0.05).

Given that these mutant variants also exhibit an in vitro mitochondrial fusion defect, we hypothesize that nucleotide dependent assembly contributes to efficient Mfn2-mediated membrane fusion. Our data would further predict that cytosolic factors, which improve in vitro fusion activity, could facilitate Mfn2 assembly. To test this, we assessed Mfn2 nucleotide-dependent assembly in the presence of recombinant purified Bax, which has been previously demonstrated to promote Mfn2-dependent mitochondrial fusion and Mfn2 assembly (Karbowski et al. 2006; Hoppins et al. 2011). In the presence of Bax, we observe more $Mfn2^{WT}$ in the 320 kDa oligomer, consistent with Bax playing a role in Mfn2 assembly (Figure 5C and 5D). Furthermore, $Mfn2^{S378P}$, $Mfn2^{A383V}$, $Mfn2^{Q386P}$, and $Mfn2^{C390F}$ also had increased abundance of the 320 kDa oligomer in the presence of Bax (Figure 5C and 5D). Together, these data support the conclusion that impaired nucleotide-dependent assembly results in diminished in vitro fusion activity and that cytosolic factors such as Bax compensate for these defects in cells.

4.3.5 Double hinge mutations reveal that HB1 and HB2 work together in mitochondrial fusion

Our data indicate that this region of Mfn2 is important for Mfn2 fusion activity. Based on structural models, S378 is predicted to be located in HB1 while C390 is part of HB2. We considered the possibility that these two distinct structural domains function in cooperatively to control the conformational state of Mfn2. If this is the case, a variant of Mfn2 with amino acid substitutions in both HB1 and HB2 would be predicted to have a more severe functional defect than variants with two substitutions in the same structural domain. To test this hypothesis, we used $Mfn2^{L710P}$, a disease-associated variant in HB2 that is located near Loop 2 in Hinge 1 (Verhoeven et al. 2006) (Figure 1, Figure S2). This amino acid substitution has been characterized in Mfn1, $Mfn1^{L691P}$, which had some fusion activity in Mfn1-null cells (Koshiba et al. 2004). We generated double mutant variants of Mfn2 with this mutation and either

Mfn2$_{S378P}$, which is located in HB1 or Mfn2$_{C390F}$, which is located in HB2 (Mfn2$_{S378P/L710P}$ and Mfn2$_{C390F/L710P}$, respectively).

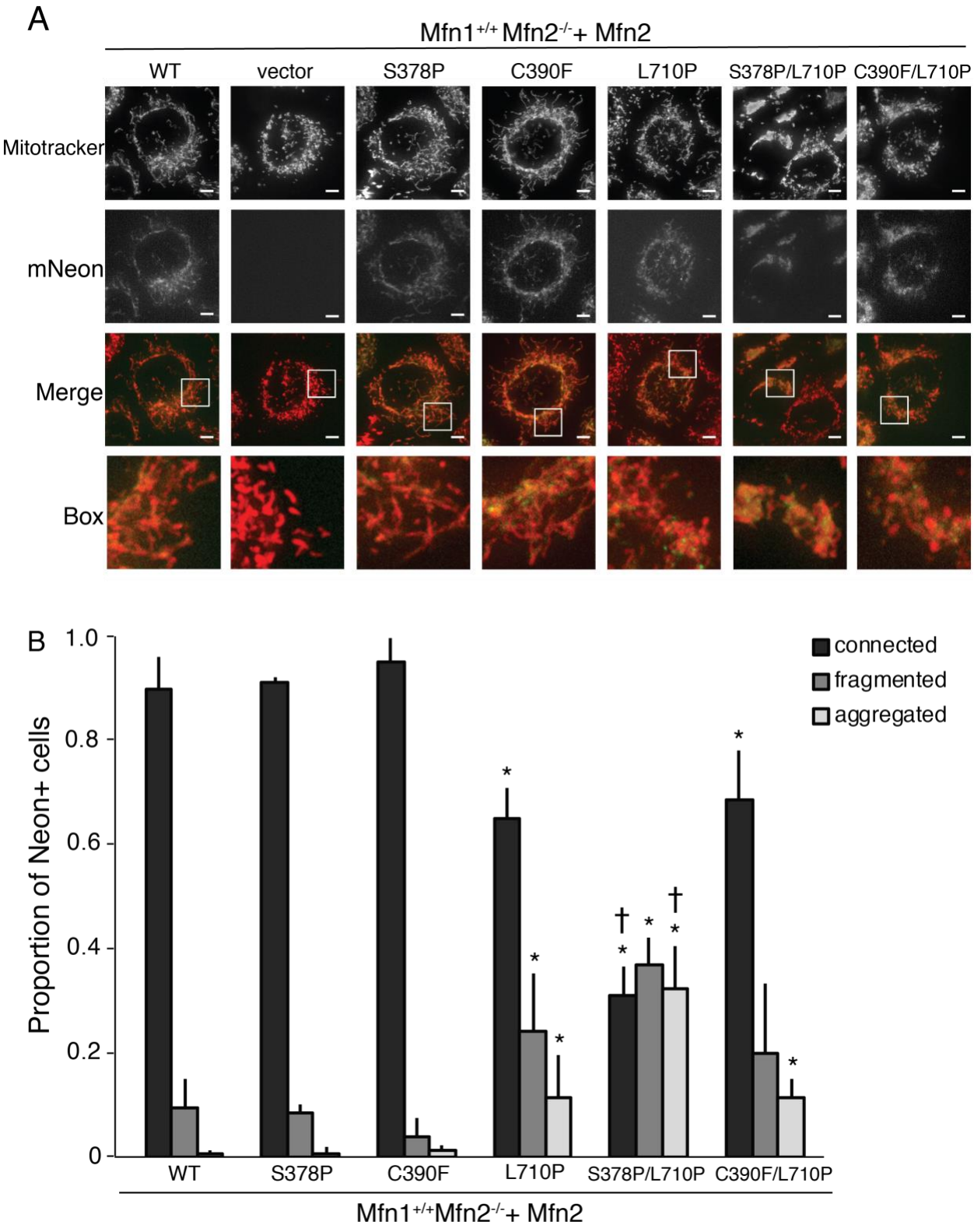

Figure 4.6. Mfn2 variants with substitutions in both HB1 and HB2 are defective for fusion in Mfn2-null cells.
(A) Representative images of mitochondrial networks in Mfn2-null ($Mfn1^{+/+}Mfn2^{-/-}$) mouse embryonic fibroblasts expressing the indicated Mfn2-mNeonGreen variant. Mitochondria were stained with Mitotracker Red CMXRos and visualized by fluorescence microscopy. Images represent a maximum intensity projection. Scale bars = 5 μm. **(B)** Quantification of mitochondrial morphology of cells represented in **(A).** Error bars indicate mean + standard deviation from at least three independent experiments and the statistical significance were determined by paired t-test analysis between the indicated data and wild type (*$P<0.05$) or between the indicated data and $Mfn2^{S378P/L710P}$ (†$P<0.05$).

To determine the fusion activity of these double mutant variants, we utilized retroviral transduction to express Mfn2-mNeonGreen (Mfn2-NG) in Mfn2-null MEFs which has previously been shown to restore fusion activity (Engelhart and Hoppins 2019). The mitochondrial morphology was scored in cells expressing Mfn2, as assessed by colocalization of Mfn2-NG with MitoTracker Red. As expected, $Mfn2^{WT}$, $Mfn2^{S378P}$ and $Mfn2^{C390F}$ restored the reticular mitochondrial network, which recapitulated our observations from the clonal populations described above (Figure 6, compare to Figure 2). Expression of $Mfn2^{L710P}$ also restored a reticular network in 65% of cells (Figure 6), indicating a mild defect in mitochondrial fusion, consistent with previous reports (Koshiba et al. 2004).

In Mfn2-null cells expressing the HB2 double mutant $Mfn2^{C390F/L710P}$, the mitochondrial morphology was comparable to that in cells expressing $Mfn2^{L710P}$ alone (Figure 6). In contrast, when both HB1 and HB2 possess an amino acid substitution, there is significantly less mitochondrial fusion. Specifically, in Mfn2-null cells expressing $Mfn2^{S378P/L710P}$, most cells possessed a mitochondrial network that was either fragmented or in fragmented aggregates, and only 30% of cells had a reticular mitochondrial network. Together, these results support the conclusion that HB1 and HB2 provide unique and separate contributions to support Mfn2-mediated membrane fusion.

4.4 Discussion

In this study, we performed an in-depth characterization of disease-associated amino acid substitutions located within Hinge 1 of Mfn2, which connects HB1 and HB2. In other DRPs, hinges mediate conformational changes that are required for membrane remodeling activity. The results presented here are consistent with structural models that suggest this region functions as a hinge and for the first time connects Hinge 1 integrity to nucleotide-dependent assembly of the mitofusins. These molecular defects also correspond to a decrease in mitochondrial fusion efficiency in vitro. Both of these defects were improved by the addition of cytosolic factors, which indicates that mitofusin function is subject to complex regulation in cells. This leads to the likely involvement of other players in the model of mitochondrial outer membrane fusion (Figure 7).

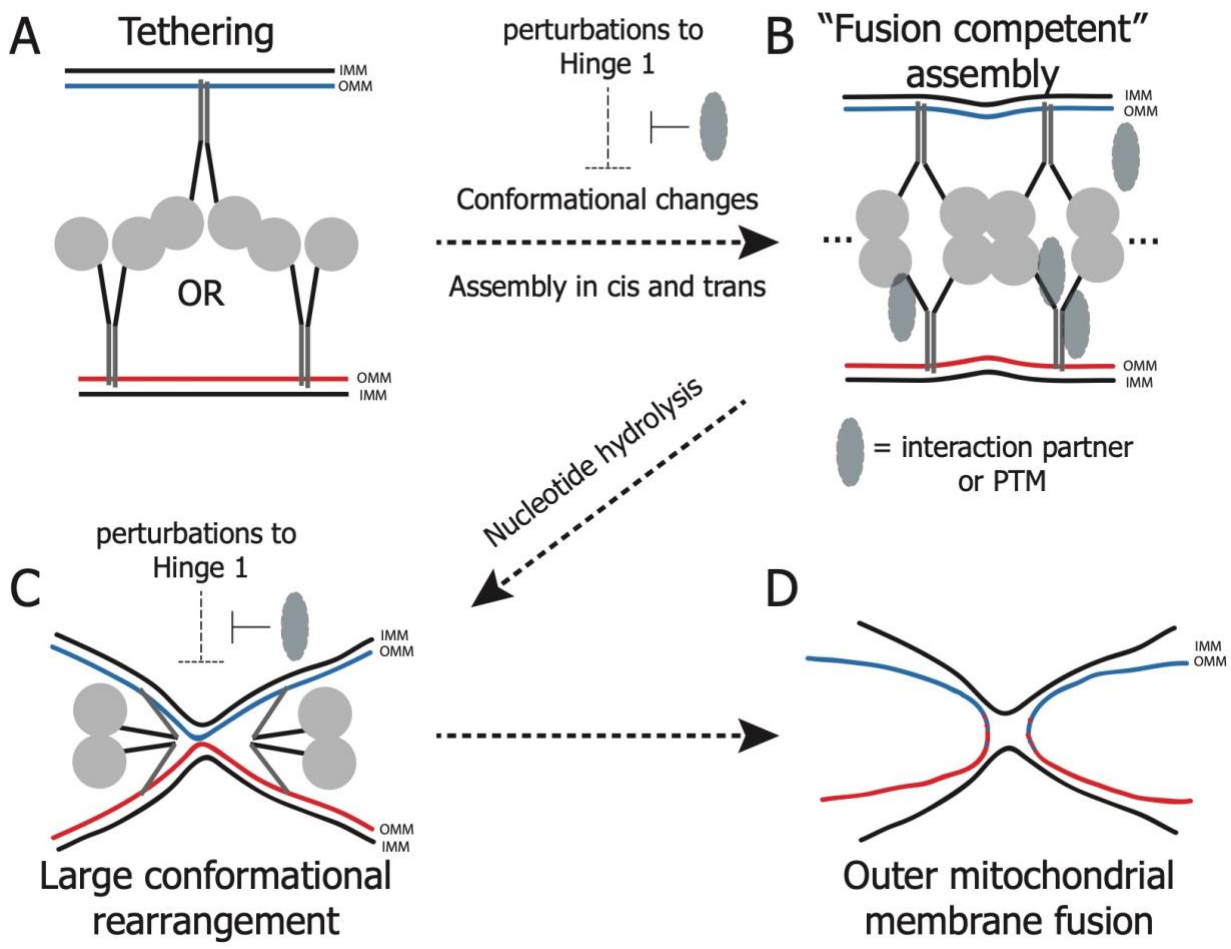

Figure 4.7. Model of outer mitochondrial membrane fusion.
A) Mitofusins on separate mitochondria are tethered by interactions between mitofusin molecules on opposite outer membranes (OMM, red and blue). **B)** Assembly of mitofusin molecules on the same membrane (in cis) and on opposite membranes (in trans) leads to the formation of an assembly that can facilitate outer mitochondrial membrane fusion. This is facilitated by conformational changes in the mitofusin proteins that can be made more inefficient by perturbations to Hinge 1, which can, in turn, be compensated for by some regulatory factor (green oval). **C)** Nucleotide hydrolysis leads to a large structural rearrangement of the mitofusin proteins that disrupts the mitochondrial membranes and brings them into close proximity. As in B), this can be slowed or destabilized by perturbations to Hinge 1 and stabilized by a regulating factor. **D)** Outer mitochondrial membranes mix completing the process of outer membrane fusion.

Our data indicate that Mfn2 exists primarily as a dimer in the mitochondrial outer membrane and this form is not altered by the amino acid substitutions tested here (consistent with Figure 7A). Furthermore, the Mfn2 variants are able to interact with Mfn1 on the same and adjacent mitochondria in a nucleotide dependent manner similarly to wild type Mfn2 (Figure 4). Together, these data suggest that these amino acid substitutions do not significantly alter the structure of Mfn2.

We demonstrate that GTP stabilizes a 450 kDa oligomer while the non-hydrolyzable analog stabilizes a 320 kDa oligomer. In the presence of GTP, most of the migration pattern of the hinge variants is similar to wild type and each can form both dimers and 450 kDa oligomers. This indicates that these variants are not unable to fold or oligomerize. In contrast, the hinge mutants do not readily form the 320 kDa state adopted when Mfn2 is bound to GMPPNP. Given that all Mfn2 hinge mutants co-immunoprecipitate Mfn1 as efficiently as wild type, interaction with Mfn1 is not likely to play a role in this assembly. Indeed, previously published data from our lab suggest that the BN-PAGE assemblies are homo-oligomers (Engelhart and Hoppins 2019). These data are consistent with the hypothesis that the nucleotide binding state of Mfn2 alters the conformational state of the protein, which results in the preferential formation of distinct oligomeric species. Therefore, the reduced assembly observed for the hinge mutants could be due to aberrant structural rearrangements of HB1 and HB2 as mediated by Hinge 1. Our data further implicate Bax in the formation or stability of these oligomers. The current mitochondrial fusion model (Figure 7) includes assembly happening before nucleotide-dependent changes in assembly state. The data presented here suggests that there may be nucleotide-dependent conformational changes around Hinge 1 prior to assembly or that the 450 and 320kDa species represent the same assembly state of Mfn2 in different conformations or including different interaction partners. The finding that Bax helps stabilize the 320kDa species, which is the only oligomer significantly affected by amino acid substitutions in Mfn2 supports

this idea. The hypothesis arising from these findings would be that the integrity of Hinge 1 is required for the conformational state and assembly that is represented in the 320 kDa band and that Bax can stabilize this conformation even with perturbations to the sequence of the hinge region.

Functional complementation has been observed between two non-functional alleles of Fzo1, the mitofusin homolog (Griffin and Chan 2006). These data indicate that different molecules in the fusion complex can contribute different properties. The amino acid substitutions tested here are predicted to be within either HB1 (S378), HB2 (C390) or a flexible loop between the two (A383V, Q386P). Given that each individual amino acid substitution was associated with a similar partial loss of function, we considered that these structural domains may work cooperatively to evoke nucleotide-dependent conformational changes. To test this, we assessed the fusion activity of variants with two amino acid substitutions, either in the same domain (HB2, C390F & L710P) or in different domains (HB1, S378P & HB2, L710P). When amino acid substitutions were both in HB2, the fusion activity in cells was more substantial than when the substitutions were in HB1 and HB2. Therefore, our data indicate that distinct structural domains provide unique contributions to Mfn2 fusion activity within the same molecule. As a whole, the data presented here are consistent with the hypothesis that different nucleotide-dependent conformations support either the formation or stabilization of different assembly states and that the integrity of the hinge that connects HB1 and HB2 plays a role in this process (Figure 7C). We have further shown that this assembly is supported not only by intramolecular interactions, but also by regulating cytosolic factors such as Bax.

4.5 Supplemental figures

Table 4.S1 Clinical characterization of the Hinge 1 Loop 1 CMT2A mutations in this study.

Mutation	Age at onset	Severity of symptoms	Other	Reference
S378P	7	Mild compared to others in the same study		Brockmann, et al. 2007
A383V	various	Various; apparent incomplete penetrance	2 unrelated families with same mutation	Muglia, et al., 2007
Q386P	1.5	Severe	De novo mutation	Verhoeven, et al., 2006
C390F	1	Severe	De novo mutation	Feely et al., 2011

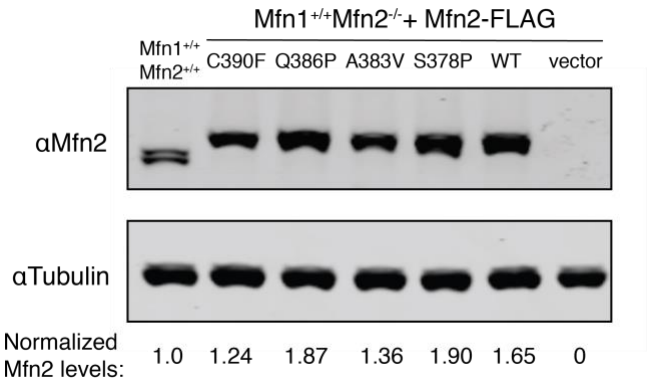

Figure 4.S1 Mfn2 protein expression in MEF clonal populations.
Whole-cell lysates prepared from the indicated cell lines were subject to SDS-PAGE and immunoblotting with α-Mfn2 and α-tubulin.

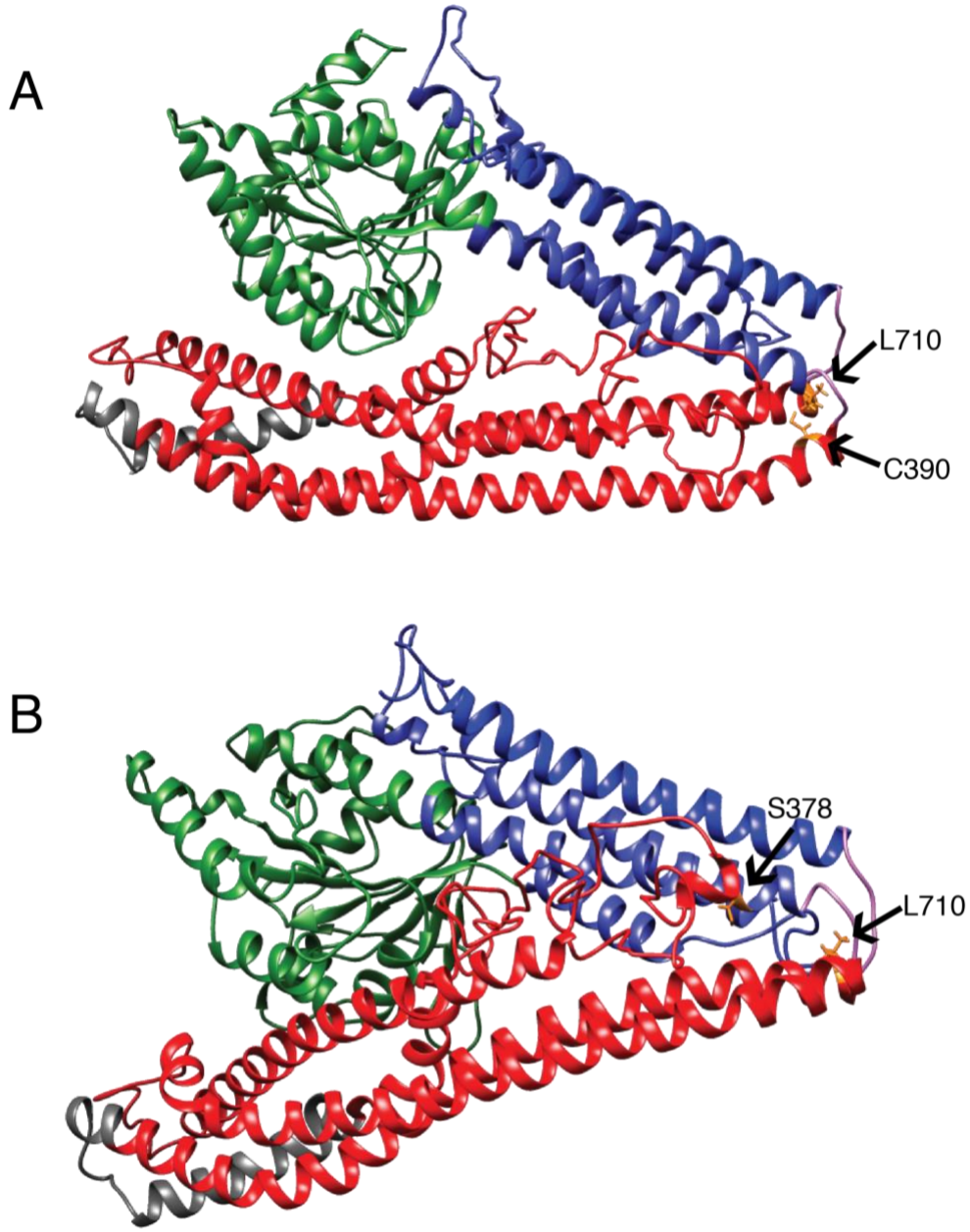

Figure 4.S2 Structural model of the positions of hinge amino acid substitutions associated with CMT2A.
Structural models of the predicted closed structure of Mfn2 based on the crystal structure of the structurally related protein BDLP with GDP (PDB 2J69). The GTPase domain is green, HB1 is blue, HB2 is red, the transmembrane (TM) domain is grey, and Loops 1/ 2 are purple. **(A)** The positions of C390 and L710 are indicated in orange and labeled. **(B)** The positions of S378 and L710 are indicated in orange and labeled. Structural prediction performed by I-TASSER server (Zhang 2009; Yang and Zhang 2015).

4.6 Materials and methods

4.6.1 Cell culture

All cells were grown at 37°C and 5% CO_2 and cultured in DMEM (Thermo Fisher Scientific) containing 1X GlutaMAX (Thermo Fisher Scientific) with 10% FBS (Seradigm) and 1% penicillin/streptomycin (Thermo Fisher Scientific). Mouse embryonic fibroblasts cells (Mfn wildtype and Mfn2-null) were purchased from ATCC.

4.6.2 Retroviral transduction and generation of clonal populations

Plat-E cells (Cell Biolabs) were maintained in complete media supplemented with 1 μg/mL puromycin and 10 μg/mL blasticidin and plated at approximately 80% confluency the day prior to transfection. Plat-E cells were transfected with FuGENE™ HD (Promega) and transfection regent was incubated overnight before a media change. Viral supernatants were collected at approximately 48, 56, 72, and 80 hours post transfection and incubated with MEFs in the presence of 8 mg/ml polybrene. Approximately 16 hours after the last viral transduction, MEF cells were split and selection was added if needed (1 μg/mL puromycin or 200 μg/mL hygromycin).

Clonal populations were generated by plating cells at very low density and clones were collected onto sterile filter paper dots soaked in trypsin. Following expansion, whole cell extract from clonal populations were screened by western blot analysis for mitofusin against wildtype controls.

4.6.3 Transfection and microscopy

All cells were plated in No. 1.5 glass-bottomed dishes (MatTek). Mouse embryonic fibroblasts were incubated with 0.1 μg/mL Mitotracker Red CMX Ros (Invitrogen) for 15 minutes at 37°C with 5% CO_2, washed and incubated with complete media for at least 45 minutes prior to imaging.

MEFs were imaged at 37°C with 5% CO_2. A Z-series with a step size of 0.3 μm was collected with a Nikon Ti-E widefield microscope with a 63X NA 1.4 oil objective (Nikon), a solid-state light source (Spectra X, Lumencor), and an sCMOS camera (Zyla 5.5 Megapixel). Each cell line was imaged by a blinded researcher on at least three separate occasions (n > 100 cells per experiment).

4.6.4 Image analysis

Images were deconvolved using 8-15 iterations of 3D Landweber deconvolution. Deconvolved images were then analyzed using Nikon Elements software. Maximum intensity projections were created using Photoshop (Adobe). Mitochondrial morphology was scored as follows: reticular indicates that fewer than 30% of the mitochondria in the cell were fragments (fragments defined as mitochondria less than 2 μm in length); fragmented indicates that most of the mitochondria in the cell were less than 2 μm in length; aggregated indicates fragmented mitochondria that were not distributed throughout the cytosol.

4.6.5 Preparation of mitochondria or cytosol-enriched fraction

For each experiment, three to five 15 cm plates each of MEFs were grown to ~90% confluency. Cells were harvested by cell scrapping, pelleted, and washed in mitochondrial isolation buffer (MIB) (0.2 M sucrose, 10 mM Tris-MOPS [pH 7.4], 1 mM EGTA). The cell pellet was resuspended in one cell pellet volume of cold MIB, and cells were homogenized by 10 to 14 strokes on ice with a Kontes Potter-Elvehjem tissue grinder set at 400 RPM. The homogenate was centrifuged (500 × *g*, 5 min, 4°C) to remove nuclei and unbroken cells, and homogenization of the pellet fraction was repeated followed by centrifugation at 500 × *g*, 5 min, 4°C. The supernatant fractions were combined and centrifuged again at 500 × *g*, 5 min, 4°C to remove remaining debris. The supernatant was transferred to a clean microfuge tube and centrifuged (7400 × *g*, 10 min, 4°C) to pellet a crude mitochondrial fraction. The post-mitochondrial

supernatant fraction was saved as the cytosol-enriched fraction. The crude mitochondrial pellet was resuspended in a small volume of MIB. Protein concentration of fractions was determined by Bradford assay (Bio-Rad Laboratories).

4.6.6 In vitro mitochondrial fusion

An equivalent mass (12.5 μg) of mtTagRFP and mtCFP mitochondria were mixed, washed in 500uL MIB and concentrated by centrifugation (7400 × *g*, 10 min, 4°C). Following a 10 min incubation on ice, the supernatant was removed and the mitochondrial pellet was resuspended in 10 μl fusion buffer (20 mM PIPES-KOH [pH 6.8], 150 mM KOAc, 5 mM $Mg(OAc)_2$, 0.4 M sorbitol, 0.12 mg/ml creatine phosphokinase, 40 mM creatine phosphate, 1.5 mM ATP, 1.5 mM GTP) or 10 μl cytosol-enriched buffer (2.5 μL of the cytosol-enriched fraction obtained from WT MEFs and 7.5 μL fusion buffer). Fusion reactions were incubated at 37°C for 60 minutes.

4.6.7 Analysis of mitochondrial fusion

Mitochondria were imaged on depression microscope slides by pipetting 4μL fusion reaction onto a 3% low-melt agarose bed, made in modified fusion buffer (20 mM PIPES-KOH [pH 6.8], 150 mM KOAc, 5 mM $Mg(OAc)_2$, 0.4 M sorbitol). A Z-series of 6 0.2 μm steps was collected with a Nikon Ti-E widefield microscope with a 100X NA 1.4 oil objective (Nikon), a solid state light source (Spectra X, Lumencor), and a sCMOS camera (Zyla 5.5 Megapixel). For each condition tested, mitochondrial fusion was assessed by counting ≥ 300 total mitochondria per condition from ≥ 4 images per condition (50 – 200 mitochondria per image collected), and fusion was scored by colocalization of the red and cyan fluorophores in three dimensions.

4.6.8 BN-PAGE

Isolated mitochondria (15 – 30 μg) were incubated with or without 2 mM nucleotide (GTP or GMPPNP) and 1μM purified recombinant Bax as indicated in modified mitochondrial isolation buffer (0.2 M sucrose, 10 mM Tris-MOPS [pH 7.4], 1 mM EGTA, 5 mM $Mg(OAc)_2$, 50mM KOAc, 1X HALT protease inhibitor (Thermo Scientific), 0.5mM phenylmethylsulfonyl fluoride (PMSF)) at 37°C for 30 minutes. Mitochondria were then lysed in 1% w/v digitonin, 50 mM Bis-Tris, 50 mM NaCl, 10% w/v glycerol, 0.001% Ponceau S; pH 7.2 for 15 minutes on ice. Lysates were centrifuged at 16,000 x *g* at 4° C for 30 minutes. The cleared lysate was mixed with Invitrogen NativePAGE™ 5% G-250 Sample Additive to a final concentration of 0.25%. Samples were separated on a Novex™ NativePAGE™ 4 - 16% Bis-Tris Protein Gels (Invitrogen) at 4°C. Gels were run at 40 V for 30 minutes then 100 V for 30 minutes with dark cathode buffer (1X NativePAGE™ Running Buffer (Invitrogen), 0.02% (w/v) Coomassie G-250). Dark cathode buffer was replaced with light cathode buffer (1X NativePAGE™ Running Buffer (Invitrogen), 0.002% (w/v) Coomassie G-250) and the gel was run at 100 V for 30 minutes and subsequently at 250 V for 60-75 minutes until the dye front ran off the gel. After electrophoresis was complete, gels were transferred to PVDF membrane (Bio-Rad Laboratories) at 30 volts for 16 hours in transfer buffer (25 mM Tris, 192 mM glycine, 20% methanol). Membranes were incubated with 8% acetic acid for 15 minutes and washed with H_2O for 5 minutes. Membranes were dried at 37°C for 20 minutes and then rehydrated in 100% methanol and washed in H_2O. Membranes were blocked in 4% milk for 20 minutes and were probed with anti-FLAG (Sigma) for 4 hours at room temperature or overnight at 4°C. Membranes were incubated with HRP-linked secondary antibody (Cell Signaling Technology) at room temperature for 1 hour. Membranes were developed in SuperSignal Femto ECL reagent (Thermo Fisher Scientific) for 5 minutes and imaged on iBright Imaging System (Thermo Fisher Scientific). Band intensities were quantified using ImageJ software (NIH). NativeMark Unstained Protein Standard (Life Technologies) was used to estimate molecular weights of mitofusin protein complexes.

4.6.9 Co-immunoprecipitation

Differentially tagged isolated mitochondrial populations (50 □g each) were mixed together. Mitochondria were incubated at 37°C for 30 minutes with beryllium fluoride (2.5 mM $BeSO_4$, 25 mM NaF) with or without 2 mM GDP in fusion buffer (20 mM PIPES-KOH [pH 6.8], 150 mM KOAc, 5 mM $Mg(OAc)_2$, 0.4 M sorbitol with 0.12 mg/mL creatine kinase, 40 mM creatine phosphate, 1.5 mM ATP). Mitochondria were solubilized in lysis buffer (20 mM HEPES-KOH [pH 7.4], 50 mM KCl, 5 mM $MgCl_2$) with 1.5% w/v n-Dodecyl β-D-maltoside (DDM), and 1X Halt Protease Inhibitor (Thermo Scientific) for 30 minutes on ice. Lysates were cleared at 10,000 x *g* for 15 minutes at 4°C. Supernatant was incubated with 50 mL magnetic μMACS Anti-DYKDDDDK MicroBeads (Miltenyi Biotec) for 30 minutes on ice. The sample was applied to a MACS Column (Miltenyi Biotec) placed in the magnetic field using a μMACS Separator (Miltenyi Biotec) and washed once with 300 mL 20 mM HEPES-KOH [pH 7.4], 50 mM KCl, 5 mM $MgCl_2$, 0.1% DDM and once with 200 mL 20 mM HEPES-KOH [pH 7.4], 50 mM KCl, 5 mM $MgCl_2$. One column volume (25 ml) SDS-PAGE loading buffer (60 mM Tris-HCl [pH 6.8], 2.5% sodium dodecyl sulfate, 5% βME, 5% sucrose, 0.1% bromophenol blue) was incubated for 15 minutes at room temperature and proteins were eluted once with 40 mL SDS-PAGE loading buffer. Samples were run on an SDS-PAGE gel and transferred onto nitrocellulose at 94V for 1 hour in 1X transfer buffer (25 mM Tris, 192 mM glycine, 20% methanol). Membranes were blocked in 4% Milk for at least 45 minutes and were probed with anti-Mfn1 antibody and anti-Mfn2 antibody for 4 hours at room temperature or overnight at 4°C. Membranes were incubated with DyLight secondary antibody (Invitrogen) at room temperature for 1 hour. Membranes were imaged on LI-COR Imaging System (LI-COR Biosciences).

4.6.10 Western Blot Analysis

Protein lysates from MEFs were obtained by resuspending PBS washed cells in RIPA lysis buffer (150 mM NaCl, 1% Nonidet P-40, 1% Sodium deoxycholate, 0.1% SDS, 25 mM Tris [pH 7.4], 1X Halt Protease Inhibitor Cocktail, EDTA-Free [Thermo Scientific]). Samples were incubated on ice for 5 minutes and then spun at 21,000 x g for 15 minutes at 4°C. Supernatant was transferred to a clean tube and protein concentration was measured by BCA assay (Thermo Scientific). Samples were run on an SDS-PAGE gel and transferred onto nitrocellulose at 100 V for 50 minutes in 1X transfer buffer. Membranes were blocked in 4% milk for at least 45 minutes and were probed with anti-Mfn1, anti-Mfn2 (Sigma), anti-VDAC (Invitrogen) or anti-alpha Tubulin (Invitrogen) antibody for 4 hours at room temperature or overnight at 4°C. Membranes were incubated with DyLight secondary antibody (Invitrogen) at room temperature for 1 hour. Membranes were imaged on LI-COR Imaging System (LI-COR Biosciences).

4.6.11 Bax expression and purification

Bax was purified as previously described (Suzuki et al. 2000). Briefly, pTYB1-Bax was expressed in E. coli strain BL21(DE3) grown in Luria-Bertani medium with 150 μg/mL ampicillin at 37°C to an OD600 ~ 0.6, and protein expression was induced by the addition of 1 mM isopropyl 1-thio-β-D-galactopyranoside. Induced cultures were grown for about 3 hours at 37°C and then cells were harvested and frozen in liquid nitrogen and stored at -80°C. The pellet was resuspended in TEN buffer (20 mM Tris-HCl pH 8.0, 1 mM EDTA, 500 mM NaCl) and cells were lysed using a microfluidizer (Avestin). The lysate was subjected to centrifugation at 14,000 rpm for 45 min and the cleared lysate was passed through a 0.2 μm filter before binding to a chitin column equilibrated with TEN buffer. The column was washed with TEN buffer and then incubated with TEN buffer + 30 mM DTT for 48 hours at 4°C. Cleaved protein was eluted with TEN buffer and buffer exchange was performed with 20 mM Tris-HCl, pH 8.0 with 10%

glycerol. Protein was bound to Q-sepharose and eluted with a linear gradient of NaCl. TCEP was added to Bax-containing fractions to a final concentration of 1 mM before the protein was aliquoted and frozen at -80°C.

4.6.12 Plasmids & primers

The following plasmids were purchased from Addgene: pBABE-hygro (#1765), pBABE-puro (#1764), mito-paGFP (#23348), pclbw-mito TagRFP (#58425), pclbw-mitoCFP (#58426). The following primers were used to for site directed mutagenesis by Gibson Assembly:

$Mfn2_{S378P}$ F: (5' – CCGTTCGTCTCATCATGGATCCCCTGCACATCGCAGC – 3')

$Mfn2_{S378P}$ R: (5' – GCTGCGATGTGCAGGGGATCCATGATGAGACGAACGG – 3')

$Mfn2_{A383V}$ F: (5' – ATTCCCTGCACATCGCAGTTCAGGAGCAGCGGG – 3')

$Mfn2_{A383V}$ R: (5' – CCCGCTGCTCCTGAACTGCGATGTGCAGGGAAT – 3')

$Mfn2_{Q386P}$ F: (5' –GCACATCGCAGCTCAGGAGCCGCGGGTTTATTGCCTAGAAATGCGG -3')

$Mfn2_{Q386P}$ R: (5'- CCGCATTTCTAGGCAATAAACCCGCGGCTCCTGAGCTGCGATGTGC -3')

$Mfn2_{C390F}$ F: (5' – GGGTTTATTTCCTAGAAATGCGG – 3')

$Mfn2_{C390F}$ R: (5' – CCGCATTTCTAGGAAATAAACCC – 3')

$Mfn2_{L710P}$ F: (5' – GACATCACCCGAGATAATCCGGAGCAGGAAATTGCTGC – 3')

$Mfn2_{L710P}$ R: (5' – GCAGCAATTTCCTGCTCCGGATTATCTCGGGTGATGTC – 3')

4.7 Acknowledgements

We thank the members of the Hoppins lab and Laura Lackner for critical scientific discussions and critical reading of the manuscript. We would also like to thank Richard Youle for sharing the pTYB1-Bax plasmid and Bax purification protocol. NBS was supported by National Institute of General Medical Sciences (NIH NIGMS) Training grant No. T32GM007270 and SCH is supported by NIH NIGMS Grant No. R01GM-118509.

4.8 References

Atkins K, Dasgupta A, Chen K, Mewburn J, Archer SL. 2016. The role of Drp1 adaptor proteins MiD49 and MiD51 in mitochondrial fission : implications for human disease. :1861–1874. doi:10.1042/CS20160030.

Baloh RH, Schmidt RE, Pestronk A, Milbrandt J. 2007. Altered axonal mitochondrial transport in the pathogenesis of Charcot-Marie-Tooth disease from mitofusin 2 mutations. *J Neurosci*. 27(2):422–430. doi:10.1523/JNEUROSCI.4798-06.2007.

Bian X, Xu J, Zhao H, Zheng Q, Xiao X, Ma X, Li Y, Du X, Liu X. 2019. Zinc-Induced SUMOylation of Dynamin-Related Protein 1 Protects the Heart against Ischemia-Reperfusion Injury. *Oxid Med Cell Longev*. 2019:1–11. doi:10.1155/2019/1232146.

Brandt T, Cavellini L, Kühlbrandt W, Cohen MM. 2016. A mitofusin-dependent docking ring complex triggers mitochondrial fusion in vitro. *Elife*. 5:1–23. doi:10.7554/eLife.14618.

de Brito OM, Scorrano L. 2008. Mitofusin 2 tethers endoplasmic reticulum to mitochondria. *Nature*. 456(7222):605–10. doi:10.1038/nature07534.

Cairns RA, Harris IS, Mak TW. 2011. Regulation of cancer cell metabolism. *Nat Rev Cancer*. 11(2):85–95. doi:10.1038/nrc2981.

Calvo J, Funalot B, Ouvrier R a, Lazaro L, Toutain A, De Mas P, Bouche P, Gilbert-Dussardier B, Arne-Bes M-C, Carrière J-P, et al. 2009. Genotype-phenotype correlations in Charcot-Marie-Tooth disease type 2 caused by mitofusin 2 mutations. *Arch Neurol*. 66(12):1511–1516. doi:10.1001/archneurol.2009.284.

Cao Y-L, Meng S, Chen Y, Feng J-X, Gu D-D, Yu B, Li Y-J, Yang J-Y, Liao S, Chan DC, et al. 2017. MFN1 structures reveal nucleotide-triggered dimerization critical for mitochondrial fusion. *Nature*.:1–5. doi:10.1038/nature21077.

Cartoni R, Arnaud E, Médard JJ, Poirot O, Courvoisier DS, Chrast R, Martinou JC. 2010. Expression of mitofusin 2R94Q in a transgenic mouse leads to Charcot-Marie-Tooth neuropathy type 2A. *Brain*. 133(5):1460–1469. doi:10.1093/brain/awq082.

Cartoni R, Martinou JC. 2009. Role of mitofusin 2 mutations in the physiopathology of Charcot-Marie-Tooth disease type 2A. *Exp Neurol*. 218(2):268–273. doi:10.1016/j.expneurol.2009.05.003.

Celardo I, Martins LM, Gandhi S. 2014. Unravelling mitochondrial pathways to Parkinson's disease. *Br J Pharmacol*. 171(8):1943–1957. doi:10.1111/bph.12433.

Chandel NS, Maltepe E, Goldwasser E, Mathieu CE, Simon MC, Schumacker PT. 1998. Mitochondrial reactive oxygen species trigger hypoxia-induced transcription. *Proc Natl Acad Sci U S A*. 95(September):11715–11720.

Chappie JS, Acharya S, Liu Y-W, Leonard M, Pucadyil TJ, Schmid SL. 2009. An Intramolecular Signaling Element that Modulates Dynamin Function In Vitro and In Vivo. *Mol Biol Cell*. 20:3561–3571. doi:10.1091/mbc.E09.

Chen H, Detmer SA, Ewald AJ, Griffin EE, Fraser SE, Chan DC. 2003. Mitofusins Mfn1 and Mfn2 coordinately regulate mitochondrial fusion and are essential for embryonic development. *J Cell Biol*. 160:189–200. doi:10.1083/jcb.200211046.

Chen K-H, Guo X, Ma D, Guo Y, Li Q, Yang D, Li P, Qiu X, Wen S, Xiao R-P, et al. 2004. Dysregulation of HSG triggers vascular proliferative disorders. *Nat Cell Biol*. 6(9):872–883. doi:10.1038/ncb1161.

Chen KH, Dasgupta A, Ding J, Indig FE, Ghosh P, L. Longo D. 2014. Role of mitofusin 2 (Mfn2) in controlling cellular proliferation. *FASEB J*. 28(1):382–394. doi:10.1096/fj.13-230037.

Chen KH, Guo X, Ma D, Guo Y, Li Q, Yang D, Li P, Qiu X, Wen S, Xiao RP, et al. 2004. Dysregulation of HSG triggers vascular proliferative disorders. *Nat Cell Biol*. 6(9):872–883. doi:10.1038/ncb1161.

Chen Y, Dorn GW. 2013. PINK1-Phosphorylated Mitofusin 2 is a Parkin Receptor for Culling Damaged Mitochondria. *Science (80-)*. 340(April):471–476.

Cleland MM, Norris KL, Karbowski M, Wang C, Suen D-F, Jiao S, George NM, Luo X, Li Z, Youle RJ. 2011. Bcl-2 family interaction with the mitochondrial morphogenesis machinery. *Cell*

Death Differ. 18(2):235–247. doi:10.1038/cdd.2010.89.

Cribbs JT, Strack S. 2007. Reversible phosphorylation of Drp1 by cyclic AMP-dependent protein kinase and calcineurin regulates mitochondrial fission and cell death. *EMBO Rep*. 8(10):939–944. doi:10.1038/sj.embor.7401062.

Delaunay A, Isnard AD, Toledano MB. 2000. H2O2 sensing through oxidation of the Yap1 transcription factor. *EMBO J*. 19(19):5157–5166. doi:10.1093/emboj/19.19.5157.

Detmer Scott A, Chan DC. 2007a. Complementation between mouse Mfn1 and Mfn2 protects mitochondrial fusion defects caused by CMT2A disease mutations. *J Cell Biol*. 176(4):405–14. doi:10.1083/jcb.200611080.

Detmer Scott A, Chan DC. 2007b. Functions and dysfunctions of mitochondrial dynamics. *Nat Rev Mol Cell Biol*. 8(november):870–879. doi:10.1038/nrm2275.

Detmer Scott A., Chan DC. 2007. Complementation between mouse Mfn1 and Mfn2 protects mitochondrial fusion defects caused by CMT2A disease mutations. *J Cell Biol*. 176(4):405–414. doi:10.1083/jcb.200611080.

Detmer SA, Velde C Vande, Cleveland DW, Chan DC. 2008. Hindlimb gait defects due to motor axon loss and reduced distal muscles in a transgenic mouse model of Charcot - Marie - Tooth type 2A. *Hum Mol Genet*. 17(3):367–375. doi:10.1093/hmg/ddm314.

Du C, Fang M, Li Y, Li L, Wang X. 2000. Smac, a Mitochondrial Protein that Promotes Cytochrome c-Dependent Caspase Activation by Eliminating IAP Inhibition Hid, and Grim in terms of IAP neutralization and is the. *Cell*. 102:33–42.

Ekman D, Björklund ÅK, Frey-Skött J, Elofsson A. 2005. Multi-domain proteins in the three kingdoms of life: Orphan domains and other unassigned regions. *J Mol Biol*. 348(1):231–243. doi:10.1016/j.jmb.2005.02.007.

Engelhart EA, Hoppins S. 2019. A catalytic domain variant of Mitofusin requiring a wildtype paralog for function uncouples mitochondrial outer-membrane tethering and fusion. *J Biol Chem*. 1(8):jbc.RA118.006347. doi:10.1074/jbc.RA118.006347.

Ernster L, Schatz G. 1981. Mitochondria : A Historical Review. 91(December).

Eura Y. 2003. Two Mitofusin Proteins, Mammalian Homologues of FZO, with Distinct Functions Are Both Required for Mitochondrial Fusion. *J Biochem*. 134(3):333–344. doi:10.1093/jb/mvg150.

Federico A, Cardaioli E, Da Pozzo P, Formichi P, Gallus GN, Radi E. 2012. Mitochondria, oxidative stress and neurodegeneration. *J Neurol Sci*. 322(1–2):254–262. doi:10.1016/j.jns.2012.05.030.

Feely SME, Laura M, Siskind CE, Sottile S, Davis M, Gibbons VS, Reilly MM, Shy ME. 2011. MFN2 mutations cause severe phenotypes in most patients with CMT2A. *Neurology*. 76(20):1690–6. doi:10.1212/WNL.0b013e31821a441e.

Ferreira JCB, Campos JC, Qvit N, Qi X, Bozi LHM, Bechara LRG, Lima VM, Queliconi BB, Disatnik MH, Dourado PMM, et al. 2019. A selective inhibitor of mitofusin 1-βIIPKC association improves heart failure outcome in rats. *Nat Commun*. 10(1). doi:10.1038/s41467-018-08276-6.

Filadi R, Greotti E, Turacchio G, Luini A, Pozzan T, Pizzo P. 2015. Mitofusin 2 ablation increases endoplasmic reticulum–mitochondria coupling. *Proc Natl Acad Sci*. doi:10.1073/pnas.1504880112.

Franco A, Kitsis RN, Fleischer JA, Gavathiotis E, Kornfeld OS, Gong G, Biris N, Benz A, Qvit N, Donnelly SK, et al. 2016. Correcting mitochondrial fusion by manipulating mitofusin conformations. *Nature*.:1–20. doi:10.1038/nature20156.

Fransson Å, Ruusala A, Aspenström P. 2006. The atypical Rho GTPases Miro-1 and Miro-2 have essential roles in mitochondrial trafficking. *Biochem Biophys Res Commun*. 344(2):500–510. doi:10.1016/j.bbrc.2006.03.163.

Ganesan V, Willis SD, Chang KT, Beluch S, Cooper KF, Strich R. 2019. Cyclin C directly stimulates Drp1 GTP affinity to mediate stress-induced mitochondrial hyperfission. *Mol Biol Cell*. 30(3):302–311. doi:10.1091/mbc.E18-07-0463.

Gawlowski T, Suarez J, Scott B, Torres-Gonzalez M, Wang H, Schwappacher R, Han X, Yates JR,

Hoshijima M, Dillmann W. 2012. Modulation of dynamin-related protein 1 (DRP1) function by increased O-linked-β-N-acetylglucosamine modification (O-GlcNAc) in cardiac myocytes. *J Biol Chem*. 287(35):30024–30034. doi:10.1074/jbc.M112.390682.

Gemignani F, Marbini A. 2001. Charcot-Marie-Tooth disease (CMT): Distinctive phenotypic and genotypic features in CMT type 2. *J Neurol Sci*. 184(1):1–9. doi:10.1016/S0022-510X(00)00497-4.

Giarmarco MM, Cleghorn WM, Sloat SR, Hurley JB, Brockerhoff SE. 2017. Mitochondria Maintain Distinct Ca 2+ Pools in Cone Photoreceptors . *J Neurosci*. 37(8):2061–2072. doi:10.1523/jneurosci.2689-16.2017.

Gilbert HF. 1995. Thiol-Disulfide Exchange Equilibria and Bond Stability. *Methods Enzymol*. 251:8–28.

Giustarini D, Colombo G, Garavaglia ML, Astori E, Portinaro NM, Reggiani F, Badalamenti S, Aloisi AM, Santucci A, Rossi R, et al. 2017. Assessment of glutathione/glutathione disulphide ratio and S-glutathionylated proteins in human blood, solid tissues, and cultured cells. *Free Radic Biol Med*. 112(August):360–375. doi:10.1016/j.freeradbiomed.2017.08.008.

Giustarini D, Dalle-Donne I, Tsikas D, Rossi R. 2009. Oxidative stress and human diseases: Origin, link, measurement, mechanisms, and biomarkers. *Crit Rev Clin Lab Sci*. 46(5–6):241–281. doi:10.3109/10408360903142326.

Gomes LC, Benedetto G Di, Scorrano L. 2011. During autophagy mitochondria elongate, are spared from degradation and sustain cell viability. *Nat Cell Biol*. 13(5):589–598. doi:10.1038/ncb2220.

Grek CL, Zhang J, Manevich Y, Townsend DM, Tew KD. 2013. Causes and consequences of cysteine s-glutathionylation. *J Biol Chem*. 288(37):26497–26504. doi:10.1074/jbc.R113.461368.

Griffin EE, Chan DC. 2006. Domain interactions within Fzo1 oligomers are essential for mitochondrial fusion. *J Biol Chem*. 281(24):16599–606. doi:10.1074/jbc.M601847200.

Guo C, Hildick KL, Luo J, Dearden L, Wilkinson KA, Henley JM. 2013. SENP3-mediated

deSUMOylation of dynamin-related protein 1 promotes cell death following ischaemia. *EMBO J*. 32(11):1514–1528. doi:10.1038/emboj.2013.65.

Guo X, Chen KH, Guo Y, Liao H, Tang J, Xiao RP. 2007. Mitofusin 2 triggers vascular smooth muscle cell apoptosis via mitochondrial death pathway. *Circ Res*. 101(11):1113–1122. doi:10.1161/CIRCRESAHA.107.157644.

Han X, Lu Y, Li S, Kaitsuka T, Sato Y, Tomizawa K, Nairn AC, Takei K, Matsui H, Matsushita M. 2008. JCB : ARTICLE. 182(3):573–585. doi:10.1083/jcb.200802164.

Harder Z, Zunino R, McBride H. 2004. Sumo1 conjugates mitochondrial substrates and participates in mitochondrial fission. *Curr Biol*. 14(4):340–345. doi:10.1016/S0960-9822(04)00084-3.

Hoppins S, Edlich F, Cleland MM, Banerjee S, McCaffery JM, Youle RJ, Nunnari J. 2011. The Soluble Form of Bax Regulates Mitochondrial Fusion via MFN2 Homotypic Complexes. *Mol Cell*. 41(2):150–160. doi:10.1016/j.molcel.2010.11.030.

Horbay R, Bilyy R. 2016. Mitochondrial dynamics during cell cycling. *Apoptosis*. 21(12):1327–1335. doi:10.1007/s10495-016-1295-5.

Iqbal S, Hood DA. 2014. Oxidative stress-induced mitochondrial fragmentation and movement in skeletal muscle myoblasts. *Am J Physiol - Cell Physiol*. 306(12):1176–1183. doi:10.1152/ajpcell.00017.2014.

Ishihara N, Eura Y, Mihara K. 2004. Mitofusin 1 and 2 play distinct roles in mitochondrial fusion reactions via GTPase activity. *J Cell Sci*. 117(26):6535–6546. doi:10.1242/jcs.01565.

James SJ, Rose S, Melnyk S, Jernigan S, Blossom S, Pavliv O, Gaylor DW. 2009. Cellular and mitochondrial glutathione redox imbalance in lymphoblastoid cells derived from children with autism. *FASEB J*. 23(8):2374–2383. doi:10.1096/fj.08-128926.

Jendrach M, Mai S, Pohl S, Vöth M, Bereiter-Hahn J. 2008. Short- and long-term alterations of mitochondrial morphology, dynamics and mtDNA after transient oxidative stress. *Mitochondrion*. 8(4):293–304. doi:10.1016/j.mito.2008.06.001.

Jimah JR, Hinshaw JE. 2019. Structural Insights into the Mechanism of Dynamin Superfamily Proteins. *Trends Cell Biol*. 29(3):257–273. doi:10.1016/j.tcb.2018.11.003.

Karbowski M, Lee Y, Gaume B, Jeong S, Frank S, Nechushtan A, Santel A, Fuller M, Smith CL, Youle RJ. 2002. Spatial and temporal association of Bax with during apoptosis. 159(6):931–938. doi:10.1083/jcb.200209124.

Karbowski M, Norris KL, Cleland MM, Jeong S-Y, Youle RJ. 2006. Role of Bax and Bak in mitochondrial morphogenesis. *Nature*. 443(October):658–662. doi:10.1038/nature05111.

Kim YM, Youn SW, Sudhahar V, Das A, Chandhri R, Cuervo Grajal H, Kweon J, Leanhart S, He L, Toth PT, et al. 2018. Redox Regulation of Mitochondrial Fission Protein Drp1 by Protein Disulfide Isomerase Limits Endothelial Senescence. *Cell Rep*. 23(12):3565–3578. doi:10.1016/j.celrep.2018.05.054.

Koshiba T, Detmer S a, Kaiser JT, Chen H, McCaffery JM, Chan DC. 2004. Structural basis of mitochondrial tethering by mitofusin complexes. *Science*. 305(5685):858–862. doi:10.1126/science.1099793.

Kosower NS, Kosower EM, Wertheim B, Correa WS. 1969. Diamide, a new reagent for the intracellular oxidation of glutathione to the disulfide. *Biochem Biophys Res Commun*. 37(4):593–596. doi:10.1016/0006-291X(69)90850-X.

Koutsopoulos OS, Laine D, Osellame L, Chudakov DM, Parton RG, Frazier AE, Ryan MT. 2010. Human Miltons associate with mitochondria and induce microtubule-dependent remodeling of mitochondrial networks. *Biochim Biophys Acta - Mol Cell Res*. 1803(5):564–574. doi:10.1016/j.bbamcr.2010.03.006.

Labbé K, Murley A, Nunnari J. 2014. Determinants and Functions of Mitochondrial Behavior. *Annu Rev Cell Dev Biol*. 30(1):357–391. doi:10.1146/annurev-cellbio-101011-155756.

Lebeau J, Saunders JM, Moraes VWR, Madhavan A, Madrazo N, Anthony MC, Wiseman RL. 2018. The PERK Arm of the Unfolded Protein Response Regulates Mitochondrial Morphology during Acute Endoplasmic Reticulum Stress. *Cell Rep*. 22(11):2827–2836.

doi:10.1016/j.celrep.2018.02.055.

Lee D, Redfern O, Orengo C. 2007. Predicting protein function from sequence and structure. *Nat Rev Mol Cell Biol*. 8(12):995–1005. doi:10.1038/nrm2281.

Lee J-Y, Kapur M, Li M, Choi M-C, Choi S, Kim H-J, Kim I, Lee E, Taylor JP, Yao T-P. 2014. MFN1 deacetylation activates adaptive mitochondrial fusion and protects metabolically challenged mitochondria. *J Cell Sci*. 127(22):4954–4963. doi:10.1242/jcs.157321.

Liu J, Noel JK, Low HH. 2018. Structural basis for membrane tethering by a bacterial dynamin-like pair. *Nat Commun*. 9(1):1–12. doi:10.1038/s41467-018-05523-8.

Liu X, Kim CN, Yang J, Jemmerson R, Wang X. 1996. Induction of Apoptotic Program in Cell-Free Extracts: Requirement for dATP and Cytochrome C. *Cell*. 86(July):147–157.

Loson OC, Song Z, Chen H, Chan DC. 2013. Fis1, Mff, MiD49, and MiD51 mediate Drp1 recruitment in mitochondrial fission. *Mol Biol Cell*. 24(5):659–667. doi:10.1091/mbc.e12-10-0721.

Low HH, Löwe J. 2006. A bacterial dynamin-like protein. *Nature*. 444(7120):766–769. doi:10.1038/nature05312.

Low HH, Sachse C, Amos LA, Löwe J. 2009. Structure of a Bacterial Dynamin-like Protein Lipid Tube Provides a Mechanism For Assembly and Membrane Curving. *Cell*. 139(7):1342–1352. doi:10.1016/j.cell.2009.11.003.

Mattie S, Riemer J, Wideman JG, McBride HM. 2018. A new mitofusin topology places the redox-regulated C terminus in the mitochondrial intermembrane space. *J Cell Biol*. 217(2):507–515. doi:10.1083/jcb.201611194.

McLelland GL, Goiran T, Yi W, Dorval G, Chen CX, Lauinger ND, Krahn AI, Valimehr S, Rakovic A, Rouiller I, et al. 2018. Mfn2 ubiquitination by PINK1/parkin gates the p97-dependent release of ER from mitochondria to drive mitophagy. *Elife*. 7:1–35. doi:10.7554/eLife.32866.

Mears JA, Lackner LL, Fang S, Ingerman E, Nunnari J, Hinshaw JE. 2011. Conformational changes in Dnm1 support a contractile mechanism for mitochondrial fission. *Nat Struct Mol*

Biol. 18(1):20–27. doi:10.1038/nsmb.1949.

Mishra P, Chan DC. 2014. Mitochondrial dynamics and inheritance during cell division, development and disease. *Nat Rev Mol Cell Biol*. 15(10):634–646. doi:10.1038/nrm3877.

Mitra K, Wunder C, Roysam B, Lin G, Lippincott-Schwartz J. 2009. A hyperfused mitochondrial state achieved at G1-S regulates cyclin E buildup and entry into S phase. *Proc Natl Acad Sci*. 106(29):11960–11965. doi:10.1073/pnas.0904875106.

Olichon A, Baricault L, Gas N, Guillou E, Valette A, Belenguer P, Lenaers G. 2003. Loss of OPA1 perturbates the mitochondrial inner membrane structure and integrity, leading to cytochrome c release and apoptosis. *J Biol Chem*. 278(10):7743–7746. doi:10.1074/jbc.C200677200.

Ong S-B, Kalkhoran SB, Cabrera-Fuentes H a., Hausenloy DJ. 2015. Mitochondrial fusion and fission proteins as novel therapeutic targets for treating cardiovascular disease. *Eur J Pharmacol*.:1–11. doi:10.1016/j.ejphar.2015.04.056.

Østergaard H, Tachibana C, Winther JR. 2004. Monitoring disulfide bond formation in the eukaryotic cytosol. *J Cell Biol*. 166(3):337–345. doi:10.1083/jcb.200402120.

Otera H, Wang C, Cleland MM, Setoguchi K, Yokota S, Youle RJ, Mihara K. 2010. Mff is an essential factor for mitochondrial recruitment of Drp1 during mitochondrial fission in mammalian cells. *J Cell Biol*. 191(6):1141–1158. doi:10.1083/jcb.201007152.

Pareyson D, Saveri P, Sagnelli A, Piscosquito G. 2015. Mitochondrial dynamics and inherited peripheral nerve diseases. *Neurosci Lett*. 596:66–77. doi:10.1016/j.neulet.2015.04.001.

Park YY, Nguyen OTK, Kang H, Cho H. 2014. MARCH5-mediated quality control on acetylated Mfn1 facilitates mitochondrial homeostasis and cell survival. *Cell Death Dis*. 5(4):e1172-12. doi:10.1038/cddis.2014.142.

Pernas L, Scorrano L. 2015. Mito-Morphosis: Mitochondrial Fusion, Fission, and Cristae Remodeling as Key Mediators of Cellular Function. *Annu Rev Physiol*. 78(1):505–531. doi:10.1146/annurev-physiol-021115-105011.

Picard M, Wallace DC, Burelle Y. 2016. The rise of mitochondria in medicine. *Mitochondrion*.

30:105–116. doi:10.1016/j.mito.2016.07.003.

Pilling AD, Horiuchi D, Lively CM, Saxton WM. 2006. Kinesin-1 and Dynein are the primary motors for fast transport of mitochondria in Drosophila motor axons. *Mol Biol Cell*. 17(April):2057–2068. doi:10.1091/mbc.E05.

Pócsi I, Miskei M, Karányi Z, Emri T, Ayoubi P, Pusztahelyi T, Balla G, Prade RA. 2005. Comparison of gene expression signatures of diamide, H2O2 and menadione exposed Aspergillus nidulans cultures - Linking genome-wide transcriptional changes to cellular physiology. *BMC Genomics*. 6:1–18. doi:10.1186/1471-2164-6-182.

Prudent J, Zunino R, Sugiura A, Mattie S, Shore GC, McBride HM. 2015. MAPL SUMOylation of Drp1 Stabilizes an ER/Mitochondrial Platform Required for Cell Death. *Mol Cell*. 59(6):941–955. doi:10.1016/j.molcel.2015.08.001.

Pyakurel A, Savoia C, Scorrano L, Pyakurel A, Savoia C, Hess D, Scorrano L. 2015. Extracellular Regulated Kinase Phosphorylates Mitofusin 1 to Control Mitochondrial Morphology and Article Extracellular Regulated Kinase Phosphorylates Mitofusin 1 to Control Mitochondrial Morphology and Apoptosis. *Mol Cell*.:1–11. doi:10.1016/j.molcel.2015.02.021.

Qi Y, Yan L, Yu C, Guo X, Zhou X, Hu X, Huang X, Rao Z, Lou Z, Hu J. 2016. Structures of human mitofusin 1 provide insight into mitochondrial tethering.

Rambold AS, Kostelecky B, Elia N, Lippincott-Schwartz J. 2011. Tubular network formation protects mitochondria from autophagosomal degradation during nutrient starvation. *Proc Natl Acad Sci*. 108(25):10190–10195. doi:10.1073/pnas.1107402108.

Redpath CJ, Bou Khalil M, Drozdzal G, Radisic M, McBride HM. 2013. Mitochondrial Hyperfusion during Oxidative Stress Is Coupled to a Dysregulation in Calcium Handling within a C2C12 Cell Model. *PLoS One*. 8(7). doi:10.1371/journal.pone.0069165.

Rocha AG, Franco A, Krezel AM, Rumsey JM, Alberti JM, Knight WC, Biris N, Zacharioudakis E, Janetka JW, Baloh RH, et al. 2018a. MFN2 agonists reverse mitochondrial defects in preclinical models of Charcot-Marie-Tooth disease type 2A. *Science (80-)*. 360(6386):336–341.

doi:10.1126/science.aao1785.

Rocha AG, Franco A, Krezel AM, Rumsey JM, Alberti JM, Knight WC, Biris N, Zacharioudakis E, Janetka JW, Baloh RH, et al. 2018b. MFN2 agonists reverse mitochondrial defects in preclinical models of Charcot-Marie-Tooth disease type 2A. *Science (80-)*. 360(6386):336–341. doi:10.1126/science.aao1785.

Rovira-Llopis S, Bañuls C, Diaz-Morales N, Hernandez-Mijares A, Rocha M, Victor VM. 2017. Mitochondrial dynamics in type 2 diabetes: Pathophysiological implications. *Redox Biol*. 11(January):637–645. doi:10.1016/j.redox.2017.01.013.

Santel a, Fuller MT. 2001. Control of mitochondrial morphology by a human mitofusin. *J Cell Sci*. 114:867–874.

Scorrano L. 2013. Keeping mitochondria in shape: A matter of life and death. *Eur J Clin Invest*. 43(8):886–893. doi:10.1111/eci.12135.

Sena LA, Chandel NS. 2012. Physiological roles of mitochondrial reactive oxygen species. *Mol Cell*. 48(2):158–167. doi:10.1016/j.molcel.2012.09.025.

Shen T, Zheng M, Cao C, Chen C, Tang J, Zhang W, Cheng H, Chen KH, Xiao RP. 2007. Mitofusin-2 is a major determinant of oxidative stress-mediated heart muscle cell apoptosis. *J Biol Chem*. 282(32):23354–23361. doi:10.1074/jbc.M702657200.

SHITARA H, SHIMANUKI M, HAYASHI J-I, YONEKAWA H. 2010. Global Imaging of Mitochondrial Morphology in Tissues Using Transgenic Mice Expressing Mitochondrially Targeted Enhanced Green Fluorescent Protein. *Exp Anim*. 59(1):99–103. doi:10.1538/expanim.59.99.

Shutt T, Geoffrion M, Milne R, McBride HM. 2012. The intracellular redox state is a core determinant of mitochondrial fusion. *EMBO Rep*. 13(10):909–915. doi:10.1038/embor.2012.128.

Shutt TE, McBride HM. 2013. Staying cool in difficult times: Mitochondrial dynamics, quality control and the stress response. *Biochim Biophys Acta - Mol Cell Res*. 1833(2):417–424.

doi:10.1016/j.bbamcr.2012.05.024.

Slater EC, Cleland KW. 1953. The effect of calcium on the respiratory and phosphorylative activities of heart-muscle sarcosomes. *Biochem J*. 55(4):566–580. doi:10.1042/bj0550566.

Slivka A, Spina MB, Cohen G. 1987. Reduced and oxidized glutathione in human and monkey brain. *Neurosci Lett*. 74(1):112–118. doi:10.1016/0304-3940(87)90061-9.

Smirnova E, Griparic L, Shurland D-L, van der Bliek AM. 2001. Dynamin-related Protein Drp1 Is Required for Mitochondrial Division in Mammalian Cells. *Mol Biol Cell*. 12(8):2245–2256. doi:10.1091/mbc.12.8.2245.

Sorrentino V, Menzies KJ, Auwerx J. 2017. Repairing Mitochondrial Dysfunction in Disease. *Annu Rev Pharmacol Toxicol*. 58(1):353–389. doi:10.1146/annurev-pharmtox-010716-104908.

De Stefani D, Rizzuto R, Pozzan T. 2016. Enjoy the Trip: Calcium in Mitochondria Back and Forth. *Annu Rev Biochem*. 85(1):161–192. doi:10.1146/annurev-biochem-060614-034216.

Strickland A V, Rebelo AP, Zhang F, Price J, Bolon B, Silva JP, Wen R, Züchner S. 2014. Characterization of the Mitofusin 2 R94W Mutation in a Knock-in Mouse Model. *J Peripher Nerv Syst*. 164:152–164. doi:10.1111/jns5.12066.

Stuppia G, Rizzo F, Riboldi G, Del Bo R, Nizzardo M, Simone C, Comi GP, Bresolin N, Corti S. 2015. MFN2-related neuropathies: Clinical features, molecular pathogenesis and therapeutic perspectives. *J Neurol Sci*. doi:10.1016/j.jns.2015.05.033.

Suen D, Norris KL, Youle RJ. 2008. Mitochondrial dynamics and apoptosis. (301):1577–1590. doi:10.1101/gad.1658508.GENES.

Sugiura A, Nagashima S, Tokuyama T, Amo T, Matsuki Y, Ishido S, Kudo Y, McBride HM, Fukuda T, Matsushita N, et al. 2013. MITOL regulates endoplasmic reticulum-mitochondria contacts via Mitofusin2. *Mol Cell*. 51(1):20–34. doi:10.1016/j.molcel.2013.04.023.

Susin SA, Zamzami N, Castedo M, Hirsch T, Marchetti P, Macho A, Daugas E, Geuskens M, Kroemer G. 1996. Bcl-2 Inhibits the Mitochondrial Release of an Apoptotic Protease. *J Exp Med*. 184(October):1331–1341.

Suzuki M, Youle RJ, Tjandra N. 2000. Structure of Bax. *Cell*. 103(4):645–654. doi:10.1016/s0092-8674(00)00167-7.

Suzuki Y, Imai Y, Nakayama H, Takahashi K, Takio K, Takahashi R. 2001. A serine protease, HtrA2, is released from the mitochondria and interacts with XIAP, inducing cell death. *Mol Cell*. 8(3):613–621. doi:10.1016/S1097-2765(01)00341-0.

Thaher O, Wolf C, Dey PN, Pouya A, Wüllner V, Tenzer S, Methner A. 2017. The thiol switch C684 in Mitofusin-2 mediates redox-induced alterations of mitochondrial shape and respiration. *Neurochem Int*.:5–11. doi:10.1016/j.neuint.2017.05.009.

Thorpe GW, Fong CS, Alic N, Higgins VJ, Dawes IW. 2004. Cells have distinct mechanisms to maintain protection against different reactive oxygen species: Oxidative-stress-response genes. *Proc Natl Acad Sci*. 101(17):6564–6569. doi:10.1073/pnas.0305888101.

Tondera D, Grandemange S, Jourdain A, Karbowski M, Mattenberger Y, Herzig S, Da Cruz S, Clerc P, Raschke I, Merkwirth C, et al. 2009. SLP-2 is required for stress-induced mitochondrial hyperfusion. *EMBO J*. 28(November 2008):1589–1600. doi:10.1038/emboj.2009.89.

Twig G, Elorza A, Molina AJA, Mohamed H, Wikstrom JD, Walzer G, Stiles L, Haigh SE, Katz S, Las G, et al. 2008. Fission and selective fusion govern mitochondrial segregation and elimination by autophagy. *EMBO J*. 27(2):433–446. doi:10.1038/sj.emboj.7601963.

Vallat J-M, Ouvrier R a, Pollard JD, Magdelaine C, Zhu D, Nicholson G a, Grew S, Ryan MM, Funalot B. 2008. Histopathological findings in hereditary motor and sensory neuropathy of axonal type with onset in early childhood associated with mitofusin 2 mutations. *J Neuropathol Exp Neurol*. 67(11):1097–1102. doi:10.1097/NEN.0b013e31818b6cbc.

Verhagen AM, Ekert PG, Pakusch M, Silke J, Connonlly LM, Reid GE, Moritz RL, Simpson RJ, Vaux DL. 2000. Identification of DIABLO, a Mammalian Protein that Promotes Apoptosis by Binding to and Antagonizing IAP Proteins. *Cell*. 102(1):43–53. doi:10.1016/S0896-6273(00)80282-2.

Verhoeven K, Claeys KG, Züchner S, Schröder JM, Weis J, Ceuterick C, Jordanova A, Nelis E, De

Vriendt E, Van Hul M, et al. 2006. MFN2 mutation distribution and genotype/phenotype correlation in Charcot-Marie-Tooth type 2. *Brain*. 129(8):2093–2102. doi:10.1093/brain/awl126.

Vital A, Vital C. 2012. Mitochondria and peripheral neuropathies. *J Neuropathol Exp Neurol*. 71(12):1036–46. doi:10.1097/NEN.0b013e3182764d47.

Wada J, Nakatsuka A. 2016. Mitochondrial Dynamics and Mitochondrial Dysfunction in Diabetes. *Acta Med Okayama*. 70(3):151–8. doi:10.18926/AMO/54413.

Wallace DC, Fan W, Procaccio V. 2010. Mitochondrial Energetics and Therapeutics. *Annu Rev Pathol Mech Dis*. 5(1):297–348. doi:10.1146/annurev.pathol.4.110807.092314.

Wang C, Youle RJ. 2011. The role of mitochondria in apoptosis. *BMB Rep*. 41(1):11–22. doi:10.5483/bmbrep.2008.41.1.011.

Wang H, Song P, Du L, Tian W, Yue W, Liu M, Li D, Wang B, Zhu Y, Cao C, et al. 2011. Parkin ubiquitinates Drp1 for proteasome-dependent degradation: Implication of dysregulated mitochondrial dynamics in Parkinson disease. *J Biol Chem*. 286(13):11649–11658. doi:10.1074/jbc.M110.144238.

Wang K, Yan R, Cooper KF, Strich R. 2015. Cyclin C mediates stress-induced mitochondrial fission and apoptosis. *Mol Biol Cell*. 26(6):1030–1043. doi:10.1091/mbc.E14-08-1315.

Wang W, Zhang F, Li L, Tang F, Siedlak SL, Fujioka H, Liu Y, Su B, Pi Y, Wang X. 2015. MFN2 couples glutamate excitotoxicity and mitochondrial dysfunction in motor neurons. *J Biol Chem*. 290(1):168–182. doi:10.1074/jbc.M114.617167.

Wemmie JA, Steggerda SM, Moye-Rowley WS. 1997. The Saccharomyces cerevisiae AP-1 protein discriminates between oxidative stress elicited by the oxidants H 2O 2 and diamide. *J Biol Chem*. 272(12):7908–7914. doi:10.1074/jbc.272.12.7908.

Willems P, Wanschers BFJ, Esseling J, Szklarczyk R, Kudla U, Duarte I, Forkink M, Nooteboom M, Swarts H, Gloerich J, et al. 2013. BOLA1 is an aerobic protein that prevents mitochondrial morphology changes induced by glutathione depletion. *Antioxidants Redox Signal*. 18(2):129–

138. doi:10.1089/ars.2011.4253.

Wu S, Zhou F, Zhang Z, Xing D. 2011. Mitochondrial oxidative stress causes mitochondrial fragmentation via differential modulation of mitochondrial fission-fusion proteins. *FEBS J*. 278(6):941–954. doi:10.1111/j.1742-4658.2011.08010.x.

Xiying F, Rajaa H, George A. B. 2013. H2O2-induced mitochondrial fragmentation in C2C12 myocytes. *Free Radic Biol Med*. 18(9):1199–1216. doi:10.1016/j.micinf.2011.07.011.Innate.

Xu K, Chen G, Li X, Wu X, Chang Z, Xu J, Zhu Y, Yin P, Liang X, Dong L. 2017. MFN2 suppresses cancer progression through inhibition of mTORC2/Akt signaling. *Sci Rep*. 7(February):1–13. doi:10.1038/srep41718.

Yan L, Qi Y, Huang X, Yu C, Lan L, Guo X, Rao Z, Hu J, Lou Z. 2018. Structural basis for GTP hydrolysis and conformational change of MFN1 in mediating membrane fusion. *Nat Struct Mol Biol*. 25(3):233–243. doi:10.1038/s41594-018-0034-8.

Yang J, Zhang Y. 2015. I-TASSER server: New development for protein structure and function predictions. *Nucleic Acids Res*. 43(W1):W174–W181. doi:10.1093/nar/gkv342.

Yesylevskyy SO, Kharkyanen VN, Demchenko AP. 2006. Dynamic protein domains: Identification, interdependence, and stability. *Biophys J*. 91(2):670–685. doi:10.1529/biophysj.105.078584.

Yoon Y-S, Yoon D-S, Lim IK, Yoon S-H, Chung H-Y, Rojo M, Malka F, Jou M-J, Martinou J-C, Yoon G. 2006. Formation of Elongated Giant Mitochondria in DFO-Induced Cellular Senescence: Involvement of Enhanced Fusion Process Through Modulation of Fis1. *J Cell Physiol*. 209(1):468–480. doi:10.1002/JCP.

Zahedi A, Phandthong R, Chaili A, Leung S, Omaiye E, Talbot P. 2019. Mitochondrial Stress Response in Neural Stem Cells Exposed to Electronic Cigarettes. *iScience*. 16:250–269. doi:10.1016/j.isci.2019.05.034.

Zhang G-E, Jin H-L, Lin X-K, Chen C, Liu X-S, Zhang Q, Yu J-R. 2013. Anti-tumor effects of mfn2 in gastric cancer. *Int J Mol Sci*. 14:13005–21. doi:10.3390/ijms140713005.

Zhang Y. 2009. I-TASSER: Fully automated protein structure prediction in CASP8. *Proteins Struct Funct Bioinforma*. 77(SUPPL. 9):100–113. doi:10.1002/prot.22588.

Zheng M, Xiao RP. 2010. Role of mitofusin 2 in cardiovascular oxidative injury. *J Mol Med*. 88(10):987–991. doi:10.1007/s00109-010-0675-5.

Zhou Y, Lutz CM, Baloh RH, Zhou Y, Carmona S, Muhammad AKMG, Bell S, Landeros J, Vazquez M, Ho R, et al. 2019. Restoring mitofusin balance prevents axonal degeneration in a Charcot-Marie-Tooth type 2A model Graphical abstract Find the latest version : Restoring mitofusin balance prevents axonal degeneration in a Charcot-Marie-Tooth type 2A model.

Zorov DB, Filburn CR, Klotz LO, Zweier JL, Sollott SJ. 2000. Reactive oxygen species (ROS)-induced ROS release: A new phenomenon accompanying induction of the mitochondrial permeability transition in cardiac myocytes. *J Exp Med*. 192(7):1001–1014. doi:10.1084/jem.192.7.1001.

Züchner S, Mersiyanova I V, Muglia M, Bissar-Tadmouri N, Rochelle J, Dadali EL, Zappia M, Nelis E, Patitucci A, Senderek J, et al. 2004. Mutations in the mitochondrial GTPase mitofusin 2 cause Charcot-Marie-Tooth neuropathy type 2A. *Nat Genet*. 36(5):449–451. doi:10.1038/ng1341.

Chapter 5: Conclusions

My research, like most good research, has both added a brick to the tower of knowledge in my field of study and helped direct potential future directions of study. Here I present my contribution to the study of Mfn2 as well as future avenues of study that I find particularly interesting.

5.1 Summary of findings and implications for models of mitochondrial outer membrane fusion

My analysis of disease-associated mutations of Mfn2 has contributed an increase in our understanding of how this protein functions. I have shown that Mfn2 variants in three different regions of the protein have different effects on the ability of Mfn2 to facilitate mitochondrial fusion in Mfn2-null mouse embryonic fibroblasts (Chapter 2). This analysis allowed me to determine that disease-associated mutations distal to the transmembrane domain result in proteins that cannot facilitate mitochondrial fusion in MEFs. The heterogeneity of the mitochondrial morphology points toward the importance of studying other activities and regulation of Mfn2 in different cell types or physiological states.

I also found that Mfn2 mediates the hyperfusion of mitochondria during diamide-induced oxidative stress (Chapter 3). Substituting the cysteine at amino acid position 390 alters this activity in in vitro biochemical analysis, but in mouse embryonic fibroblasts, these variants act similarly to wild type Mfn2 both under "standard" conditions, and during oxidative stress induced by both hydrogen peroxide and diamide. This leads to the hypothesis that a cytosolic factor that influences or interacts with Mfn2 allows $Mfn2_{C390R \text{ or } F}$ to function effectively in these cells, but without this factor (i.e. in assays involving isolated mitochondria), a defect is apparent.

I have furthermore found that the integrity of the putative Hinge 1 is vital for proper Mfn2 assembly (Chapter 4). Disease-associated Mfn2 variants in this region have fusion and assembly

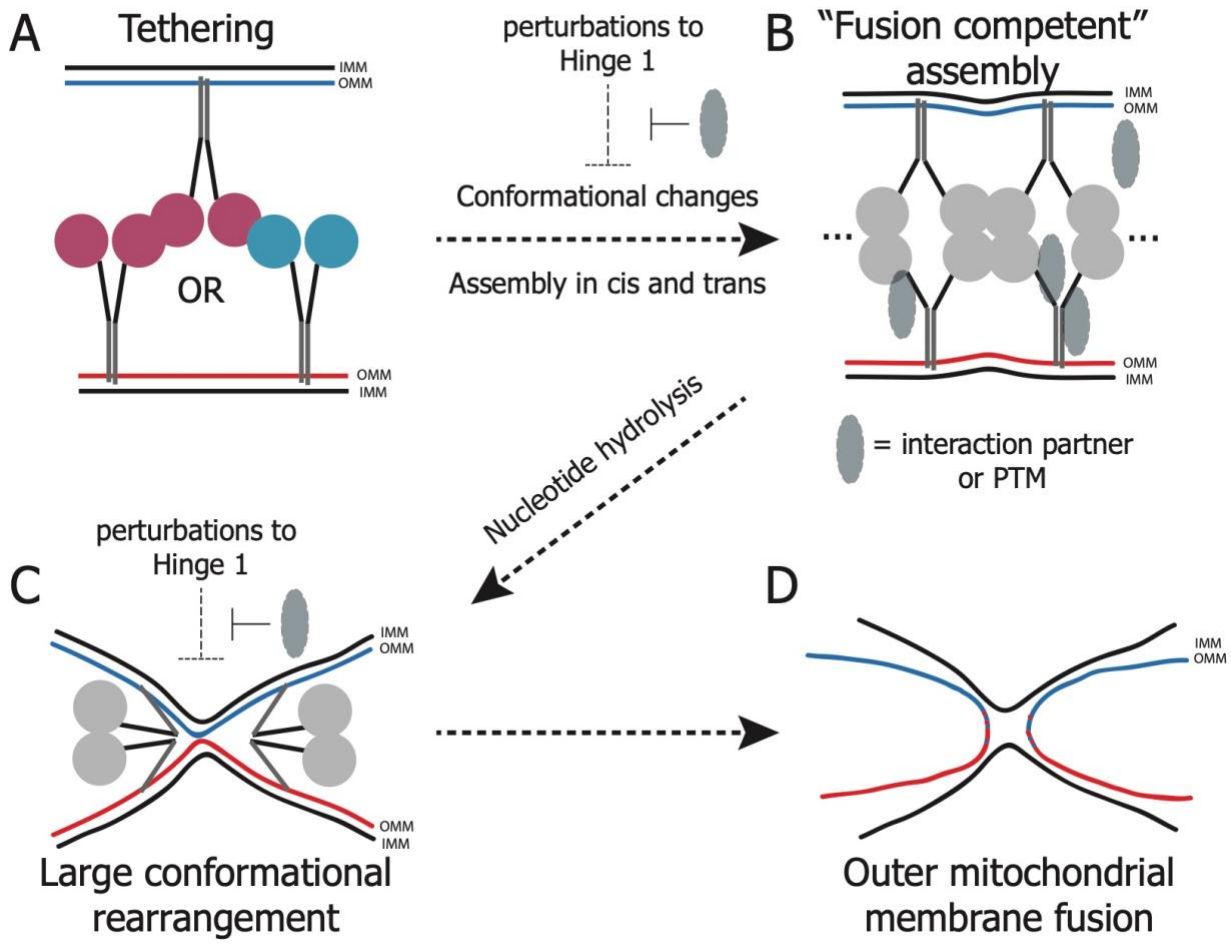

Figure 5.1. Updated model of outer mitochondrial membrane fusion.
A) Mitofusins on separate mitochondria are tethered by interactions between mitofusin molecules on opposite outer membranes (OMM, red and blue). This is facilitated by interactions between Mfn1-Mfn1 (pink) or Mfn1 (pink) - Mfn2 (blue). **B)** Assembly of mitofusin molecules on the same membrane (in cis) and on opposite membranes (in trans) leads to the formation of an assembly that can facilitate outer mitochondrial membrane fusion. This is facilitated by conformational changes in the mitofusin proteins that can be made more inefficient by perturbations to Hinge 1, which can, in turn, be compensated for by some regulatory factor (green oval). **C)** Nucleotide hydrolysis leads to a large structural rearrangement of the mitofusin proteins that disrupts the mitochondrial membranes and brings them into close proximity. As in B), this can be slowed or destabilized by perturbations to Hinge 1 and stabilized by a regulating factor. **D)** Outer mitochondrial membranes mix completing the process of outer membrane fusion.

defects which also seem to be mitigated by interaction with a cytosolic factor(s). The focus on the hinge region in this study suggests that the cytosolic factor is assisting Mfn2 function by stabilizing conformations or by conformational changes that rely on the integrity of this hinge.

My research has highlighted that the current model of mitochondrial fusion is incomplete. The differences in results between biochemical assays and cellular studies indicate that there are likely other factors involved in the fusion process, especially in the assembly and conformational change steps. While these factors may not be necessary for the occurrence of the biochemical steps laid out in the model, they are likely necessary for the efficiency of mitochondrial fusion in cells and for the correct regulation of changes in fusion rate in cells. It also indicates that the model may not be identical for Mfn1 and Mfn2. Mfn1 can form trans interactions between mitochondria with another Mfn1 molecule, which is likely a proxy for tethering. Mfn2 can interact with Mfn1 in trans, but not with Mfn2, indicating that Mfn2 homodimers are not efficient tethers between mitochondria. (Figure 5.1)

5.2 Future Directions

5.2.1 Mfn2 regulation

All of my data points to the importance of other cellular factors in Mfn2-mediated mitochondrial fusion. These factors could include an interaction partner, a post translational modification enacted by a cytosolic enzyme, or both. Regulation of Mfn2 is likely to be vital to its function in both physiological and stressful conditions. The profile of mitofusin interactors and modifiers expressed in different cell types likely varies, which may help explain the susceptibility of certain cell types to mutations in MFN2 as well as the inconsistency of results from biochemical analyses and cellular data I have reported. The experiments I reported should be repeated in different cell types. Stress conditions may also affect the signaling pathways that impinge on

Mfn2, so exposing cells to various types of stress may also help to discover the regulation of Mfn2.

Most other dynamin related proteins have other interacting proteins and post translational modifications that allow regulate their ability to perform their membrane remodeling functions (REFS, examples). Mfn2 has been shown to interact with Bax, and indeed, I discovered that adding Bax to isolated mitochondria enhanced the ability of Mfn2 to assemble. There may also be other interaction partners. I have piloted experiments that suggest that the composition of elutions from co-immunoprecipitation of Mfn2 contain many proteins and that different variants may have slightly different interactors. A pilot experiment of mass spectrometry to identify binding partners of Mfn2 has indicated that this may be a viable method to identify other potential interaction factors and to determine if different variants have differences in their affinity for these partners. I have additionally developed a co-immunoprecipitation based mass spec analysis protocol to find post translational modifications of Mfn1 which could be easily adapted to examine post translational modifications of Mfn2.

5.2.2 Conformational changes

To test the hypothesis that it is conformational changes or stability that are affected by interaction partners or post translational modifications, protocols to monitor the conformational state of the mitofusin proteins will need to be developed. FRET based assays to measure Mfn2 in open versus closed conformations have been reported (Franco et al. 2016; Rocha et al. 2018b), but they would likely need to be optimized to give data on subtle conformational changes or stability alterations. Additionally, the two FRET fluorophores were added to the N- and C-terminus of Mfn2 in these studies, which may complicate data interpretation if the C-terminus does fold up into HB1 as it does in Mfn1 (see Figure 5.2), or if the poorly modeled N-terminal 21 amino acids of Mfn2 complicate the fluorophore interaction.

Linkers would need to be optimized to ensure Mfn2 folding was not disrupted and that FRET signal was specific to Mfn2 conformational changes. Additionally, Mfn2 homooligomers could also display FRET emission depending on the assembly interface between them, especially if they form “back to back” dimers as seen in BDLP studies (Low et al. 2009). Therefore, any FRET-based assay to determine Mfn2 conformation should be rigorously tested and controlled.

Crystallographic information has been helpful for identifying conformational changes in a minimal Mfn1 construct (Yan et al. 2018). Purification and crystallization of full-length mitofusin under various conditions would be of great value to the field in addressing hypotheses about conformational states and changes within both mitofusins.

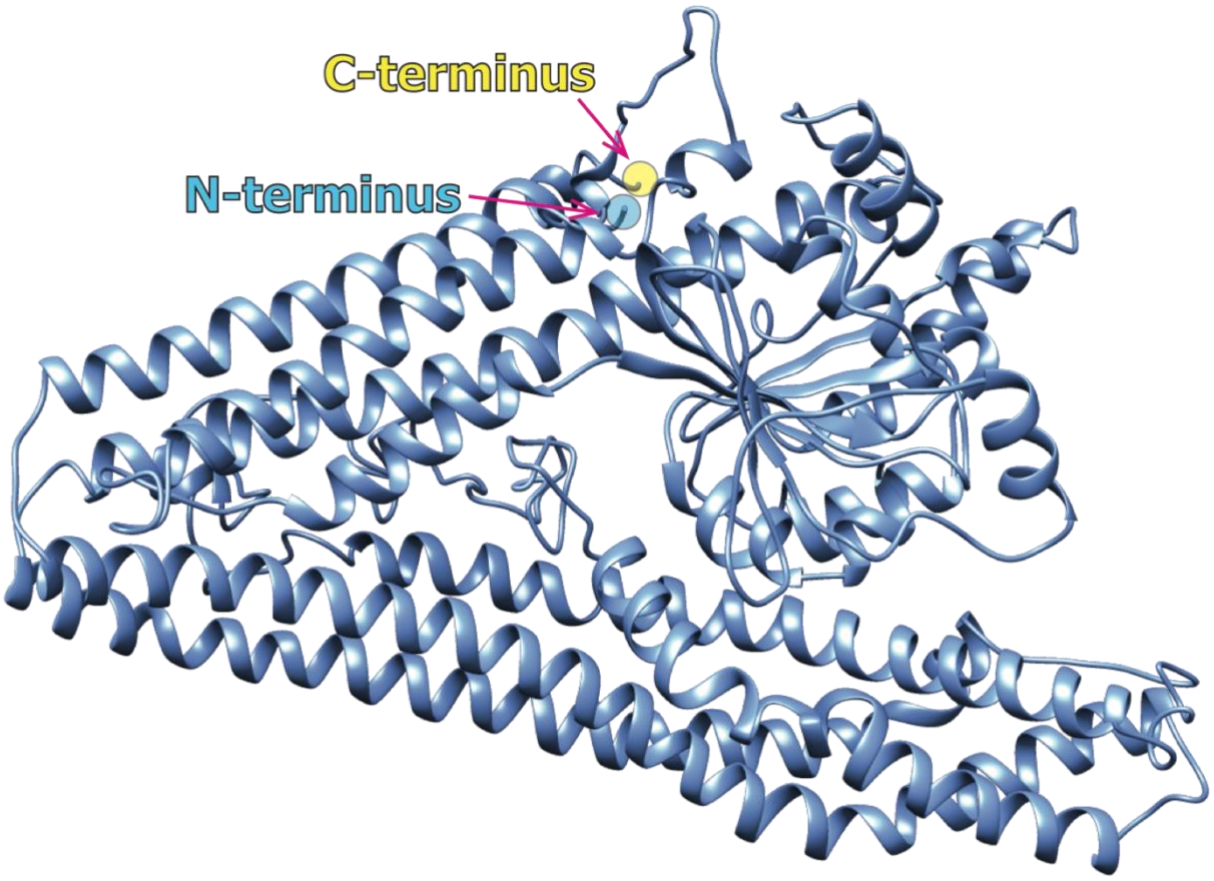

Figure 5.2. Model of Mfn2 with predicted locations of FRET fluorophores marked. An N-terminal mCerulean (modeled as a blue circle) and a C-terminal mVenus (modeled as a yellow circle) would potentially be close to one another whether Hinge 1 is in the open or closed conformation.

5.2.3 Assembly interfaces

My work along with other studies show that assembly of mitofusins is essential to their membrane fusion capability in biochemical analyses. Multiple mitofusin variants that have different effects on mitochondrial morphology in cells lead to disruption in the assembly of mitofusin. Because the assembly that is capable of facilitating fusion as assumed to be different

from the tethering assembly, and because interactions need to happen between two different mitofusins in both cis and trans, there are likely several assembly interfaces or domains within the mitofusins. Future work could focus on defining these different interfaces. For example, it seems that Mfn2 interacts differently in trans (in that it does not appear to interact strongly) with itself than it does with Mfn1 or that Mfn1 does with itself. This could indicate that the domain that facilitates these interactions is slightly different between the two mitofusins. One attractive area of research here would be to examine the first 21 amino acids of Mfn2, which are not conserved in Mfn1. If removing these allows Mfn2 to interact with itself in trans, we could then assume that having two of these regions interferes with the trans assembly.

5.2.4 Mfn2 vs Mfn1 differences

The implication of Mfn2 rather than Mfn1 in multiple diseases may reflect the trend in the field to only study Mfn2 or true differences between the two paralogues. The truth likely lies in a combination of these two factors. To directly address this, a direct, systematic analysis of both these proteins is required. Because these proteins are so similar at the structural and amino acid level, examining the regulation, interaction and modification of these two proteins may be more fruitful in discovering differences between the two. There is certainly evidence that the two behave differently even in baseline mitochondrial fusion and assembly in biochemical analyses gathered by myself, my lab, and others. Comparison of interaction profiles, post-translational modifications, and assembly interfaces would greatly enhance our understanding of the differences between the two.

Conversely, Mfn2 may be the mitofusin associated with disease because it is the mitofusin that responds to oxidative stress. Mfn2 has been implicated not only in CMT2A, but in cardiac disease, diabetes, other neurodegenerative diseases, and cancer (K.H. Chen et al. 2004; Zhang et

al. 2013; W. Wang et al. 2015; Ong et al. 2015; Wada and Nakatsuka 2016; Xu et al. 2017). Research on all of these conditions suggest that reactive oxygen species are involved in the pathophysiology of the disease (Zheng and Xiao 2010; Cairns et al. 2011; Federico et al. 2012; Sena and Chandel 2012; Rovira-Llopis et al. 2017). For CMT2A specifically, if disease etiology relies on the ability of Mfn2 to respond to oxidative stress, this may help to explain the heterogeneity and incomplete penetrance of disease. Exposure of the cells to oxidative stress may alter the progression and severity of the disease, for example, by ROS-induced ROS release (Zorov et al. 2000).

5.3 References

Atkins K, Dasgupta A, Chen K, Mewburn J, Archer SL. 2016. The role of Drp1 adaptor proteins MiD49 and MiD51 in mitochondrial fission : implications for human disease. :1861–1874. doi:10.1042/CS20160030.

Baloh RH, Schmidt RE, Pestronk A, Milbrandt J. 2007. Altered axonal mitochondrial transport in the pathogenesis of Charcot-Marie-Tooth disease from mitofusin 2 mutations. *J Neurosci*. 27(2):422–430. doi:10.1523/JNEUROSCI.4798-06.2007.

Bian X, Xu J, Zhao H, Zheng Q, Xiao X, Ma X, Li Y, Du X, Liu X. 2019. Zinc-Induced SUMOylation of Dynamin-Related Protein 1 Protects the Heart against Ischemia-Reperfusion Injury. *Oxid Med Cell Longev*. 2019:1–11. doi:10.1155/2019/1232146.

Brandt T, Cavellini L, Kühlbrandt W, Cohen MM. 2016. A mitofusin-dependent docking ring complex triggers mitochondrial fusion in vitro. *Elife*. 5:1–23. doi:10.7554/eLife.14618.

de Brito OM, Scorrano L. 2008. Mitofusin 2 tethers endoplasmic reticulum to mitochondria. *Nature*. 456(7222):605–10. doi:10.1038/nature07534.

Cairns RA, Harris IS, Mak TW. 2011. Regulation of cancer cell metabolism. *Nat Rev Cancer*. 11(2):85–95. doi:10.1038/nrc2981.

Calvo J, Funalot B, Ouvrier R a, Lazaro L, Toutain A, De Mas P, Bouche P, Gilbert-Dussardier B, Arne-Bes M-C, Carrière J-P, et al. 2009. Genotype-phenotype correlations in Charcot-Marie-Tooth disease type 2 caused by mitofusin 2 mutations. *Arch Neurol*. 66(12):1511–1516. doi:10.1001/archneurol.2009.284.

Cao Y-L, Meng S, Chen Y, Feng J-X, Gu D-D, Yu B, Li Y-J, Yang J-Y, Liao S, Chan DC, et al. 2017. MFN1 structures reveal nucleotide-triggered dimerization critical for mitochondrial fusion. *Nature*.:1–5. doi:10.1038/nature21077.

Cartoni R, Arnaud E, Médard JJ, Poirot O, Courvoisier DS, Chrast R, Martinou JC. 2010. Expression of mitofusin 2R94Q in a transgenic mouse leads to Charcot-Marie-Tooth neuropathy type 2A. *Brain*. 133(5):1460–1469. doi:10.1093/brain/awq082.

Cartoni R, Martinou JC. 2009. Role of mitofusin 2 mutations in the physiopathology of Charcot-Marie-Tooth disease type 2A. *Exp Neurol*. 218(2):268–273. doi:10.1016/j.expneurol.2009.05.003.

Celardo I, Martins LM, Gandhi S. 2014. Unravelling mitochondrial pathways to Parkinson's disease. *Br J Pharmacol*. 171(8):1943–1957. doi:10.1111/bph.12433.

Chandel NS, Maltepe E, Goldwasser E, Mathieu CE, Simon MC, Schumacker PT. 1998. Mitochondrial reactive oxygen species trigger hypoxia-induced transcription. *Proc Natl Acad Sci U S A*. 95(September):11715–11720.

Chappie JS, Acharya S, Liu Y-W, Leonard M, Pucadyil TJ, Schmid SL. 2009. An Intramolecular Signaling Element that Modulates Dynamin Function In Vitro and In Vivo. *Mol Biol Cell*. 20:3561–3571. doi:10.1091/mbc.E09.

Chen H, Detmer SA, Ewald AJ, Griffin EE, Fraser SE, Chan DC. 2003. Mitofusins Mfn1 and Mfn2 coordinately regulate mitochondrial fusion and are essential for embryonic development. *J Cell Biol*. 160:189–200. doi:10.1083/jcb.200211046.

Chen K-H, Guo X, Ma D, Guo Y, Li Q, Yang D, Li P, Qiu X, Wen S, Xiao R-P, et al. 2004. Dysregulation of HSG triggers vascular proliferative disorders. *Nat Cell Biol*. 6(9):872–883. doi:10.1038/ncb1161.

Chen KH, Dasgupta A, Ding J, Indig FE, Ghosh P, L. Longo D. 2014. Role of mitofusin 2 (Mfn2) in controlling cellular proliferation. *FASEB J*. 28(1):382–394. doi:10.1096/fj.13-230037.

Chen KH, Guo X, Ma D, Guo Y, Li Q, Yang D, Li P, Qiu X, Wen S, Xiao RP, et al. 2004. Dysregulation of HSG triggers vascular proliferative disorders. *Nat Cell Biol*. 6(9):872–883. doi:10.1038/ncb1161.

Chen Y, Dorn GW. 2013. PINK1-Phosphorylated Mitofusin 2 is a Parkin Receptor for Culling Damaged Mitochondria. *Science (80-)*. 340(April):471–476.

Cleland MM, Norris KL, Karbowski M, Wang C, Suen D-F, Jiao S, George NM, Luo X, Li Z, Youle RJ. 2011. Bcl-2 family interaction with the mitochondrial morphogenesis machinery. *Cell*

Death Differ. 18(2):235–247. doi:10.1038/cdd.2010.89.

Cribbs JT, Strack S. 2007. Reversible phosphorylation of Drp1 by cyclic AMP-dependent protein kinase and calcineurin regulates mitochondrial fission and cell death. *EMBO Rep*. 8(10):939–944. doi:10.1038/sj.embor.7401062.

Delaunay A, Isnard AD, Toledano MB. 2000. H2O2 sensing through oxidation of the Yap1 transcription factor. *EMBO J*. 19(19):5157–5166. doi:10.1093/emboj/19.19.5157.

Detmer Scott A, Chan DC. 2007a. Complementation between mouse Mfn1 and Mfn2 protects mitochondrial fusion defects caused by CMT2A disease mutations. *J Cell Biol*. 176(4):405–14. doi:10.1083/jcb.200611080.

Detmer Scott A, Chan DC. 2007b. Functions and dysfunctions of mitochondrial dynamics. *Nat Rev Mol Cell Biol*. 8(november):870–879. doi:10.1038/nrm2275.

Detmer Scott A., Chan DC. 2007. Complementation between mouse Mfn1 and Mfn2 protects mitochondrial fusion defects caused by CMT2A disease mutations. *J Cell Biol*. 176(4):405–414. doi:10.1083/jcb.200611080.

Detmer SA, Velde C Vande, Cleveland DW, Chan DC. 2008. Hindlimb gait defects due to motor axon loss and reduced distal muscles in a transgenic mouse model of Charcot - Marie - Tooth type 2A. *Hum Mol Genet*. 17(3):367–375. doi:10.1093/hmg/ddm314.

Du C, Fang M, Li Y, Li L, Wang X. 2000. Smac, a Mitochondrial Protein that Promotes Cytochrome c-Dependent Caspase Activation by Eliminating IAP Inhibition Hid, and Grim in terms of IAP neutralization and is the. *Cell*. 102:33–42.

Ekman D, Björklund ÅK, Frey-Skött J, Elofsson A. 2005. Multi-domain proteins in the three kingdoms of life: Orphan domains and other unassigned regions. *J Mol Biol*. 348(1):231–243. doi:10.1016/j.jmb.2005.02.007.

Engelhart EA, Hoppins S. 2019. A catalytic domain variant of Mitofusin requiring a wildtype paralog for function uncouples mitochondrial outer-membrane tethering and fusion. *J Biol Chem*. 1(8):jbc.RA118.006347. doi:10.1074/jbc.RA118.006347.

Ernster L, Schatz G. 1981. Mitochondria : A Historical Review. 91(December).

Eura Y. 2003. Two Mitofusin Proteins, Mammalian Homologues of FZO, with Distinct Functions Are Both Required for Mitochondrial Fusion. *J Biochem*. 134(3):333–344. doi:10.1093/jb/mvg150.

Federico A, Cardaioli E, Da Pozzo P, Formichi P, Gallus GN, Radi E. 2012. Mitochondria, oxidative stress and neurodegeneration. *J Neurol Sci*. 322(1–2):254–262. doi:10.1016/j.jns.2012.05.030.

Feely SME, Laura M, Siskind CE, Sottile S, Davis M, Gibbons VS, Reilly MM, Shy ME. 2011. MFN2 mutations cause severe phenotypes in most patients with CMT2A. *Neurology*. 76(20):1690–6. doi:10.1212/WNL.0b013e31821a441e.

Ferreira JCB, Campos JC, Qvit N, Qi X, Bozi LHM, Bechara LRG, Lima VM, Queliconi BB, Disatnik MH, Dourado PMM, et al. 2019. A selective inhibitor of mitofusin 1-βIIPKC association improves heart failure outcome in rats. *Nat Commun*. 10(1). doi:10.1038/s41467-018-08276-6.

Filadi R, Greotti E, Turacchio G, Luini A, Pozzan T, Pizzo P. 2015. Mitofusin 2 ablation increases endoplasmic reticulum–mitochondria coupling. *Proc Natl Acad Sci*. doi:10.1073/pnas.1504880112.

Franco A, Kitsis RN, Fleischer JA, Gavathiotis E, Kornfeld OS, Gong G, Biris N, Benz A, Qvit N, Donnelly SK, et al. 2016. Correcting mitochondrial fusion by manipulating mitofusin conformations. *Nature*.:1–20. doi:10.1038/nature20156.

Fransson Å, Ruusala A, Aspenström P. 2006. The atypical Rho GTPases Miro-1 and Miro-2 have essential roles in mitochondrial trafficking. *Biochem Biophys Res Commun*. 344(2):500–510. doi:10.1016/j.bbrc.2006.03.163.

Ganesan V, Willis SD, Chang KT, Beluch S, Cooper KF, Strich R. 2019. Cyclin C directly stimulates Drp1 GTP affinity to mediate stress-induced mitochondrial hyperfission. *Mol Biol Cell*. 30(3):302–311. doi:10.1091/mbc.E18-07-0463.

Gawlowski T, Suarez J, Scott B, Torres-Gonzalez M, Wang H, Schwappacher R, Han X, Yates JR,

Hoshijima M, Dillmann W. 2012. Modulation of dynamin-related protein 1 (DRP1) function by increased O-linked-β-N-acetylglucosamine modification (O-GlcNAc) in cardiac myocytes. *J Biol Chem*. 287(35):30024–30034. doi:10.1074/jbc.M112.390682.

Gemignani F, Marbini A. 2001. Charcot-Marie-Tooth disease (CMT): Distinctive phenotypic and genotypic features in CMT type 2. *J Neurol Sci*. 184(1):1–9. doi:10.1016/S0022-510X(00)00497-4.

Giarmarco MM, Cleghorn WM, Sloat SR, Hurley JB, Brockerhoff SE. 2017. Mitochondria Maintain Distinct Ca 2+ Pools in Cone Photoreceptors . *J Neurosci*. 37(8):2061–2072. doi:10.1523/jneurosci.2689-16.2017.

Gilbert HF. 1995. Thiol-Disulfide Exchange Equilibria and Bond Stability. *Methods Enzymol*. 251:8–28.

Giustarini D, Colombo G, Garavaglia ML, Astori E, Portinaro NM, Reggiani F, Badalamenti S, Aloisi AM, Santucci A, Rossi R, et al. 2017. Assessment of glutathione/glutathione disulphide ratio and S-glutathionylated proteins in human blood, solid tissues, and cultured cells. *Free Radic Biol Med*. 112(August):360–375. doi:10.1016/j.freeradbiomed.2017.08.008.

Giustarini D, Dalle-Donne I, Tsikas D, Rossi R. 2009. Oxidative stress and human diseases: Origin, link, measurement, mechanisms, and biomarkers. *Crit Rev Clin Lab Sci*. 46(5–6):241–281. doi:10.3109/10408360903142326.

Gomes LC, Benedetto G Di, Scorrano L. 2011. During autophagy mitochondria elongate, are spared from degradation and sustain cell viability. *Nat Cell Biol*. 13(5):589–598. doi:10.1038/ncb2220.

Grek CL, Zhang J, Manevich Y, Townsend DM, Tew KD. 2013. Causes and consequences of cysteine s-glutathionylation. *J Biol Chem*. 288(37):26497–26504. doi:10.1074/jbc.R113.461368.

Griffin EE, Chan DC. 2006. Domain interactions within Fzo1 oligomers are essential for mitochondrial fusion. *J Biol Chem*. 281(24):16599–606. doi:10.1074/jbc.M601847200.

Guo C, Hildick KL, Luo J, Dearden L, Wilkinson KA, Henley JM. 2013. SENP3-mediated

deSUMOylation of dynamin-related protein 1 promotes cell death following ischaemia. *EMBO J*. 32(11):1514–1528. doi:10.1038/emboj.2013.65.

Guo X, Chen KH, Guo Y, Liao H, Tang J, Xiao RP. 2007. Mitofusin 2 triggers vascular smooth muscle cell apoptosis via mitochondrial death pathway. *Circ Res*. 101(11):1113–1122. doi:10.1161/CIRCRESAHA.107.157644.

Han X, Lu Y, Li S, Kaitsuka T, Sato Y, Tomizawa K, Nairn AC, Takei K, Matsui H, Matsushita M. 2008. JCB : ARTICLE. 182(3):573–585. doi:10.1083/jcb.200802164.

Harder Z, Zunino R, McBride H. 2004. Sumo1 conjugates mitochondrial substrates and participates in mitochondrial fission. *Curr Biol*. 14(4):340–345. doi:10.1016/S0960-9822(04)00084-3.

Hoppins S, Edlich F, Cleland MM, Banerjee S, McCaffery JM, Youle RJ, Nunnari J. 2011. The Soluble Form of Bax Regulates Mitochondrial Fusion via MFN2 Homotypic Complexes. *Mol Cell*. 41(2):150–160. doi:10.1016/j.molcel.2010.11.030.

Horbay R, Bilyy R. 2016. Mitochondrial dynamics during cell cycling. *Apoptosis*. 21(12):1327–1335. doi:10.1007/s10495-016-1295-5.

Iqbal S, Hood DA. 2014. Oxidative stress-induced mitochondrial fragmentation and movement in skeletal muscle myoblasts. *Am J Physiol - Cell Physiol*. 306(12):1176–1183. doi:10.1152/ajpcell.00017.2014.

Ishihara N, Eura Y, Mihara K. 2004. Mitofusin 1 and 2 play distinct roles in mitochondrial fusion reactions via GTPase activity. *J Cell Sci*. 117(26):6535–6546. doi:10.1242/jcs.01565.

James SJ, Rose S, Melnyk S, Jernigan S, Blossom S, Pavliv O, Gaylor DW. 2009. Cellular and mitochondrial glutathione redox imbalance in lymphoblastoid cells derived from children with autism. *FASEB J*. 23(8):2374–2383. doi:10.1096/fj.08-128926.

Jendrach M, Mai S, Pohl S, Vöth M, Bereiter-Hahn J. 2008. Short- and long-term alterations of mitochondrial morphology, dynamics and mtDNA after transient oxidative stress. *Mitochondrion*. 8(4):293–304. doi:10.1016/j.mito.2008.06.001.

Jimah JR, Hinshaw JE. 2019. Structural Insights into the Mechanism of Dynamin Superfamily Proteins. *Trends Cell Biol*. 29(3):257–273. doi:10.1016/j.tcb.2018.11.003.

Karbowski M, Lee Y, Gaume B, Jeong S, Frank S, Nechushtan A, Santel A, Fuller M, Smith CL, Youle RJ. 2002. Spatial and temporal association of Bax with during apoptosis. 159(6):931–938. doi:10.1083/jcb.200209124.

Karbowski M, Norris KL, Cleland MM, Jeong S-Y, Youle RJ. 2006. Role of Bax and Bak in mitochondrial morphogenesis. *Nature*. 443(October):658–662. doi:10.1038/nature05111.

Kim YM, Youn SW, Sudhahar V, Das A, Chandhri R, Cuervo Grajal H, Kweon J, Leanhart S, He L, Toth PT, et al. 2018. Redox Regulation of Mitochondrial Fission Protein Drp1 by Protein Disulfide Isomerase Limits Endothelial Senescence. *Cell Rep*. 23(12):3565–3578. doi:10.1016/j.celrep.2018.05.054.

Koshiba T, Detmer S a, Kaiser JT, Chen H, McCaffery JM, Chan DC. 2004. Structural basis of mitochondrial tethering by mitofusin complexes. *Science*. 305(5685):858–862. doi:10.1126/science.1099793.

Kosower NS, Kosower EM, Wertheim B, Correa WS. 1969. Diamide, a new reagent for the intracellular oxidation of glutathione to the disulfide. *Biochem Biophys Res Commun*. 37(4):593–596. doi:10.1016/0006-291X(69)90850-X.

Koutsopoulos OS, Laine D, Osellame L, Chudakov DM, Parton RG, Frazier AE, Ryan MT. 2010. Human Miltons associate with mitochondria and induce microtubule-dependent remodeling of mitochondrial networks. *Biochim Biophys Acta - Mol Cell Res*. 1803(5):564–574. doi:10.1016/j.bbamcr.2010.03.006.

Labbé K, Murley A, Nunnari J. 2014. Determinants and Functions of Mitochondrial Behavior. *Annu Rev Cell Dev Biol*. 30(1):357–391. doi:10.1146/annurev-cellbio-101011-155756.

Lebeau J, Saunders JM, Moraes VWR, Madhavan A, Madrazo N, Anthony MC, Wiseman RL. 2018. The PERK Arm of the Unfolded Protein Response Regulates Mitochondrial Morphology during Acute Endoplasmic Reticulum Stress. *Cell Rep*. 22(11):2827–2836.

doi:10.1016/j.celrep.2018.02.055.

Lee D, Redfern O, Orengo C. 2007. Predicting protein function from sequence and structure. *Nat Rev Mol Cell Biol*. 8(12):995–1005. doi:10.1038/nrm2281.

Lee J-Y, Kapur M, Li M, Choi M-C, Choi S, Kim H-J, Kim I, Lee E, Taylor JP, Yao T-P. 2014. MFN1 deacetylation activates adaptive mitochondrial fusion and protects metabolically challenged mitochondria. *J Cell Sci*. 127(22):4954–4963. doi:10.1242/jcs.157321.

Liu J, Noel JK, Low HH. 2018. Structural basis for membrane tethering by a bacterial dynamin-like pair. *Nat Commun*. 9(1):1–12. doi:10.1038/s41467-018-05523-8.

Liu X, Kim CN, Yang J, Jemmerson R, Wang X. 1996. Induction of Apoptotic Program in Cell-Free Extracts: Requirement for dATP and Cytochrome C. *Cell*. 86(July):147–157.

Loson OC, Song Z, Chen H, Chan DC. 2013. Fis1, Mff, MiD49, and MiD51 mediate Drp1 recruitment in mitochondrial fission. *Mol Biol Cell*. 24(5):659–667. doi:10.1091/mbc.e12-10-0721.

Low HH, Löwe J. 2006. A bacterial dynamin-like protein. *Nature*. 444(7120):766–769. doi:10.1038/nature05312.

Low HH, Sachse C, Amos LA, Löwe J. 2009. Structure of a Bacterial Dynamin-like Protein Lipid Tube Provides a Mechanism For Assembly and Membrane Curving. *Cell*. 139(7):1342–1352. doi:10.1016/j.cell.2009.11.003.

Mattie S, Riemer J, Wideman JG, McBride HM. 2018. A new mitofusin topology places the redox-regulated C terminus in the mitochondrial intermembrane space. *J Cell Biol*. 217(2):507–515. doi:10.1083/jcb.201611194.

McLelland GL, Goiran T, Yi W, Dorval G, Chen CX, Lauinger ND, Krahn AI, Valimehr S, Rakovic A, Rouiller I, et al. 2018. Mfn2 ubiquitination by PINK1/parkin gates the p97-dependent release of ER from mitochondria to drive mitophagy. *Elife*. 7:1–35. doi:10.7554/eLife.32866.

Mears JA, Lackner LL, Fang S, Ingerman E, Nunnari J, Hinshaw JE. 2011. Conformational changes in Dnm1 support a contractile mechanism for mitochondrial fission. *Nat Struct Mol*

Biol. 18(1):20–27. doi:10.1038/nsmb.1949.

Mishra P, Chan DC. 2014. Mitochondrial dynamics and inheritance during cell division, development and disease. *Nat Rev Mol Cell Biol*. 15(10):634–646. doi:10.1038/nrm3877.

Mitra K, Wunder C, Roysam B, Lin G, Lippincott-Schwartz J. 2009. A hyperfused mitochondrial state achieved at G1-S regulates cyclin E buildup and entry into S phase. *Proc Natl Acad Sci*. 106(29):11960–11965. doi:10.1073/pnas.0904875106.

Olichon A, Baricault L, Gas N, Guillou E, Valette A, Belenguer P, Lenaers G. 2003. Loss of OPA1 perturbates the mitochondrial inner membrane structure and integrity, leading to cytochrome c release and apoptosis. *J Biol Chem*. 278(10):7743–7746. doi:10.1074/jbc.C200677200.

Ong S-B, Kalkhoran SB, Cabrera-Fuentes H a., Hausenloy DJ. 2015. Mitochondrial fusion and fission proteins as novel therapeutic targets for treating cardiovascular disease. *Eur J Pharmacol*.:1–11. doi:10.1016/j.ejphar.2015.04.056.

Østergaard H, Tachibana C, Winther JR. 2004. Monitoring disulfide bond formation in the eukaryotic cytosol. *J Cell Biol*. 166(3):337–345. doi:10.1083/jcb.200402120.

Otera H, Wang C, Cleland MM, Setoguchi K, Yokota S, Youle RJ, Mihara K. 2010. Mff is an essential factor for mitochondrial recruitment of Drp1 during mitochondrial fission in mammalian cells. *J Cell Biol*. 191(6):1141–1158. doi:10.1083/jcb.201007152.

Pareyson D, Saveri P, Sagnelli A, Piscosquito G. 2015. Mitochondrial dynamics and inherited peripheral nerve diseases. *Neurosci Lett*. 596:66–77. doi:10.1016/j.neulet.2015.04.001.

Park YY, Nguyen OTK, Kang H, Cho H. 2014. MARCH5-mediated quality control on acetylated Mfn1 facilitates mitochondrial homeostasis and cell survival. *Cell Death Dis*. 5(4):e1172-12. doi:10.1038/cddis.2014.142.

Pernas L, Scorrano L. 2015. Mito-Morphosis: Mitochondrial Fusion, Fission, and Cristae Remodeling as Key Mediators of Cellular Function. *Annu Rev Physiol*. 78(1):505–531. doi:10.1146/annurev-physiol-021115-105011.

Picard M, Wallace DC, Burelle Y. 2016. The rise of mitochondria in medicine. *Mitochondrion*.

30:105–116. doi:10.1016/j.mito.2016.07.003.

Pilling AD, Horiuchi D, Lively CM, Saxton WM. 2006. Kinesin-1 and Dynein are the primary motors for fast transport of mitochondria in Drosophila motor axons. *Mol Biol Cell*. 17(April):2057–2068. doi:10.1091/mbc.E05.

Pócsi I, Miskei M, Karányi Z, Emri T, Ayoubi P, Pusztahelyi T, Balla G, Prade RA. 2005. Comparison of gene expression signatures of diamide, H2O2 and menadione exposed Aspergillus nidulans cultures - Linking genome-wide transcriptional changes to cellular physiology. *BMC Genomics*. 6:1–18. doi:10.1186/1471-2164-6-182.

Prudent J, Zunino R, Sugiura A, Mattie S, Shore GC, McBride HM. 2015. MAPL SUMOylation of Drp1 Stabilizes an ER/Mitochondrial Platform Required for Cell Death. *Mol Cell*. 59(6):941–955. doi:10.1016/j.molcel.2015.08.001.

Pyakurel A, Savoia C, Scorrano L, Pyakurel A, Savoia C, Hess D, Scorrano L. 2015. Extracellular Regulated Kinase Phosphorylates Mitofusin 1 to Control Mitochondrial Morphology and Article Extracellular Regulated Kinase Phosphorylates Mitofusin 1 to Control Mitochondrial Morphology and Apoptosis. *Mol Cell*.:1–11. doi:10.1016/j.molcel.2015.02.021.

Qi Y, Yan L, Yu C, Guo X, Zhou X, Hu X, Huang X, Rao Z, Lou Z, Hu J. 2016. Structures of human mitofusin 1 provide insight into mitochondrial tethering.

Rambold AS, Kostelecky B, Elia N, Lippincott-Schwartz J. 2011. Tubular network formation protects mitochondria from autophagosomal degradation during nutrient starvation. *Proc Natl Acad Sci*. 108(25):10190–10195. doi:10.1073/pnas.1107402108.

Redpath CJ, Bou Khalil M, Drozdzal G, Radisic M, McBride HM. 2013. Mitochondrial Hyperfusion during Oxidative Stress Is Coupled to a Dysregulation in Calcium Handling within a C2C12 Cell Model. *PLoS One*. 8(7). doi:10.1371/journal.pone.0069165.

Rocha AG, Franco A, Krezel AM, Rumsey JM, Alberti JM, Knight WC, Biris N, Zacharioudakis E, Janetka JW, Baloh RH, et al. 2018a. MFN2 agonists reverse mitochondrial defects in preclinical models of Charcot-Marie-Tooth disease type 2A. *Science (80-)*. 360(6386):336–341.

doi:10.1126/science.aao1785.

Rocha AG, Franco A, Krezel AM, Rumsey JM, Alberti JM, Knight WC, Biris N, Zacharioudakis E, Janetka JW, Baloh RH, et al. 2018b. MFN2 agonists reverse mitochondrial defects in preclinical models of Charcot-Marie-Tooth disease type 2A. *Science (80-)*. 360(6386):336–341. doi:10.1126/science.aao1785.

Rovira-Llopis S, Bañuls C, Diaz-Morales N, Hernandez-Mijares A, Rocha M, Victor VM. 2017. Mitochondrial dynamics in type 2 diabetes: Pathophysiological implications. *Redox Biol*. 11(January):637–645. doi:10.1016/j.redox.2017.01.013.

Santel a, Fuller MT. 2001. Control of mitochondrial morphology by a human mitofusin. *J Cell Sci*. 114:867–874.

Scorrano L. 2013. Keeping mitochondria in shape: A matter of life and death. *Eur J Clin Invest*. 43(8):886–893. doi:10.1111/eci.12135.

Sena LA, Chandel NS. 2012. Physiological roles of mitochondrial reactive oxygen species. *Mol Cell*. 48(2):158–167. doi:10.1016/j.molcel.2012.09.025.

Shen T, Zheng M, Cao C, Chen C, Tang J, Zhang W, Cheng H, Chen KH, Xiao RP. 2007. Mitofusin-2 is a major determinant of oxidative stress-mediated heart muscle cell apoptosis. *J Biol Chem*. 282(32):23354–23361. doi:10.1074/jbc.M702657200.

SHITARA H, SHIMANUKI M, HAYASHI J-I, YONEKAWA H. 2010. Global Imaging of Mitochondrial Morphology in Tissues Using Transgenic Mice Expressing Mitochondrially Targeted Enhanced Green Fluorescent Protein. *Exp Anim*. 59(1):99–103. doi:10.1538/expanim.59.99.

Shutt T, Geoffrion M, Milne R, McBride HM. 2012. The intracellular redox state is a core determinant of mitochondrial fusion. *EMBO Rep*. 13(10):909–915. doi:10.1038/embor.2012.128.

Shutt TE, McBride HM. 2013. Staying cool in difficult times: Mitochondrial dynamics, quality control and the stress response. *Biochim Biophys Acta - Mol Cell Res*. 1833(2):417–424.

doi:10.1016/j.bbamcr.2012.05.024.

Slater EC, Cleland KW. 1953. The effect of calcium on the respiratory and phosphorylative activities of heart-muscle sarcosomes. *Biochem J*. 55(4):566–580. doi:10.1042/bj0550566.

Slivka A, Spina MB, Cohen G. 1987. Reduced and oxidized glutathione in human and monkey brain. *Neurosci Lett*. 74(1):112–118. doi:10.1016/0304-3940(87)90061-9.

Smirnova E, Griparic L, Shurland D-L, van der Bliek AM. 2001. Dynamin-related Protein Drp1 Is Required for Mitochondrial Division in Mammalian Cells. *Mol Biol Cell*. 12(8):2245–2256. doi:10.1091/mbc.12.8.2245.

Sorrentino V, Menzies KJ, Auwerx J. 2017. Repairing Mitochondrial Dysfunction in Disease. *Annu Rev Pharmacol Toxicol*. 58(1):353–389. doi:10.1146/annurev-pharmtox-010716-104908.

De Stefani D, Rizzuto R, Pozzan T. 2016. Enjoy the Trip: Calcium in Mitochondria Back and Forth. *Annu Rev Biochem*. 85(1):161–192. doi:10.1146/annurev-biochem-060614-034216.

Strickland A V, Rebelo AP, Zhang F, Price J, Bolon B, Silva JP, Wen R, Züchner S. 2014. Characterization of the Mitofusin 2 R94W Mutation in a Knock-in Mouse Model. *J Peripher Nerv Syst*. 164:152–164. doi:10.1111/jns5.12066.

Stuppia G, Rizzo F, Riboldi G, Del Bo R, Nizzardo M, Simone C, Comi GP, Bresolin N, Corti S. 2015. MFN2-related neuropathies: Clinical features, molecular pathogenesis and therapeutic perspectives. *J Neurol Sci*. doi:10.1016/j.jns.2015.05.033.

Suen D, Norris KL, Youle RJ. 2008. Mitochondrial dynamics and apoptosis. (301):1577–1590. doi:10.1101/gad.1658508.GENES.

Sugiura A, Nagashima S, Tokuyama T, Amo T, Matsuki Y, Ishido S, Kudo Y, McBride HM, Fukuda T, Matsushita N, et al. 2013. MITOL regulates endoplasmic reticulum-mitochondria contacts via Mitofusin2. *Mol Cell*. 51(1):20–34. doi:10.1016/j.molcel.2013.04.023.

Susin SA, Zamzami N, Castedo M, Hirsch T, Marchetti P, Macho A, Daugas E, Geuskens M, Kroemer G. 1996. Bcl-2 Inhibits the Mitochondrial Release of an Apoptotic Protease. *J Exp Med*. 184(October):1331–1341.

Suzuki M, Youle RJ, Tjandra N. 2000. Structure of Bax. *Cell*. 103(4):645–654. doi:10.1016/s0092-8674(00)00167-7.

Suzuki Y, Imai Y, Nakayama H, Takahashi K, Takio K, Takahashi R. 2001. A serine protease, HtrA2, is released from the mitochondria and interacts with XIAP, inducing cell death. *Mol Cell*. 8(3):613–621. doi:10.1016/S1097-2765(01)00341-0.

Thaher O, Wolf C, Dey PN, Pouya A, Wüllner V, Tenzer S, Methner A. 2017. The thiol switch C684 in Mitofusin-2 mediates redox-induced alterations of mitochondrial shape and respiration. *Neurochem Int*.:5–11. doi:10.1016/j.neuint.2017.05.009.

Thorpe GW, Fong CS, Alic N, Higgins VJ, Dawes IW. 2004. Cells have distinct mechanisms to maintain protection against different reactive oxygen species: Oxidative-stress-response genes. *Proc Natl Acad Sci*. 101(17):6564–6569. doi:10.1073/pnas.0305888101.

Tondera D, Grandemange S, Jourdain A, Karbowski M, Mattenberger Y, Herzig S, Da Cruz S, Clerc P, Raschke I, Merkwirth C, et al. 2009. SLP-2 is required for stress-induced mitochondrial hyperfusion. *EMBO J*. 28(November 2008):1589–1600. doi:10.1038/emboj.2009.89.

Twig G, Elorza A, Molina AJA, Mohamed H, Wikstrom JD, Walzer G, Stiles L, Haigh SE, Katz S, Las G, et al. 2008. Fission and selective fusion govern mitochondrial segregation and elimination by autophagy. *EMBO J*. 27(2):433–446. doi:10.1038/sj.emboj.7601963.

Vallat J-M, Ouvrier R a, Pollard JD, Magdelaine C, Zhu D, Nicholson G a, Grew S, Ryan MM, Funalot B. 2008. Histopathological findings in hereditary motor and sensory neuropathy of axonal type with onset in early childhood associated with mitofusin 2 mutations. *J Neuropathol Exp Neurol*. 67(11):1097–1102. doi:10.1097/NEN.0b013e31818b6cbc.

Verhagen AM, Ekert PG, Pakusch M, Silke J, Connonlly LM, Reid GE, Moritz RL, Simpson RJ, Vaux DL. 2000. Identification of DIABLO, a Mammalian Protein that Promotes Apoptosis by Binding to and Antagonizing IAP Proteins. *Cell*. 102(1):43–53. doi:10.1016/S0896-6273(00)80282-2.

Verhoeven K, Claeys KG, Züchner S, Schröder JM, Weis J, Ceuterick C, Jordanova A, Nelis E, De

Vriendt E, Van Hul M, et al. 2006. MFN2 mutation distribution and genotype/phenotype correlation in Charcot-Marie-Tooth type 2. *Brain*. 129(8):2093–2102. doi:10.1093/brain/awl126.

Vital A, Vital C. 2012. Mitochondria and peripheral neuropathies. *J Neuropathol Exp Neurol*. 71(12):1036–46. doi:10.1097/NEN.0b013e3182764d47.

Wada J, Nakatsuka A. 2016. Mitochondrial Dynamics and Mitochondrial Dysfunction in Diabetes. *Acta Med Okayama*. 70(3):151–8. doi:10.18926/AMO/54413.

Wallace DC, Fan W, Procaccio V. 2010. Mitochondrial Energetics and Therapeutics. *Annu Rev Pathol Mech Dis*. 5(1):297–348. doi:10.1146/annurev.pathol.4.110807.092314.

Wang C, Youle RJ. 2011. The role of mitochondria in apoptosis. *BMB Rep*. 41(1):11–22. doi:10.5483/bmbrep.2008.41.1.011.

Wang H, Song P, Du L, Tian W, Yue W, Liu M, Li D, Wang B, Zhu Y, Cao C, et al. 2011. Parkin ubiquitinates Drp1 for proteasome-dependent degradation: Implication of dysregulated mitochondrial dynamics in Parkinson disease. *J Biol Chem*. 286(13):11649–11658. doi:10.1074/jbc.M110.144238.

Wang K, Yan R, Cooper KF, Strich R. 2015. Cyclin C mediates stress-induced mitochondrial fission and apoptosis. *Mol Biol Cell*. 26(6):1030–1043. doi:10.1091/mbc.E14-08-1315.

Wang W, Zhang F, Li L, Tang F, Siedlak SL, Fujioka H, Liu Y, Su B, Pi Y, Wang X. 2015. MFN2 couples glutamate excitotoxicity and mitochondrial dysfunction in motor neurons. *J Biol Chem*. 290(1):168–182. doi:10.1074/jbc.M114.617167.

Wemmie JA, Steggerda SM, Moye-Rowley WS. 1997. The Saccharomyces cerevisiae AP-1 protein discriminates between oxidative stress elicited by the oxidants H 2O 2 and diamide. *J Biol Chem*. 272(12):7908–7914. doi:10.1074/jbc.272.12.7908.

Willems P, Wanschers BFJ, Esseling J, Szklarczyk R, Kudla U, Duarte I, Forkink M, Nooteboom M, Swarts H, Gloerich J, et al. 2013. BOLA1 is an aerobic protein that prevents mitochondrial morphology changes induced by glutathione depletion. *Antioxidants Redox Signal*. 18(2):129–

138. doi:10.1089/ars.2011.4253.

Wu S, Zhou F, Zhang Z, Xing D. 2011. Mitochondrial oxidative stress causes mitochondrial fragmentation via differential modulation of mitochondrial fission-fusion proteins. *FEBS J*. 278(6):941–954. doi:10.1111/j.1742-4658.2011.08010.x.

Xiying F, Rajaa H, George A. B. 2013. H2O2-induced mitochondrial fragmentation in C2C12 myocytes. *Free Radic Biol Med*. 18(9):1199–1216. doi:10.1016/j.micinf.2011.07.011.Innate.

Xu K, Chen G, Li X, Wu X, Chang Z, Xu J, Zhu Y, Yin P, Liang X, Dong L. 2017. MFN2 suppresses cancer progression through inhibition of mTORC2/Akt signaling. *Sci Rep*. 7(February):1–13. doi:10.1038/srep41718.

Yan L, Qi Y, Huang X, Yu C, Lan L, Guo X, Rao Z, Hu J, Lou Z. 2018. Structural basis for GTP hydrolysis and conformational change of MFN1 in mediating membrane fusion. *Nat Struct Mol Biol*. 25(3):233–243. doi:10.1038/s41594-018-0034-8.

Yang J, Zhang Y. 2015. I-TASSER server: New development for protein structure and function predictions. *Nucleic Acids Res*. 43(W1):W174–W181. doi:10.1093/nar/gkv342.

Yesylevskyy SO, Kharkyanen VN, Demchenko AP. 2006. Dynamic protein domains: Identification, interdependence, and stability. *Biophys J*. 91(2):670–685. doi:10.1529/biophysj.105.078584.

Yoon Y-S, Yoon D-S, Lim IK, Yoon S-H, Chung H-Y, Rojo M, Malka F, Jou M-J, Martinou J-C, Yoon G. 2006. Formation of Elongated Giant Mitochondria in DFO-Induced Cellular Senescence: Involvement of Enhanced Fusion Process Through Modulation of Fis1. *J Cell Physiol*. 209(1):468–480. doi:10.1002/JCP.

Zahedi A, Phandthong R, Chaili A, Leung S, Omaiye E, Talbot P. 2019. Mitochondrial Stress Response in Neural Stem Cells Exposed to Electronic Cigarettes. *iScience*. 16:250–269. doi:10.1016/j.isci.2019.05.034.

Zhang G-E, Jin H-L, Lin X-K, Chen C, Liu X-S, Zhang Q, Yu J-R. 2013. Anti-tumor effects of mfn2 in gastric cancer. *Int J Mol Sci*. 14:13005–21. doi:10.3390/ijms140713005.

Zhang Y. 2009. I-TASSER: Fully automated protein structure prediction in CASP8. *Proteins Struct Funct Bioinforma*. 77(SUPPL. 9):100–113. doi:10.1002/prot.22588.

Zheng M, Xiao RP. 2010. Role of mitofusin 2 in cardiovascular oxidative injury. *J Mol Med*. 88(10):987–991. doi:10.1007/s00109-010-0675-5.

Zhou Y, Lutz CM, Baloh RH, Zhou Y, Carmona S, Muhammad AKMG, Bell S, Landeros J, Vazquez M, Ho R, et al. 2019. Restoring mitofusin balance prevents axonal degeneration in a Charcot-Marie-Tooth type 2A model Graphical abstract Find the latest version : Restoring mitofusin balance prevents axonal degeneration in a Charcot-Marie-Tooth type 2A model.

Zorov DB, Filburn CR, Klotz LO, Zweier JL, Sollott SJ. 2000. Reactive oxygen species (ROS)-induced ROS release: A new phenomenon accompanying induction of the mitochondrial permeability transition in cardiac myocytes. *J Exp Med*. 192(7):1001–1014. doi:10.1084/jem.192.7.1001.

Züchner S, Mersiyanova I V, Muglia M, Bissar-Tadmouri N, Rochelle J, Dadali EL, Zappia M, Nelis E, Patitucci A, Senderek J, et al. 2004. Mutations in the mitochondrial GTPase mitofusin 2 cause Charcot-Marie-Tooth neuropathy type 2A. *Nat Genet*. 36(5):449–451. doi:10.1038/ng1341.